AOSPR 2019 SEOUL KOREA

September 26 - 28, 2019

19th Annual Scientific Meeting of
Asian and Oceanic Society for Paediatric Radiology

AOfPR

CONTENTS

AOSPR 2019 Seoul Conference Awardees Presentation

In-One Kim, M.D.
Professor Emeritus,
Seoul National University,
Seoul, KOREA.

Better Imaging for Children, Better Imaging for the Future

Dear AOSPR colleagues,

On behalf of Korean Society of Pediatric Radiology, I have the honor and privilege to write a welcome message to 6thissue of the Asian Oceanic forum for Pediatric Radiology.

In this issue, we included 10 excellent presentations that were awarded in AOSPR 2019 held in Seoul, Korea.

Reminding the Seoul AOSPR meeting, we had a great time sharing our knowledge and friendship, and enjoyed Seoul as well. We had 203 international participants from 27 countries including 47 invited guests. I deeply appreciate all the attendants and organizing committee members for such vivid participations to achieve another step of a very successful meeting after the previous AOSPR Seoul meeting in 2003.

Out of 124 presentations, 4 oral and 8 e-poster presentations were awarded. And special thanks to the authors for the generous acceptance of our invitation and the outstanding contributions.

Just as the theme of AOSPR 2019 meeting, we hope these presentations contribute for the better imaging for the children and the future.

I also thank for the enormous works of the members of Editorial Board and webmasters to make this forum possible.

Please enjoy the forum!

Convolutional Neural Network for the Diagnosis of Pediatric Developmental Dysplasia of the Hip on Conventional Radiography

Yeon Jin Cho[1], Ga Young Choi[1], Seul Bi Lee[1],YoungHun Choi[1], Seung Hyun Lee[1], Jung-Eun Cheon[1] , Woo Sun Kim[1] , In-One Kim[1] , Young Jin Ryu[2] , Jae-Yeon Hwang[3] , Hyoung Suk Park[4] , Kiwan Jeon[4]

[1]Department of Radiology, Seoul National University College of Medicine, and Institute of Radiation Medicine, Seoul National University Medical Research Center, Seoul, Korea
[2]Department of Radiology, Seoul National University Bundang Hospital, Bundang-gu, Seongnam, Republic of Korea
[3]Department of Radiology, Pusan National University Yangsan Hospital, Mulgeum-eup, Yangsan-si, Gyeongsangnam-do, Republic of Korea
[4]Division of Medical Mathematics, National Institute for Mathematical Sciences, Daejeon, Republic of Korea

- ***Developmental Dysplasia Of the Hip (DDH):***

  The most common orthopedic disorder in newborns

  Incidence: 1.5 in 1,000

  Spectrum of structural abnormalities

  (mild acetabular dysplasia ~ dislocation of the femoral head)

- ***Diagnosis and Treatment:***

  - Modality of choice: Conventional radiography and Ultrasound

  - Ossification center of femoral head: 4-6 month of age

  - US: < 4-6 months of age

  - Conventional radiography: > 4-6 month of age

  - Articulation of the femoral head and acetabulum → normal development

  - Early diagnosis and treatment are important

Siegel MJ. Pediatric sonography: Lippincott Williams & Wilkins; 2011.

Starr V . Et al. AJR. 2014;203(6):1324-35.

- ***Convolutional Neural Network***

  : tremendous progress; considered to be an emerging technique for the classification of images

  : potential of deep learning in the field of lesion detection, classification and image improvement in radiologic image

- To evaluate the diagnostic performance of a deep learning algorithm for DDH using conventional radiography.

- **Inclusion**

 - Younger than 12 months of age who were suspected of DDH and were undergoing hip AP conventional radiography

 - SNUH: between January 2011 and June 2018

 - SNUBH & PNUYH: between January 2016 and June 2018

- **Exclusion**

 - Inappropriate images for reading

 - Images taken with not proper position

 - Postoperative images

- **Dataset**

- 2,601 Hip radiographs → 5,202 hip joints images
- Exclusion: 126 inappropriate images
- 5,076 hip joint images→ Dataset (Training 80% / Validation 10% / Test 10%)

Hospitals	Total	Training Set		Validation Set		Test Set	
		Normal	DDH	Normal	DDH	Normal	DDH
SNUH	3433	2406	341	300	43	300	43
SNUBH	1036	800	32	97	5	97	5
PNUYH	607	452	19	65	3	66	2
Total	5076	4050		513		513	

- **Labeling**

- Image Review and Labeling: By two pediatric radiologists in consensus
- Binary Classification: Normal and DDH
- Diagnosis of DDH
  1) high acetabular index (> 30 degree)
  2) abnormal acetabular morphology and delayed femoral head
  3) abnormal femoral head location; out of inferior medial quadrant of acetabulum
  4) disruption of Shenton line

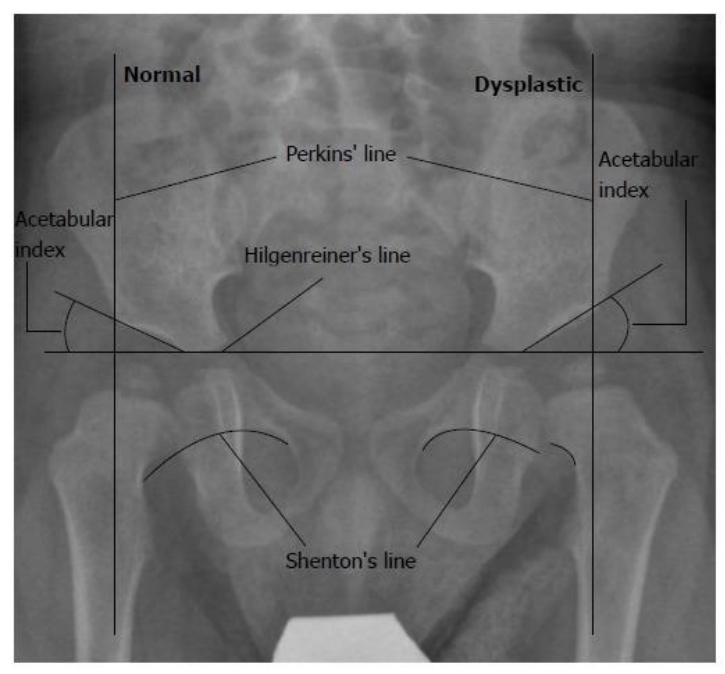

Pavel Kotlarsky, World J Orthop. 2015 Dec 18; 6(11): 886–901

- **Image Processing**

- Manually cropping: include single hip joint with the femoral head in the center of the cropped image
- To avoid overfitting, the training datasets were augmented (x 10 in DDH, x4 in normal)
- 3,920 DDH and 14,632 normal patches were used for training.
- Training was performed after resizing patch size from 414×414 to 128×128

- **Deep Learning Algorithm**

- **Tensorflow**
- **GPU (NVIDIA, Titan Xp. 12GB) system**
- **Network minimization: using the Adam optimizer**
- **Learning rate: 0.0001**
- **Mini-batch size: 16**
- **Epoch: 100**

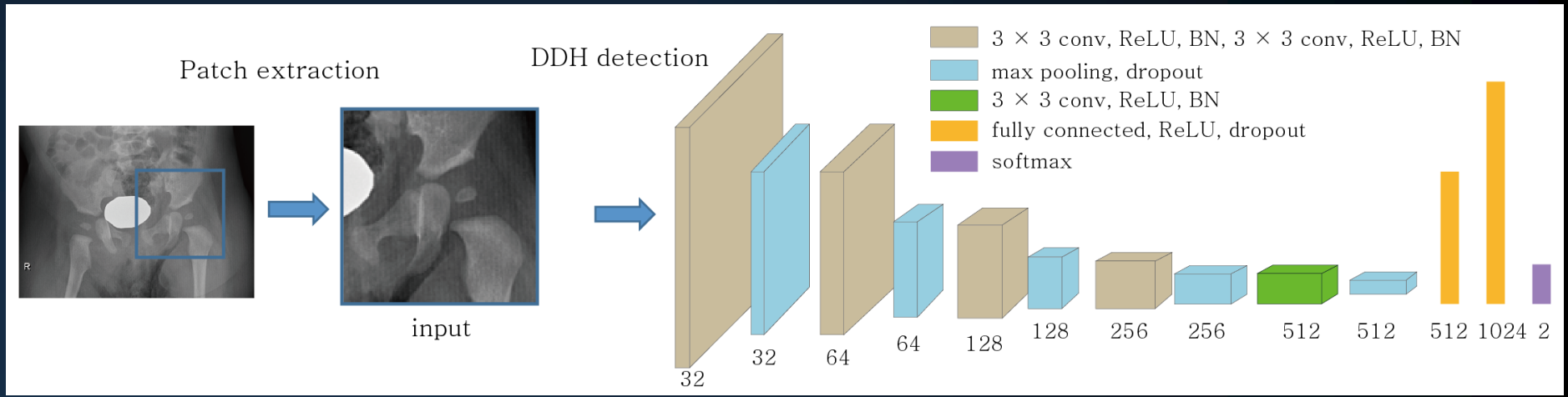

- **Human Readout**

- Three invited radiologists performed image review
  - Reviewer 1: pediatric experts
  - Reviewer 2: experienced radiologist without experience in pediatric radiology
  - Reviewer 3: inexperienced radiologist without experience in pediatric radiology

- No clinical information, No contralateral Hip image

- Labeling: 5-point scale
  - 1, definitely normal; 2, probably normal; 3, indeterminate; 4, probable DDH; and 5, definite DDH

- **Statistical analysis**

- **Diagnostic Performance of the deep learning algorithm**
  - construction of 2x2 table
  - calculation of sensitivity, specificity, positive predictive value (PPV), negative predictive value (NPV)
  - construction of receiver an operating curve (ROC) plot and a precision-recall (PRC) plot → calculate area under the curve (AUC)

- **Comparison with Human Readout**
  - 5-point scale → dichotomization into normal (1, 2)and D오 (3, 4, 5)
  - calculation of sensitivity, specificity , PPV and NPV
  - McNemar`s test
  - AUC of ROC and PRC plot comparison (algorithm vs. human readout)

	Sensitivity	Specificity	PPV	NPV	AUC of ROC plot	AUC of PRC plot
Deep learning algorithm	**94.0 (83.5-98.7)**	**98.9 (97.5-99.6)**	**90.4 (79.7-95.8)**	**99.4 (98.1-99.8)**	**0.988 (0.974-0.995)**	**0.979**
Radiologist 1 (p= 1.000)	96.0 (86.3-99.5)	99.1 (97.8–99.8)	92.3 (81.9-97.0)	99.6 (98.3-99.9)	0.988 (0.974-0.995)	0.958
Radiologist 2 (p<0.001)	96.0 (86.3-99.5)	89.0 (85.8-91.7)	**48.5 (41.9-55.1)**	99.5 (98.1-99.9)	0.959 (0.939-0.975)	0.835
Radiologist 3 (p<0.001)	**84.0 (70.9-92.8)**	**85.8 (82.2-88.8)**	**38.9 (33.0-45.1)**	**98.0 (96.3-98.9)**	**0.919 (0.892-0.941)**	**0.618**

Results

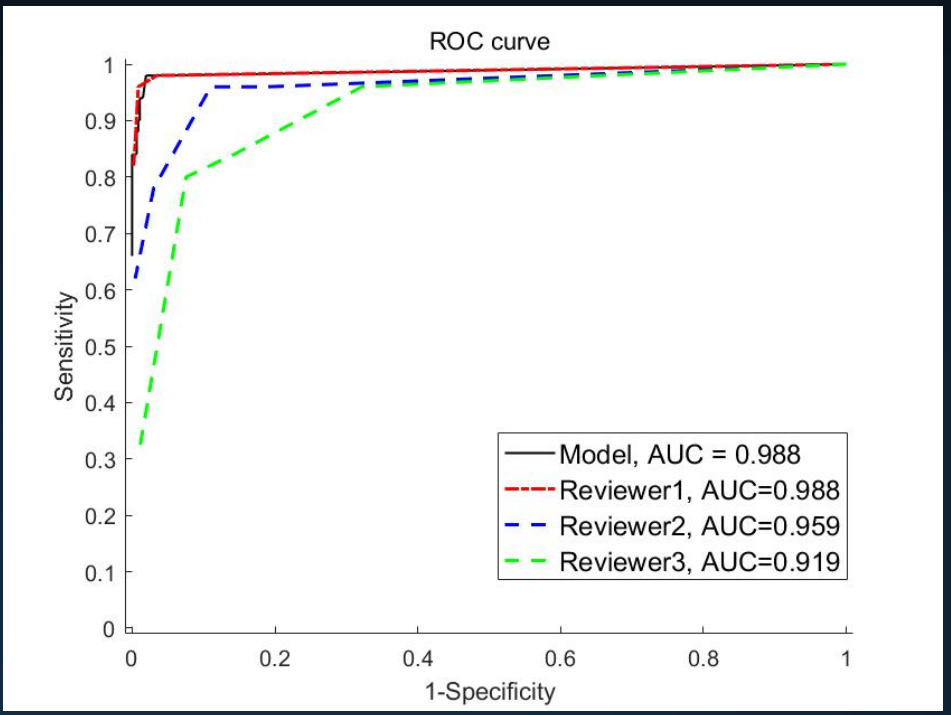
ROC curve
Sensitivity
1-Specificity
Model, AUC = 0.988
Reviewer1, AUC=0.988
Reviewer2, AUC=0.959
Reviewer3, AUC=0.919

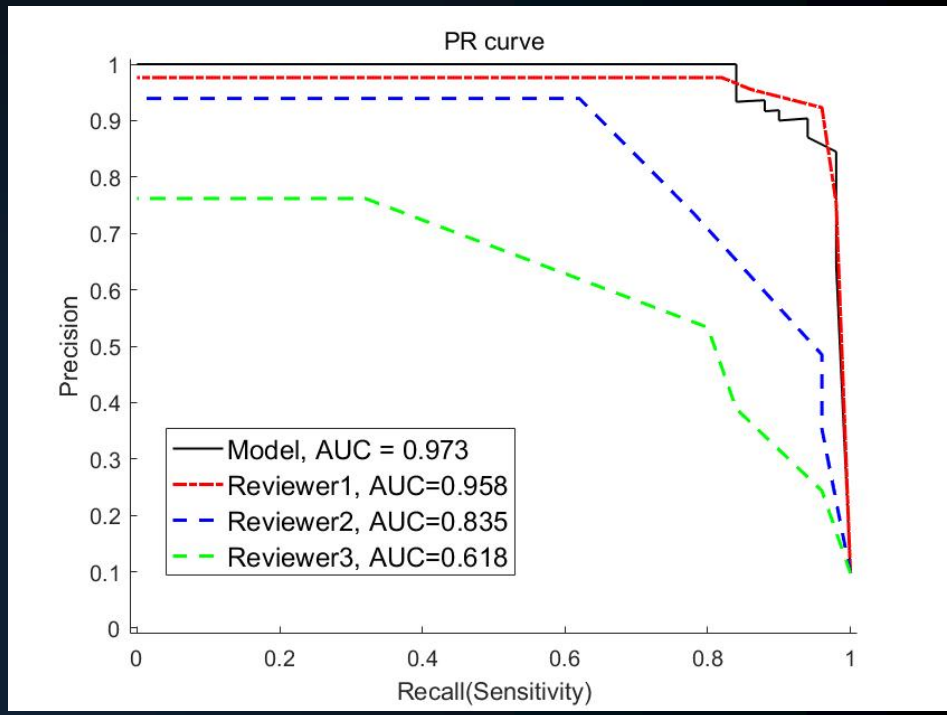
PR curve
Precision
Recall(Sensitivity)
Model, AUC = 0.973
Reviewer1, AUC=0.958
Reviewer2, AUC=0.835
Reviewer3, AUC=0.618

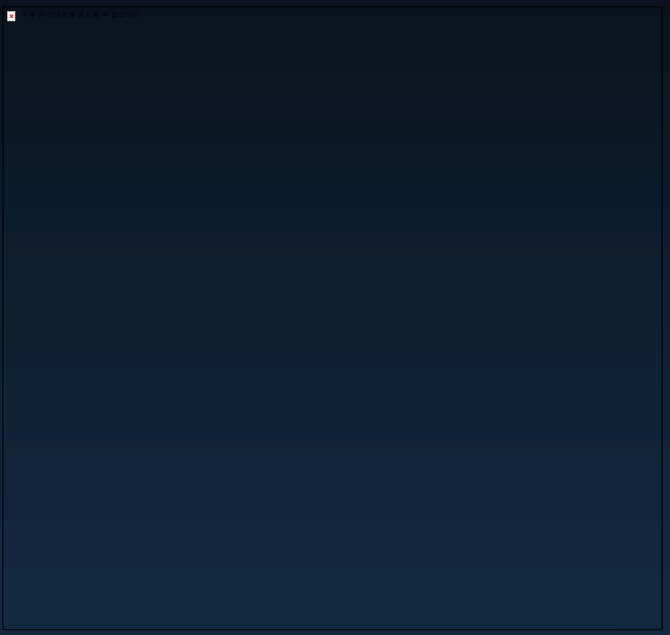

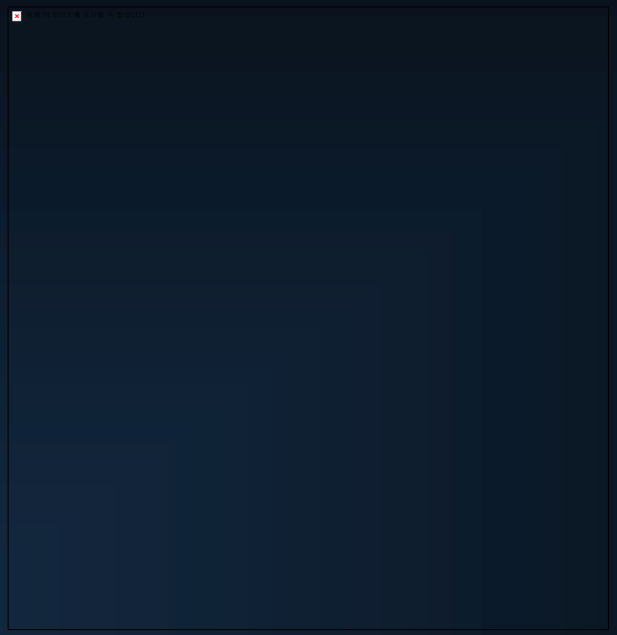

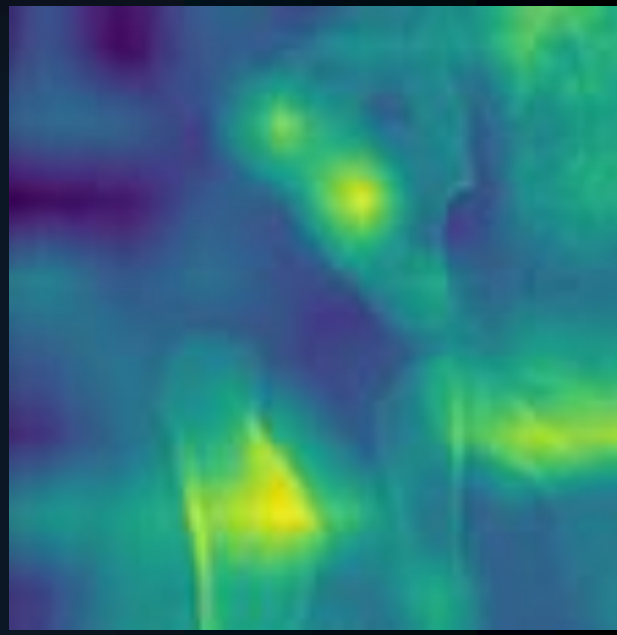


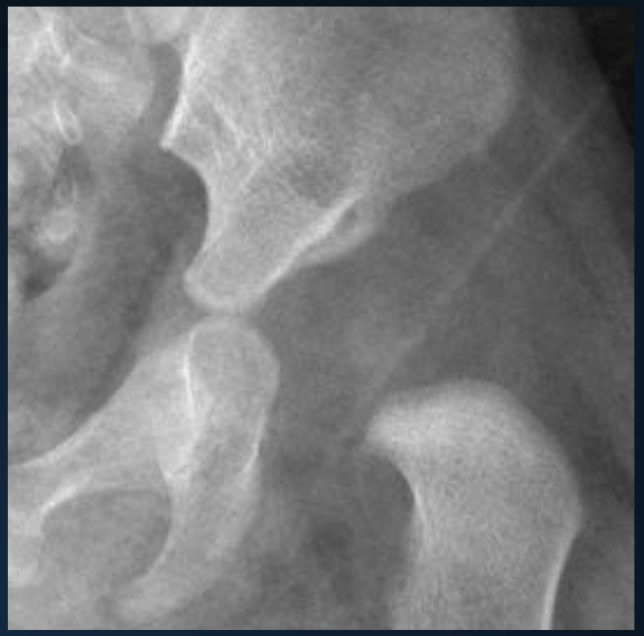
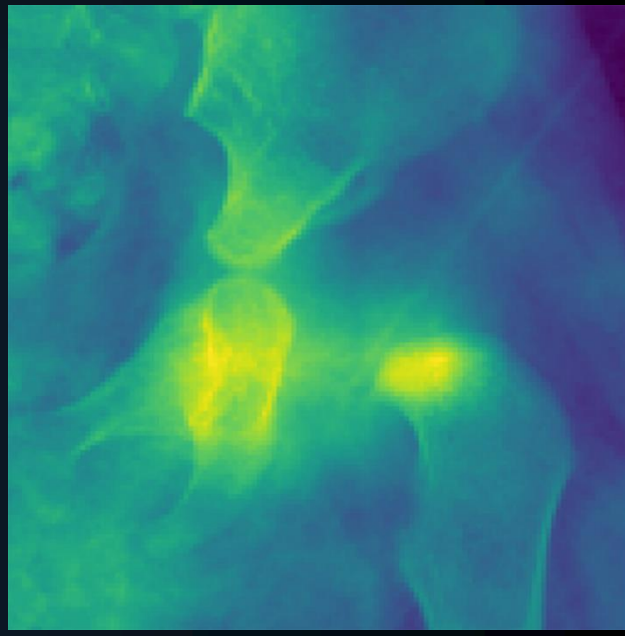



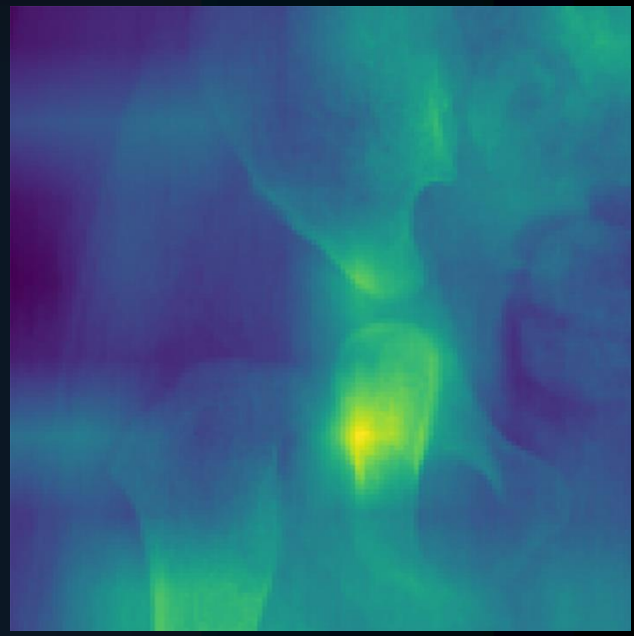

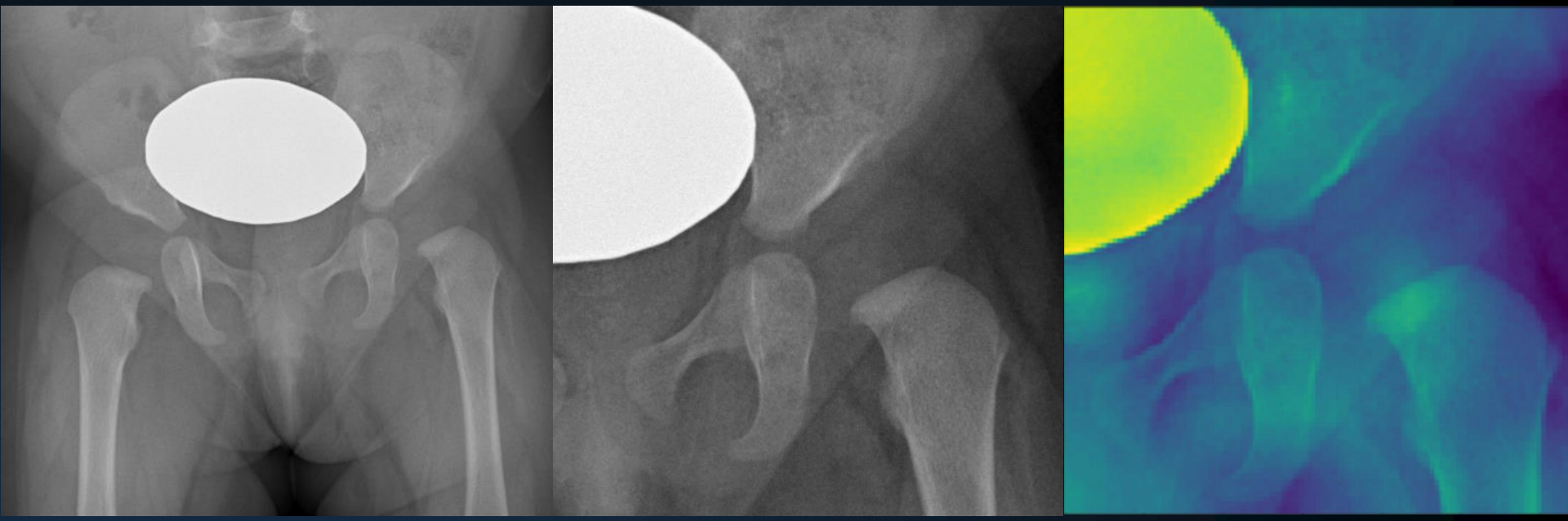

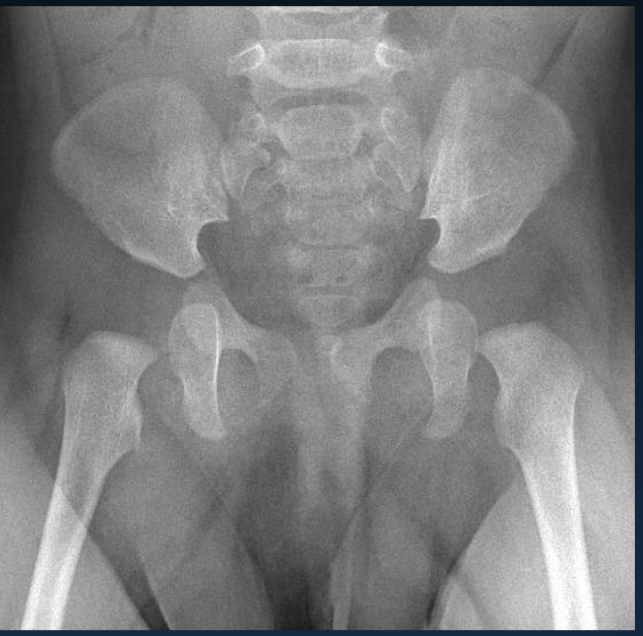

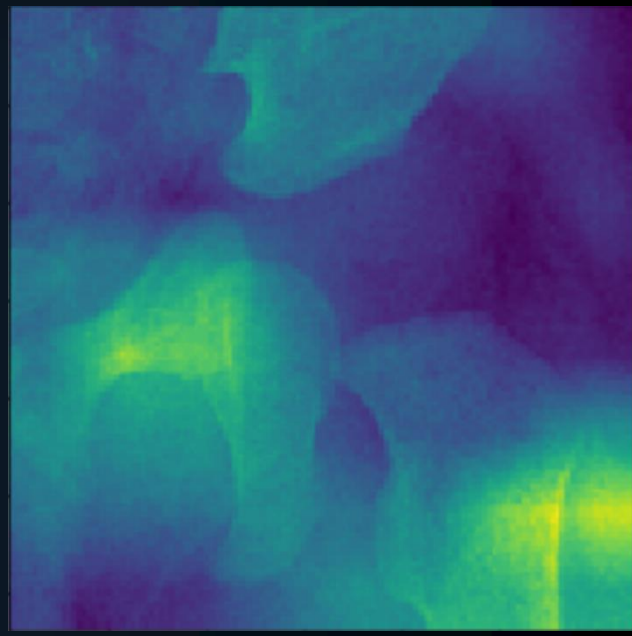

Conclusion

- The proposed deep learning algorithm provided an accurate diagnosis of developmental dysplasia of the hip on hip AP conventional radiographs, which was comparable to an experienced radiologist.

Thank you for your attentions

ARE ACADEMIC INVOLVEMENTS OF RADIOLOGY TRAINEES IN PEDIATRICS ENOUGH?

PRELIMINARY RESULTS OF A GLOBAL PERSPECTIVE

JM Choa-Go (Philippines), F Vernuccio (Italy), D Haroun (Egypt), E Terrazas Torres (Mexico), B Bold (Mongolia), M Arzanauskaite (UK)

choa.jmd@gmail.com

DISCLOSURE

NONE

“Radiology, being one of the most technologically intensive and rapidly evolving disciplines in medicine, relies heavily on **research** for its continuing clinical relevance and utility” [1]

“**Research** is an aspect of the profession that should be paid more attention to, in order to invest in the intellectual development of the next generation of radiologists.” [2]

INTRODUCTION AND BACKGROUND OF THE STUDY

- "The future of radiology was threatened by the paucity of **competent researchers** who are radiologists" [3]
  - Only **32% of residents** and **44% of fellows** were engaged in prospective clinical research
- Almost 30 years after, there is still **inadequate involvement** of radiology residents in research during core training
  - About **39% of residents** [4] involved, and approximately **41% of radiology residents** are not satisfied with the research opportunities available to them [5].

To assess the involvement in **research and teaching** of radiology trainees who are interested in pediatric imaging as well as to identify the **challenges and difficulties** they encounter

PURPOSE

MATERIALS AND METHODS

35-item online survey

Distributed through

Components

Composition: introduction of study, voluntary consent to participate, demographics, information on work place, core radiology residency, participation in academic activities during residency

Format: multiple questions (multiple choice tick-box format) and open-ended questions

Participants

Radiology trainees and radiologists within two years of graduation from fellowship with interest in

PEDIATRIC IMAGING

Formal request distributed to
almost 30 societies,
wherein 15 of them agreed

Descriptive Statistics

Fisher’s Exact test for comparison with $p<0.05$ as significant

RESULTS

3161

2 undisclosed

94

Total participants

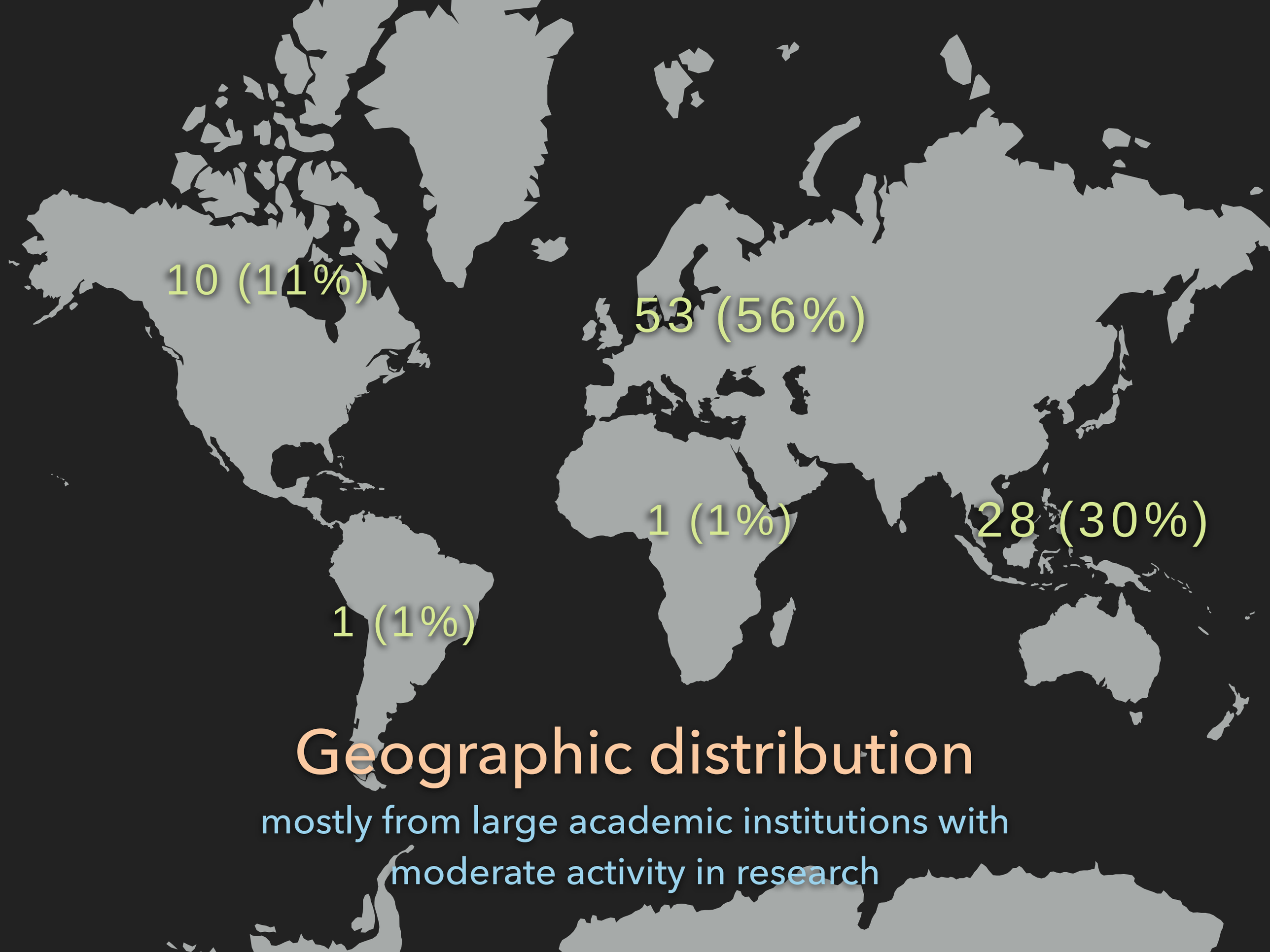

Geographic distribution

mostly from large academic institutions with moderate activity in research

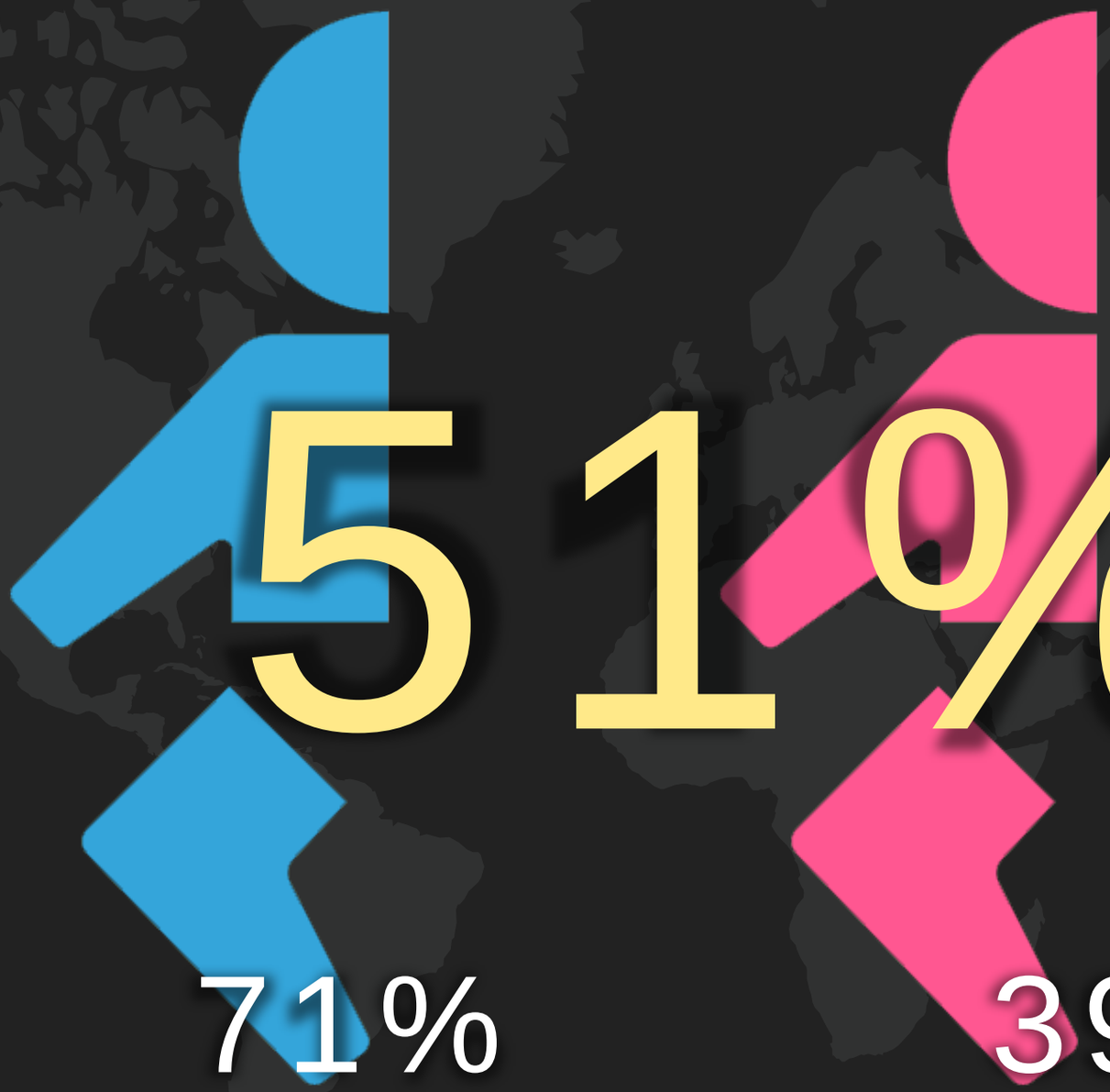

Engaged in Research

26%

26%
8/31

28%
17/61

Involved in Teaching

59/94 (63%)

Research and teaching activities during training

NO ALLOCATED TIME

Allocated hours per week for RESEARCH

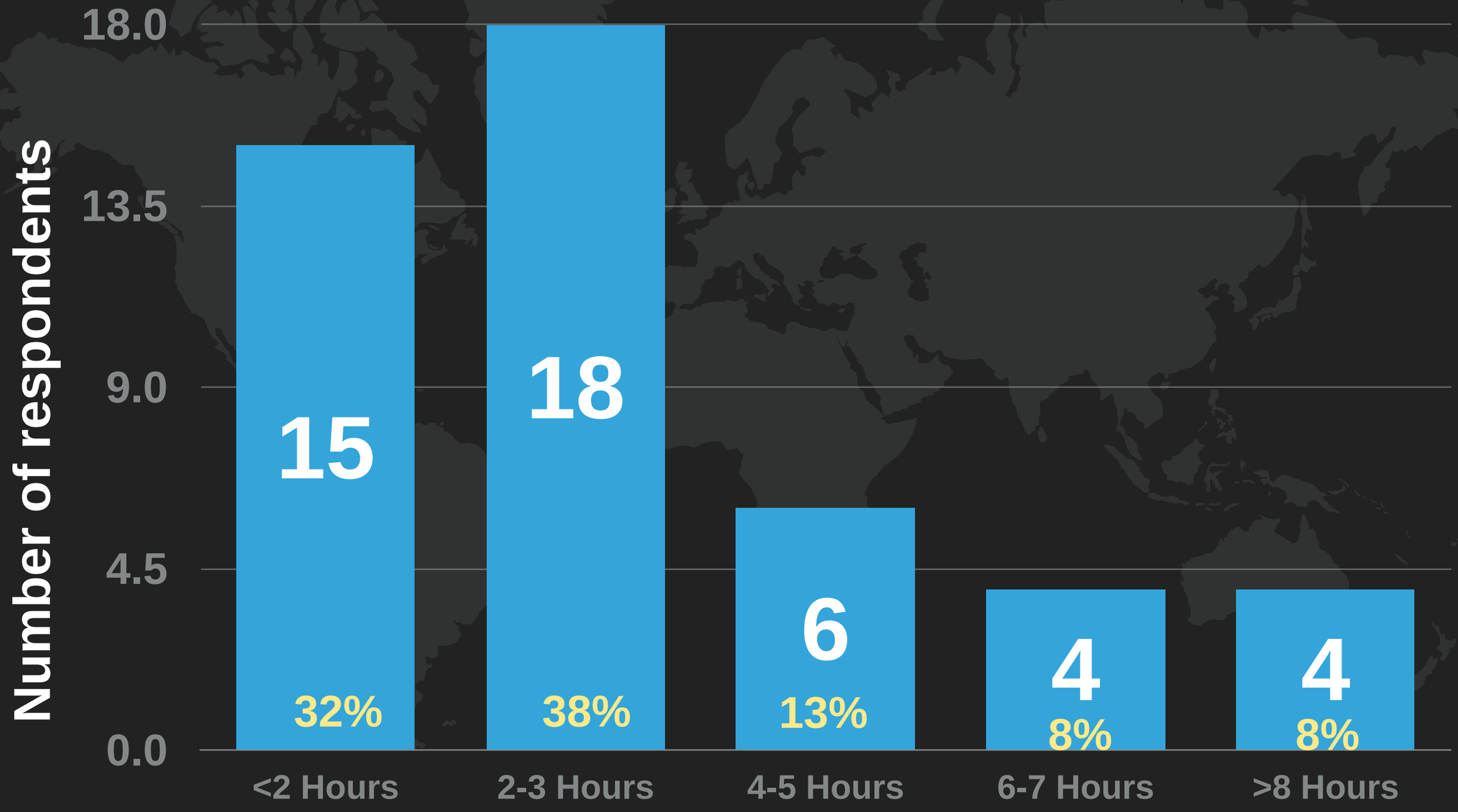

Allocated hours per week for RESEARCH

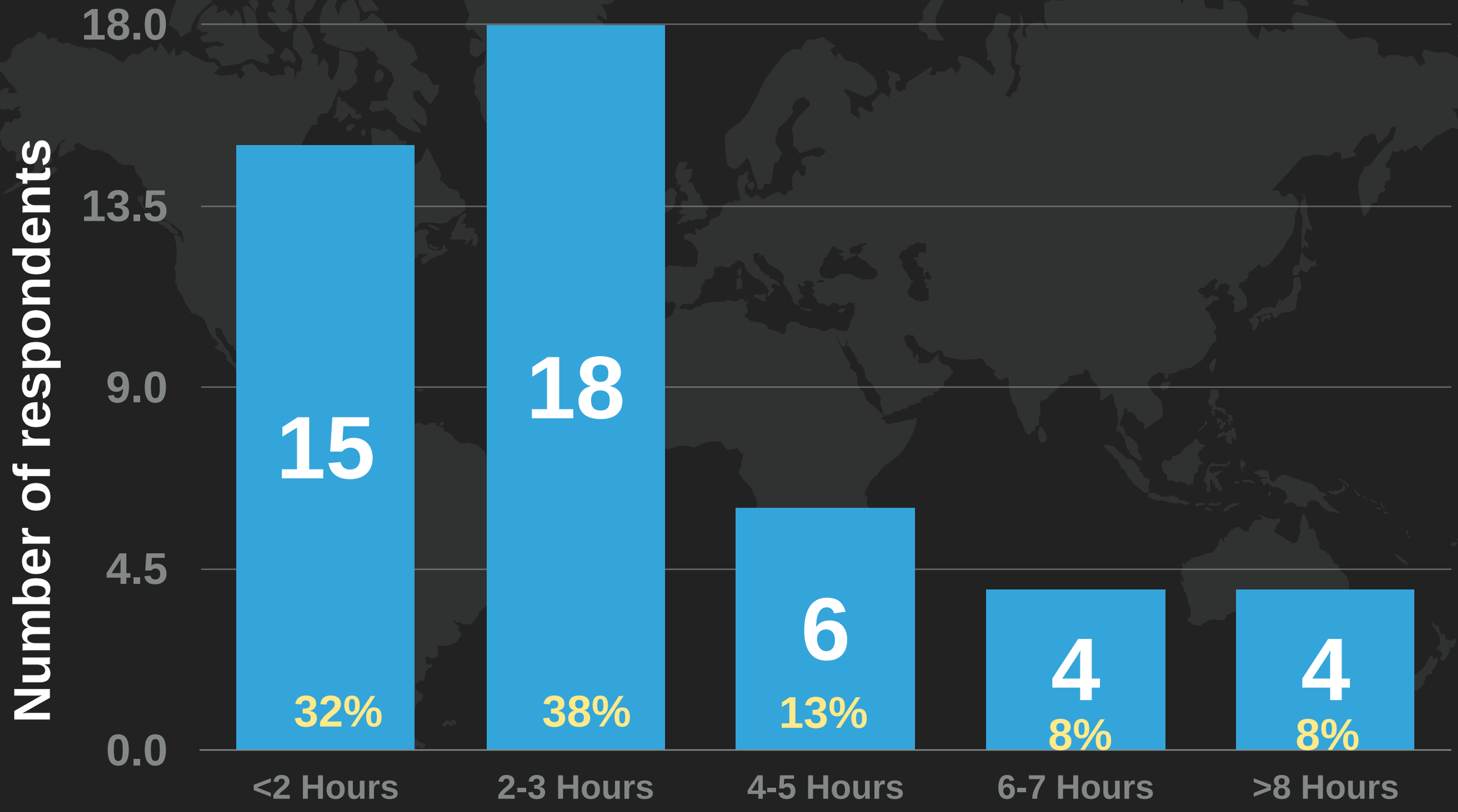

67/72 (86%) willing to have allocated time

Allocated hours per week for TEACHING

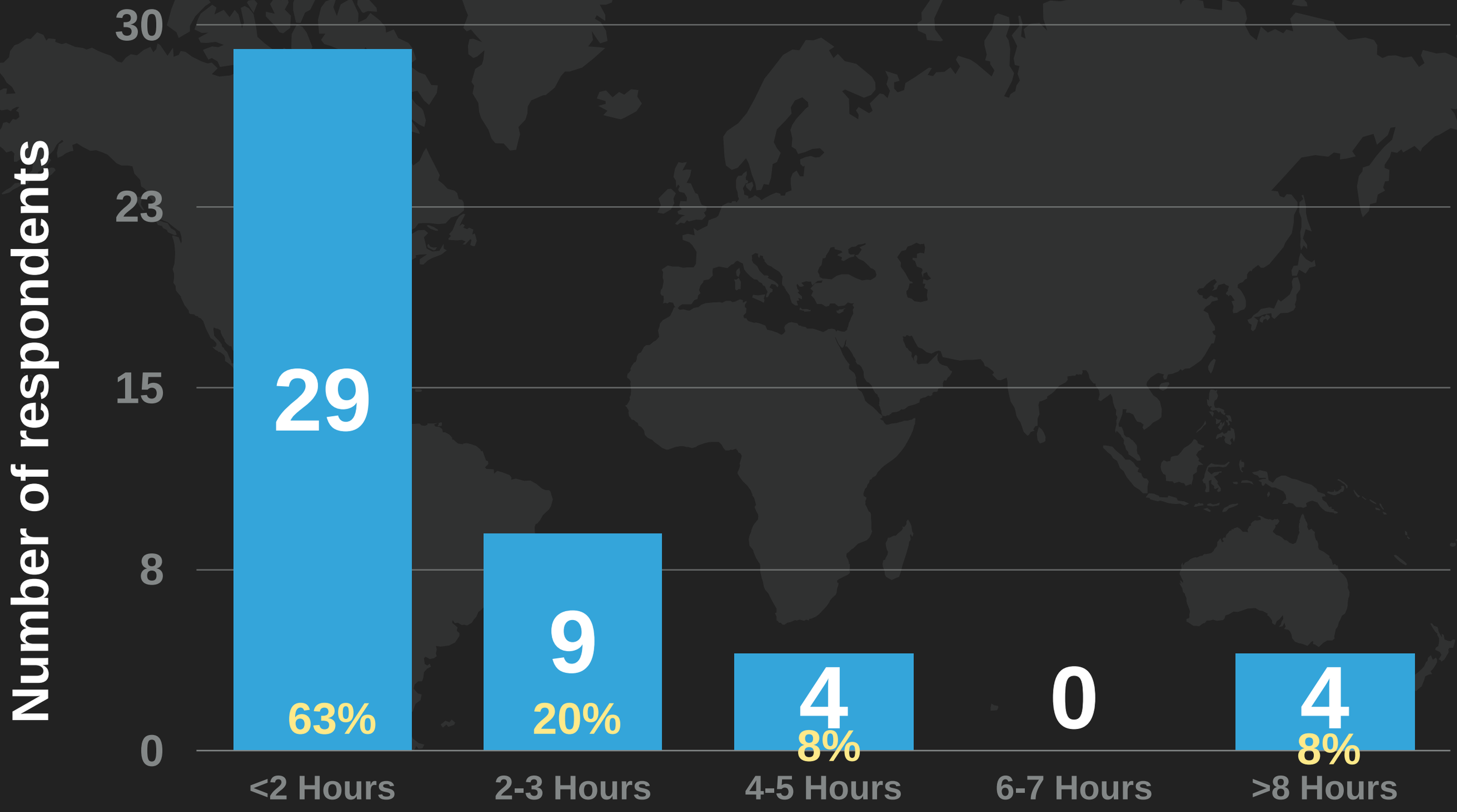

Allocated hours per week for TEACHING

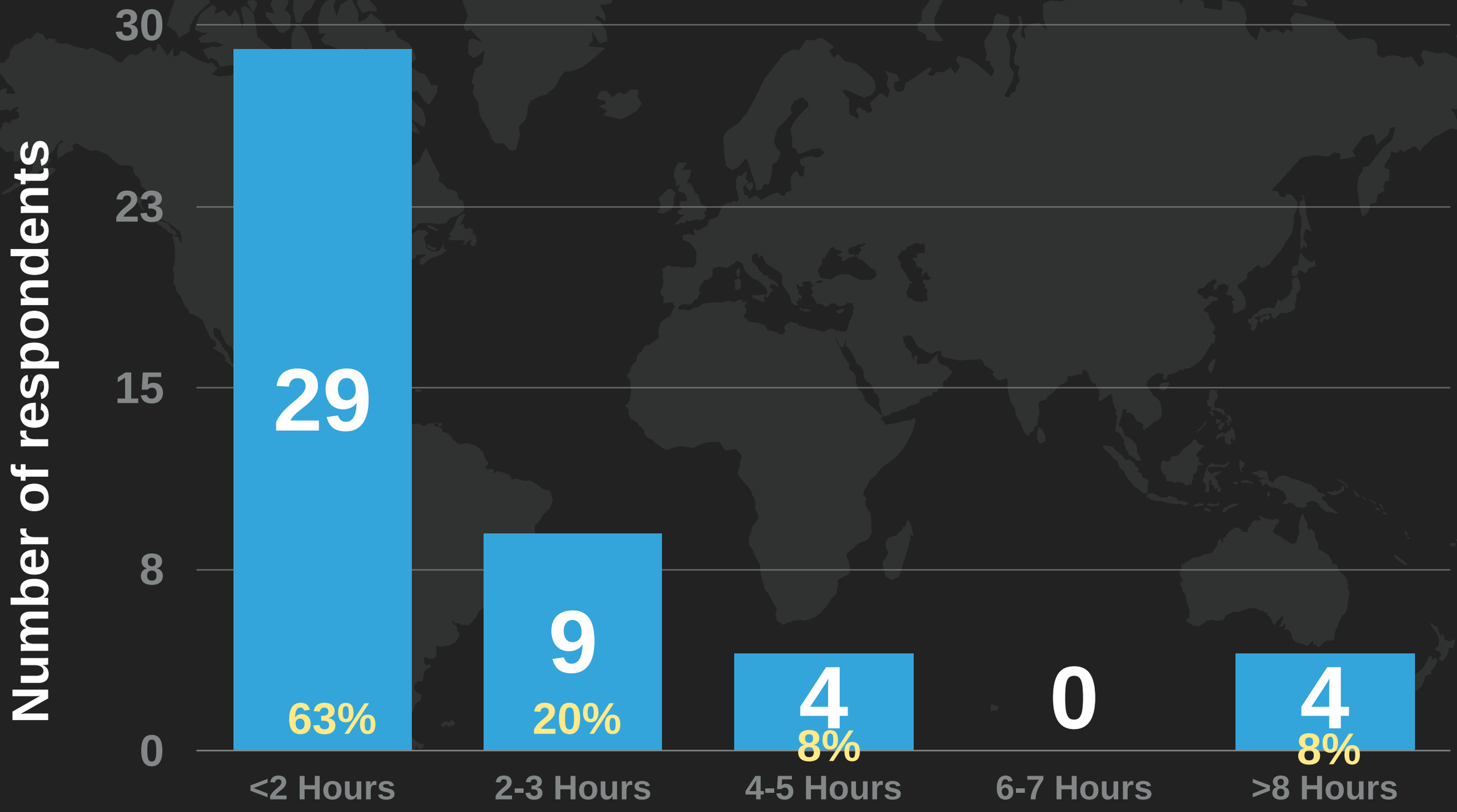

59/90 (66%) willing to have allocated time

Allocated time for research

Amount of research presented/published

p = 0.052

Research and teaching activities during training

IMPROVE CLINICAL COMPETENCY

Research: 62/94 (66%) Teaching: 70/94 (74%)

Research and teaching activities during training

SHOULD BE MANDATORY

Research: 42/94 (45%) **Teaching: 38/94 (40%)**

Publications and Poster or Paper presentation in conferences

No publication: 48/94 (51%)

Able to present poster/paper: 55/94 (59%)

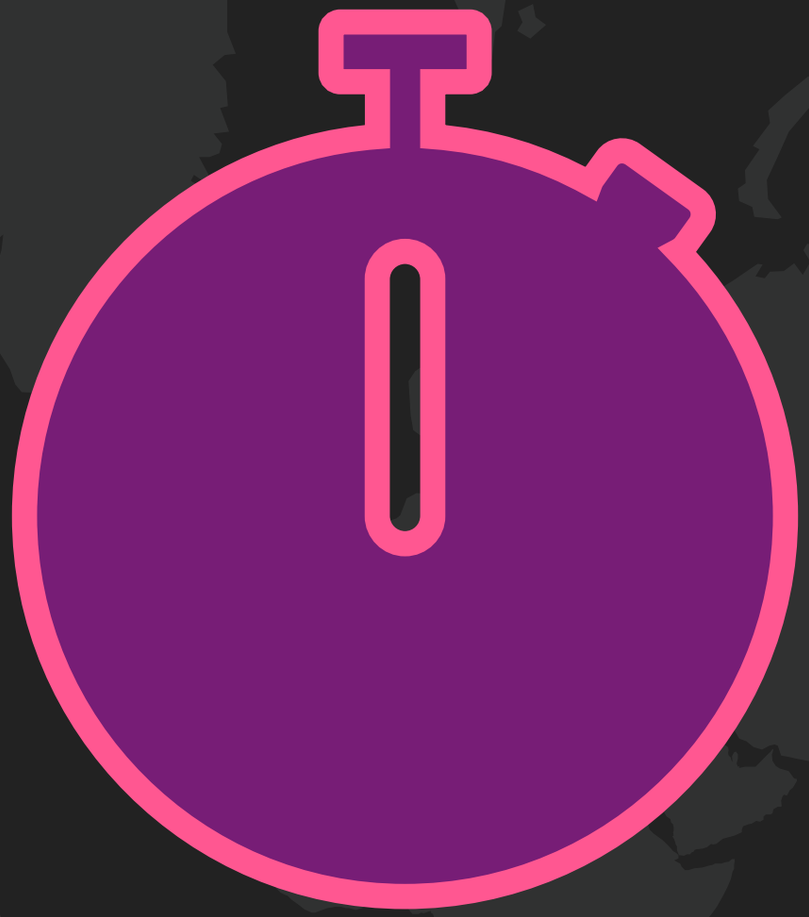

lack of TIME

56/94 (60%)

TOP CHALLENGES

lack of MENTORSHIP

41/94 (44%)

TOP CHALLENGES

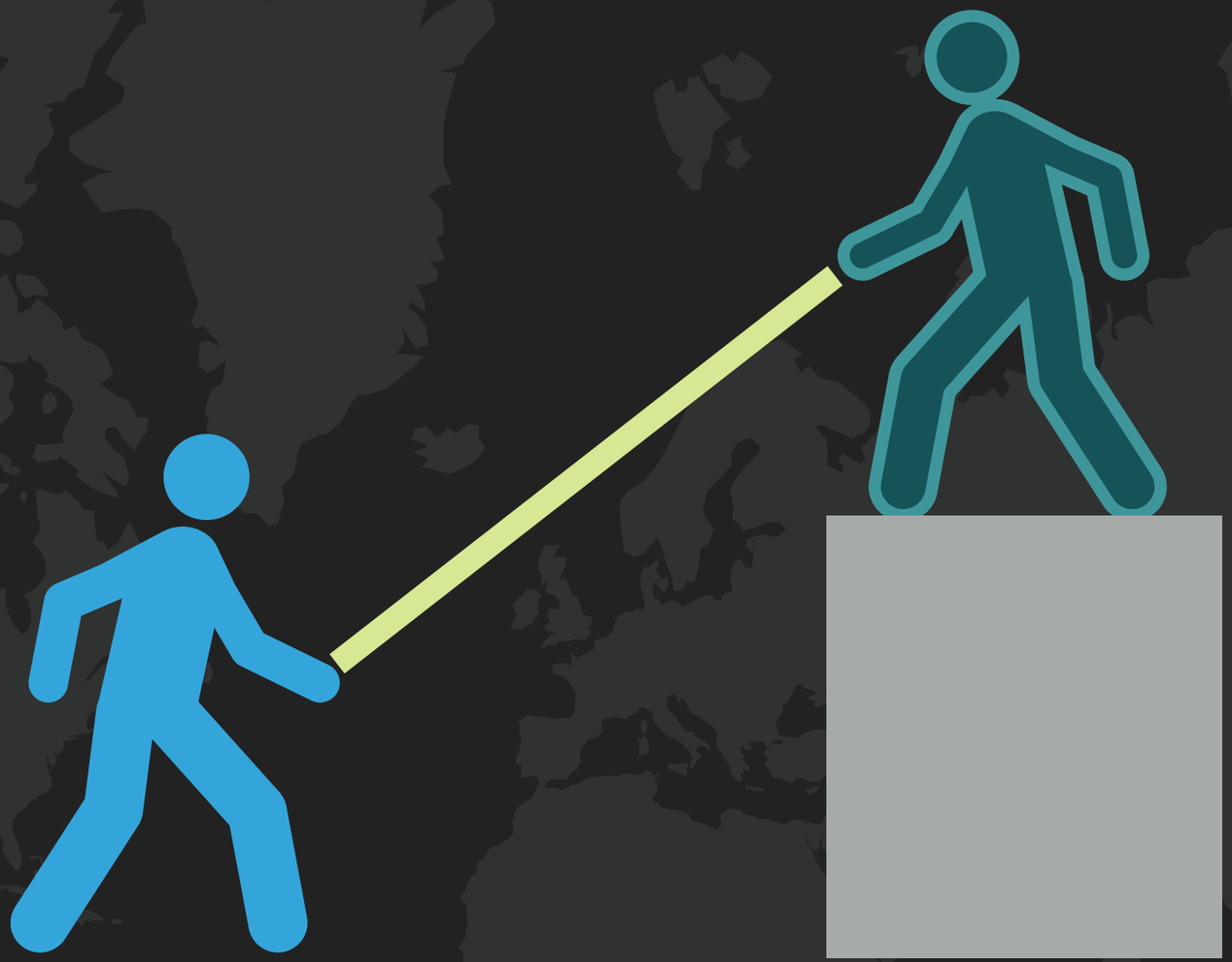

lack of SUPPORT from faculty/ senior radiologists

41/94 (44%)

TOP CHALLENGES

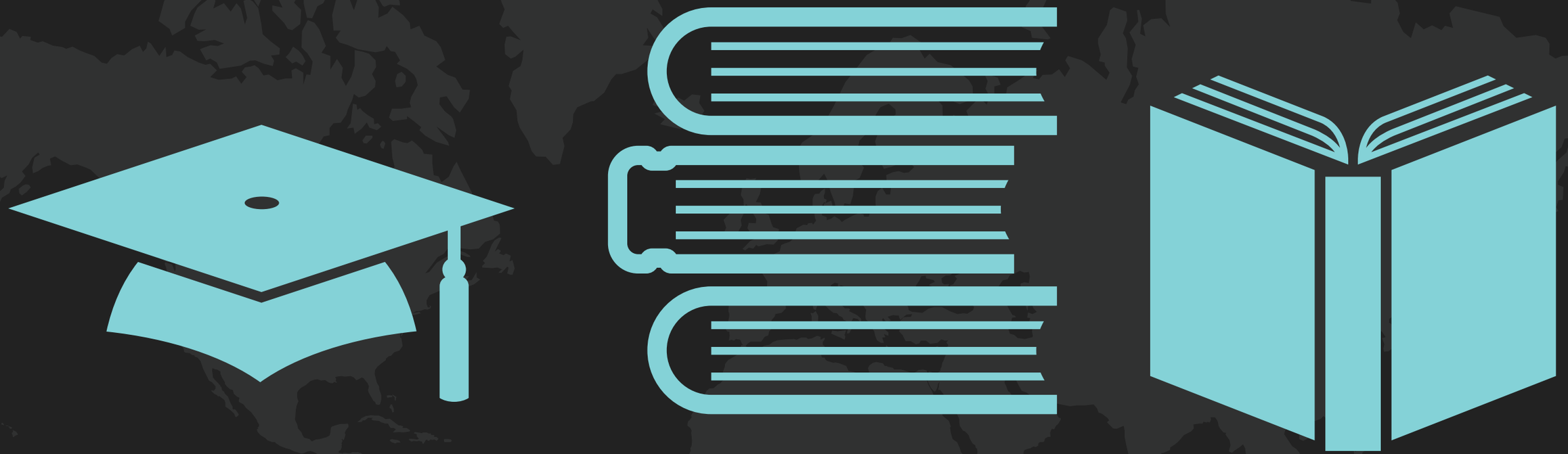

lack of teaching EXPERIENCE

32/94 (34%)

TOP CHALLENGES

51%

pediatric radiology trainees are currently involved in RESEARCH

26%

pediatric radi
are curren

3 out of 5

pediatric radiology trainees have NO allocated time in research and teaching

3 out of 5

pediatric radiology trainees think that academic activities improve clinical competency

2.5 out of 5

pediatric radiology trainees agree that academic activities should be mandatory in training

TOP CHALLENGES

IN RESEARCH AND TEACHING

TIME

MENTORSHIP

SUPPORT

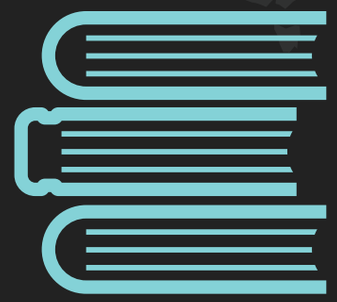

EXPERIENCE

CONCLUSION

POINTS

- **Lack of allocated time, support from faculty, mentorship and teaching experience contribute to the low involvement in academic activities of pediatric imaging trainees.**
- **Institutions and societies should give additional importance to research and teaching in training programs**
- **RESEARCH and TEACHING are keys to the continuing development of radiology**

LIMITATIONS

- **Online** distribution of survey ***(cannot assess how many trainees read the advertisement and chose to not participate and how many residents did not receive the call participation)***
- Use of **Google** survey ***(banned in some countries, hence, cohort does not accurately reflect worldwide radiology training; this was countered with the use of other social media platforms such as Facebook and Twitter)***
- Not linked to local or institutional training programs and did not assess **perceived workload** in clinical and academic parts of training
- **Limited** respondents, poor geographic distribution

REFERENCES

1. Gunderman RB, Nyce JM and Steele J. Radiologic research: The residents' perspective. *Radiology.* 2002; 223:308-310
2. Gunderman RB. Letter to the Editor: Radiologic research and residency. *Radiology*. 2003; 226(2):593
3. Hillman BJ, Fajardo LL, Witzke DB, Cardenas D, Irion M, Fulginiti JV. Factors influencing radiologists to choose research careers. *Invest Radiol.* 1989;24(11):842-8.
4. European Society of Radiology (ESR). Radiology trainees forum survey report on workplace satisfaction, ESR education, mobility and stress level. *Insights Imaging*. 2018;9(5):755-759.
5. Lam CZ, Nguyen HN, Ferguson EC. Radiology residents' satisfaction with their training and education in the United States: Effect of program directors, teaching faculty, and other factors on program success. *AJR Am J Roentgenol*. 2016;206(5):907-16.

ACKNOWLEDGMENT

RSNA-IRIYA 2017

Thank you!

MULTIFOCAL ENHANCEMENT IN FANCONI ANEMIA

A manifestation of IRIS and chronic polyoma virus infection?

Blaise V. Jones, M.D.
Neuroradiology
Cincinnati Children's Hospital Medical Center
Professor of Radiology
University of Cincinnati School of Medicine

Fanconi Anemia

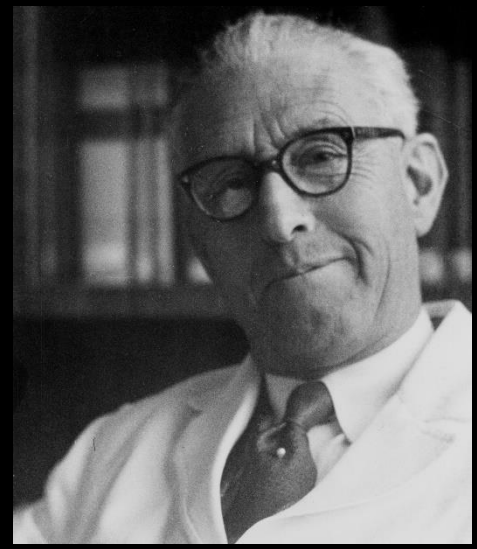

- Inherited bone marrow failure syndromes
  - Fanconi Anemia
  - Dyskeratosis congenita
  - Shwachman Diamond syndrome
  - Diamond-Blackfan anemia
  - Severe congenital neutropenia - Kostmann syndrome
  - Congenital amegakaryocytic thrombocytopenia
- Mutation in genes involved in DNA repair
- Increased risk of malignancy – viral associated
  - 1000x increased risk of HNSCC
    - 84% associated with HPV
- Immune dysfunction
  - Decrease in B and NK cells
  - Reduced function of cytoxic T cells and NK cells

Polyoma viruses

- 77 recognized polyoma virus species
- 13 are known to infect humans
- ~80% of the adult population is seropositive
- 2 known to cause pathology in immunocompromised
  - BK virus: hemorrhagic cystitis and nephropathy
    - exposure typically occurs by 3-4 years of age
  - JC virus: progressive multifocal leukoencephalopathy (PML)
    - exposure typically occurs by 10-14 years of age

Progressive multifocal leukoencephalopathy
PML

- Infection with JC virus
- Multifocal brain lesions in immunocompromised
  - T2/FLAIR abnl signal
  - Minimal enhancement
  - No calcification
- Progressive
  - 6 month avg survival after diagnosis
- No effective therapy in the face of a compromised immune system

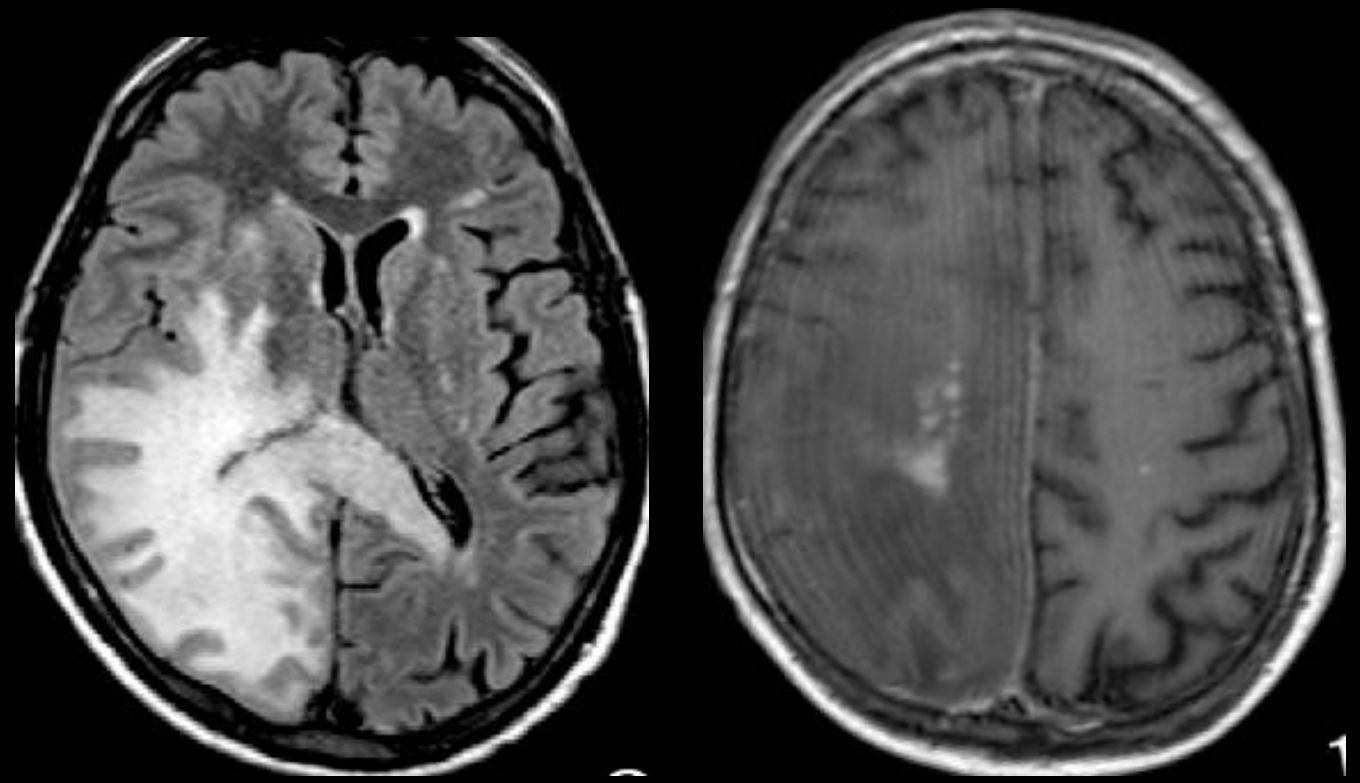

Immune Reconstitution Inflammatory Syndrome (IRIS)

- Clinical worsening of symptoms in patients with opportunistic infections due to recovery of the immune system
- Increased inflammatory (T cell) response with edema
  - HIV with PML
    - tx'd with HAART with recovery of immune fxn
    - Increased inflammation around PML
  - MS tx'd with natalizumab who develop PML
    - Increased inflammation with cessation of therapy and recovery of immune fxn
- Response to steroid therapy

Case 1

- 20 yo ♀ with Fanconi anemia treated with BMT at age 10
- Presents to ED with numbness in her right arm, hip and tongue lasting for 20 minutes
- MR demonstrates multiple small enhancing foci throughout the brain, concentrated in the posterior fossa
- Declined further evaluation; discharged and lost to follow up

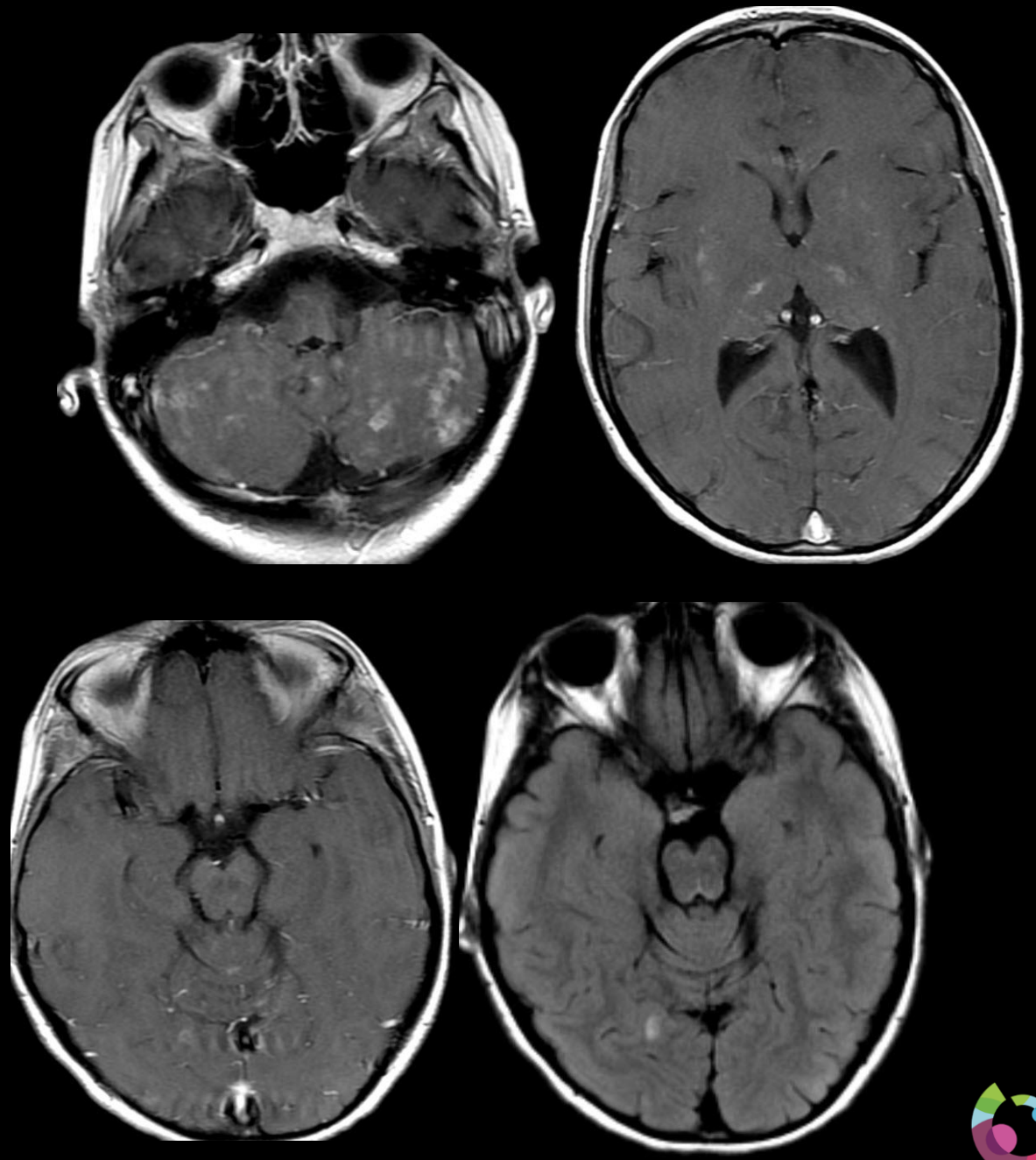

2 years later

sudden onset of left sided hemianopsia

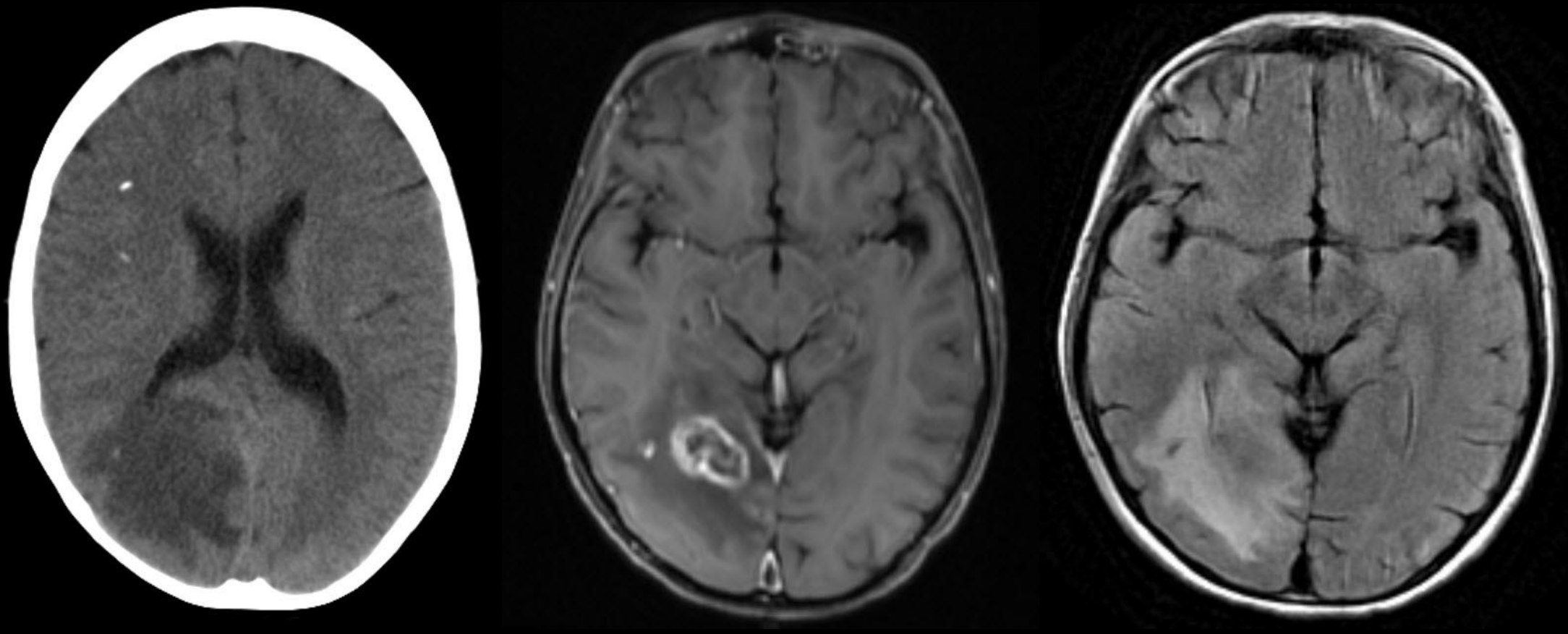

Surgical excisional biopsy

- Path
  - necroinflammatory process
  - necrosis, gliosis, scattered macrophages
  - negative for bacteria/fungus/EBV/CMV
- (+) for polyoma antigens*
  - Includes BK and JC virus
- (-) for BK virus**

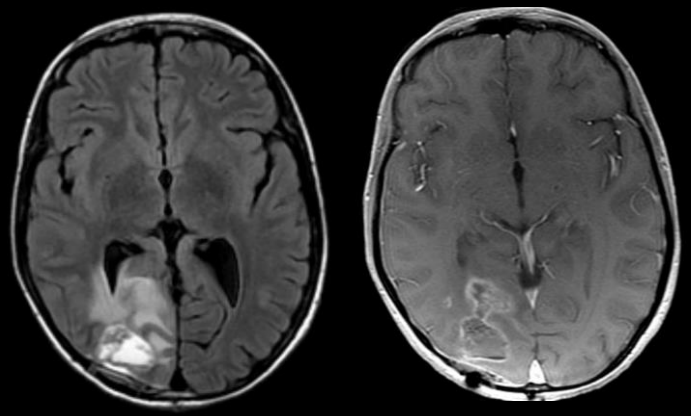

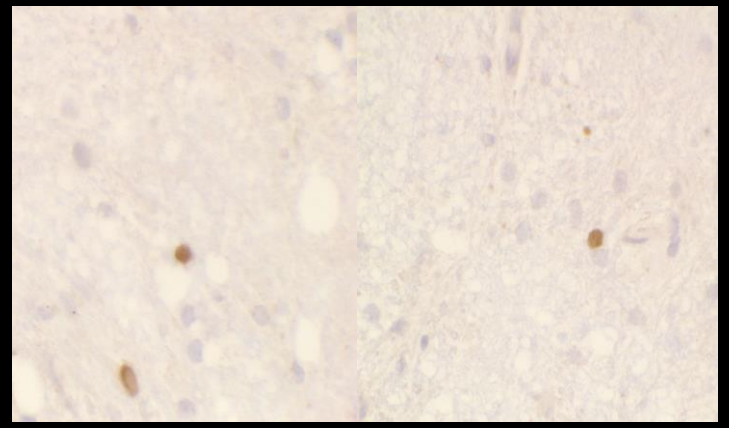

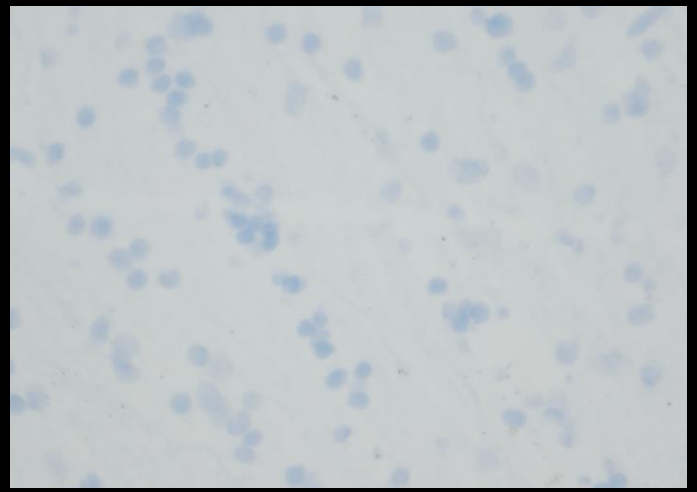

*University of Florida

**Fausto Rodriquez, Johns Hopkins University

Case 2

- 20 yo ♂ with Fanconi anemia (no BMT) who developed transient L hemiplegia after a fall

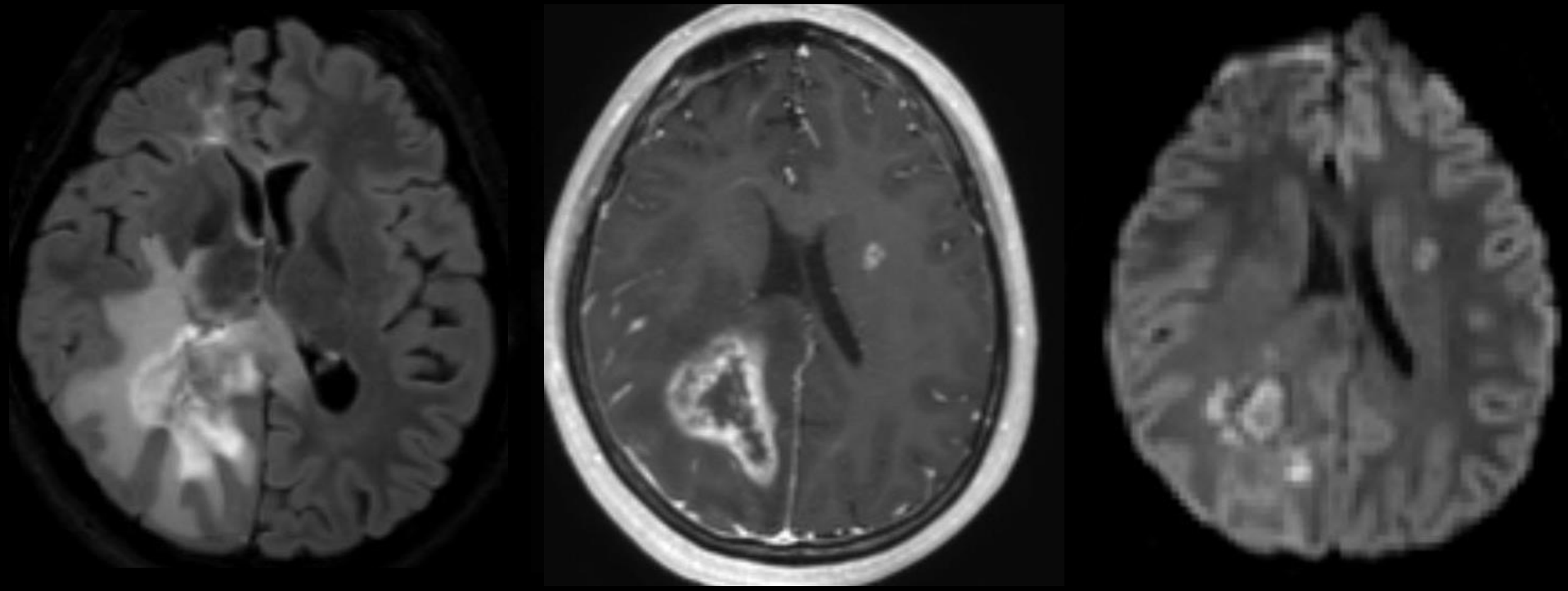

Surgical excisional biopsy

- Path
  - necroinflammatory process
  - necrosis, gliosis, scattered macrophages
  - negative for bacteria/fungus/EBV/CMV
- (+) for polyoma antigens*
  - Includes BK and JC virus
- (-) for BK virus**

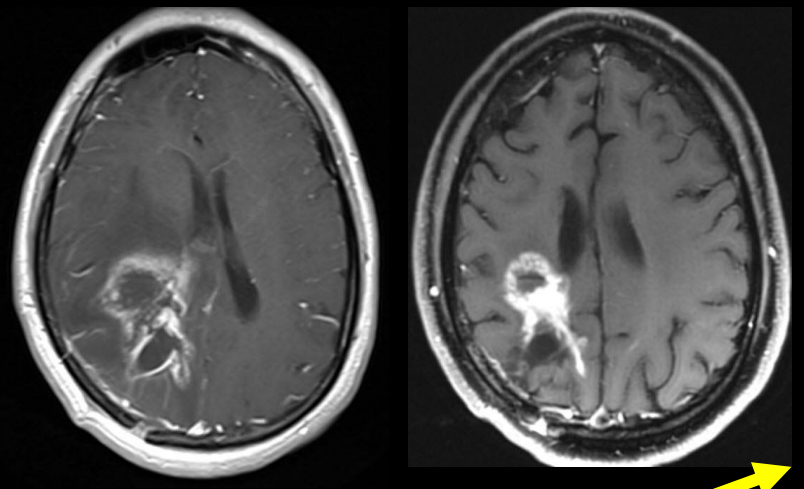

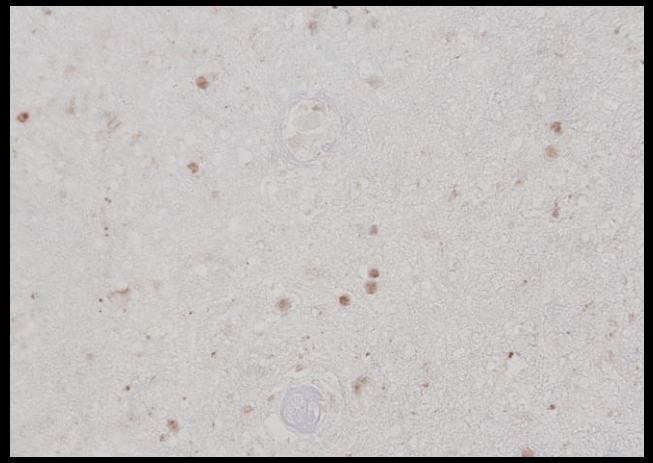

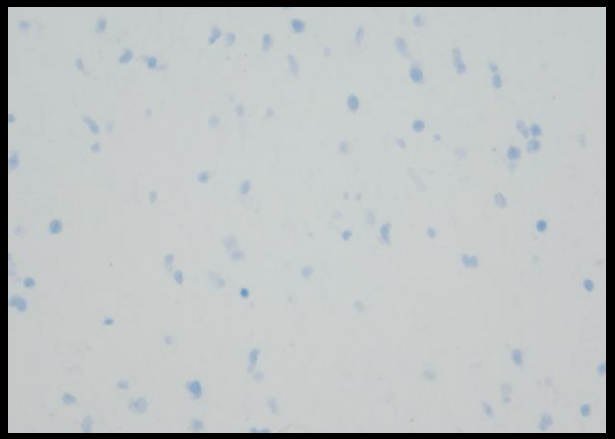

*University of Florida

**Fausto Rodriquez, Johns Hopkins University

Database search

- MR/CT on 41 patients with FA
  - 8 with normal brain studies
  - 22 with other abnormalities
    - PRES, infarct
  - 5 with some similar findings, but other diagnoses
    - Toxo, CMV
  - 6 with characteristic imaging findings
    - 4 with serologic confirmation of JC exposure
      - 2 with biopsy confirmation
    - 2 of 6 not tested yet

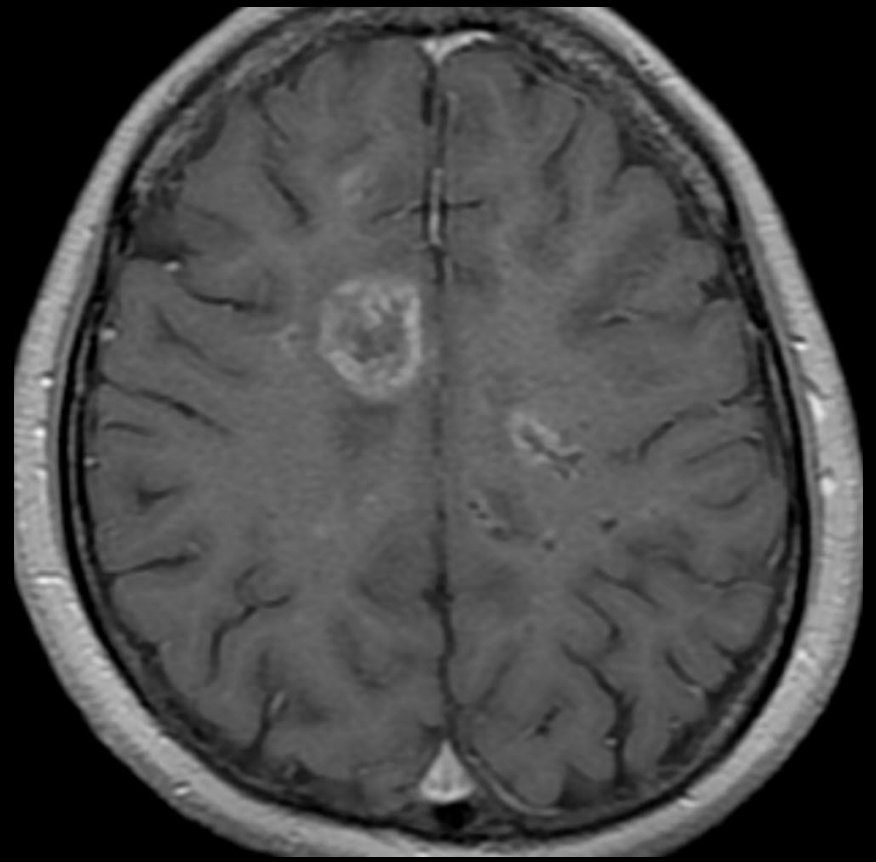

Characteristic Imaging Features

- Multiple small enhancing lesions
  - Ring enhancement
  - Little or no surrounding edema
  - Frequent cerebellar and brainstem involvement (6/6)
- Calcifications
  - Associated with many (but not all) enhancing lesions (6/6)
- Dominant mass with edema (3/6)
- 2 patients had spine imaging
  - Waxing and waning cord lesions

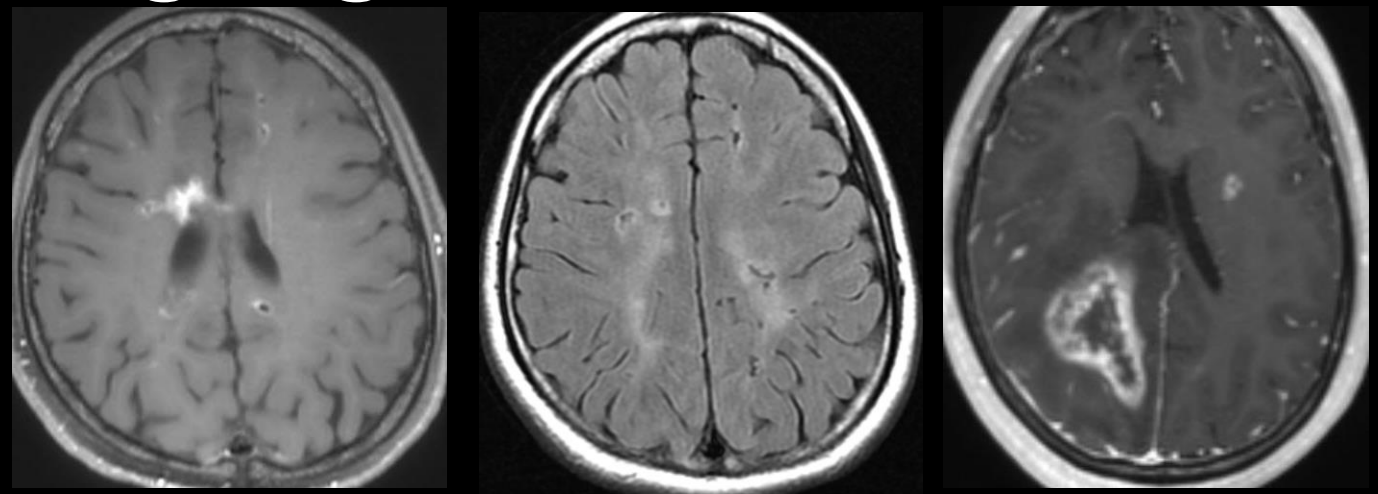

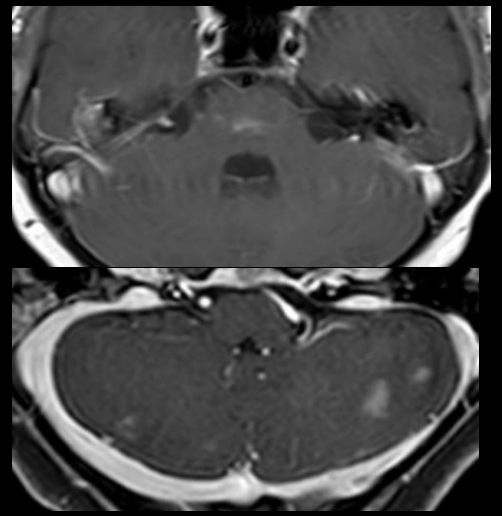

Summary of observations

- 6/41 (15%) FA patients have an unusual pattern of calcifying and enhancing brain lesions
  - 2 with spine imaging also have subtle spinal cord lesions
- 3 have developed mass-like lesions with necrosis
  - Biopsies in 2 have confirmed presence of JC virus in lesions
- Enhancement and edema respond to steroid therapy

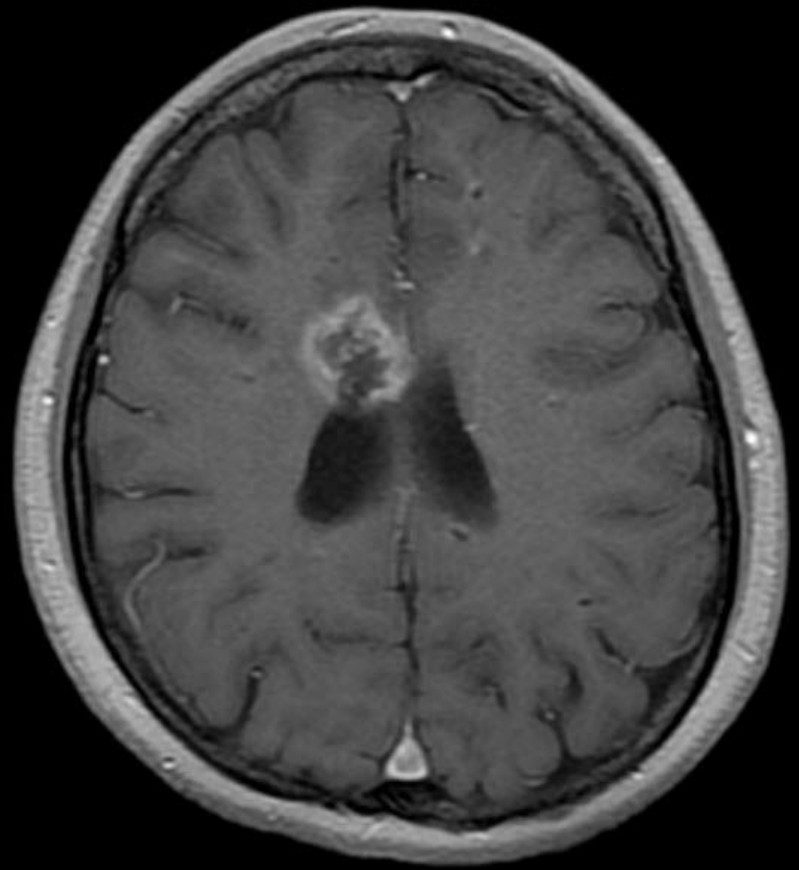

Conclusions - Hypothesis

- Increased longevity = more FA patients with JC infection
- JC infection is pathologic in FA
  - Multifocal inflammatory lesions
  - ~~Immune system dysfunction?~~
  - Hampered DNA repair
- BMT normalizes immune system function
  - DNA repair in brain cells is still hampered
    - Viral infection remains pathologic
  - May cause IRIS in response to these lesions
  - Necrotic mass lesion – not PML
    - Responsive to steroid therapy

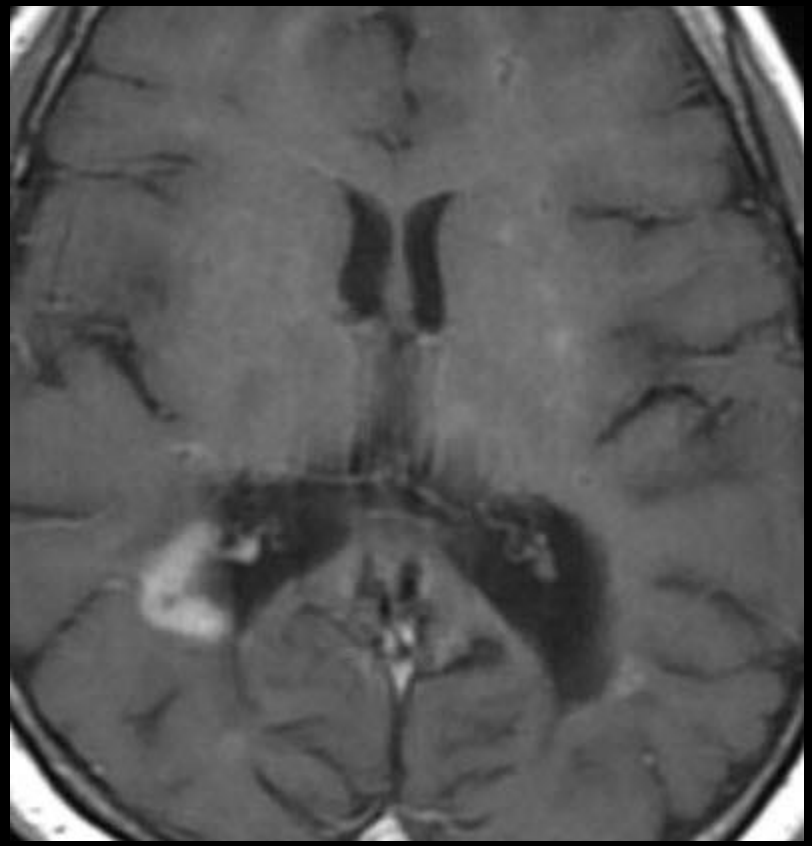

Conclusions

- FA patients are uniquely susceptible to JC virus infection
  - Because of DNA repair defects
- FA patients should be monitored for JC infection with brain MR imaging
  - Small enhancing lesions with Ca++
  - Posterior fossa, spinal cord
- Restoration of immune function with BMT does not decrease risk
  - May cause IRIS with large necrotic lesions

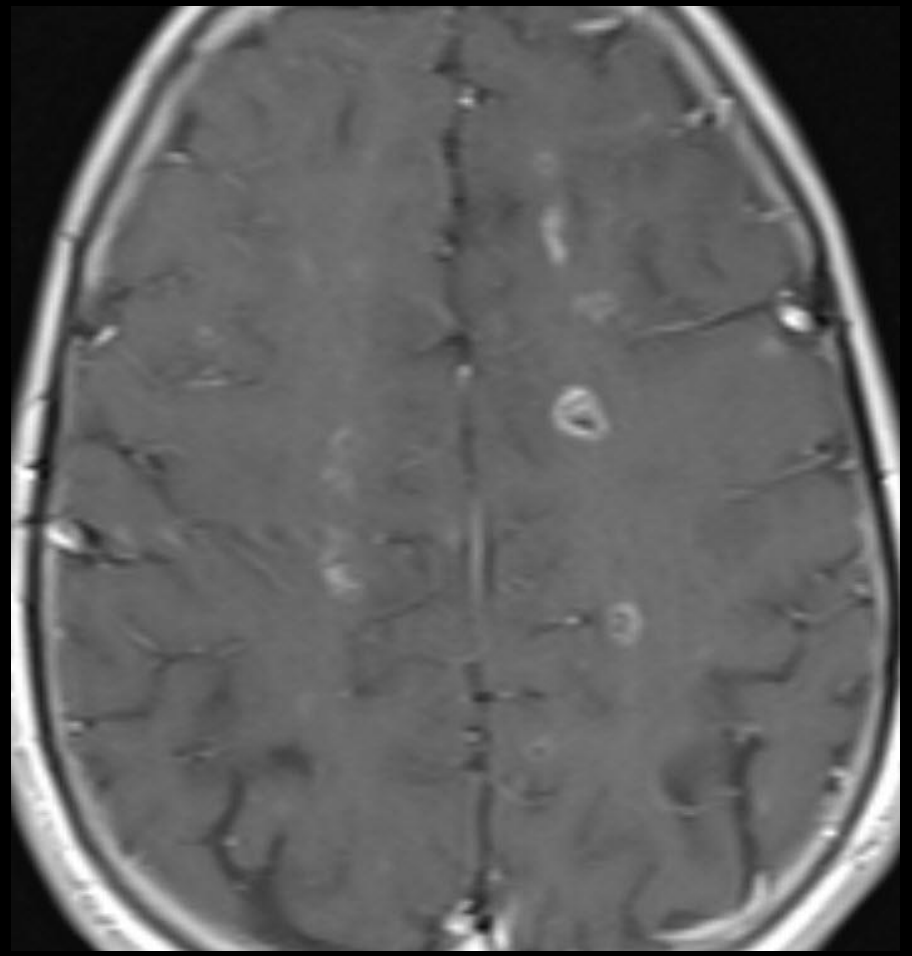

Applying the updated PRETEXT system in staging of hepatoblastoma in children: Key images to remember them

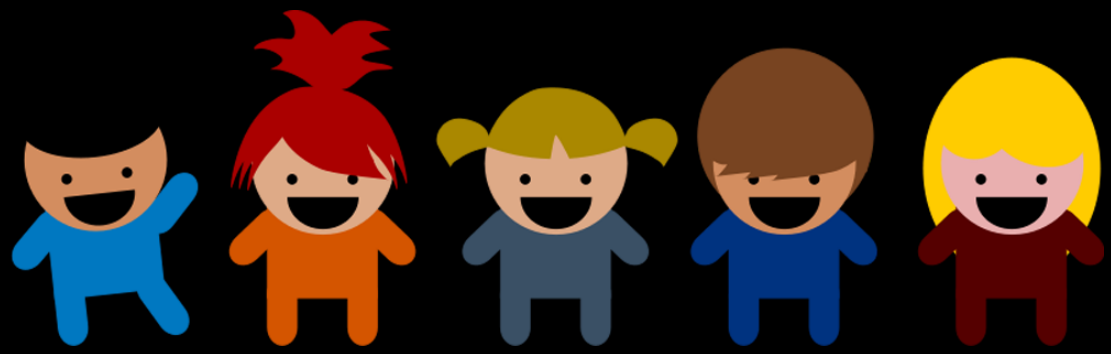

JISUN HWANG [1], M.D.

HEE MANG YOON[2], AH YOUNG JUNG[2], YOUNG AH CHO[2], JIN SEONG LEE[2]

[1] DEPARTMENT OF RADIOLOLOGY, DONGTAN SACRED HEART HOSPITAL, SOUTH KOREA

[2] DEPARTMENT OF RADIOLOLOGY, ASAN MEDICAL CENTER, SOUTH KOREA

- Learning objectives -

- To review the definitions of PRETEXT groups and annotation factors in 2017 PRETEXT system for pediatric hepatoblastoma
- To review typical CT and MRI images of PRETEXT groups and annotation factors
- To learn confusing scenarios for staging hepatoblastoma by sample cases

- OVERVIEW -

Introduction

- Clinical importance of PRETEXT system
- The background of updates to the PRETEXT system

PRETEXT groups

- Definitions and sample cases with positive findings

Annotation factors (V,P,E,F,R,C,N,M)

- Definitions and sample cases with positive findings

The background of updates to the PRETEXT system

- PRETEXT system is used to describe tumor extent before any therapy and stratify risk for treatment planning.

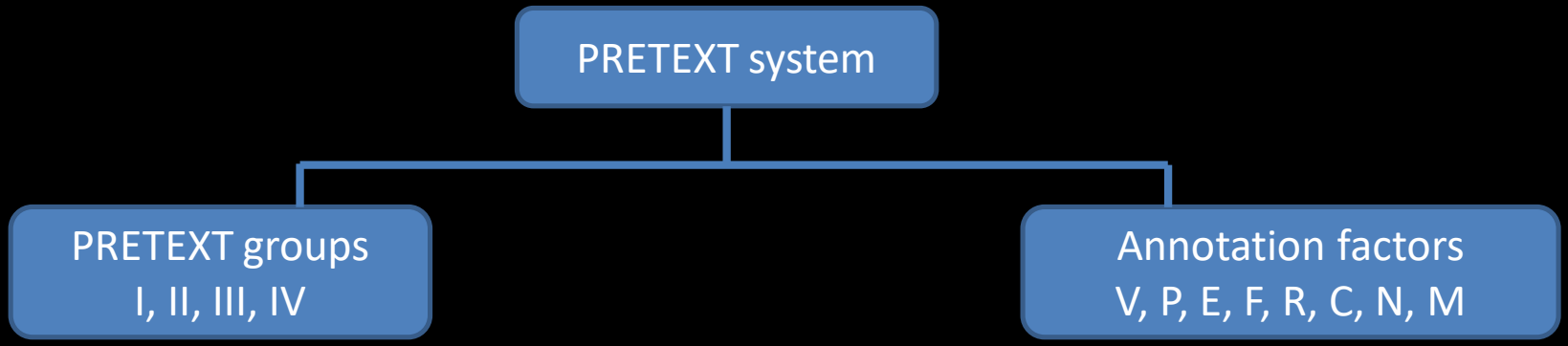

- After SIOPEL (the International Childhood Liver Tumor Strategy Group) first described the original PRETEXT system in 1990, disparate definitions and staging systems have been used by multicenter trial groups.
  - SIOPEL, the German Society for Pediatric Oncology and Hematology, and the Japanese Study Group for Pediatric Liver Tumors

- The **updated 2017 PRETEXT system** aimed to clarify and unite definitions for its use in future collaborative trial (*Pediatric Radiology* (2018) 48:536–554).

The clinical importance of the PRETEXT system

- Many studies have found poor prognostic factors such as low AFP level , advanced PRETEXT group, and distant metastases.
  - (*Journal of clinical oncology* 2005, 23, 1245-1252)(*Pediatric blood & cancer* 2009, 53, 1016-1022) (*European journal of cancer* 2012, 48, 1543-1549) (*Cancer* 2002, 95, 172-182)

- The **2017 PRETEXT** is part of the new international Hepatoblastoma Stratification system developed by the Children's Hepatic tumors International Collaboration consortium (**CHIC-HS**).

- The CHIC consortium have created **CHIC-HS**, a risk stratification tree model, from the largest dataset assembled from prior multicenter trial groups.

- All the clinical and imaging variables used in CHIC-HS were found to be associated with patient outcome.
  - Age (≤ 2, 3-7, ≥ 8), serum AFP (<100, 100-999, 1000-10^6, > 10^6)
  - PRETEXT groups, all annotation factors except C and N
  - C and N were not evaluated

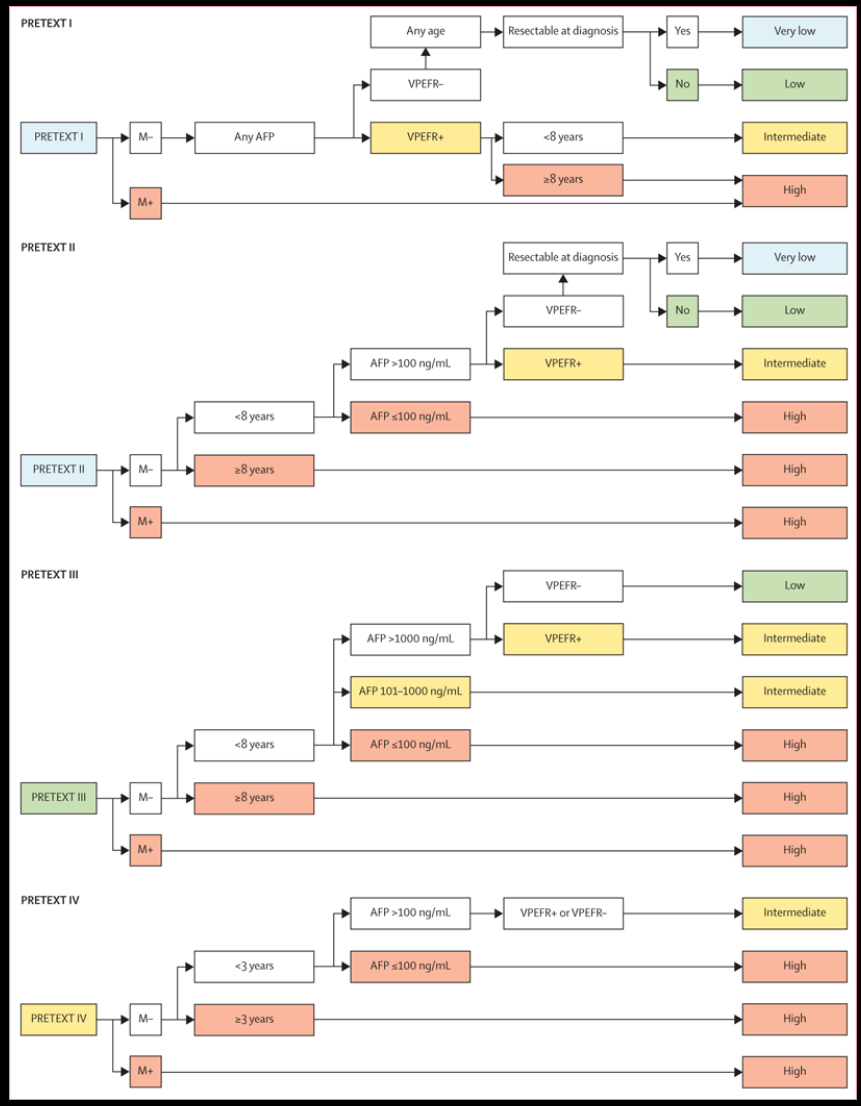

Lancet Oncol. 2017 January ; 18(1): 122–131

Part I. PRETEXT groups

- The PRETEXT group (I, II, III or IV) is based on determining the number of contiguous tumor-free liver sections
- Advanced PRETEXT group is one of the traditional poor prognostic factors in hepatoblastoma
  - - (*Journal of clinical oncology* 2005, 23, 1245-1252)(*Pediatric blood & cancer* 2009, 53, 1016-1022)

PRETEXT groups

- **PRETEXT group 1**

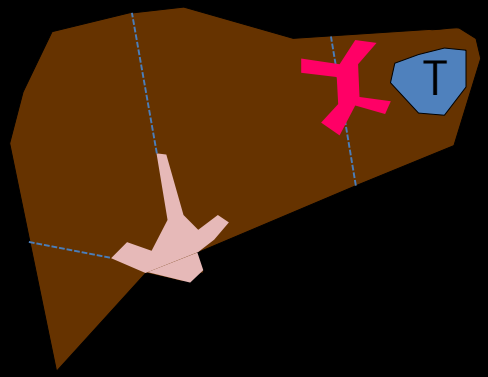

- Uncommon and are typically small
- Three contiguous hepatic sections must be free of tumor. Therefore, PRETEXT I tumors can only involve either the left lateral or right posterior section

6months/M. A heterogeneous enhancing mass involving only left lateral segment of liver. Right lobe, left medial segment, and caudate lobe are free from tumor.

PRETEXT groups

- **PRETEXT group 2**

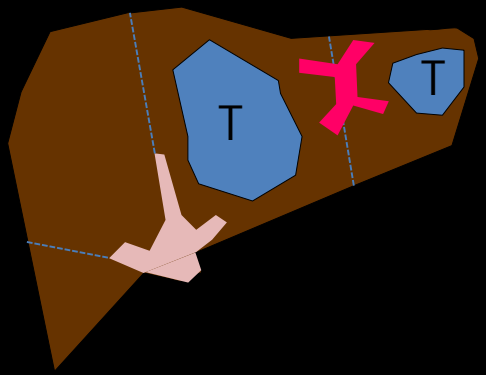

- Two contiguous hepatic sections must be free of tumor
- Limited either to the right lobe or the left lobe of the liver
- They can involve either one or two sections of the liver

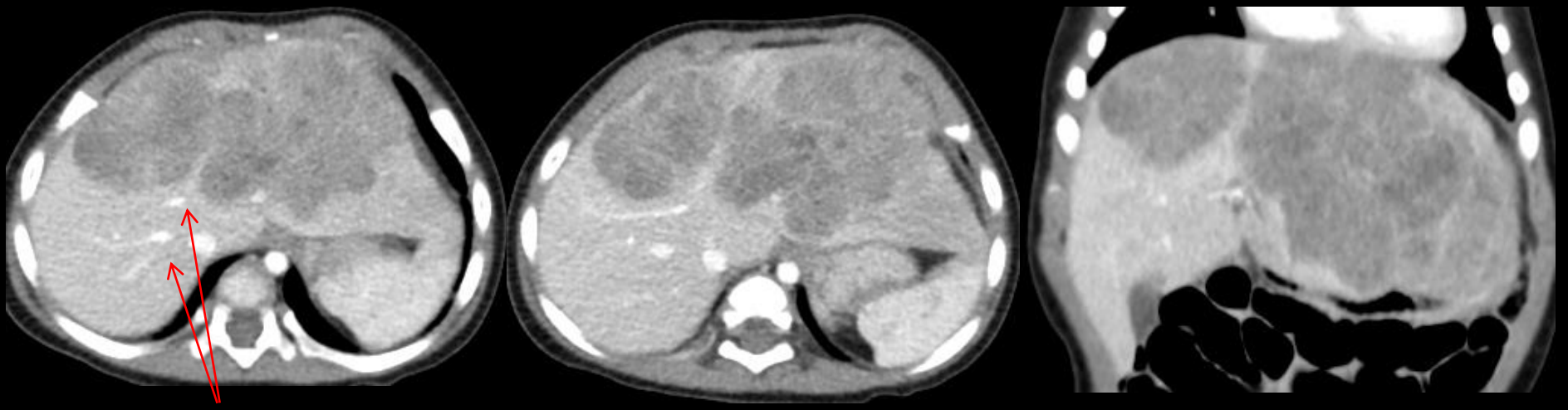

Right and middle HV

6months/F. A heterogeneous enhancing mass involving left medial and lateral segment of liver. Two contiguous hepatic sections are free from tumor.

PRETEXT groups

- **PRETEXT group3**

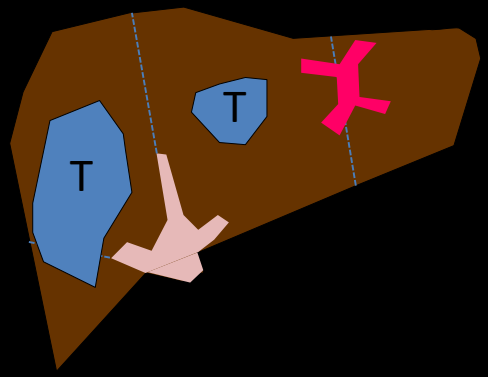

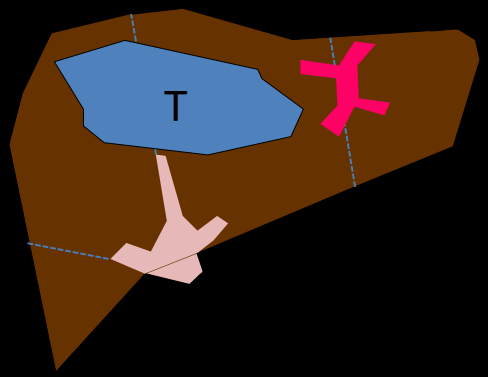

- One hepatic section must be free of tumor
- Central tumors that involve only the left medial and right anterior sections result in only one contiguous tumor-free section and are considered PRETEXT III

2/M. Multiple heterogeneous enhancing masses involving right anterior and posterior sections of liver. A small daughter nodule (arrow) is seen just medial to middle hepatic vein. Therefore, only one hepatic section is free from tumor.

PRETEXT groups

- **PRETEXT group 4**

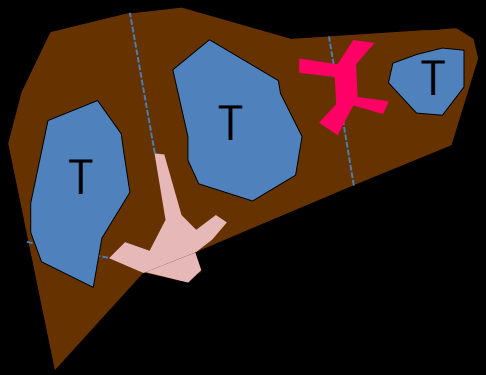

- Tumor affects all four hepatic sections
- Almost always multifocal or infiltrative tumor

1/F. A lobulating enhancing masses involving all four hepatic sections. Mass shows punctate calcifications and necrotic areas.

Part II. Annotation factors

	Annotation factors
V	Hepatic venous/IVC involvement
P	Portal venous involvement
E	Extrahepatic tumor extension
F	Multifocality
R	Tumor rupture
C	Caudate lobe
N	Lymph node metastasis
M	Distant metastasis

Hepatic venous/IVC involvement (V)

- Difference between the definitions used in the most recent SIOPEL and COG trials centers on the definitions of various degrees of vascular involvement

	SIOPEL	COG
Vascular Involvement	Completely obstructed or circumferentially encased, or findings of tumor invasion	Within 1 cm of the vessel, abutted or compressed vessels were also said to have some degree of vascular involvement
V-status	V1,V2,V3 → Number of obstructed, encased or invaded veins	Positive = If all three HV or IVC met one of the following criteria V0 – tumor within 1 cm of vessel V1 – tumor abutting vessel V2 – tumor compressing vessel V3 – intravascular tumor thrombus

Hepatic venous/IVC involvement (V)

- To address these differences, a consensus definition was created that includes information from both the SIOPEL and COG approaches

  ➔ **V-status: either V-negative or V-positive**

  ~~V 1~~, ~~V 2~~

- One of the following criteria : V (+)

1. Tumor obliterates or encases **all three HV** or the **intrahepatic IVC**
2. Tumor thrombus in **any HV** or the **intrahepatic IVC**

- Obliterates mean that the lumen is no longer visible
- Encasement by tumor means more than 50% or 180°
- "HV" definition: between the confluence of the three HV at IVC and the most central major branch of HV

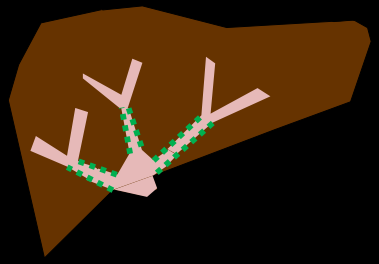

Right HV (only) obliteration → V(-)

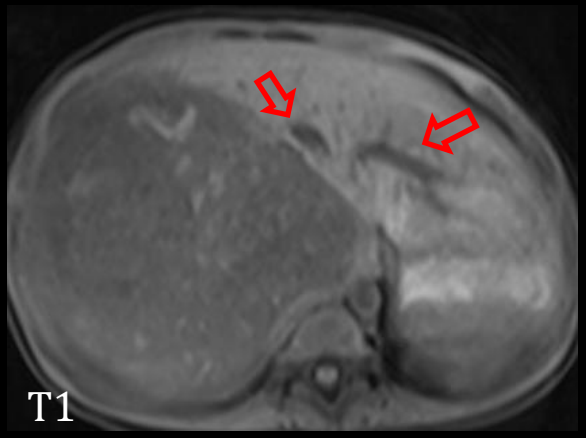

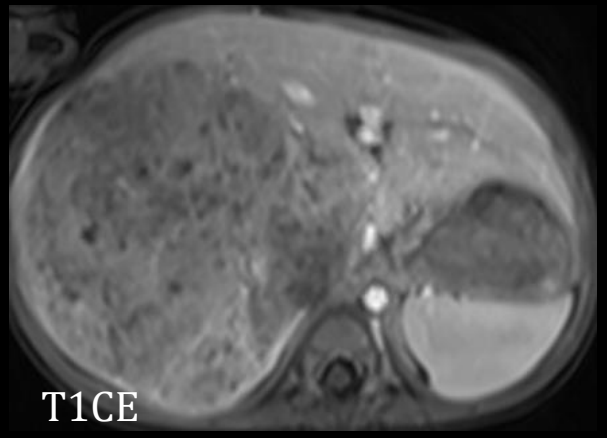

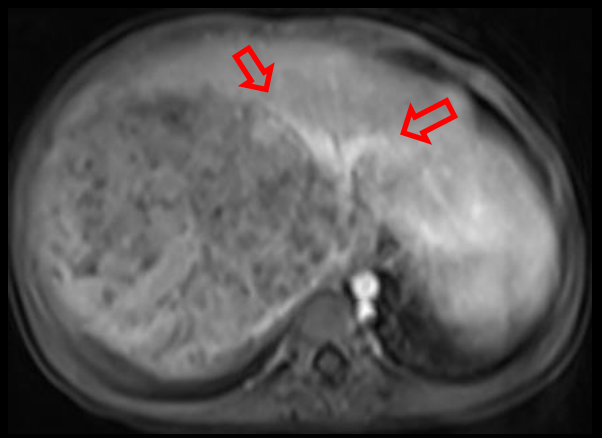

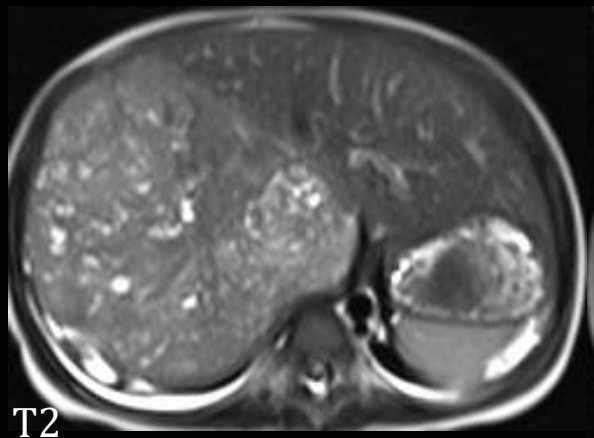

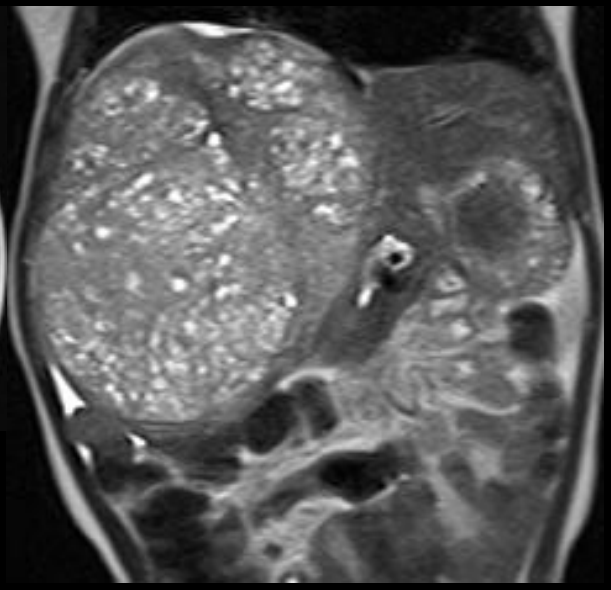

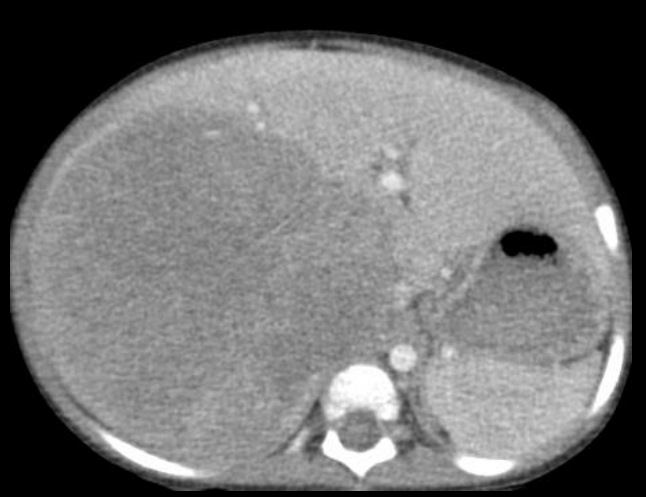

1/M. Large heterogeneous enhancing masses involving right anterior and posterior sections of liver (PRETEXT II). Right HV is obliterated due to tumor and not seen. Middle and left HV are intact (arrows). Tumor shows numerous necrotic portions.
For V (+), all three hepatic veins must be obliterated.

Middle and left HV encasement → V(-)

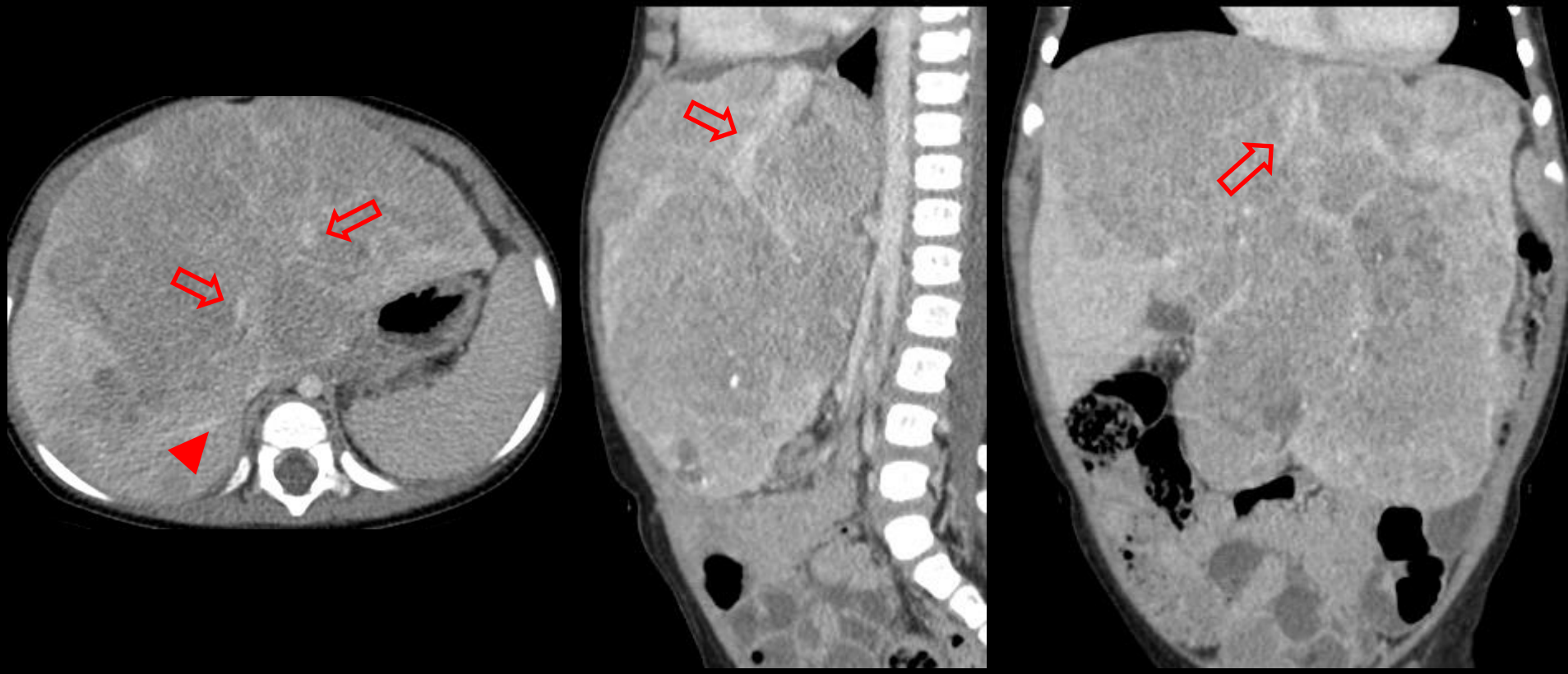

1/F. PRETEXT IV. Tumor encases both middle and left HV (arrows). In this case, annotation factor V is considered as negative. Because right HV is free from tumor (arrowhead). For V (+), all three hepatic veins must be involved.

IVC thrombus → V(+)

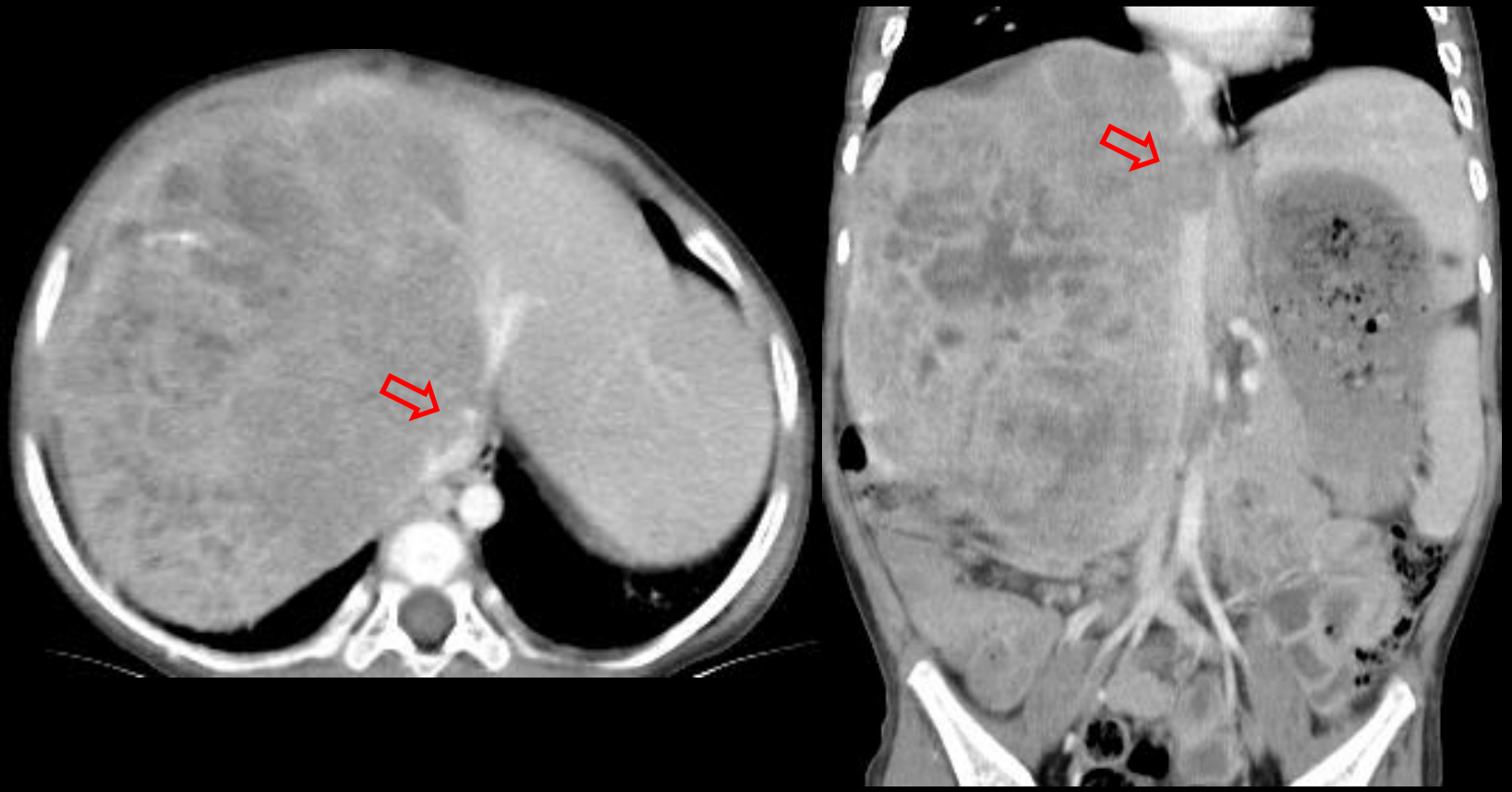

1/M. PRETEXT II. Tumor thrombus (arrow) is seen in the lumen of intrahepatic IVC. Right HV is obliterated and middle HV is encased by tumor.

Portal venous involvement (P)

- Difference between the definitions used in the most recent SIOPEL and COG trials centers on the definitions of various degrees of vascular involvement

	SIOPEL	COG
Vascular Involvement	Completely obstructed or circumferentially encased, or findings of tumor invasion	Within 1 cm of the vessel, abutted or compressed vessels were also said to have some degree of vascular involvement
P-status	P1,P2 → Number of obstructed, encased or invaded veins	Positive = If both the right and left PV, or main PV met one of the following criteria P0 – tumor within 1 cm of vessel P1 – tumor abutting vessel P2 – tumor compressing vessel P3 – intravascular tumor thrombus

Portal venous involvement (P)

- P-status has been simplified in the new international collaborative 2017 PRETEXT definitions

  ➔ **V-status: either P-negative or P-positive**

  ~~P 1, P 2~~

- One of the following criteria : P (+)

1. Tumor obliterates or encases **either both PV** or the **main PV**
2. Tumor thrombus in **either or both the right and left PV**
3. Tumor thrombus in the **main PV**

- Obliterates mean that the lumen is no longer visible
- Encasement by tumor means more than 50% or 180°
- "PV" definition : extending from the bifurcation of the main PV to the first major branch of the vein

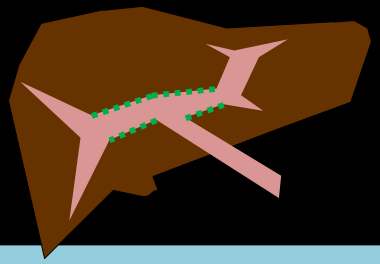

Main PV obliteration → P (+)

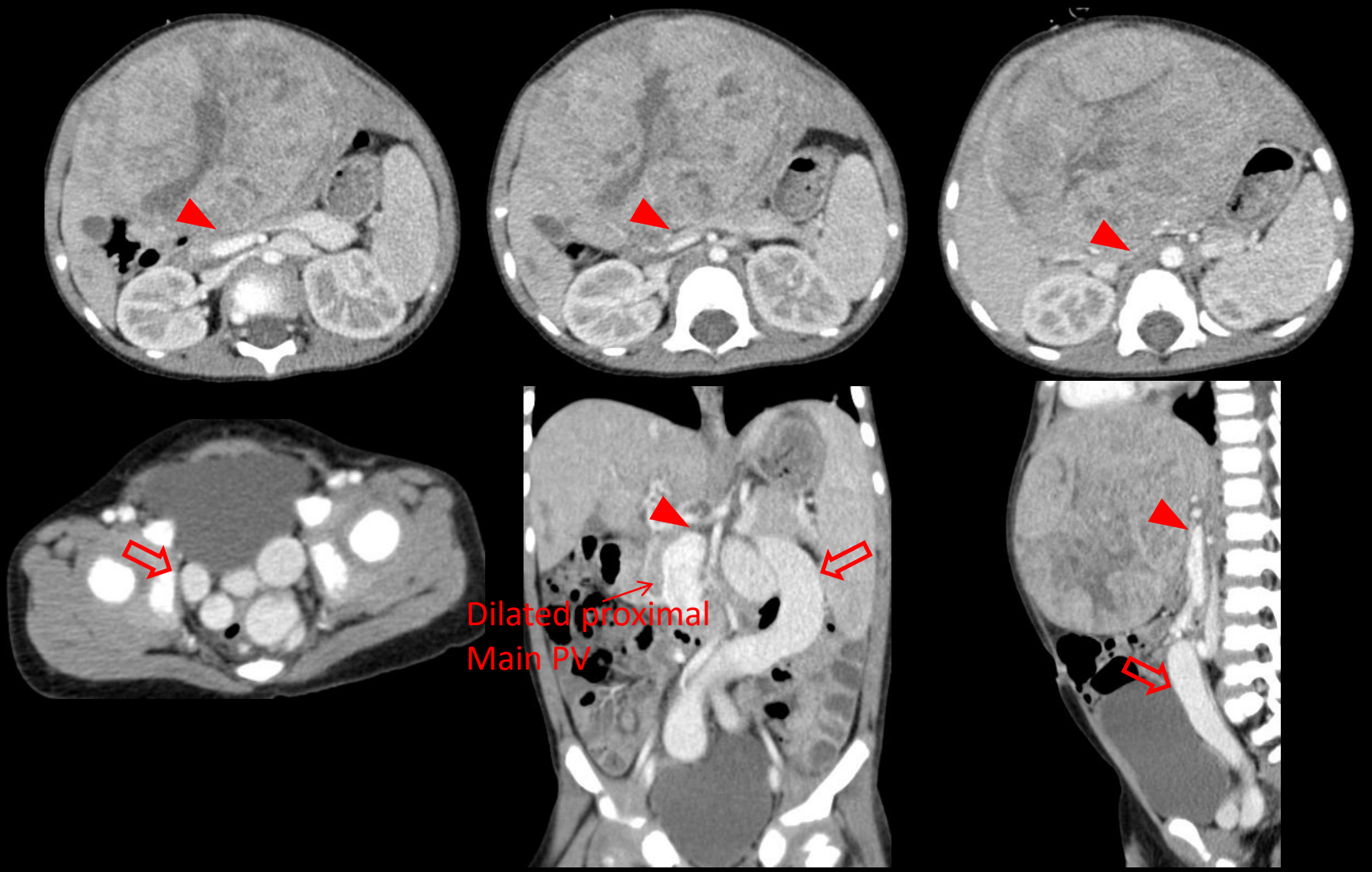

3/M. PRETEXT III. Main PV is obliterated by tumor (arrowhead) and collateral veins are developed (arrow). Splenomegaly is present.

Main PV encasement → P (+)

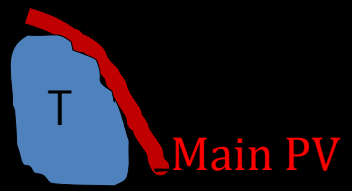

1/M. PRETEXT IV.
Half of main PV is encased by tumor (arrow). Therefore, assignment of annotation factor P is positive.

Right PV thrombus → P (+)

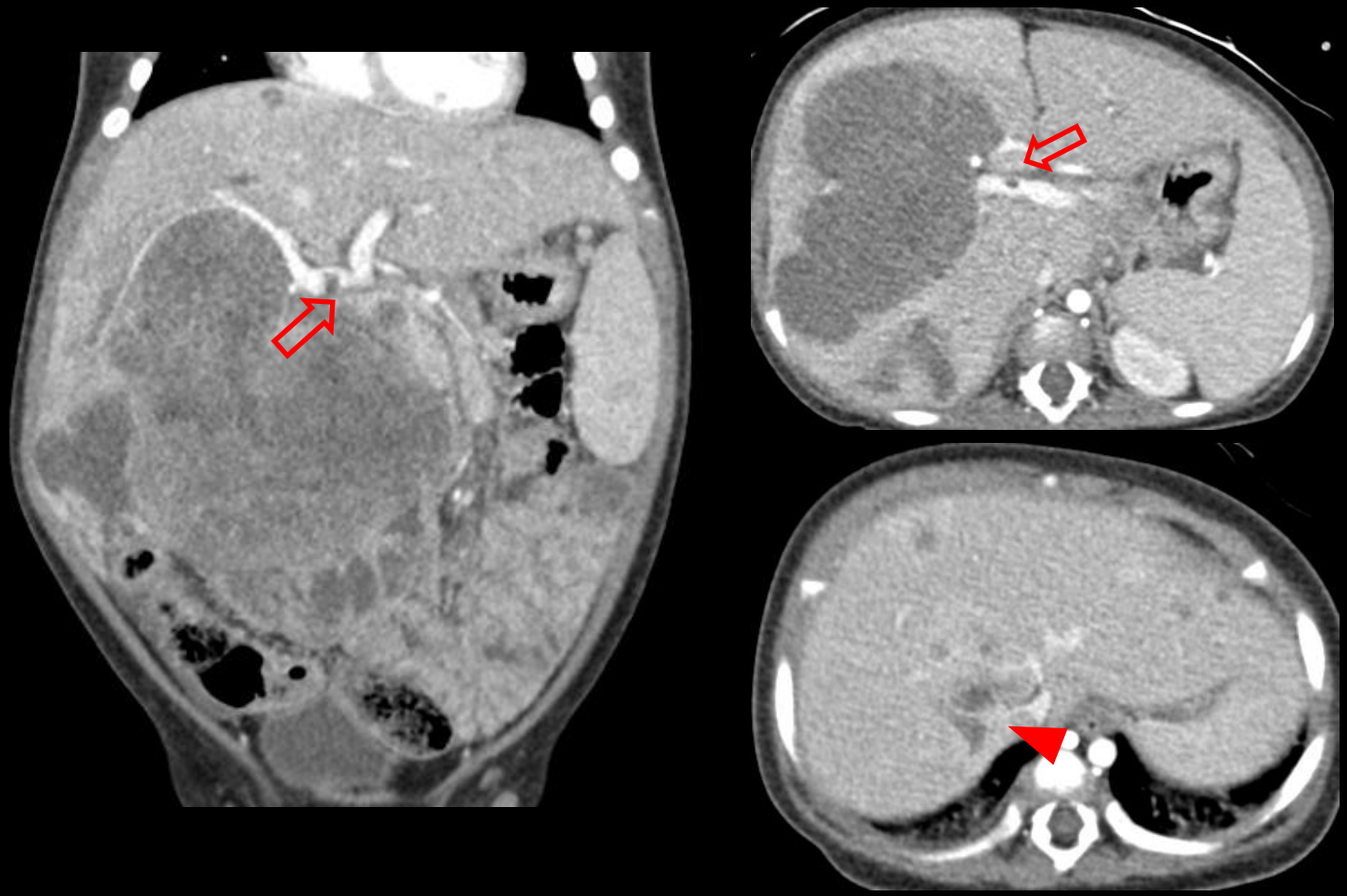

1/M. PRETEXT IV.
Thrombus in the right PV (arrow). Therefore, assignment of annotation factor P is positive. Right hepatic vein is encased by tumor (arrowhead). Tumor involves large area of right lobe and small daughter nodules are seen in the left lobe.

Cavernous transformation of main PV → P (+)

Cavernous transformation should be considered as evidence of tumor thrombus, according to 2017 PRETEXT

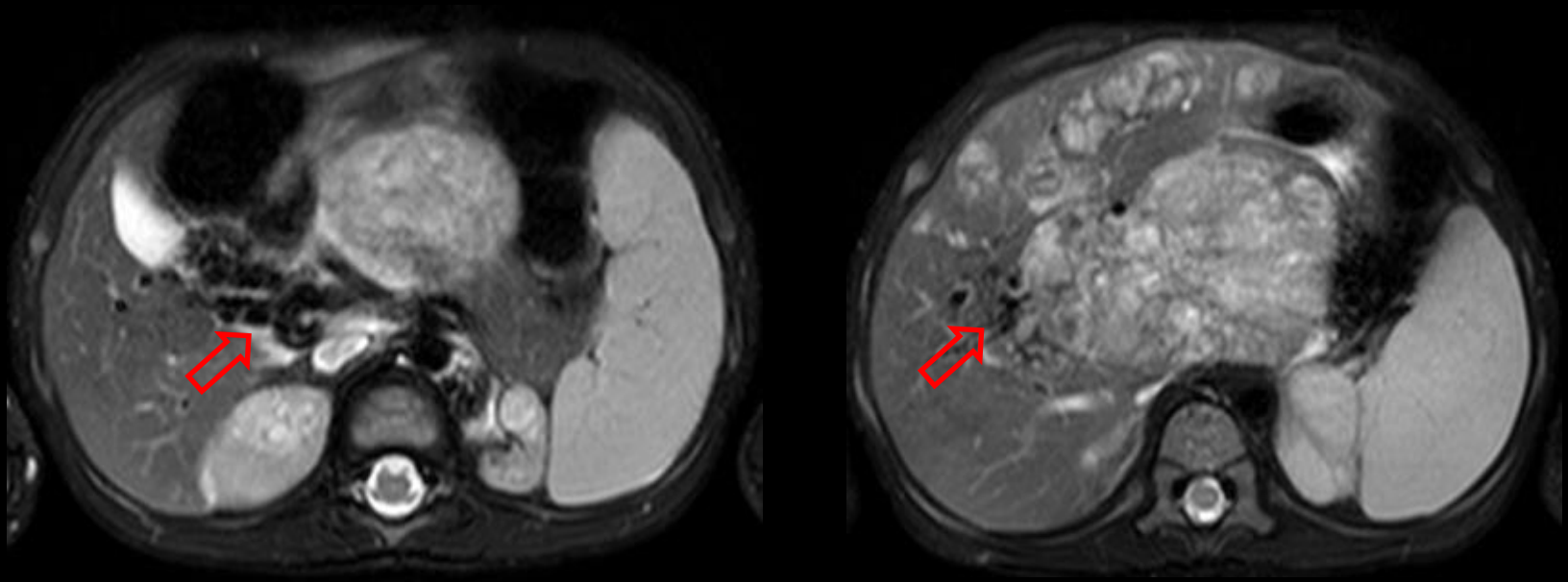

2/M. PRETEXT IV.
MR images show signal void due to cavernous transformation (arrow) of the main PV. Portal vein thrombosis/tumor thrombus should be inferred. Dominant mass involves the caudate lobe and multifocal discrete tumors are noted in both hepatic lobes.

Extrahepatic tumor extension (E)

- One of the following criteria : E (+)

1. Tumor crosses boundaries or tissue planes

   - Tumor is seen both above and below the diaphragm or extending through the abdominal wall

2. Tumor is surrounded by normal tissue more than 180°
3. Peritoneal nodules : one nodule ≥ 10mm or two or more nodules ≥ 5mm

- Extrahepatic tumor extension is uncommon (5%)
- Most times, tumor is seen to be abutting and displacing nearby structures, not invading them
- Simple ascites is not considered extrahepatic disease

Diaphragm extension → E (+)

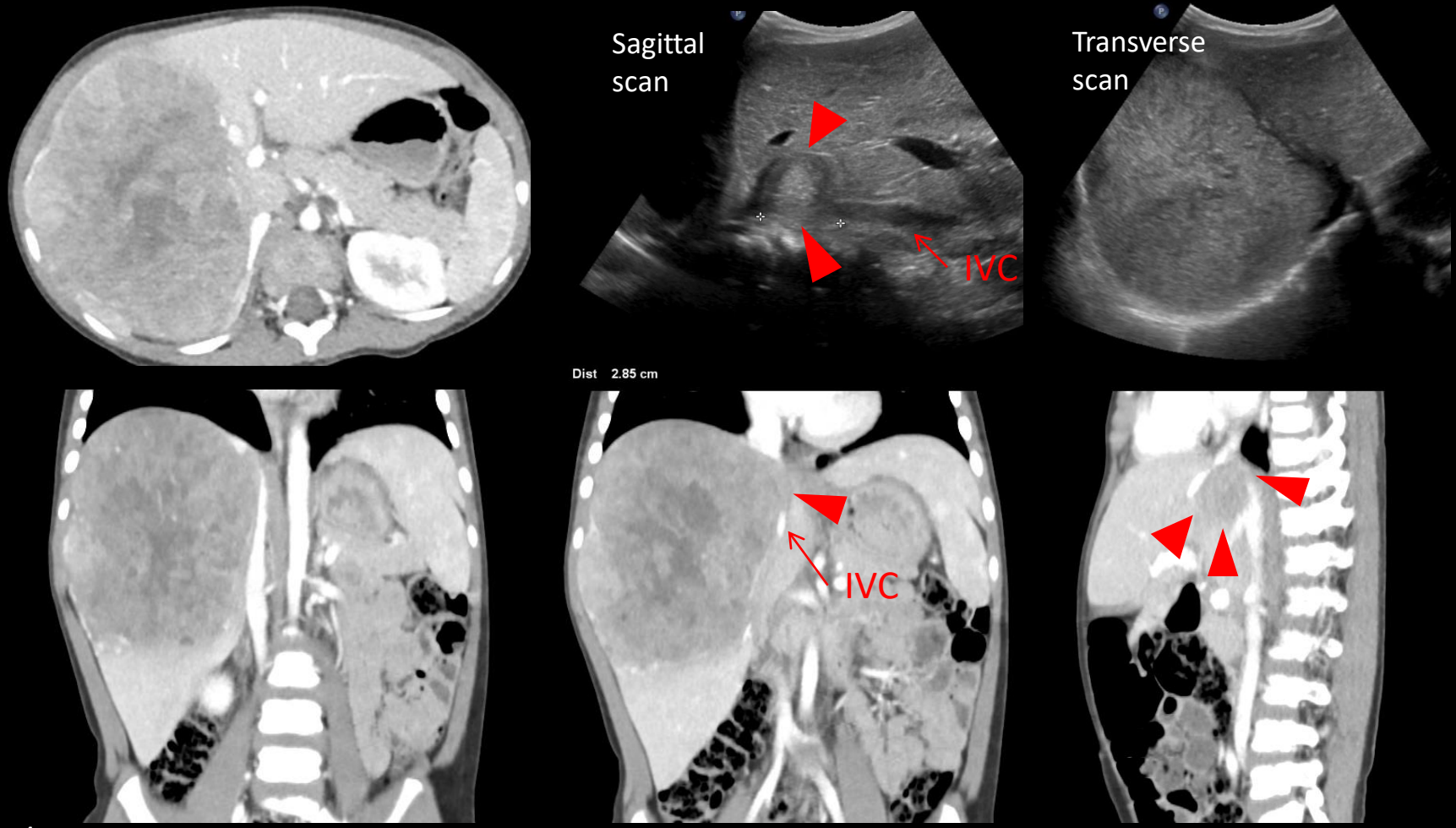

3/M. PRETEXT III (Tumor in S4 is not seen). Huge tumor in right hepatic lobe is surrounded by diaphragm more than 180 °. Diagnosis of annotation factor E could be challenging, because frequently a large tumor is seen to abut the diaphragm, causing a loss of the plane between the affected structure and the tumor. However, in this case, diaphragmatic involvement is confirmed during operation. IVC obliteration (arrowhead) is seen by tumor.

Multifocality (F)

- Two or more separate hepatic tumors with normal liver tissue between the tumors
- Present in nearly 20% of patients with hepatoblastoma.
- Multiple studies have reported a worse outcome in patients with multifocal disease than those with a solitary focus of disease

  (*European journal of cancer* 2000, 36, 1418-1425) (*European journal of cancer* 2012, 48, 1543-1549)

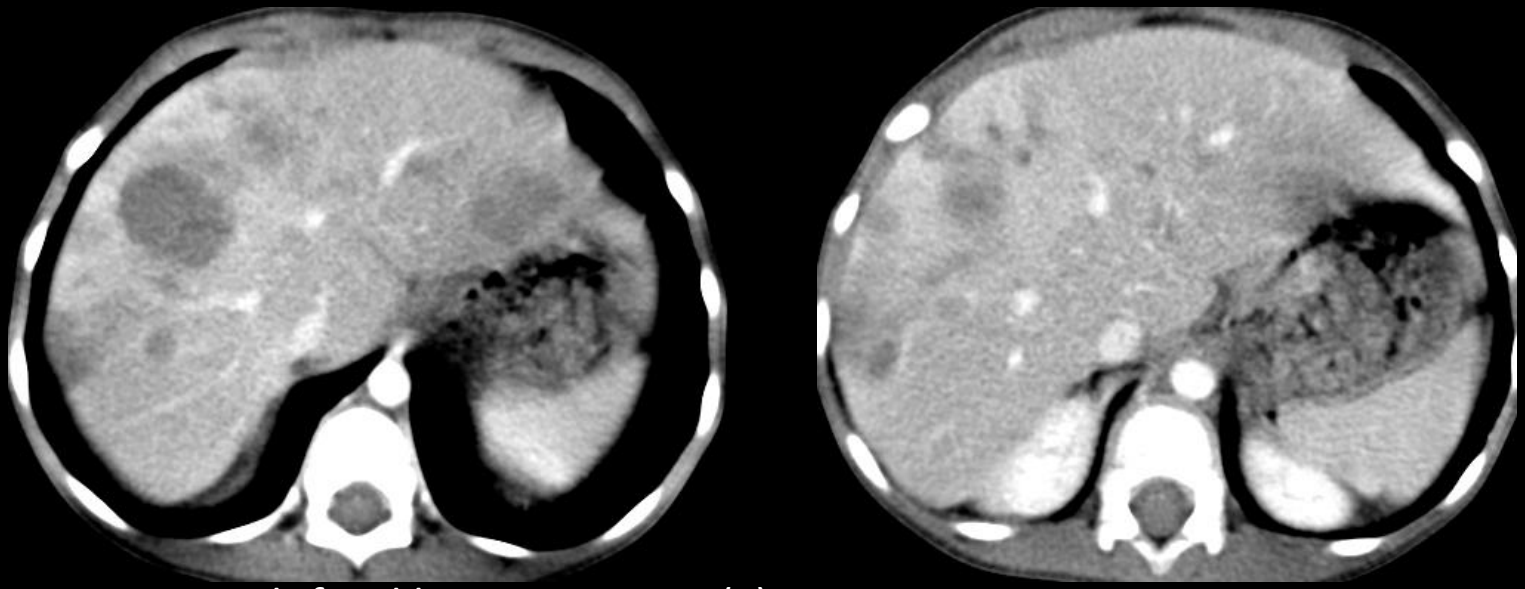

4/M. PRETEXT IV. Multifocal hepatic tumors (F)

Tumor rupture (R)

- Any findings of hemorrhage in the abdominal free fluid on imaging (US, CT, MRI)
- Visible rupture/hepatic capsular defect on imaging
- Pathologically diagnosed after paracentesis/up front resection

Tumor rupture, R (+)

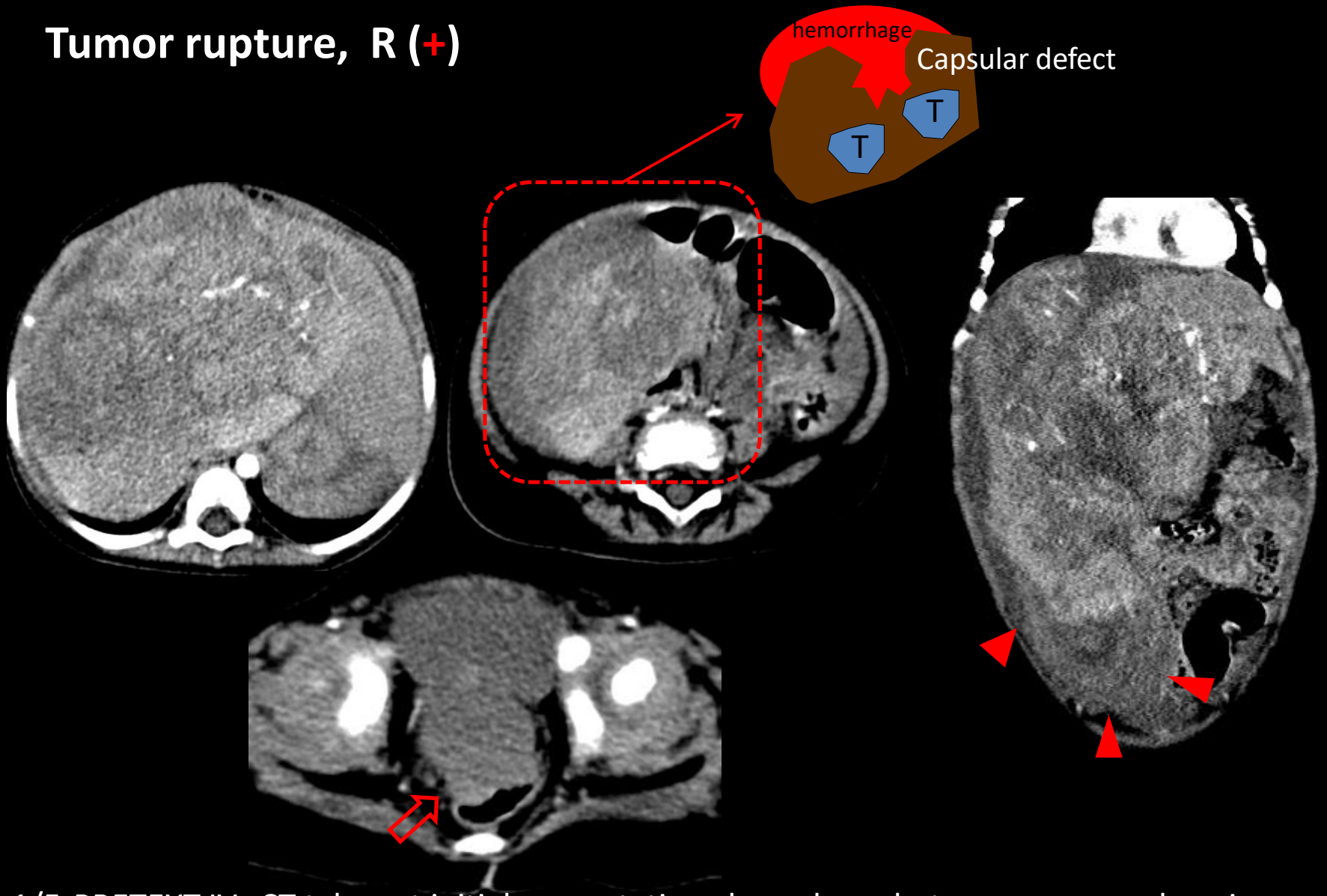

1/F. PRETEXT IV. CT taken at initial presentation shows large heterogeneous enhancing mass in both hepatic lobes. Focal capsular defect is seen in inferior aspect of S5 with surrounding hemoperitoneum (arrowhead). Free fluid of high density is demonstrated in cul-de-sac (arrow).

Caudate lobe (C)

- Involvement of the caudate lobe has implications for surgical planning
- The caudate lobe can be resected with either a right or a left hepatectomy, therefore, involvement of caudate lobe is considered at least PRETEXT II by definition

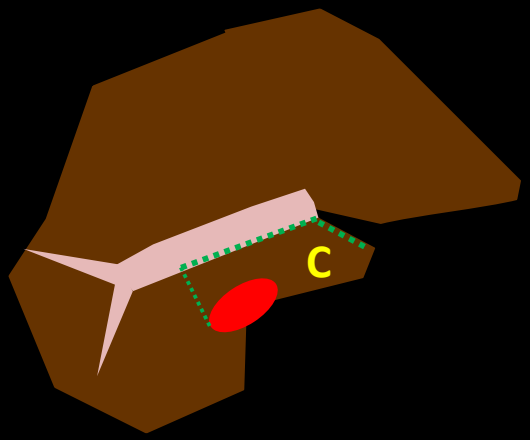

< Margins of caudate lobe >

- Right : right lateral border of IVC
- Anterior : porta hepatis and ligamentum teres
- Left : ligamentum venosum
- Superior : liver dome
- Inferior : liver passes between main PV and IVC

Caudate lobe involvement → C (+)

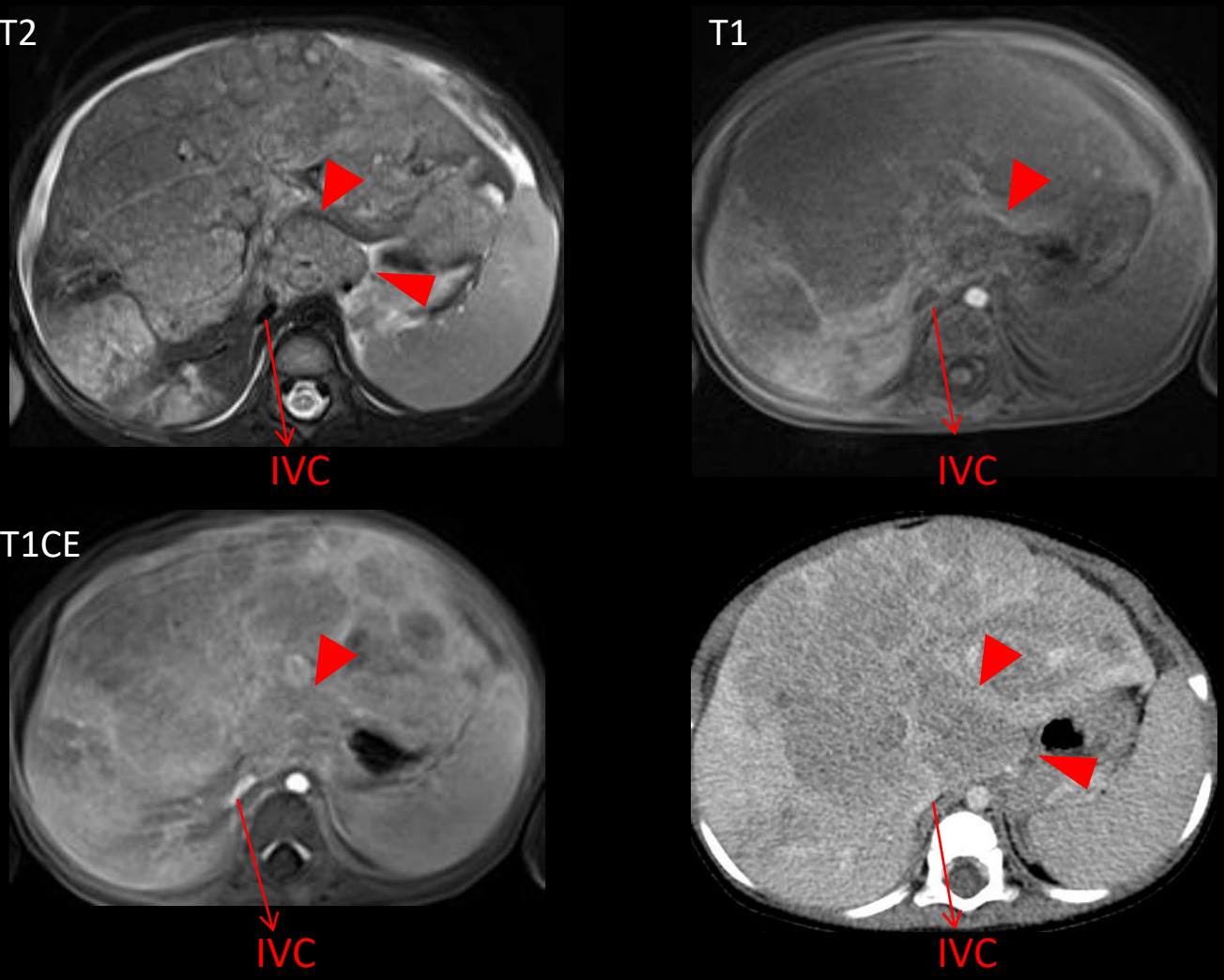

1/F. PRETEXT IV. Caudate lobe is involved by tumor (arrowhead).
Perihepatic ascites is present, however, there is no signal characteristics of blood; R (-).

Lymph node metastasis (N)

- Although lymph node metastasis is extremely rare in hepatoblastoma, one study (*European journal of cancer* 2000, 36, 1418-1425) reported that hilar lymph node enlargement is associated with reduced survival.

- Any of the following criteria:

1. Lymph node with short-axis diameter > 1cm
2. Portocaval lymph node with short-axis diameter >1.5cm
3. Spherical lymph node shape with absent fatty hilum

- It should be noted that morphologic criteria, such as in criterion 3, are less sensitive for detection of metastases

Lymph node metastasis (clinically), N (+)

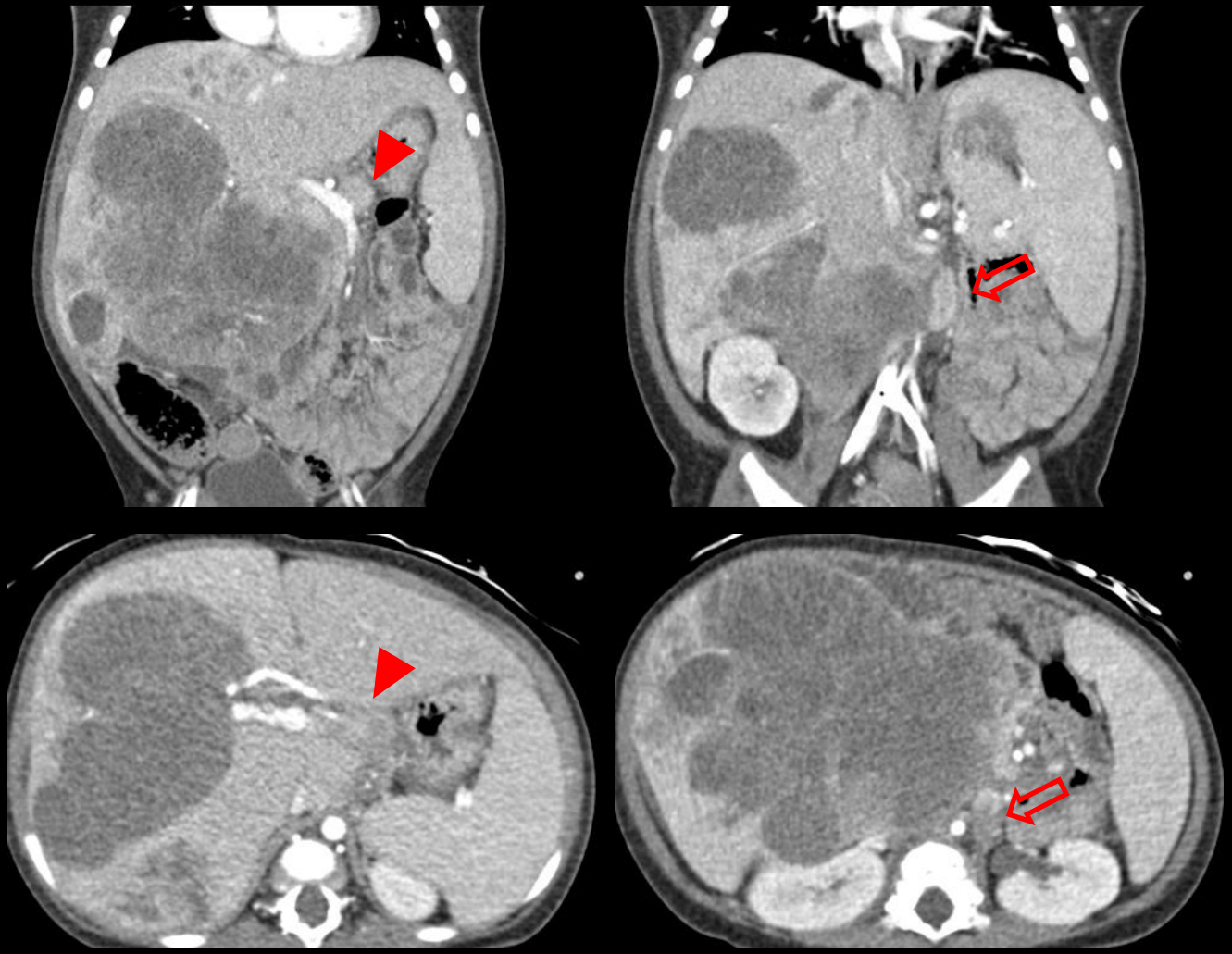

1/M. PRETEXT IV. Multiple enlarged LNs in periportal (arrowhead) and left para-aortic region (arrow). Surgical tumor resection or orthotopic liver transplantation were not performed in this patient, and lymph node metastasis is diagnosed clinically. The patient was treated with primary chemotherapy, but eventually died of refractory disease.

Distant metastasis (M)

- The lungs are the m/c site of distant metastases in children with hepatoblastoma
- Metastases can occur to other locations: bone and brain metastases

- Any of the following criteria for pulmonary metastases

1. Single non-calcified lung lesion with diameter ≥ 5mm
2. Two or more non-calcified lung lesions with each diameter ≥3mm

- Distant metastasis is one of the traditional poor prognostic factors in hepatoblastoma
  - (European journal of cancer 2012, 48, 1543-1549) (Cancer 2002, 95, 172-182)

Distant metastasis to lungs, M (+)

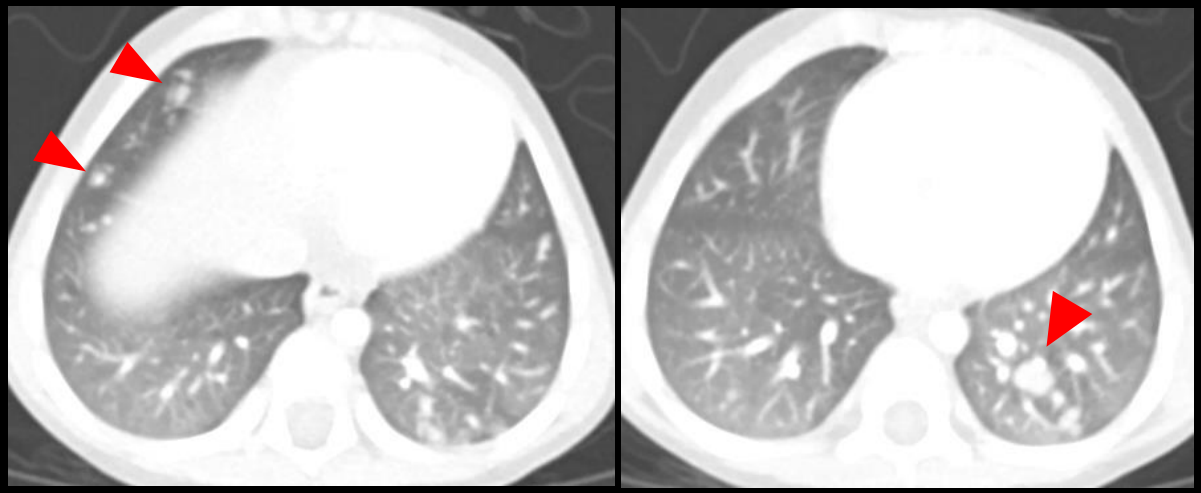

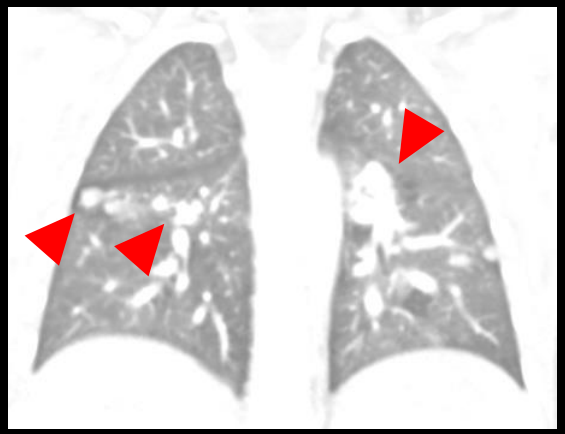

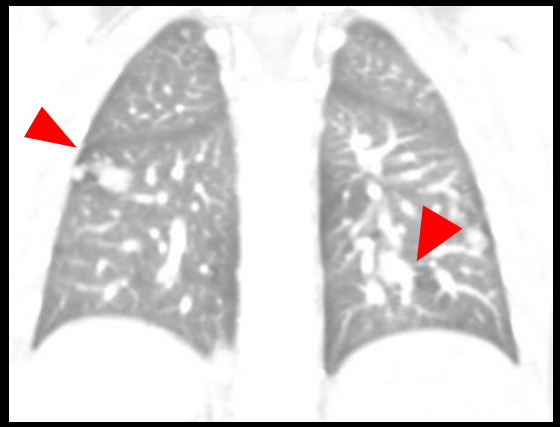

3/M. PRETEXT III.

Distant metastasis to bones, M (+)

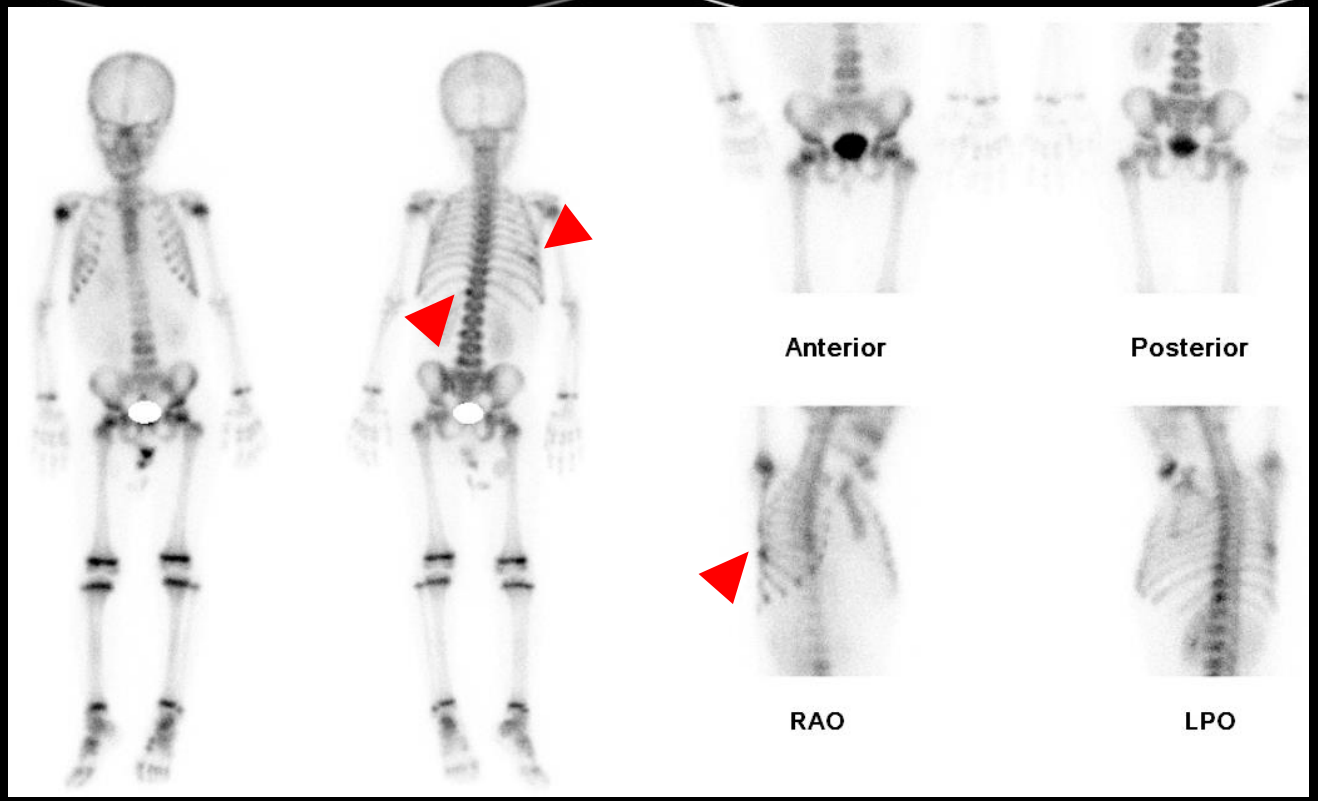

9/M. PRETEXT II. Osteolytic bone metastasis is seen in T12 verterbal body on CT.

Bone scan reveals bone metastasis in right 8th rib in addition to T12 vertebral body.

Continued.

Three months later, bone metastases progressed with new involvement of right proximal humerus, C2 and L2 vertebral bodies, and right proximal radius.

- SUMMARY (1) -

PRETEXT groups	Definition
I	3 contiguous hepatic sections are free of tumor
II	2 contiguous hepatic sections are free of tumor
III	1 contiguous hepatic section is free of tumor
IV	Tumor affects all four hepatic sections (almost always multifocal or infiltrative)
Annotation factors	**Positive definition**
Hepatic venous/IVC involvement (V)	Any of the following criteria: - Tumor obliterates or encases all three hepatic veins or the intrahepatic IVC - Tumor thrombus in any hepatic vein or the intrahepatic IVC
Portal venous involvement (P)	Any of the following criteria: - Tumor obliterates or encases either both portal veins or the main portal vein - Tumor thrombus in either or both the right and left portal veins or the main portal vein

- SUMMARY (2) -

Annotation factors	Positive definition
Extrahepatic tumor extension (E)	Any of the following criteria: - Tumor crosses boundaries or tissue planes - Tumor is surrounded by normal tissue more than 180° - Peritoneal nodules: one nodule ≥ 10 mm or two or more nodules ≥ 5 mm
Multifocality (F)	Two or more separate hepatic tumors with normal liver tissue between the tumors
Tumor rupture (R)	Any findings of hemorrhage on imaging (Ultrasound, CT, MRI) Pathologically diagnosed after paracentesis/upfront resection
Caudate lobe (C)	Tumor involving the caudate lobe
Lymph node metastasis (N)	Considered when any of the following morphologic criteria is met : - Lymph node with short-axis diameter > 1 cm - Portocaval lymph node with short-axis diameter > 1.5 cm - Spherical lymph node shape with absent fatty hilum
Distant metastasis (M)	Any of the following criteria for pulmonary metastasis: - Single non-calcified lung lesion with diameter ≥ 5 mm - Two or more non-calcified lung lesions with each diameter ≥ 3 mm Any metastases diagnosed via pathology

-Thank you-

Comparison of the Occurrence of Atelectasis between Propofol and Dexmedetomidine as a Sedative for Pediatric MRI

Pyeong Hwa Kim[1], Hee Mang Yoon[1], Yong-Seok Park[2], Ah Young Jung[1], Young Ah Cho[1], Jin Seong Lee[1], Myung-Hee Song[2]

Department of Radiology and Research Institute of Radiology[1] and Department of Anesthesiology and Pain Medicine[2],

Asan Medical Center, University of Ulsan College of Medicine, Seoul, Korea

Disclosure

There are no conflicts of interest and nothing to disclose.

Purpose

- *To compare **propofol** and **dexmedetomidine** as a sedative in regard to **occurrence of atelectasis***
- *To investigate **factors associated with atelectasis** development in children imaged whole-body MRI under sedation*

Introduction

- Prolonged sedation required for children d/t immobilization and noise issue
- However, sedation induces atelectasis→ dyspnea, fever, lung lesion mimicker
- Propofol: commonly used, providing safe and effective sedation
  - Incidence of atelectasis in pediatric patients: 42–82%

Lutterbey G, et al. Paediatr Anaesth 2007; 17: 121-5

- Dexmedetomidine: highly selective alpha-2 agonist
  - Less respiratory depression, emerged as an alternative to conventional sedative

Koroglu A, et al. Anesth Analg 2006; 103: 63-7.

Mason KP. Paediatr Anaesth 2010; 20: 265-72.

- Relationship between dexmedetomidine and atelectasis is poorly described

Materials and Methods

Study Population

- Single tertiary referral center-based retrospective study
- Patients who underwent whole-body MRI (WBMR) under sedation using propofol or dexmedetomidine in November 2017 ~ February 2018 included

Inclusion criteria

- ✓ *Age < 18 years*
- ✓ *Underwent WBMR under sedation using propofol or dexmedetomidine*
- ✓ *American Society of Anesthesiologist Physical Status Classification I or II*
- ✓ *Available medical records*

Exclusion criteria

- ✓ *Sedated using other sedatives or both propofol and dexmedetomidine*
- ✓ *Abnormalities in the thorax that interfered with the evaluation of the presence of atelectasis*
- ✓ *Underwent WBMR not following our institution's routine protocol*

Sedation Protocol

- Followed routine protocol of pediatric sedation clinic in our institution
- Sedatives selected according to anesthesiologist's preference
- Target sedation level: level 5 on the modified Ramsey sedation scale
- HR, BP, SpO_2, partial pressure of end-tidal expiratory CO_2 were monitored

Propofol

Bolus of 1 mg/kg propofol repeatedly until the patient becomes unconscious

Followed by a continuous infusion of 100 – 200 mcg/kg/min

Adjuvant agents including midazolam and/or ketamine administered as required

Dexmedetomidine

Loading dose of 1.0 – 2.0 mcg/kg for 10 minutes

Followed by a continuous infusion rate of 1.0 – 2.0 mcg/kg/hr

Image Acquisition

- Using a 3T MR system (Ingenia, Philips Medical Systems)
- 3-6 subsequent table positions to cover the head to the toes
- Including coronal and sagittal STIR images
- Coronal non-enhanced T1-weighted fast spin echo images and post-contrast scans with coronal three-dimensional fat-suppressed T1-weighted gradient echo images obtained if contrast enhancement required
- Coronal STIR at thoracic level acquired at initial and end of the WBMR to evaluate atelectasis

Evaluation of Atelectasis

- Assessed using initial & final coronal thoracic STIR images
- Evaluated by pediatric radiologist (5-yr experience) blinded to sedative types
- **Objectives of interest**
  - Rate of atelectasis
  - Atelectasis volume per total lung volume (%)
  - Overall image quality

Evaluation of Atelectasis

- **Objectives of interest**
  - Rate of atelectasis
    - Atelectasis grade
      - Grade 1: no atelectasis
      - Grade 2: linear atelectasis along the bronchovascular bundles
      - Grade 3: crescent-like subpleural atelectasis
      - Grade 4: segmental atelectasis
      - Grade 5: lobar atelectasis

Lutterbey G, et al. Paediatr Anaesth 2007; 17: 121-5

  - Atelectasis volume per total lung volume (%)
  - Overall image quality

Evaluation of Atelectasis

- **Objectives of interest**
  - Rate of atelectasis
  - Atelectasis volume per total lung volume (%)
    - Volumetric calculation by drawing the margin of atelectasis on each image slice
    - Total lung volume also calculated by drawing the margin of both lungs
  - Overall image quality

Evaluation of Atelectasis

- **Objectives of interest**
  - Rate of atelectasis
  - Atelectasis volume per total lung volume (%)
  - Overall image quality
    - 1: unreadable
    - 2: extreme artifact
    - 3: moderate artifact
    - 4: mild artifact
    - 5: no artifact

Statistical Analysis

- Chi-square test: association between additional O_2 and atelectasis
- Bonferroni correction used for multiple pairwise comparison
- Factors associated with development of atelectasis explored using multivariable logistic regression analysis
  - Sedative types, age, sex, supplemental O2, induction time, scan time, use of adjuvant agents
  - P-value < 0.1 in univariable analysis → entered in to multivariable analysis
- SPSS (version 21) and MedCalc (version 16.8) used

Results

Study Population

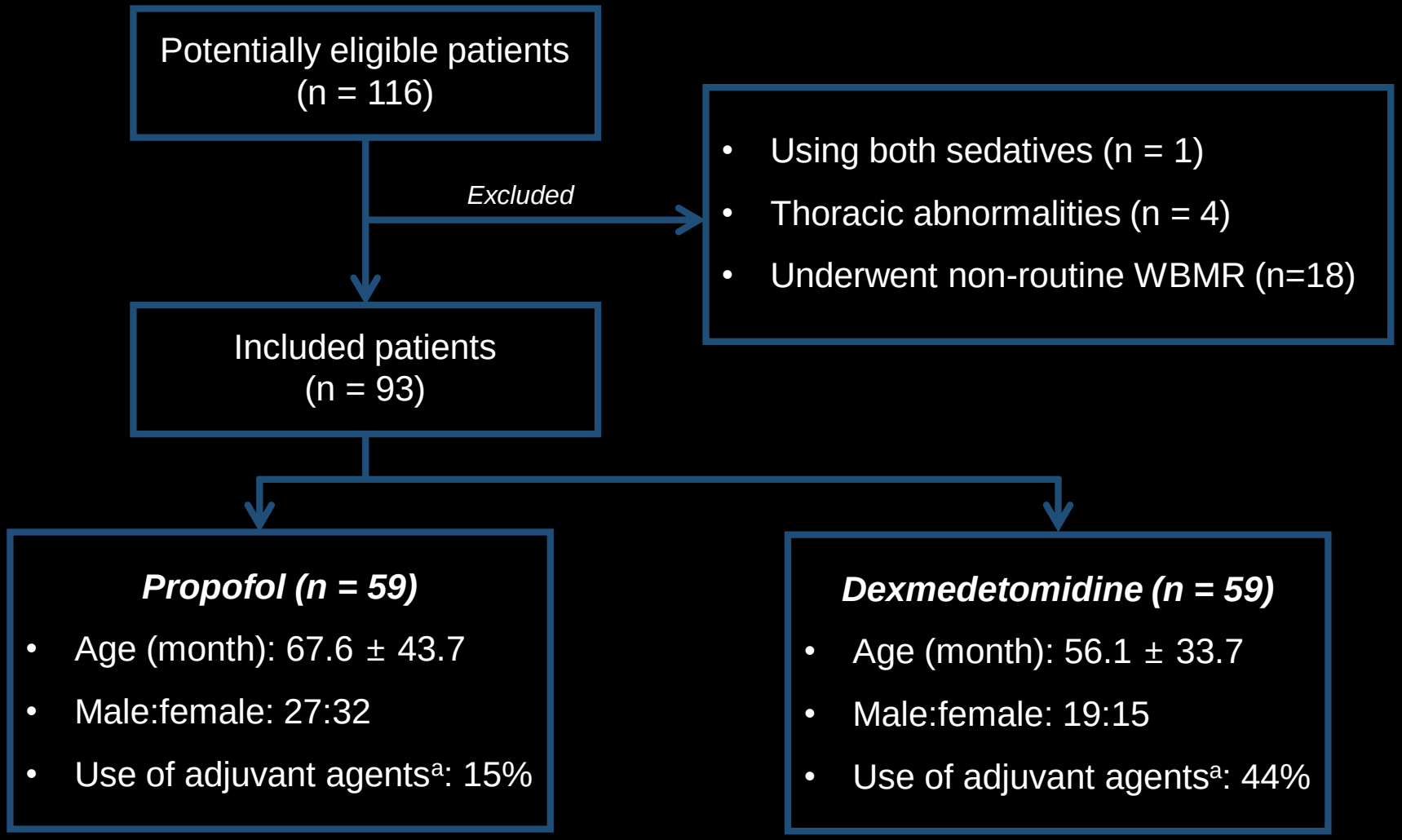

[a]*Adjuvant agents: midazolam and/or ketamine; more frequently used in dexmedetomidine group (P = 0.002)*

Rate of Atelectasis

- Requirement of additional O_2: **propofol > dexmedetomidine** (64.4% vs. 2.9%; *P* < .001)
- Atelectasis: **propofol > dexmedetomidine** (47.5% vs. 17.6%; *P* = .004)

Group		n	Atelectasis Grade					
			1	2	3	4	5	Any atelectasis
I	Propofol + O_2 (+)	38	19 (50%)	15 (39.5%)	1 (2.6%)	3 (7.9%)	NA	19 (50%)
II	Propofol + O_2 (-)	21	18 (85.7%)	3 (14.3%)	NA	NA	NA	3 (14.3%)
III	Dexmedetomidine	34	28 (82.4%)	4 (11.8%)	2 (5.9%)*	NA	NA	6 (17.6%)
		I vs. II	0.007	0.046				0.007
	P value	I vs. III	0.004	0.008	0.486			0.004
		II vs. III	0.750	0.789				0.750

Atelectasis Volume

- Atelectasis proportion: no statistical significance between groups
- Propofol: atelectasis proportion **tend to increase** during the imaging
- Dexmedetomidine: atelectasis proportion **tend to decrease** during the imaging

Group	Atelectasis volume per total lung volume on initial images (%)	Atelectasis volume per total lung volume on final images (%)	P value*
Propofol + oxygen (+)	1.37 (0.1-2.6) %	1.52 (0.8-4.4) %	0.095
Propofol + oxygen (-)	0.47 (0-3.8) %	1.23 (0.7-4.4) %	0.046
Dexmedetomidine	1.05 (0.3-3.2) %	0.63 (0.2-1.25) %	0.293
P value†	0.254	0.654	

** P values of Wilcoxon signed rank test for comparison between initial and last images.*
† P value of Kruskall Wallis test for comparison of three groups.

Factors Associated with Atelectasis

- **Requirement of additional O_2**: the only significant factor
  (Adjusted OR, 4.215; 95% CI, 1.363-13.031; *P* = 0.012)

	Univariate			Multivariate		
Parameters	Odds Ratio	95% CI	P value	Odds Ratio	95% CI	P value
Age (per 1 month)	1.008	0.998-1.019	0.122			
Sex						
Female	1					
Male	0.713	0.305-1.665	0.713			
Drug						
Propofol	1					
Dexmedetomidine	0.237	0.086-0.657	0.006	0.709	0.183-2.745	0.619
Supplemental O_2 administration	**5.619**	**2.240-14.095**	**< 0.001**	**4.215**	**1.363-13.031**	**0.012**
Induction time	0.925	0.855-0.925	0.051	0.965	0.887-1.050	0.407
Scan time	1.024	0.987-1.063	0.210			
Use of adjuvant agents	0.641	0.235-1.749	0.385			

Image Quality

- Overall image quality between propofol and dexmedetomidine was **not different**

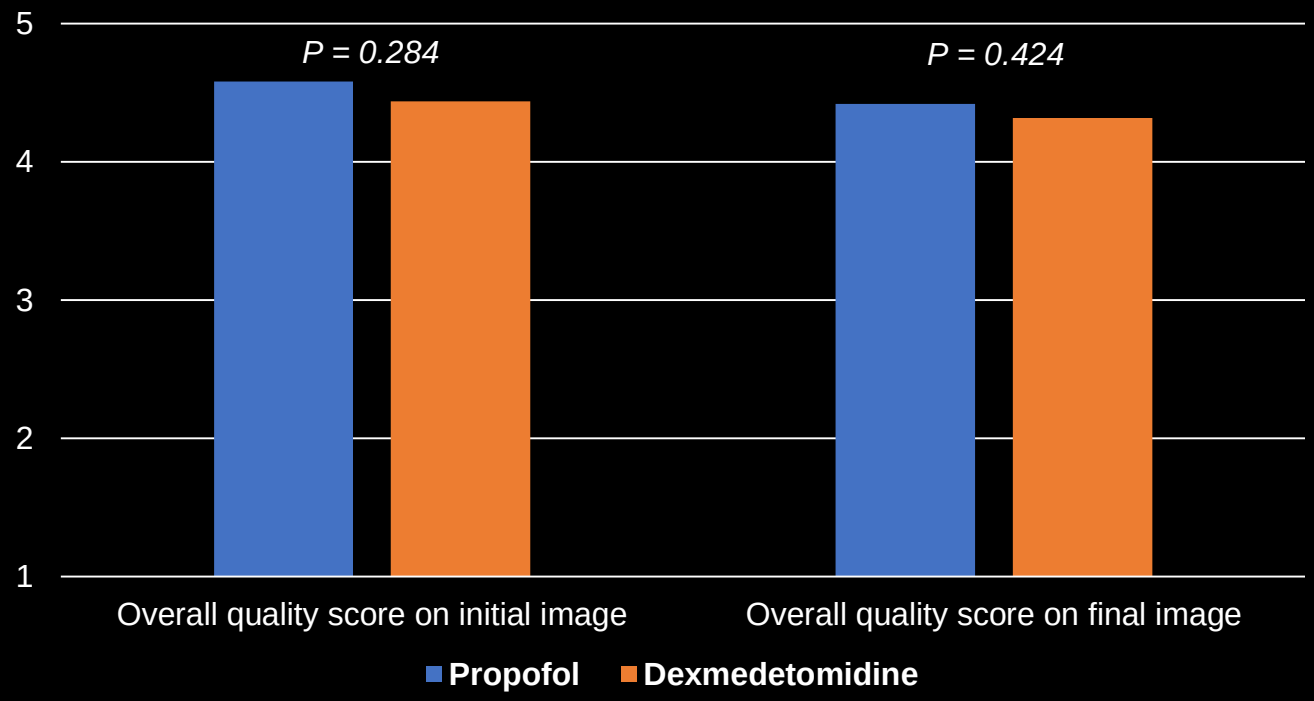

Image quality grade

5: no artifact

4: mild artifact

3: moderate artifact

2: extreme artifact

1: unreadable

Case: propofol

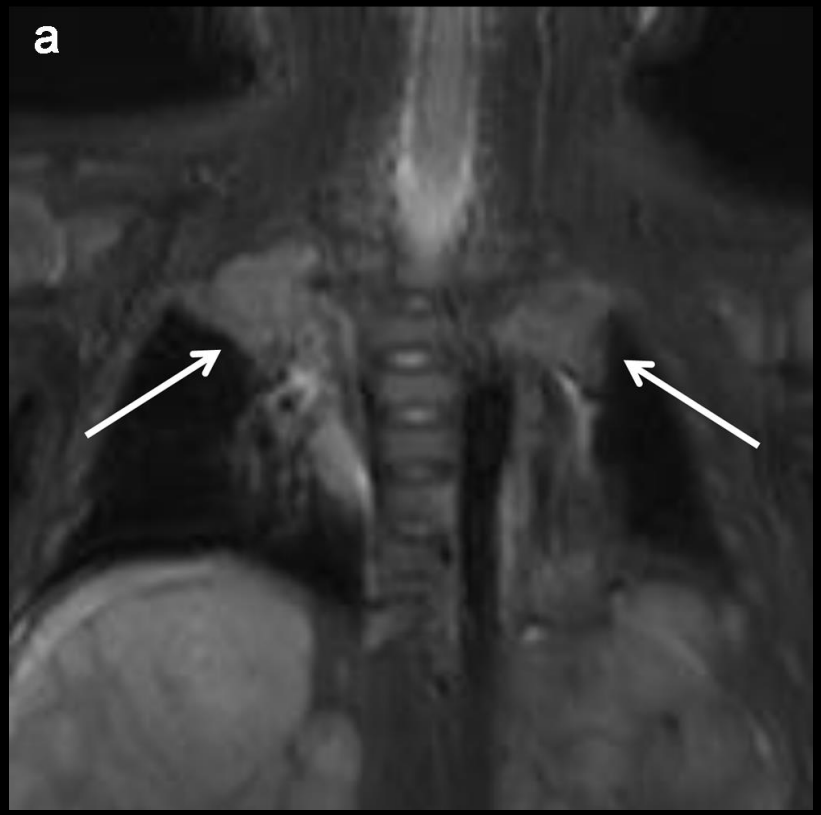

A 5-month-old male with neuroblastoma

Grade 4

Segmental atelectasis in BUL

13.6 %

Estimated atelectasis volume

Case: dexmedetomidine

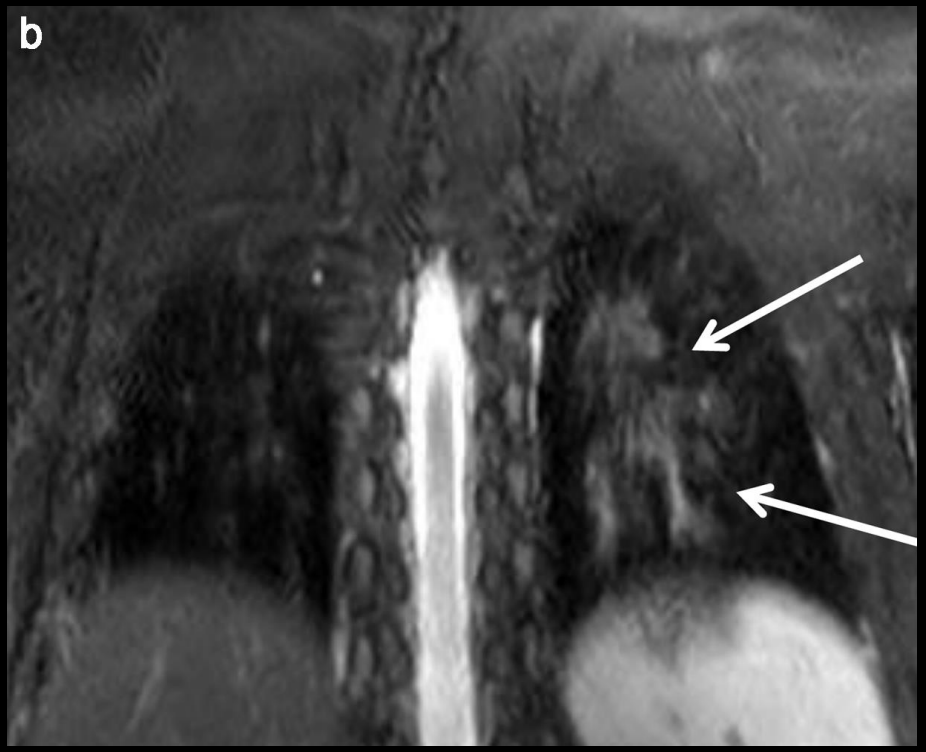

A 6-year-old male with neurofibromatosis I

Grade 2

Linear atelectasis in LLL

1.08 %

Estimated atelectasis volume

Conclusion

Conclusion

- *Pediatric patients sedated with **propofol were more likely to develop atelectasis** than those sedated with dexmedetomidine during MRI.*
- ***Supplemental oxygen** due to desaturation may be an important factor contributing to the development of atelectasis.*
- *To obtain pulmonary images without atelectasis in children under sedation, **dexmedetomidine is more likely to be suitable** as a sedative agent.*

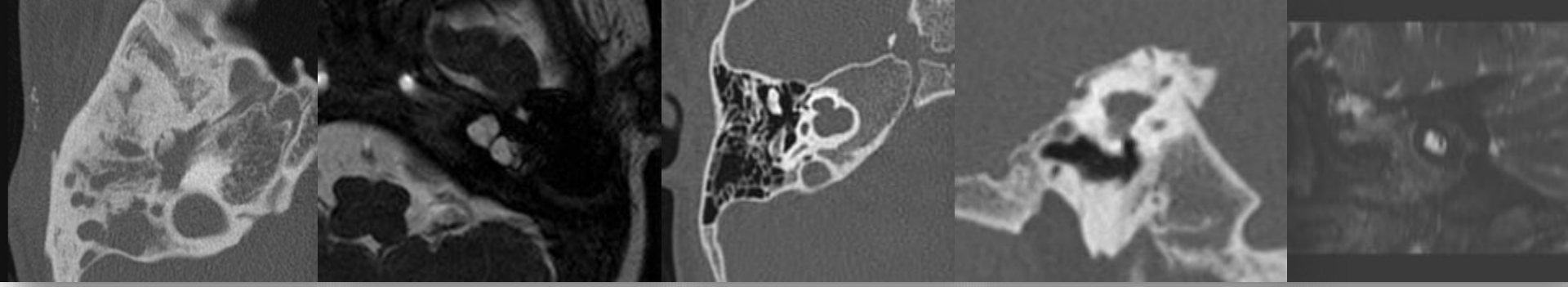

All About the Temporal Bone:
From Embryology to Congenital Pathology

Seonghwan Byun[1], MD; Ji Ye Lee[2], MD; Hyun-Sook Hong[1], MD, PhD;

[1]Department of Radiology
Soonchunhyang University Bucheon Hospital
Bucheon, Korea

[2]Department of Radiology
Eulji Medical Center, Seoul, Korea

AOSPR 2019

Disclosures

The authors declare that we have no relevant or material financial interests that related to the presentation

Learning objects

1. Embryology & development of temporal bone
2. Normal anatomy of temporal bone
3. Radiologic findings and clinical features of major congenital abnormalities
    1) Inner ear abnormalities
    2) middle ear abnormalities
    3) External ear abnormalities
4. Take home notes

1. Embryology & development

1) Inner ear
   - Membranous labyrinth
   - Perilymphatic labyrinth
   - Bony labyrinth
2) Middle ear
   - Tympanic cavity
   - Ossicles
   - Eustachian tube
3) External ear
   - Tympanic membrane
   - EAC, Auricle

1) Inner ear development

- First one to develop
- From 2 – 3 weeks of gestational age
  - Otic placode → Otic pit → Otic vesicle
- Main three phases
  ① Development (3rd – 8th weeks of gestational age)
  ② Growth (8th – 16th weeks)
  ③ Ossification (16th – 24th weeks)

1) Inner ear development

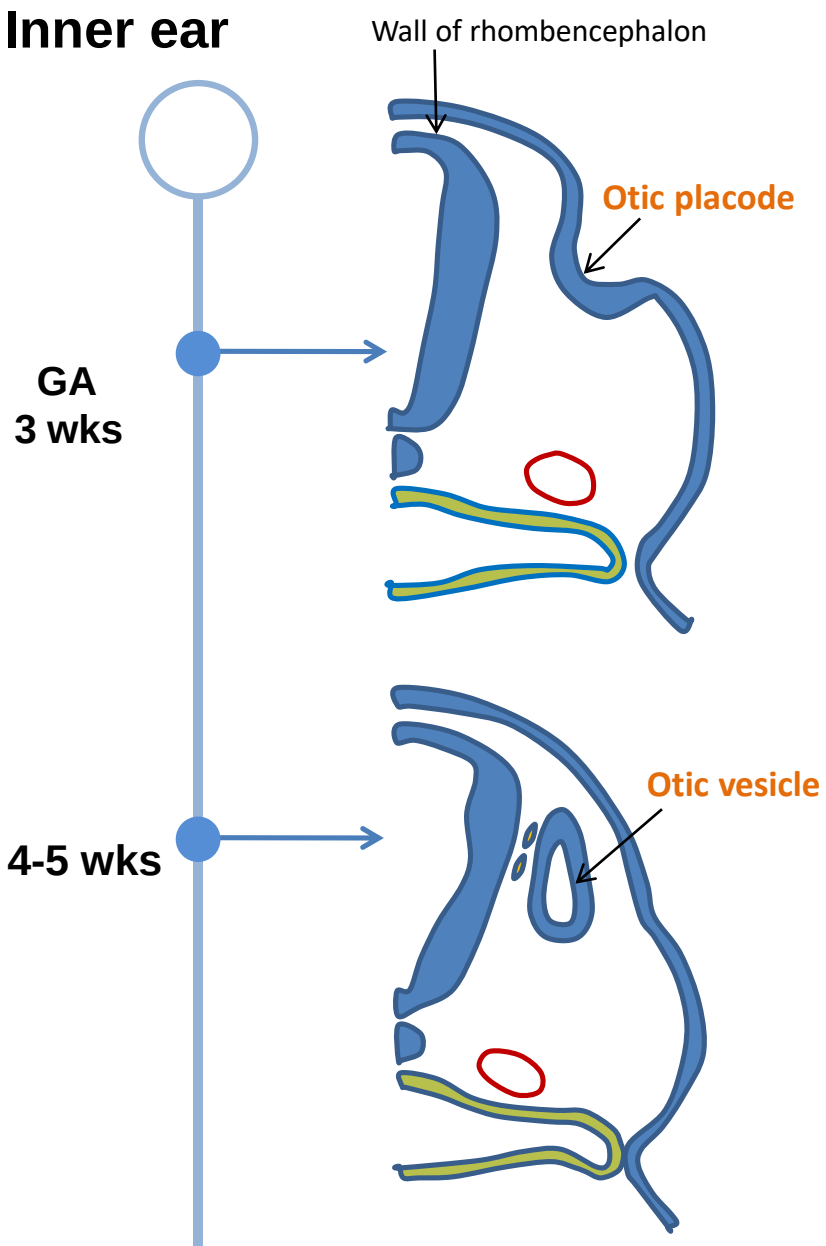

- **Otic placode** from neuroectoderm
  - Invaginating from surface

    → Loss of connection from surface

    → Otic vesicle

- **Otic vesicle (otocyst)**
  - Constitutes primitive endolymphatic and membranous labyrinth

7 wks

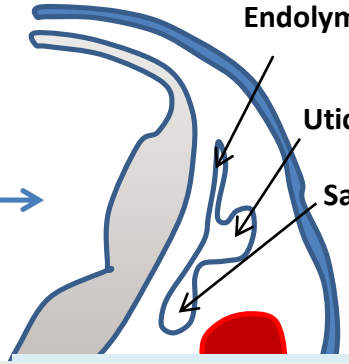

Endolymphatic duct

Uticular portion

Saccular portion

Dorsal utricular part

Ventral saccular part

Otic vesicle

- **Membranous labyrinth**
  - Differentiate to cartilage encasing entire labyrinth
  - Cartilaginous otic capsule ossifies

    : But, endolymphatic duct & sac continues to change

    : Mature anatomic configuration : Mid-term of fetal age (7 months)

7~8 wks

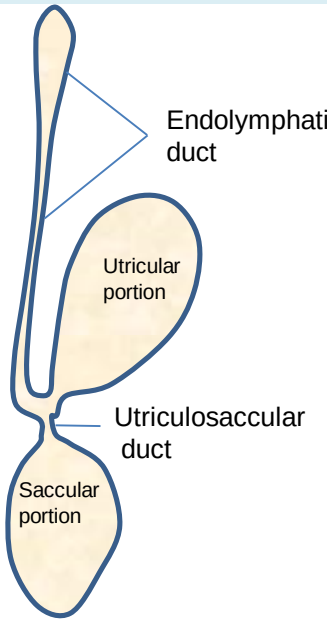

Endolymphatic sac & duct

Utricular portion

Utriculosaccular duct

Saccular portion

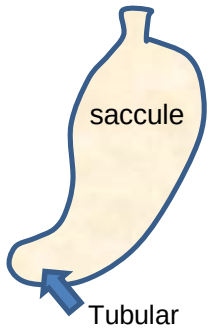

saccule

Tubular outgrowth of saccule

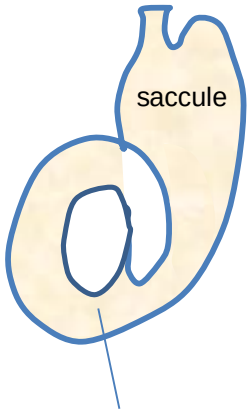

saccule

Cochlear duct

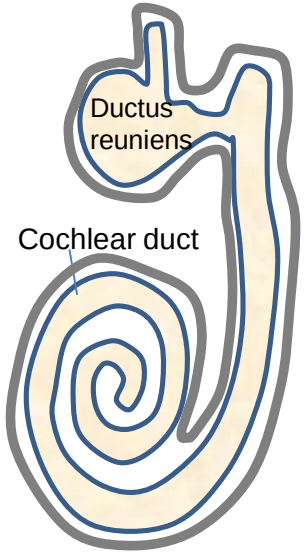

Ductus reuniens

Cochlear duct

Perilymphatic labyrinth

6~8 wks

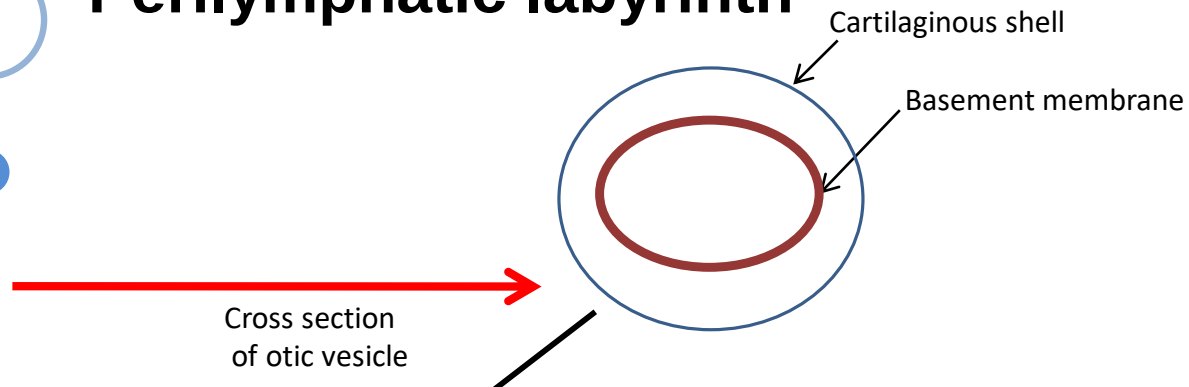

Perilymphatic labyrinth

- Cavitation within condensated mesenchyme around membranous labyrinth
- Cellular condensation → Formation of **inner / outer layer**

16 wks

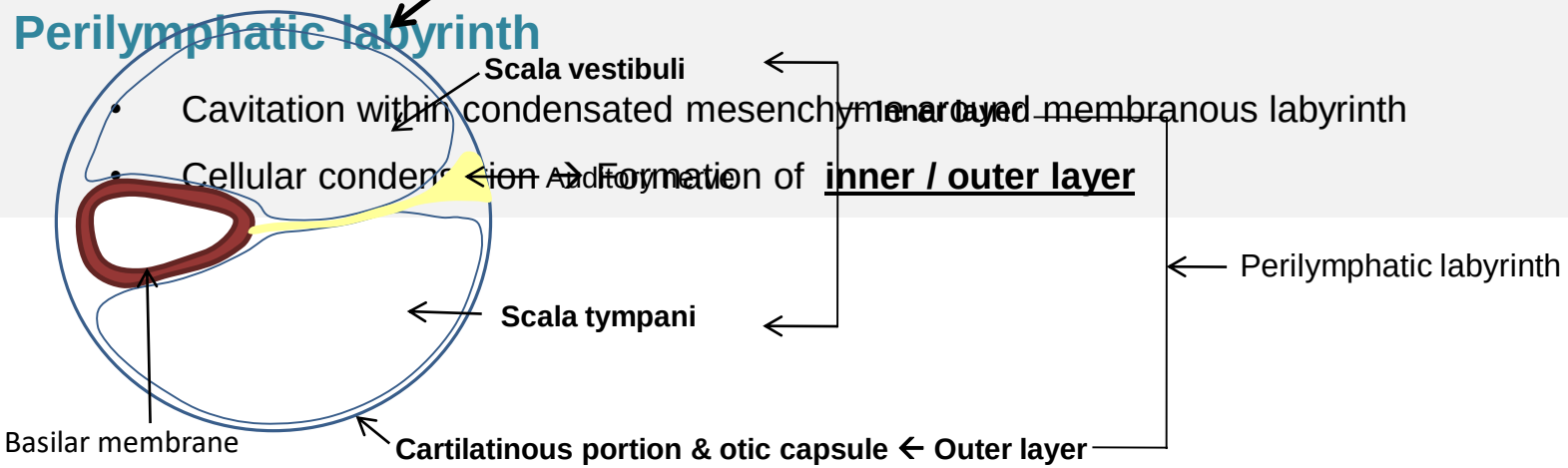

- Other 3 perilymphatic spaces into surrounding osseous otic capsule
- Cochlear aqueduct (perilymphatic duct)

  : From scala tympani near round window to subarachnoid space
- Small fissula ante fenestram / Fossula postfenestram

  : Focus of diseased bone in otosclerosis

16~ 23 wks

- **Bony labyrinth**

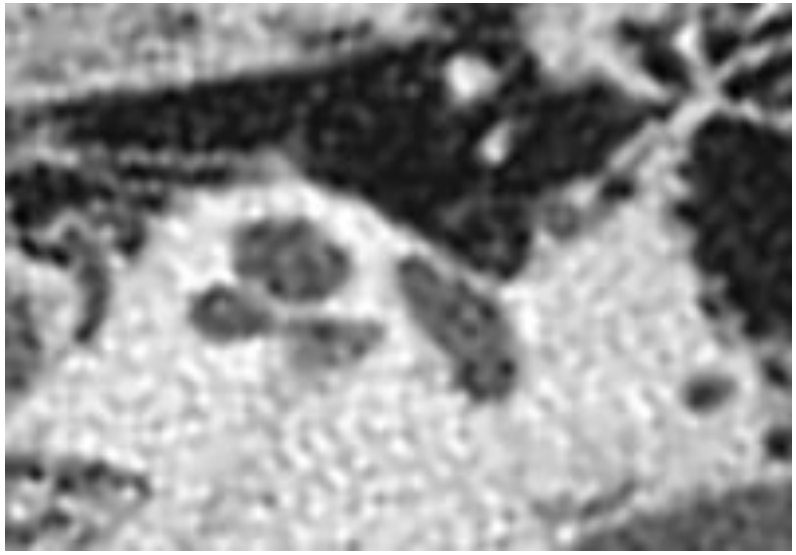

- Ossification of otic capsule (16 – 23 weeks of fetal life)
- **Enchondral bone formation** → Inner ear structures cease to grow
- Limited osteogenic repair → Labyrinthine fistula when injured
- Membraneous bone

  : Modiolus (communication with IAC) & interscalar septum
- Exception of three sites:

  1) Oval window 2) areas of fissula ante fenestram,

  3) lateral most portion of lateral SCC

2) Middle & external ear development

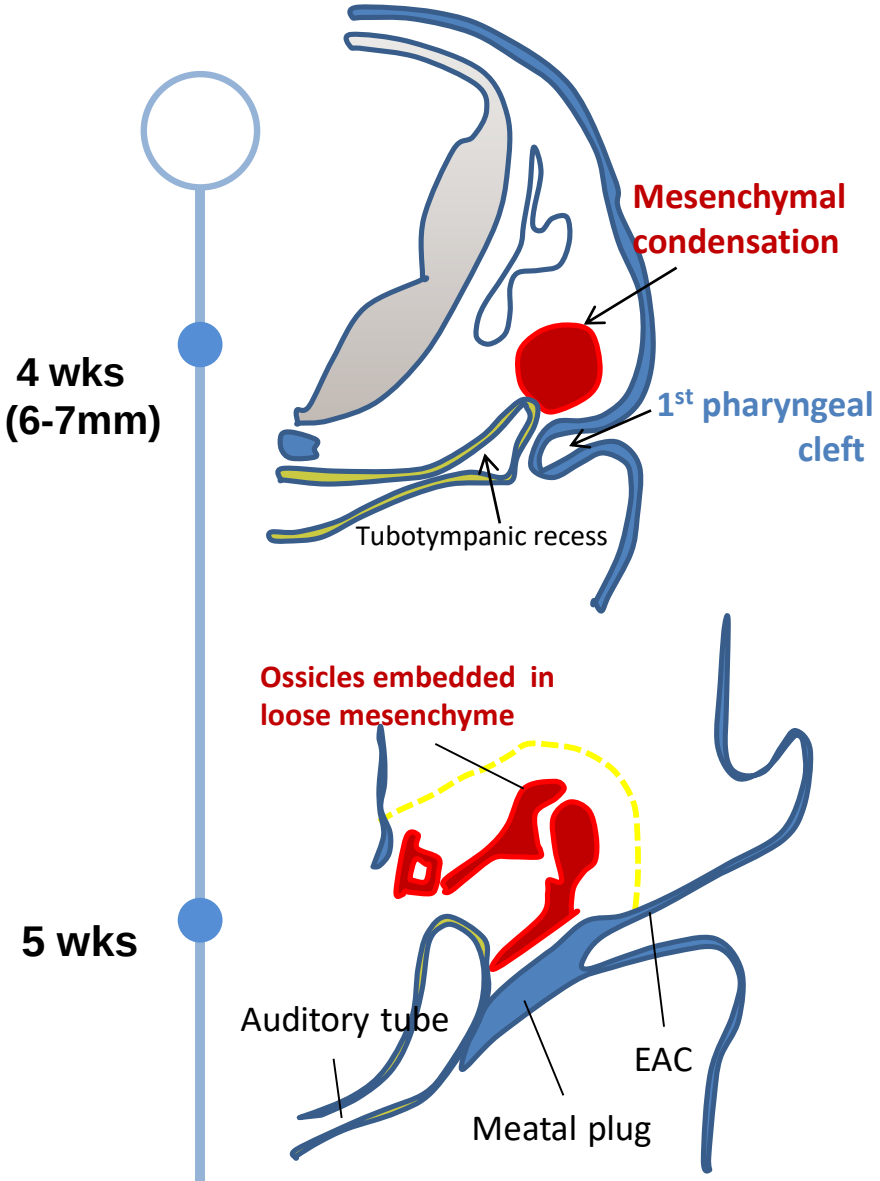

External ear development

- Begins at 3rd month of GA
- **External auditory meatus**
  - From **1st pharyngeal cleft**
    → Ectodermal cell proliferation
    → Meatal plug
    → Disolved & form external auditory meatus
- **Tympanic membrane**
  - From 1st pharyngeal membrane btw cleft & pouch
- **Auricle**
  - From proliferation six mesenchyme in 1st & 2nd pharyngeal arches
    → Swelling & fusion to form auricle

1. Embryology & development

- **Neonatal temporal bone**
  - Fully developed anatomic portions of hearing/vestibular system

    Exception of osseous portion of EAC
  - Large squamous portion, diminutive tympanic portion

    Formation & maturation of tympanic / mastoid portions
  - Pneumatization stimulated by middle ear aeration after birth

- **IAC**
  - Nearly adult vertical dimension at birth (> 4mm)
  - Length : increasing during childhood

2. Normal anatomy

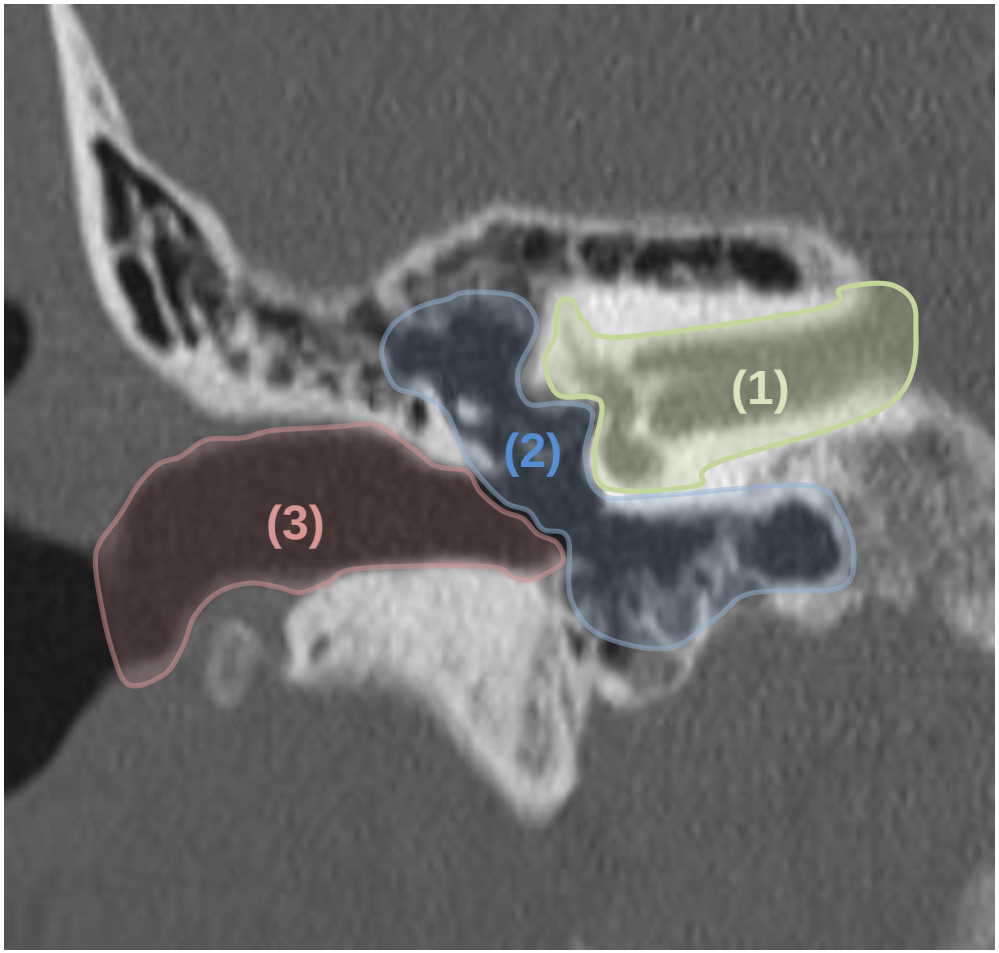

Normal temporal bone

1) **Inner ear**

2) **Middle ear**

3) **External ear**

2. Normal anatomy – 1) Inner ear

Inner ear anatomy

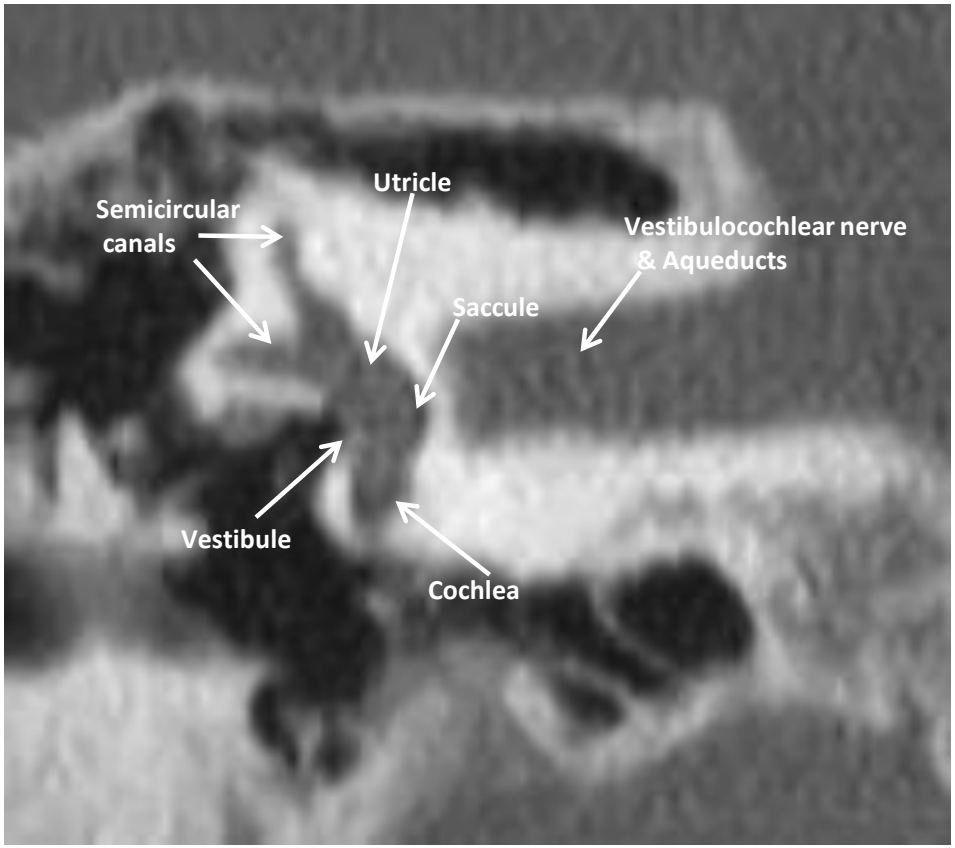

1) Bony labyrinth
   - Cochlea
   - Vestibule
   - Semicircular canals

2) Membranous labyrinth
   - Cochlear duct
   - Utricle & Saccule
   - Endolymphatic duct

3) Perilymphatic spaces
   - Oval & round window
   - Cochlear aqueduct
   - Vestibular aqueduct

1) Inner ear anatomy

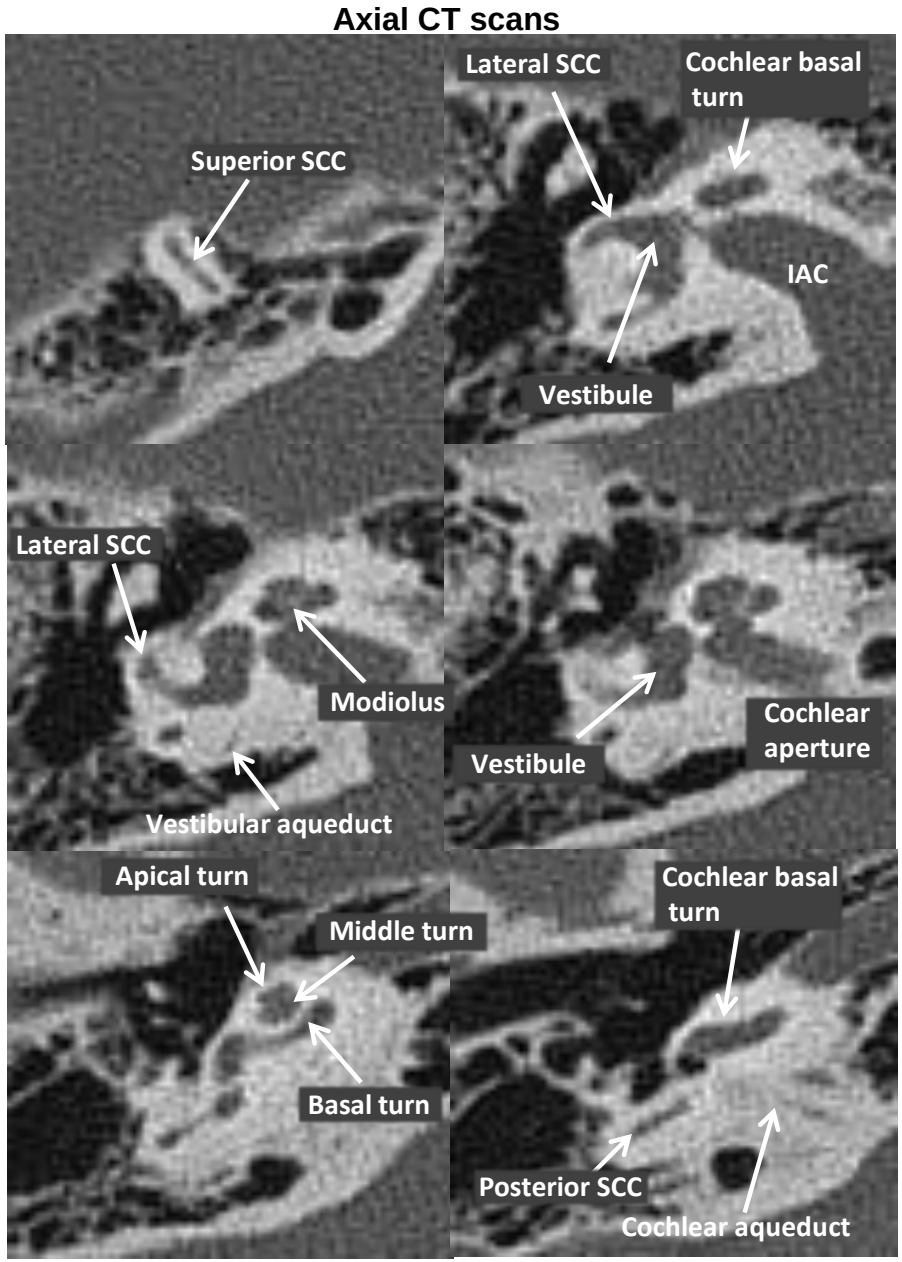

- **Bony labyrinth**
  - Cochlea, vestibule, semicircular canals
- **Vestibule**
  - Central portion of cavity of bony labyrinth
  - Oval window : Lateral wall of vestibule
  - Contains perilymphatic space
  - Superior & posterior SCC, Vestibular aqueduct
  - Posterior wall : Numerous apertures
  - Anterior wall : Cochlear aperture
  - Lateral wall : Oval window & vestibular aqueduct
- **Semicircular canals**
  - Three semicircular canals in bony labyrinth
  - Each opens into vestibule with five openings
  - Lateral SCC, Anterior & posterior SCC
  - Bony cochlear : Around modiolus (Conical central core)
  - Basilar membrane : Divide canal into scala vestibuli & tympani

1) Inner ear anatomy

Axial thin-section T2WI of MRI

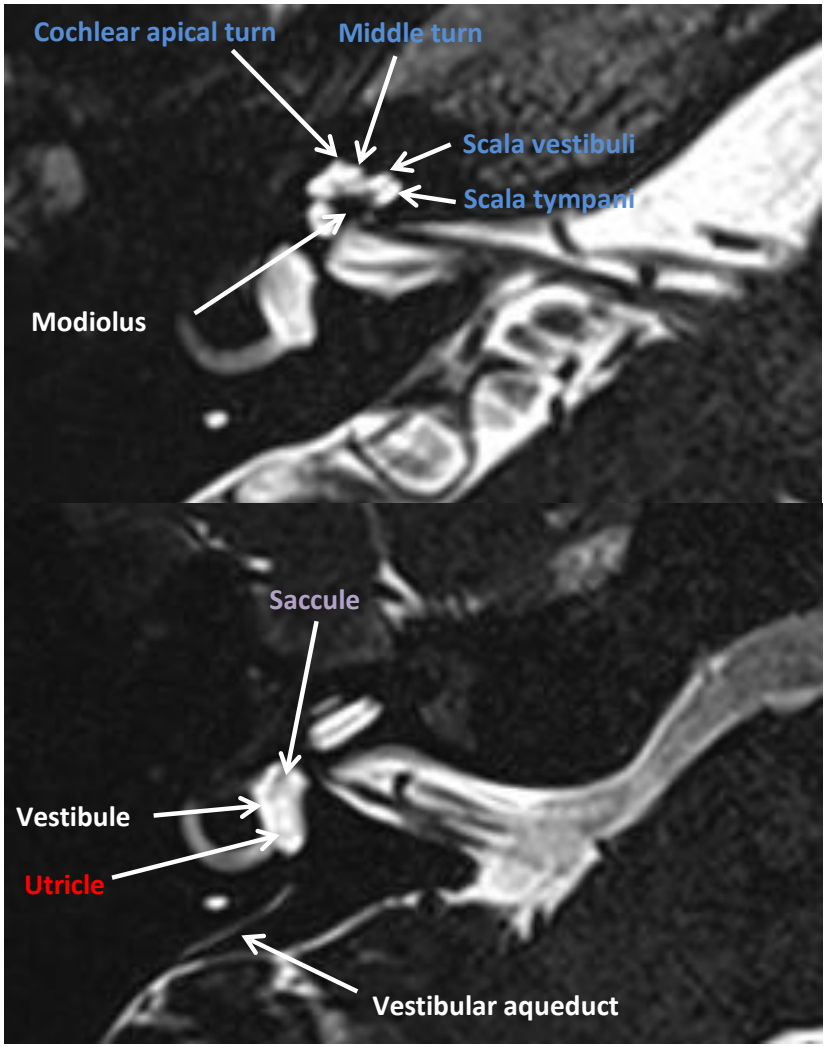

- **Membranous labyrinth**
  - Continuous openings of perilymphatic spaces
    → Vestibule ↔ Scala vestibuli & scala tympani
  - **Utricle**
  - **Cochlear aqueduct**
    : Opening of membranous semicircular canals
    : Potential communication & equilibration
  - **Saccule**
    between perilymphatic & subarachnoid spaces
    : Spherical recess near opening of scala vestibuli
  - **Vestibular aqueduct**
    : Last part of membranous labyrinth (Contains endolymph)
    : Ampullae of SCC (Angular acceleration)
  - **Endolymphatic duct & sac**
    : From vestibule, through vestibular aqueduct

1) Inner ear anatomy

3D heavily weighted T2WI with oblique sagittal reconstruction

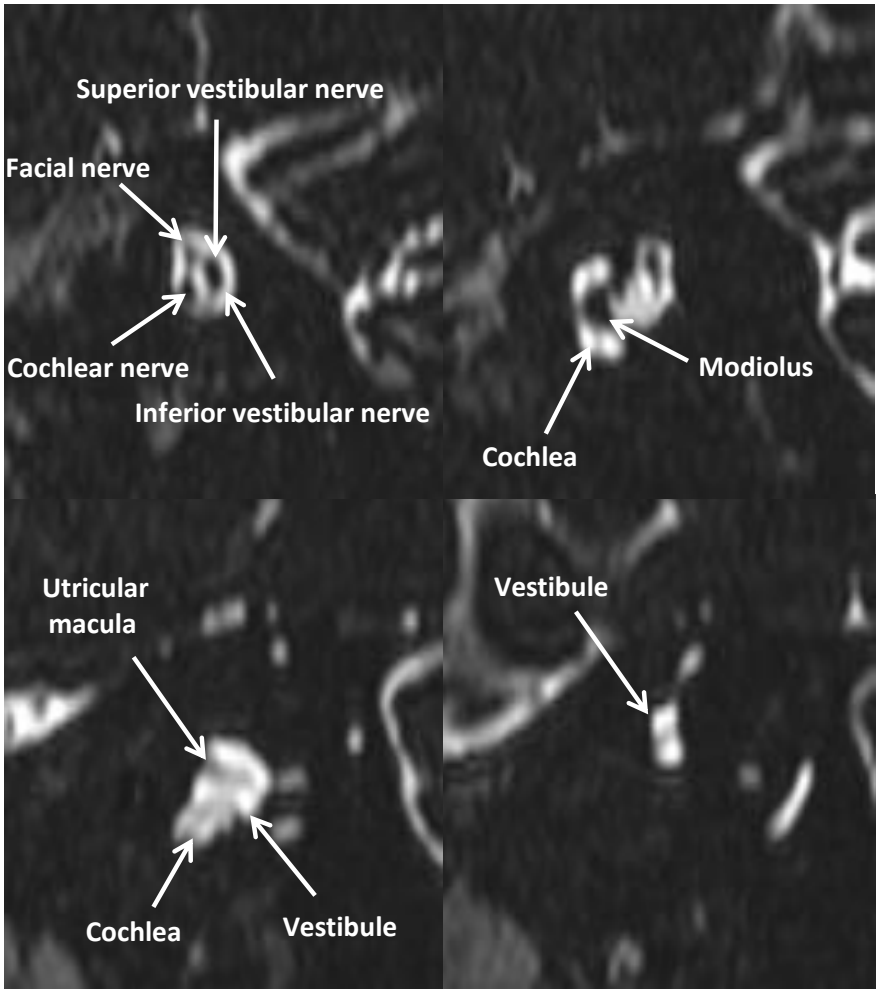

- **Internal auditory canal (IAC)**
  - Bony conduit transmitting **cranial nerve VII, VIII**
  - From pontomedullary junction to inner ear
  - Adult vertical dimension at birth
    (Average : 4mm, < 2mm : hypoplasia)

2) Middle ear anatomy

Middle ear

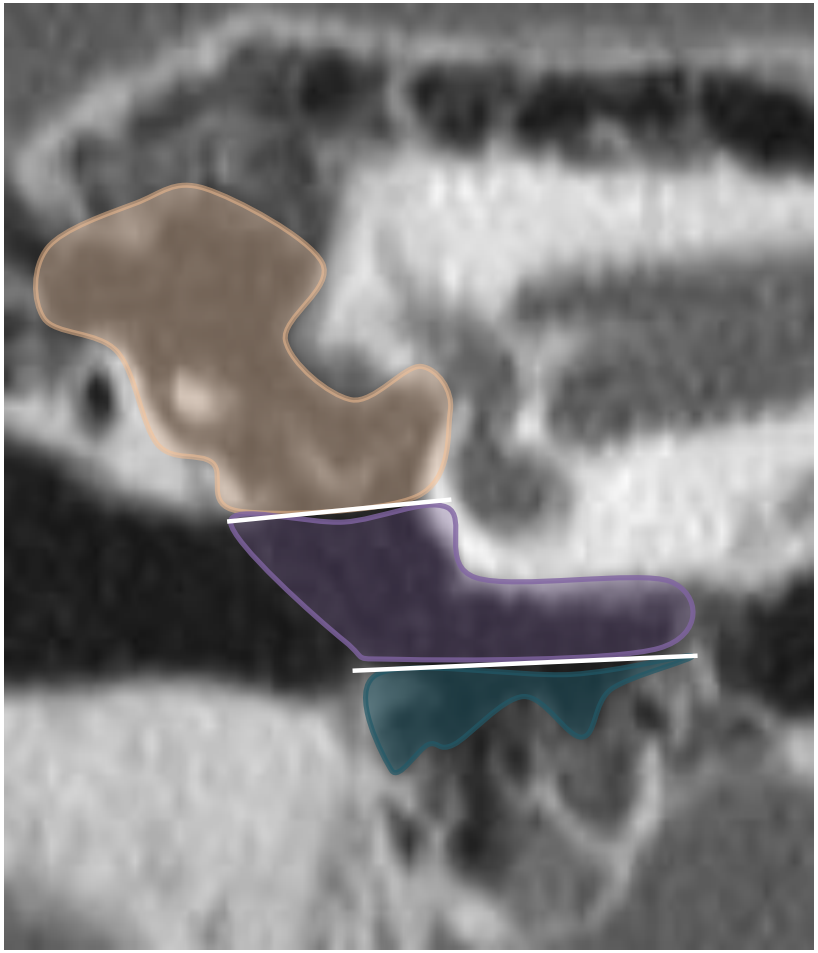

- **Main function**

  Ossicles transmitting vibration of TM to inner ear

- **Size**

  Vertical & anteroposterior dimension : 15mm,

  Transverse dimensions : 6mm

- **Space**

  Epitympanum (above level of TM)

  Mesotympanum (tympanic cavity proper)

  Hypotympanum (below level of TM)

- **6 walls (from petrous bone)**

  : Anterior (carotid wall), posterior (mastoid wall),
  roof (tegmen), floor (jugular wall),
  medial (TM) and lateral wall (membranous wall)

2) Middle ear anatomy

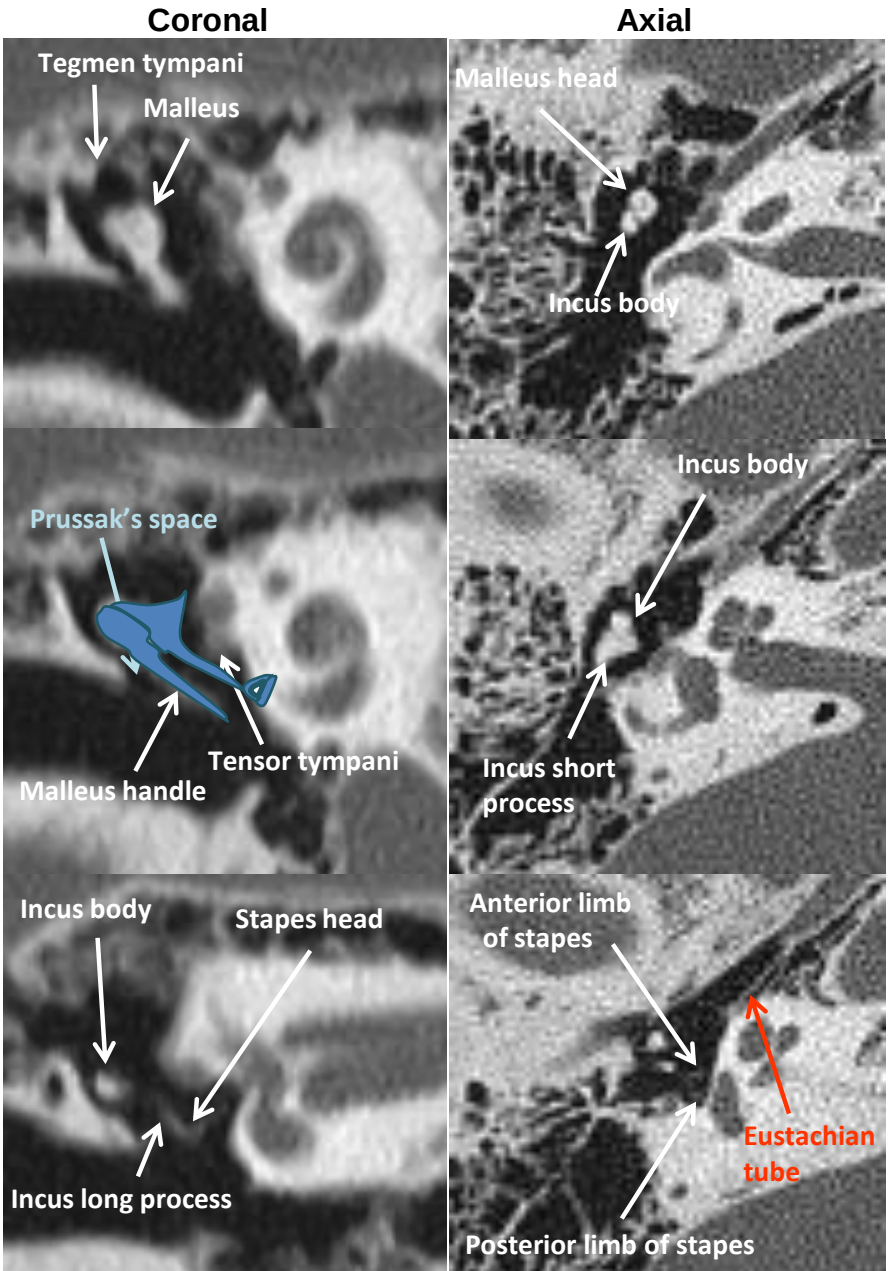

- **Middle ear ossicles**
  - : Transmitting & amplifying vibration of TM to inner ear
- **Malleus**
  - Osseous (1cm length)
  - Cartilaginous portion (2.5cm length)
  - To pharyngeal opening
  - Head, neck → Tensor / levator veli palatini, salpingopharyngeus muscles
  - Manubrium : Attached to TM
  - Lateral process : Lateral process abuts TM
  - Equilibrating pressures of middle ear and pharynx
- **Incus**
  - Body, short process
  - Long process : Descends nearly vertically behind
  - Lenticular process : Articulate with head of stapes
- **Prussak's space**
  - Small recess medial to pars flaccida of TM
  - Common location for cholesteatoma
- **Stapes**
  - Head : Articulation with incus
  - Neck, anterior & posterior crura
  - Base : To oval window with edge of cartilage

3) External ear anatomy

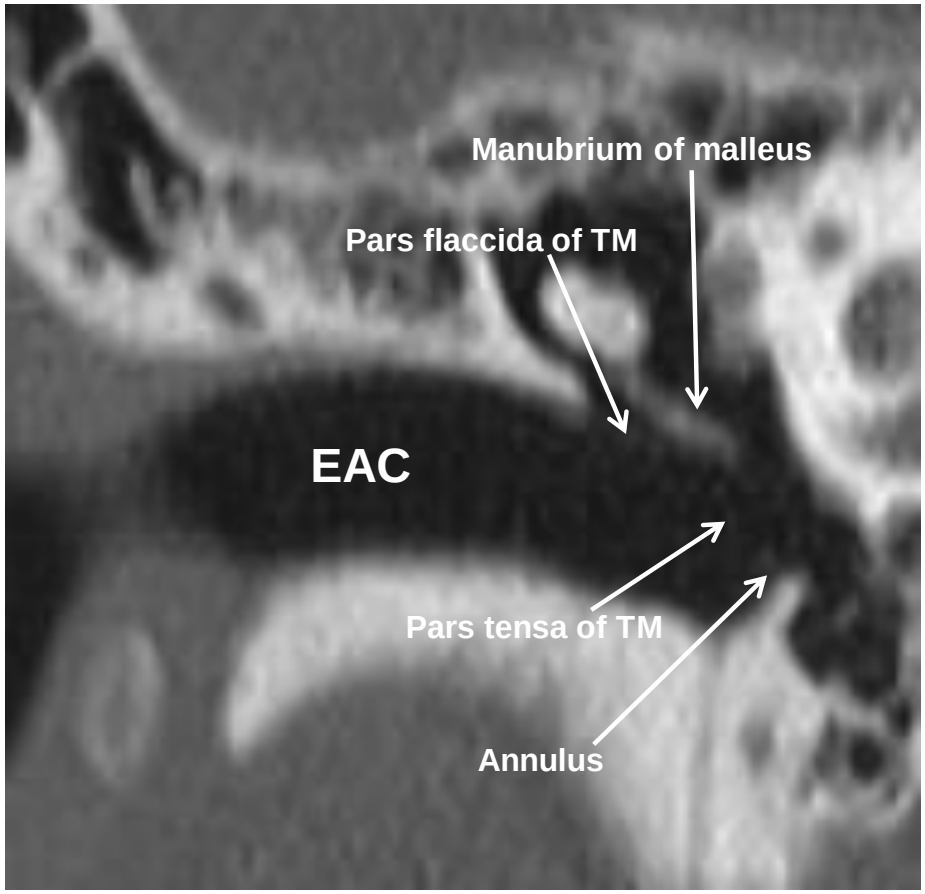

- **External auditory canal (EAC)**
  - Fibrocartilaginous (lateral), bony portion (medial)
- **Tympanic membrane**
  - Thin membrane forming medial boundary of EAC
  - Manubrium of malleus attached to TM
  - **<u>Pars flaccida</u>**

    : Superior-anterior portion of tympanic membrane

    : Triangular thin lax zone by notch of Rivinus

    : Under the scutum
  - **<u>Pars tensa</u>**

    : Remaining inferior portions of tympanic membrane

3. Major congenital abnormalities

- Inner ear abnormalities : 30%
  - Due to developmental arrest during embryogenesis
    : From otic placode & vesicle
  - Bilateral in 65%
  - Membranous labyrinthine abnormality in 80%
    : Scheibe dysplasia, Siebenmann-Bing
  - **Combined bony labyrinthine abnormality in 20%**
    → Radiologically detectable on CT / MRI
- External & middle ear abnormalities : 60%
- Complex type : 10%

Cochlear Anomalies

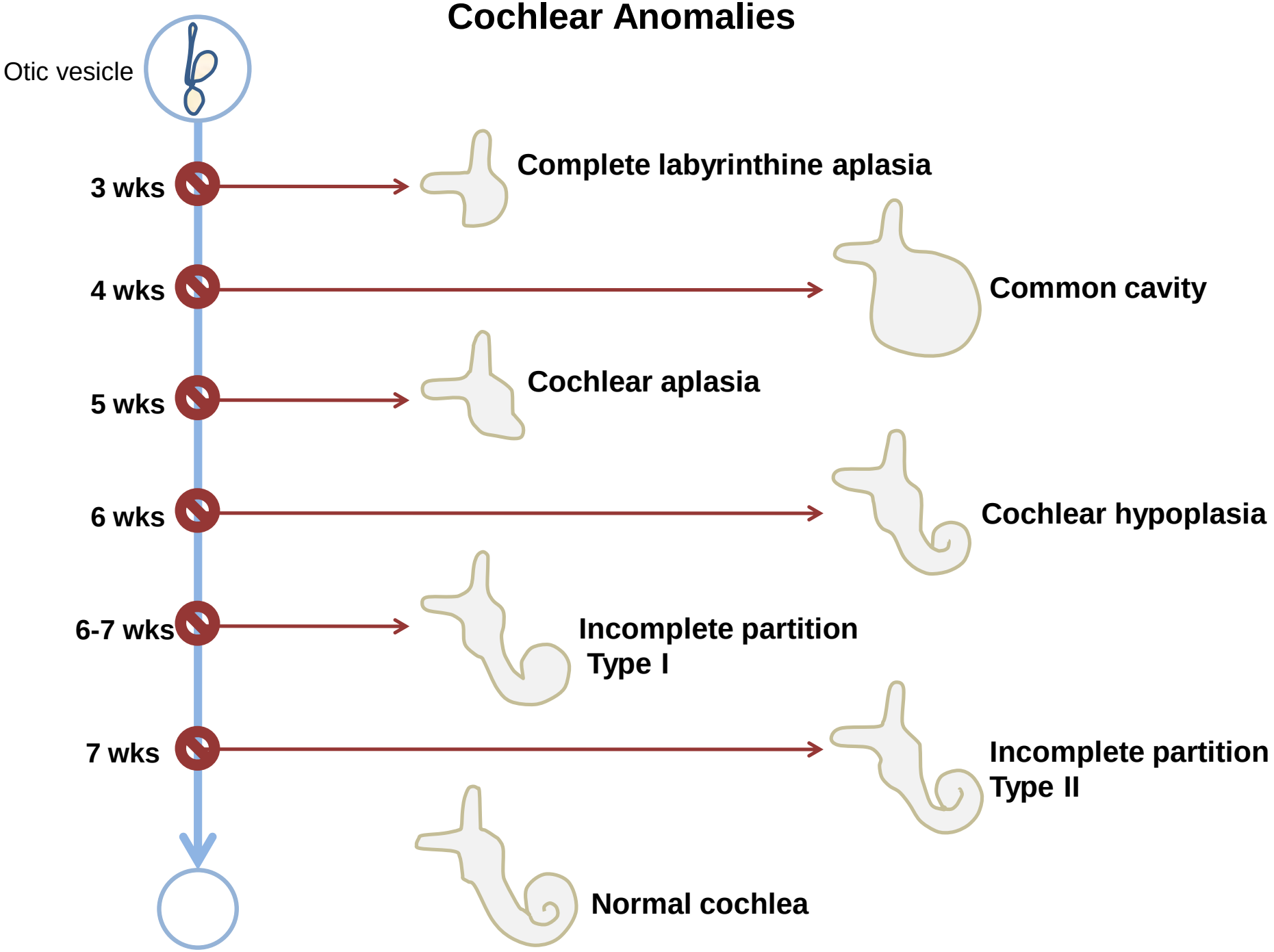

1) Inner ear abnormalities (Cochlear)

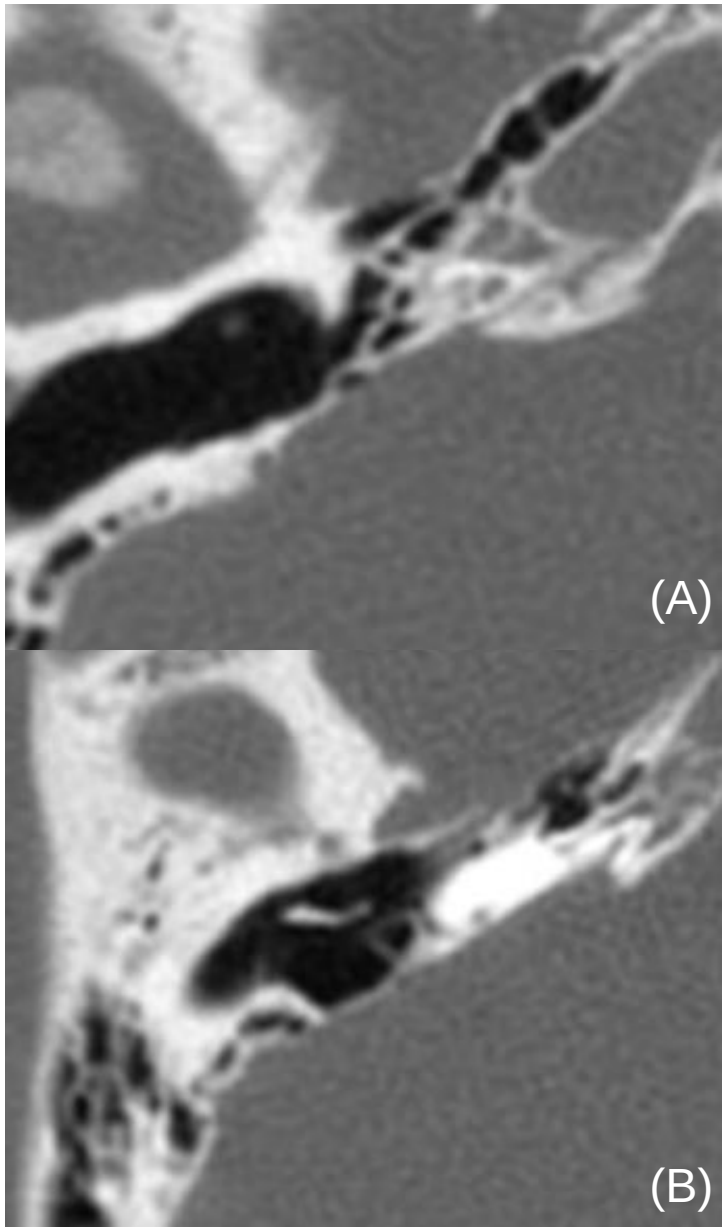

- **Complete labyrinthine aplasia (Michel's aplasia)**

Michel's aplasia

Axial CT scans (A, B) showed near complete absence of the differentiated inner ear structures including cochlea and vestibule. Note hypoplastic petrous bone.

: Single / several cystic cavity in place of inner ear

1) Inner ear abnormalities (Cochlear)

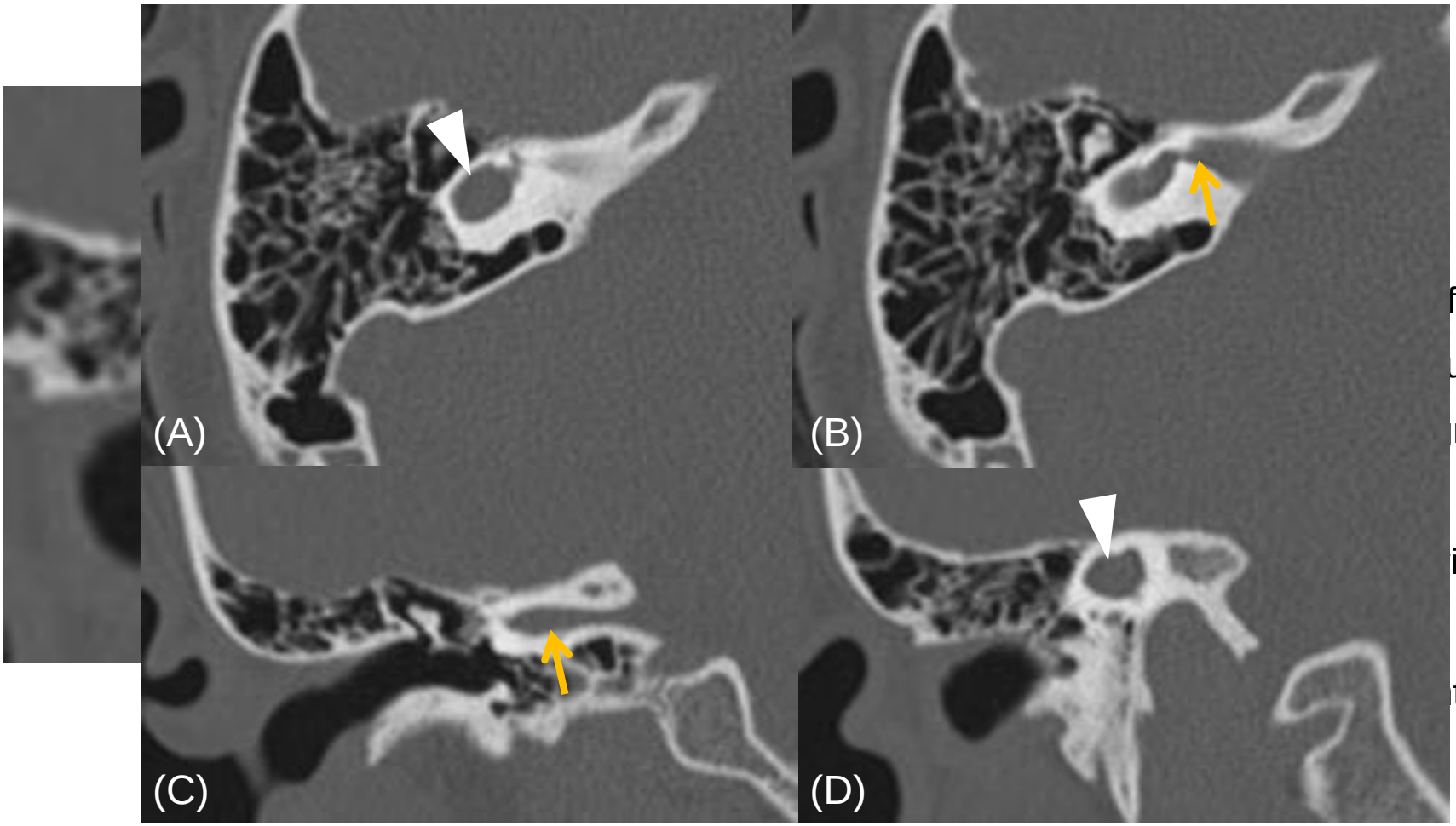

f GA
ule
nosis
ity
tal)

15/M, Common cavity type of cochlear-vestibular malformation.
Axial (A, B) and coronal (C, D) CT scans presented no distinct cochlea, vestibule, and semicircular canals and It formed large common cavity (White arrowheads). The single cavity structure showed connection with IAC (Yellow arrows). Note that there was not any cochlear structure anterior to the IAC, where the cochlea is normally situated.

1) Inner ear abnormalities (Cochlear)

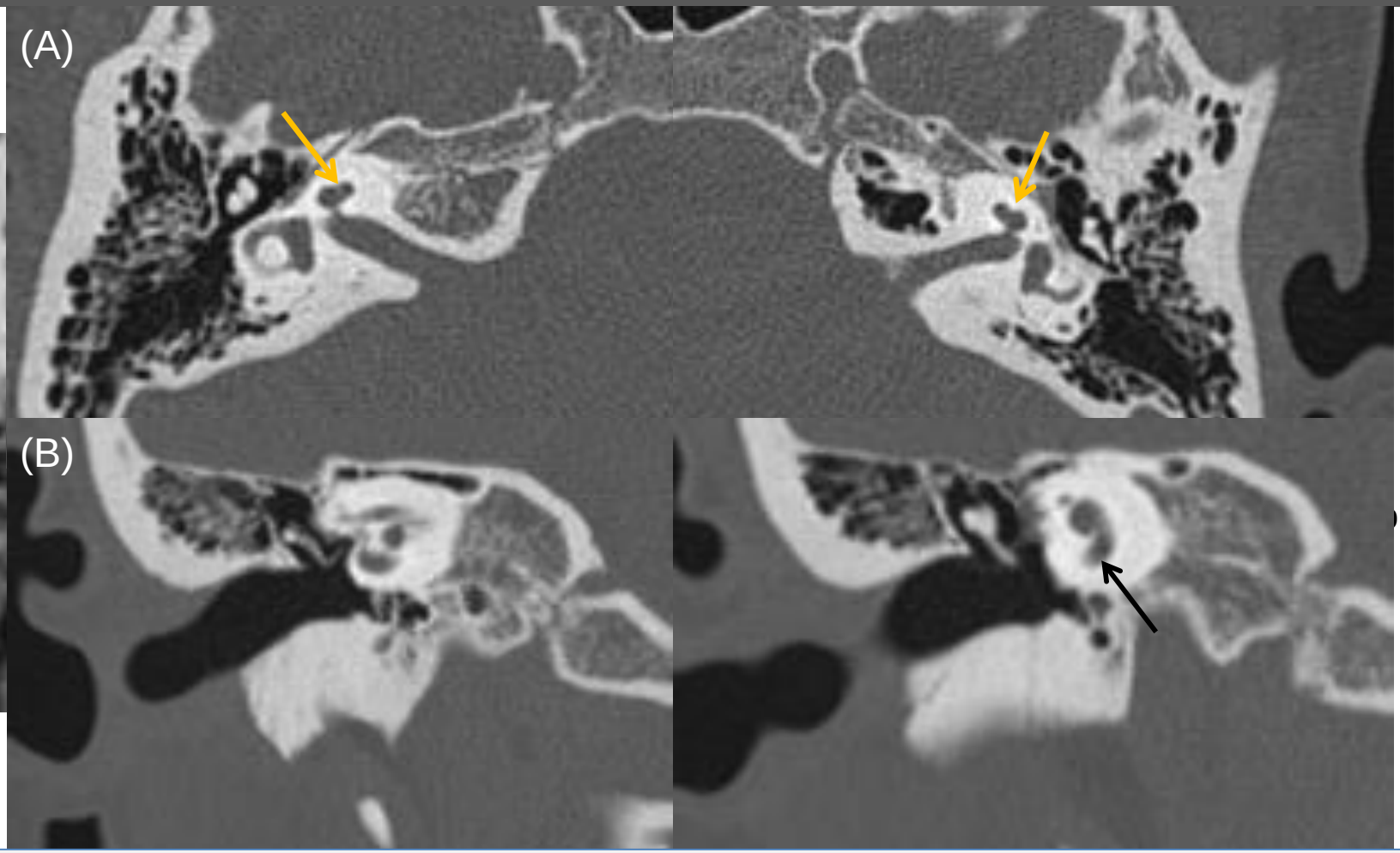

16/F, Cochlear hypoplasia.
On axial (A) and coronal (B) CT scans, aplastic apical turns of cochlea could be recognized in both sides (Yellow arrows in A). There were also reduced maximal dimension of basal turns (Black arrow in B).

1) Inner ear abnormalities (Cochlear)

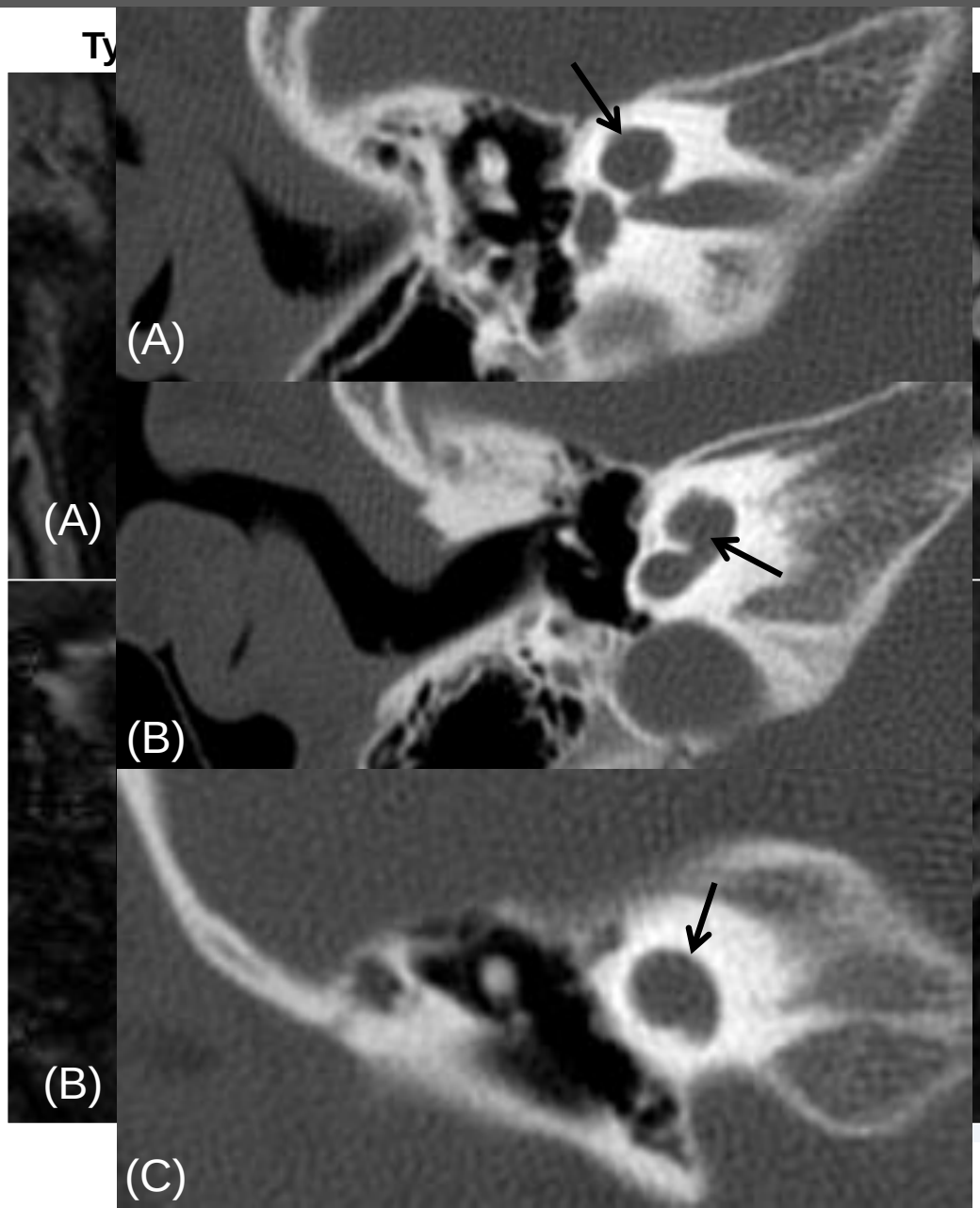

34mo/M, Bilateral Mondini dysplasia and large vestibule

On axial (A, B) and coronal (C) CT scans, the right cochlea showed shortening along its modiolar axis. The interscalar septum was not also visualized.

1) Inner ear abnormalities (Vestibular)

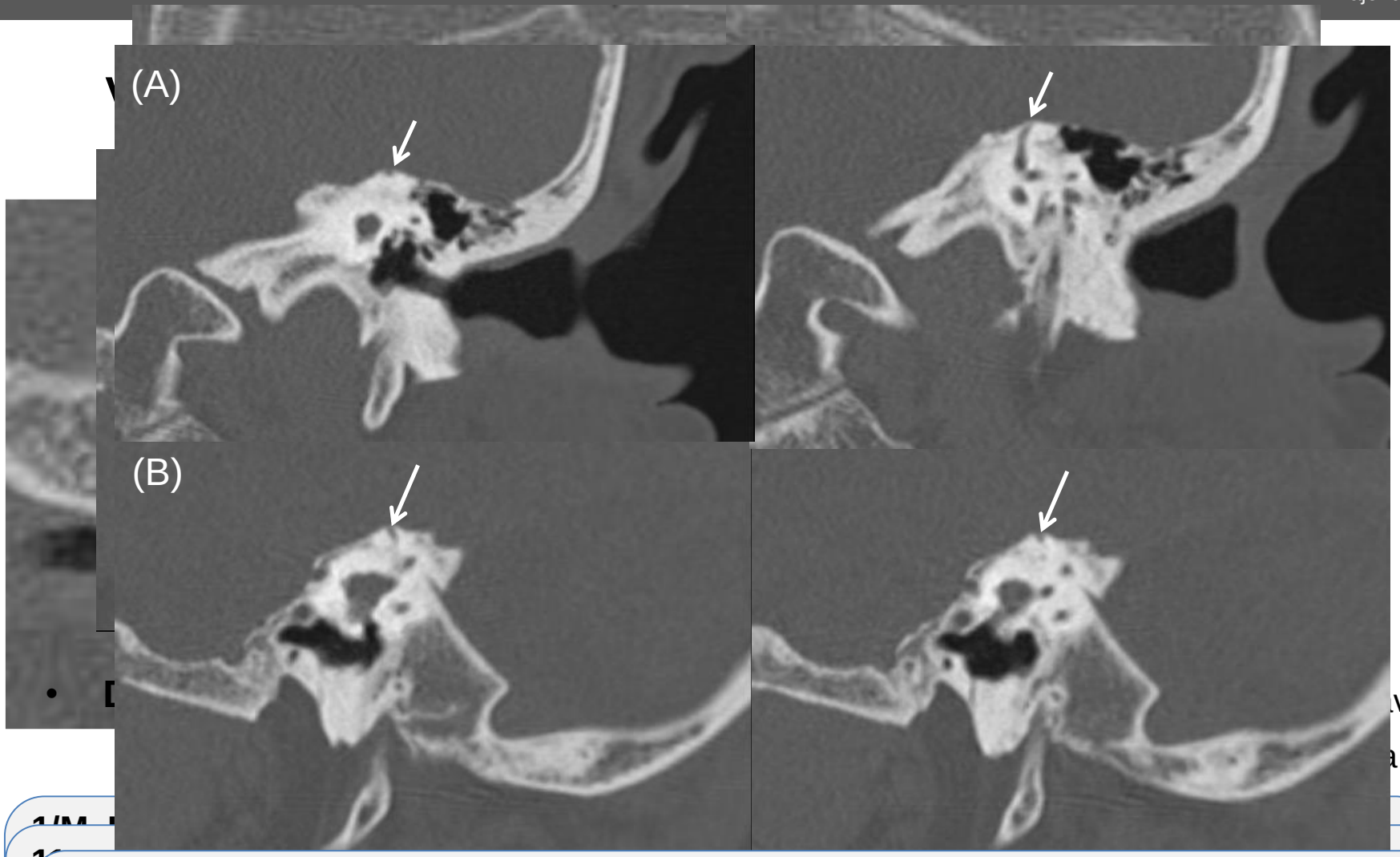

19/F, SCC dehiscence
On coronal(A) and sagittal (B) CT scans, there was bony dehiscence of the left superior semicircular canal (Arrows). She suffered from sound-induced dizziness.

1) Inner ear abnormalities (Aqueduct)

Aqueductal anomaly

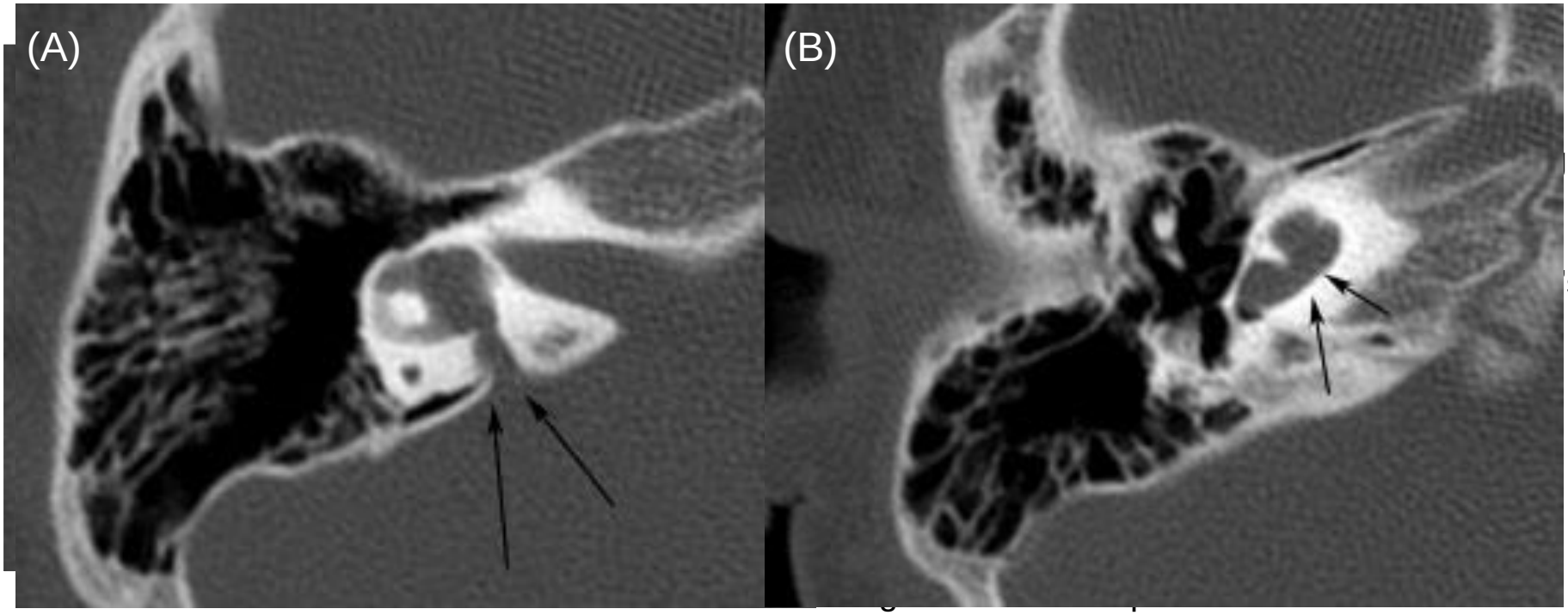

3/F, Mondini dysplasia with enlarged vestibular aqueduct.

On axial CT scans (A and B), the vestibular aqueduct (Arrows in A) was enlarged and widely opened, larger than normal posterior SCC. In addition, insufficient cochlear turns (Arrows in B) were also noted, suggesting Mondini dysplasia.

1) Inner ear abnormalities (IAC)

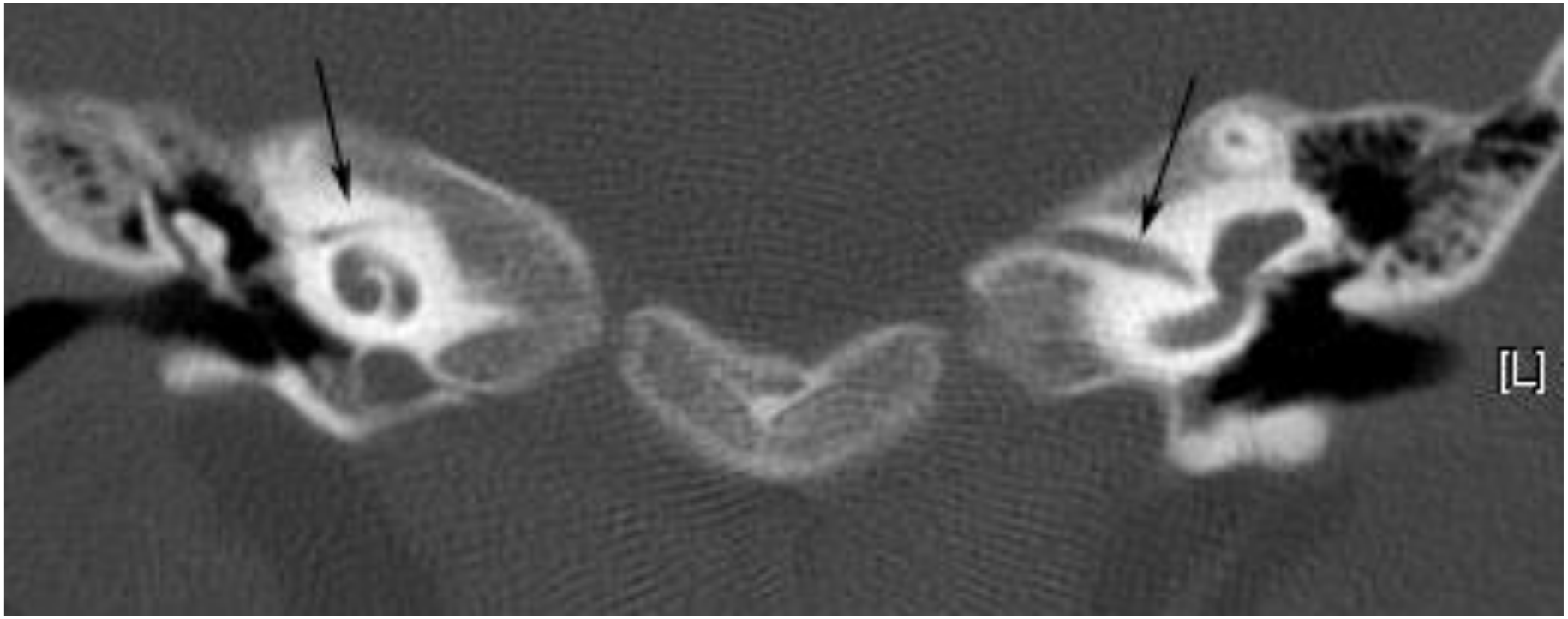

12mo/F, Bilateral small IAC

Coronal CT scan showed narrowed bilateral internal auditory canals (Arrows), measuring maximal diameter of 1.3 mm in right side and 1.6 mm in left side (Normal range : 2 – 8 mm). She had sensorineural hearing loss on both sides.

2) Middle ear abnormalities

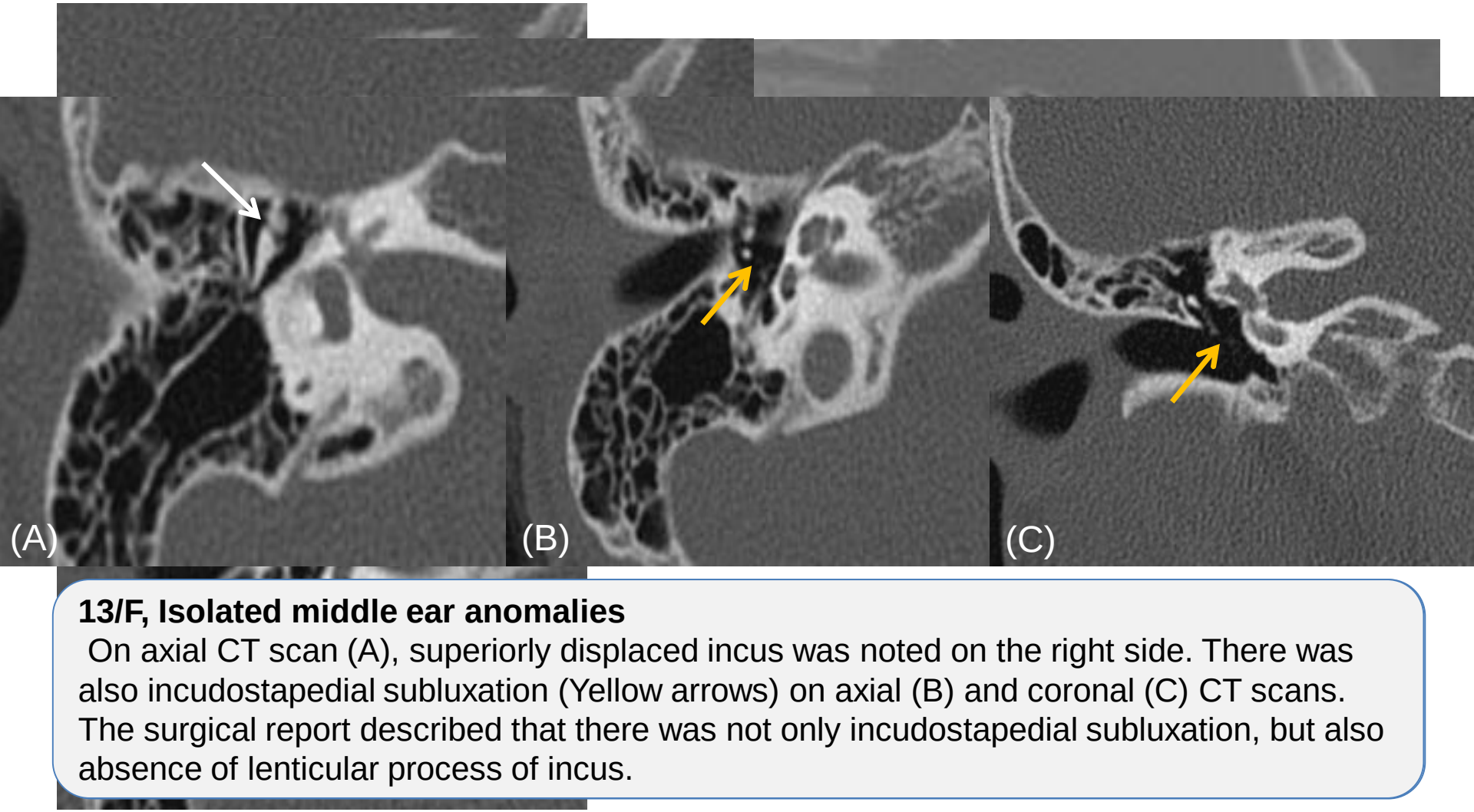

13/F, Isolated middle ear anomalies
On axial CT scan (A), superiorly displaced incus was noted on the right side. There was also incudostapedial subluxation (Yellow arrows) on axial (B) and coronal (C) CT scans. The surgical report described that there was not only incudostapedial subluxation, but also absence of lenticular process of incus.

3) External ear abnormalities

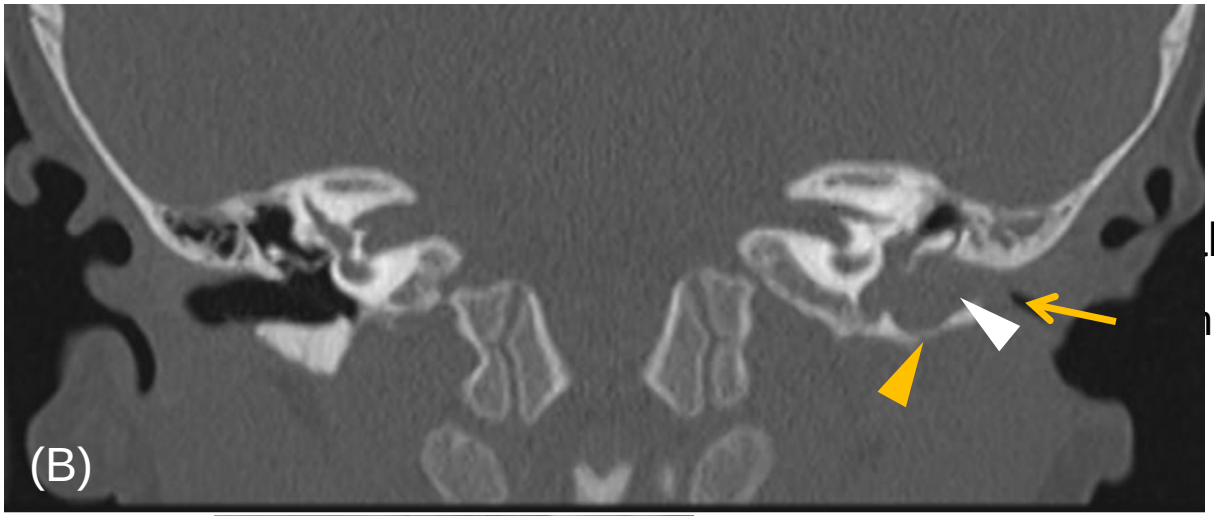

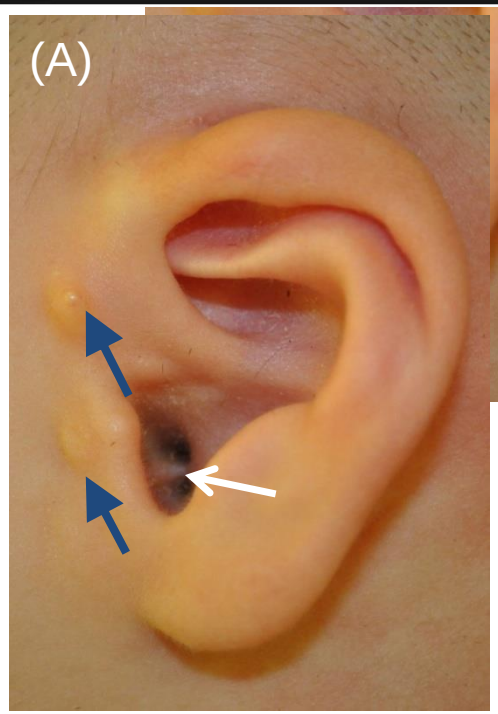

2/F, Left bifid orifice and stenosis of EAC with cholesteatoma

She had bifid orifice (White arrow in A) in EAC and skin tags (Blue arrows in A) in external ear. Coronal CT scan (B) showed atresia of left external auditory canal (Yellow arrow) with inner soft tissue density (White arrowhead), accompanying adjacent bony erosion of EAC (Yellow arrowhead). On diffusion-weighted image of MRI (C), the lesion showed diffusion restriction (White arrowhead), suggesting cholesteatoma in EAC and middle ear cavity.

4. Take home notes

- Temporal bone is one of the most elaborate and complicated structure in human body
- Development of the temporal bone
  - Inner ear –Neuroectoderm to cochleovestibular apparatus
  - Middle & external ear – 1st & 2nd branchial arches and pouch
  - Vestibular aqueduct – Last embryogenic structure, when enlarged, high suspicion for other inner ear abnormalities
- Knowledge of embryology of temporal bone assists understanding various congenital anomalies

References

- Peter M. Som, Hugh D. Curtin. Head and Neck Imaging. 4th edition. Mosby-Elsevier, 2003.
- T.W. Sadler. Langman's Medical Embryology. 13th edition. Wolters Kluwer. 2014.
- Swartz J, Loevner L. Imaging of the temporal bone. 4th edition. Thieme. 2009.
- Lorenz J, Bonell H, Liebl M, et al. CT of the normal temporal bone: Comparison of multi and single-detector row CT. Radiology. 2005; 235(1):133-141.
- Robson CD. Congenital hearing impairment. Paediat Radiol 2006;36:309-24.
- Jackler RK, Luxford WM, House WF. Congenital malformations of the inner ear: a classification based on organogenesis. Laryngoscope 1987;97:2-14.
- McClay JE, Tandy R, Grundfast K, et al. Major and minor temporal bone abnormalities in children with and without congenital sensorineural hearing loss. Arch Otolaryngol Head Neck Surg. 2002 Jun;128(6):664-71.
- Sennaroglu L, Saatci I. A new classification for cochleovestibular malformations. Laryngoscope 2002;112:2230-41.
- Rogers B. Anatomy, embryology and classification of auricular deformities. In: Tanzer R, Edgerton M, eds. Symposium on Reconstruction of the Auricle. St Louis, Mo: Mosby; 1974;10:3–11

Dual Energy Computed Tomography (DECT) For the Pediatric Radiologist: Tools to Incorporate Into Clinical Practice

Erica L Riedesel MD, FAAP [1,3] ; Ross T Christopher MD[2] ;
Sarah Sarvis Milla MD, FAAP [1,2,3] ; Stephen F Simoneaux MD, FACR [1,3]

1. Department of Radiology and Imaging Services, Emory University School of Medicine, Division of Pediatric Radiology;
2. Department of Radiology and Imaging Services, Emory University School of Medicine, Division of Neuroradiology;
3. Department of Pediatrics, Emory University School of Medicine

Disclosures

- E. Riedesel - No disclosures
- R. Christopher – No disclosures
- S. Milla – No disclosures
- S. Simoneaux – No disclosures

Learning Objectives

1. *Dual Energy CT* (DECT) basics
2. *Renal stone composition analysis*
3. *Bone subtraction imaging*
4. *Iodine material specific images*
5. *Virtual monochromatic imaging*

Dual Energy CT (DECT) – The Basics

- *What* is Dual Energy CT (DECT)?
  - Two sets of images acquired at both high- and low-energy spectra
  - Also called “multi-energy” or “spectral” CT

- Different approaches to DECT image acquisition

Dual Source

- Two independent x-ray tubes
  - Low = 70-80 kVp
  - High = sn140 – 150 kVp
- Two detector arrays

Rapid kV switching

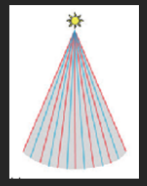

- Single x-ray tube
  - Rapidly alternates from low (80 kVp) to high (140 kVp) energies during gantry rotation
- Single detector

Dual-layer Detector

- Single x-ray tube
  - High = 120 kVp
- Single multi-layered detector
  - Separate low and high energy photons

Split Filter System

- Single x-ray tube
  - Gold (au) and Tin (sn)
  - Splits beam into two energies before reaching patient
- Single detector

Dual Energy CT (DECT) – The Basics

- *WHY* image at two different energies?
- Different materials (e.g. *calcium* , *fat*, *iodine contrast*) have unique k-edge characteristics → result in differential Hu on CT
  - Linear attenuation coefficient values are different at low and high keV
  - By evaluating HU at low and high energy we can more effectively separate different materials in the body

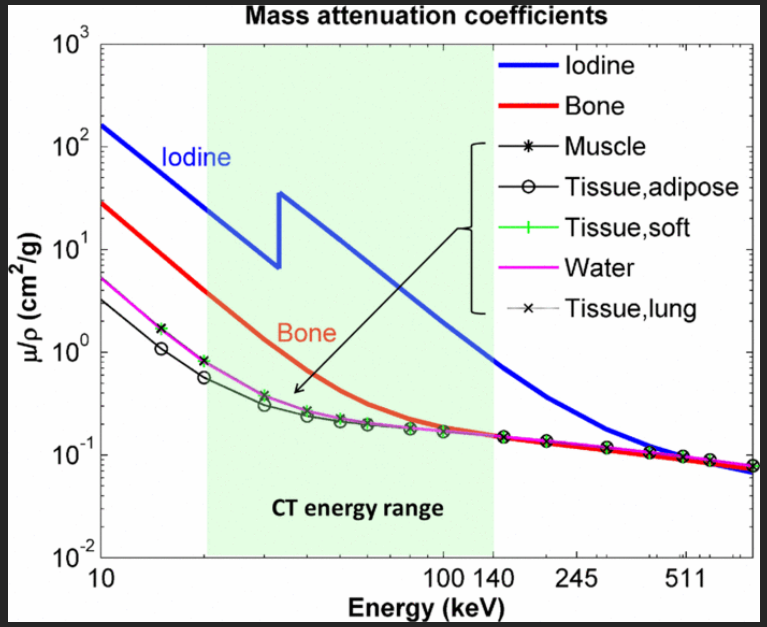

Attenuation values of MATERIALS in the body change at different energies

Dual Energy CT – The Basics

- *Material composition analysis*
  - Materials are differentiated based on attenuation characteristics
  - Several ways to utilize:
    - *"Characterize an unknown structure"* (eg. Renal stone composition)
    - *"Isolate and remove material "* (e.g. Bone subtraction, virtual non-contrast)
    - *"Isolate and overlay material "* (e.g. Iodine selective overlay)

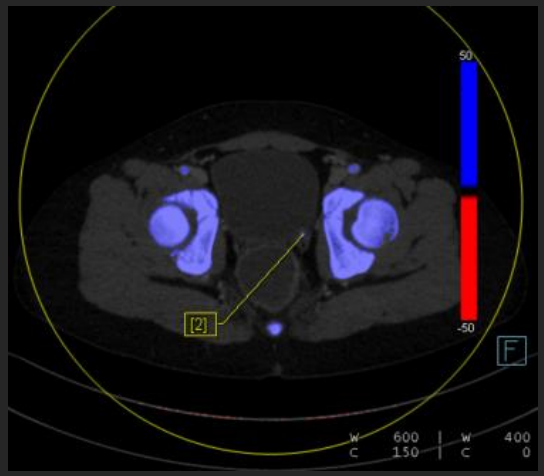

Renal Stone Composition

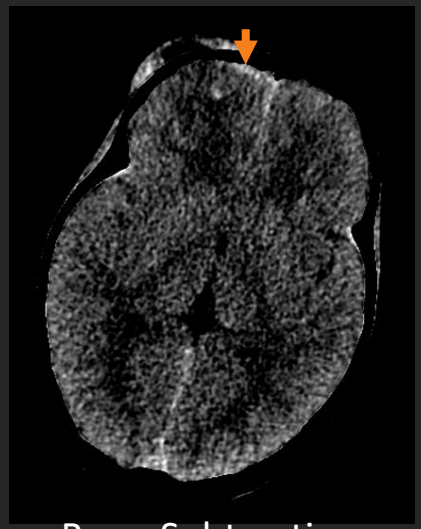
Bone Subtraction

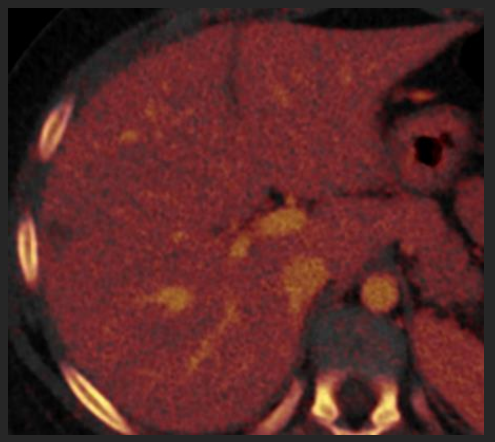
Iodine Selective Overlay

Dual Energy CT – The Basics

- *Mono-energetic imaging*
  - Extrapolate very low (40 keV) and very high (>150 keV) energy images
    - Low energy → accentuate Iodine-based contrast
    - High-energy → reduce beam hardening artifact from metal hardware

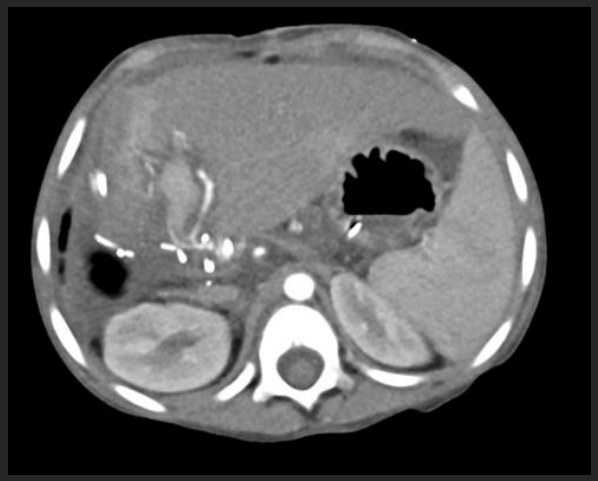

Virtual mono 40 keV

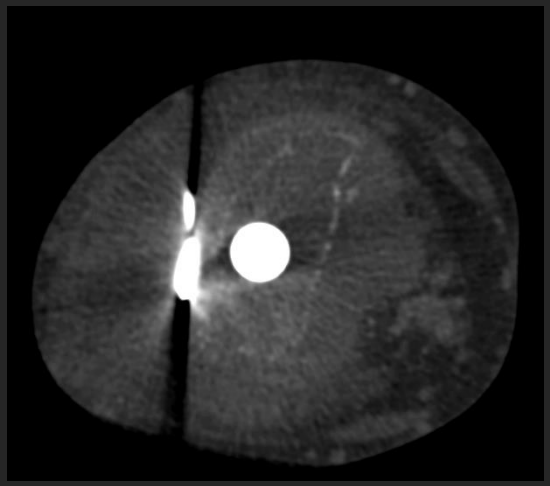

Virtual mono 150KeV

Dual Energy CT (DECT) – Radiation Exposure

- *In adults*
  - Evidence that radiation exposure of DECT is *equivalent* to conventional single energy 120 keV images

- *In pediatrics*
  - Evidence that optimized scanner technology allows DECT to deliver *equivalent* or *smaller* radiation exposure than conventional single energy CT
    - 2016 – Zhu et al. *Dual-energy compared to single energy CT in pediatric imaging: A phantom study for DECT clinical guidance.* Pediatr Radiol (2016) 46: 1671-1679
    - 2019 – Weinman et al. *Dual energy head CT to maintain image quality while reducing dose in pediatric patients.* Clinical Imaging (2019) 55: 83-88.

DECT – Incorporate Into Clinical Practice

- *How* to use DECT?

- Many clinical applications of DECT can be incorporated into daily clinical practice of Pediatric Radiology
  1. Renal stone evaluation
  2. Trauma imaging → Head CT
  3. Trauma imaging → Abdomen/Pelvic CT
  4. Vascular imaging → Neuro, Body, Chest
  5. Orthopedic imaging → Orthopedic hardware evaluation

DECT – Renal Stone Imaging

- *~70% of pediatric patients have urinary metabolic abnormality*
  - Jackson EC and Avendt-Reeber M. *Urolithiasis in Children – Treatment and Prevention*. Curr Treat Options Peds (2016) 2: 10-22.

- All children diagnosed with renal stone are evaluated for underlying stone composition
  - Serum electrolytes with serum calcium and phosphorus
  - 24 hour urine collection

- Stone composition affects both treatment and prevention strategies

- Common stones seen in pediatrics:
  - Uric Acid (5%)
  - Non-Uric Acid
    - Hydroxyapatite (~80%)
    - Calcium oxalate
    - Cystine
    - Struvite

DECT – Renal Stone Imaging

- If CT performed, *DECT* can add stone composition analysis
  - X-ray attenuation profile of the predominant materials within stones (hydroxyapatite, oxalate, cystine, uric acid) are significantly different at high and low kV
  - ROI drawn on renal stone is plotted on chart to determine stone composition

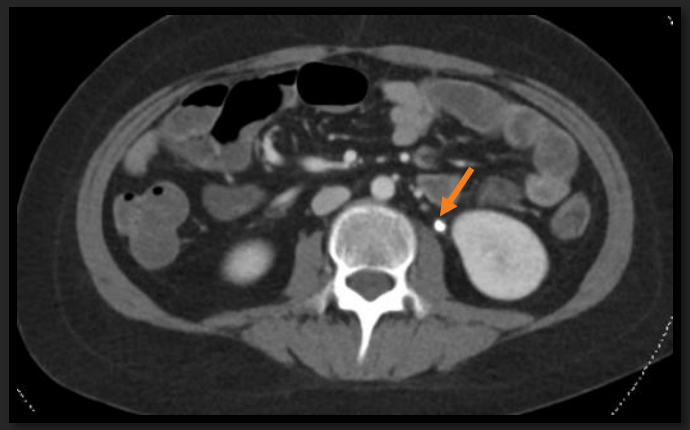

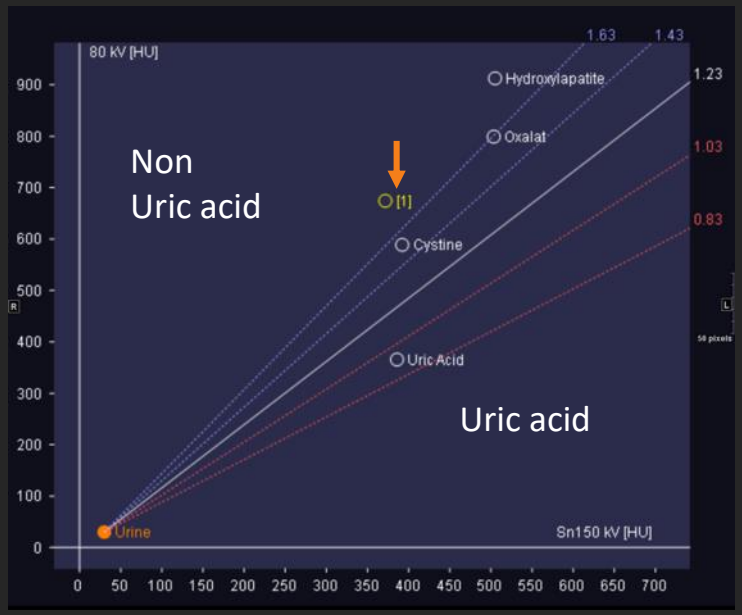

18 yo male, flank pain and hematuria

- Left hydronephrosis on ultrasound
- Hyperdense stone in the proximal LEFT ureter

DECT – Renal Stone Imaging

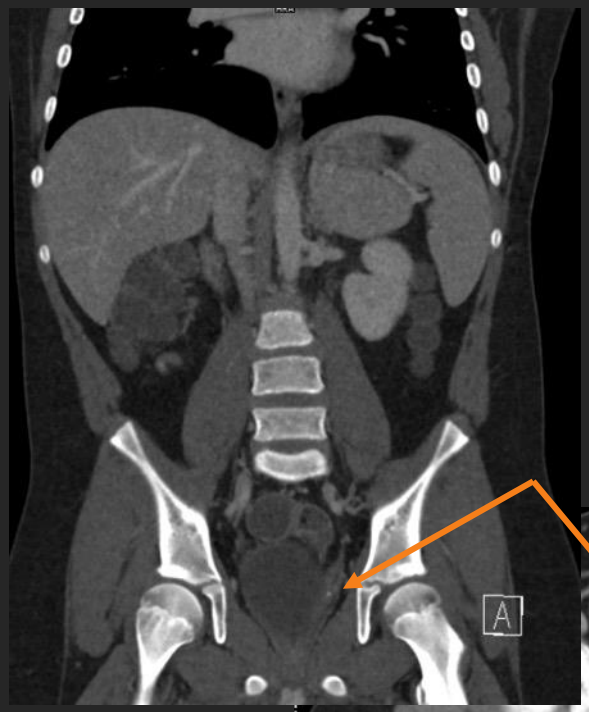

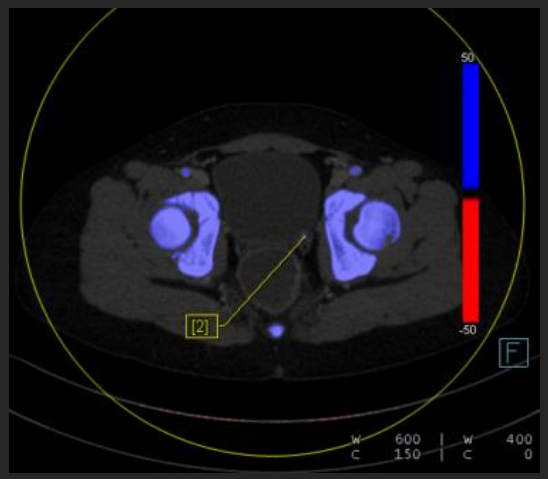

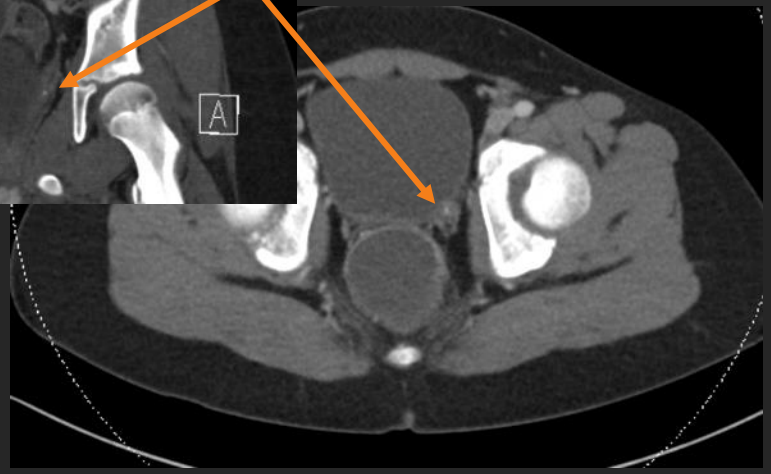

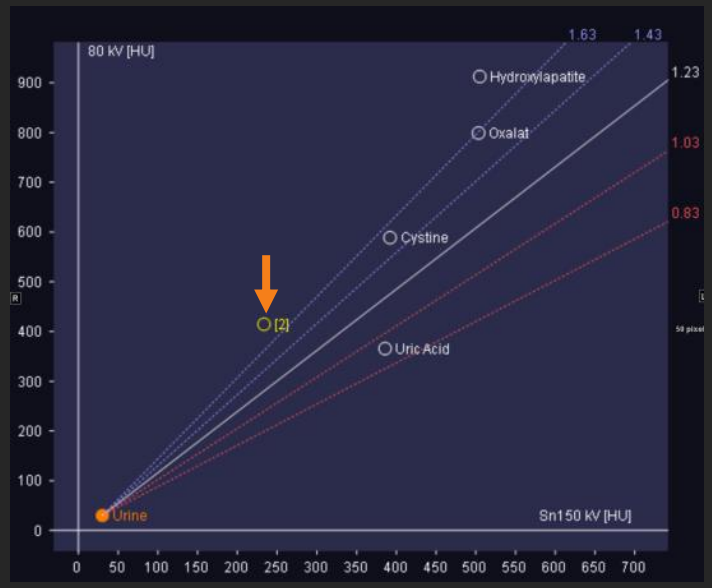

Stone composition analysis with DECT demonstrates non-uric acid stone

11 yo male; hematuria

DECT – Renal Stone Imaging

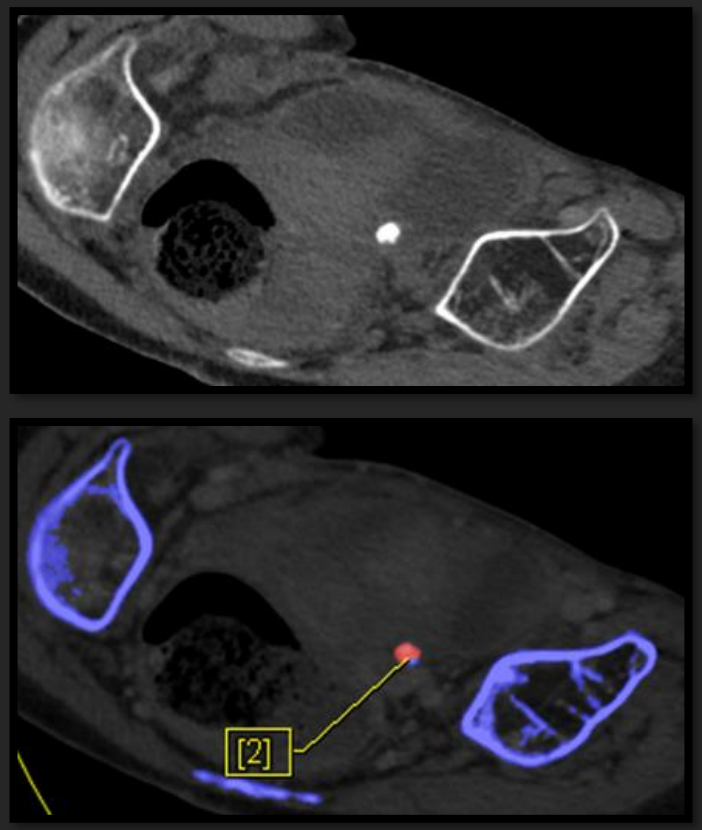

16 yo male with abdominal pain

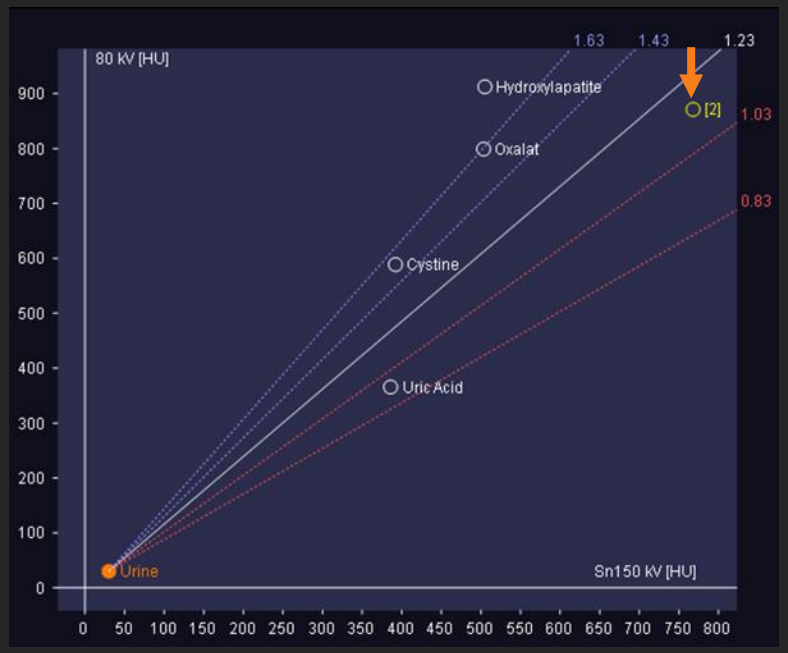

Stone analysis shows mixed composition, likely partially urate stone

DECT – Trauma Imaging(Neuro CT)

- *Non-contrast head CT* is the *recommended imaging study* for evaluation of head trauma in children
  - Acute hemorrhage higher density than normal brain parenchyma
  - However, small acute extra-axial hemorrhage adjacent to bone may be easily missed due to its size and similar density to bone

- *DECT* material composition analysis can be used to virtually *"subtract" bony calvarium*, increasing conspicuity of acute hemorrhage
  - Recent study in *Emergency Radiology* demonstrated Bone Subtraction CT images were significantly superior to simulated standard CT images in detecting small epidural/subdural hemorrhage
    - Naruto N et al. *Dual-energy bone removal computed tomography (BRCT): preliminary report of efficacy of acute intracranial hemorrhage detection. Emerg Radiol 2018(25): 29-33.*

DECT – Trauma Imaging(Neuro CT)

- 9 yo male, MVC with altered mental status

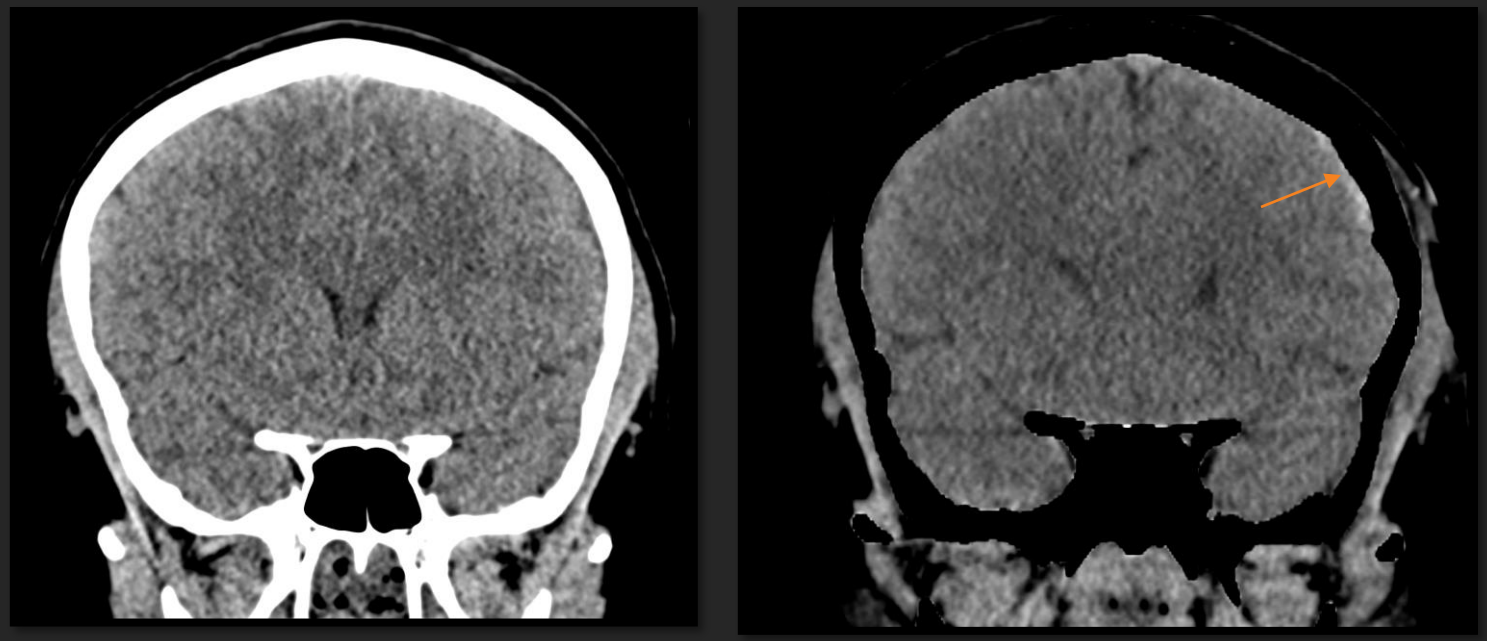

Bone subtraction increases conspicuity of small left frontal subdural hematoma.

DECT – Trauma Imaging(Neuro CT)

5 yo Female; fall with scalp hematoma

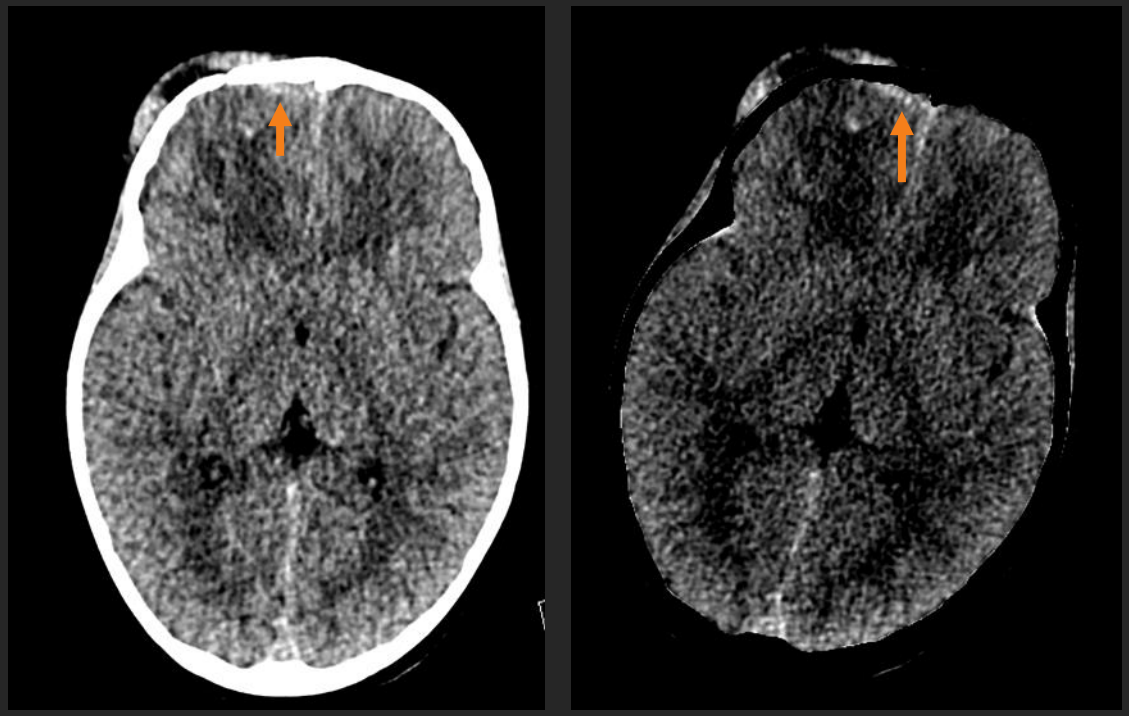

Trace subdural hemorrhage along the right frontal calvarium (→) could be mistaken for cupping artifact, but persists and is more conspicuous on bone-subtracted images.

DECT – Trauma imaging (Abdomen/Pelvic CT)

- CT plays an important part of the workup of pediatric patients with blunt abdominal and pelvic trauma
  - Identification of solid-organ and hollow-visceral injury
    - Spleen
    - Liver
    - Kidneys
    - Bowel

- *DECT* material composition analysis can be used to generate *iodine-selective imaging* can increase conspicuity of traumatic injuries making them easier to detect and categorize and assist in evaluation of active contrast extravasation

DECT – Trauma imaging (Abdomen/Pelvic CT)

- *Iodine Selective Imaging* provides qualitative assessment of contrast media distribution in solid organs, increasing conspicuity of solid organ injury

6 yo female; MVC with abdominal pain and “seatbelt sign”

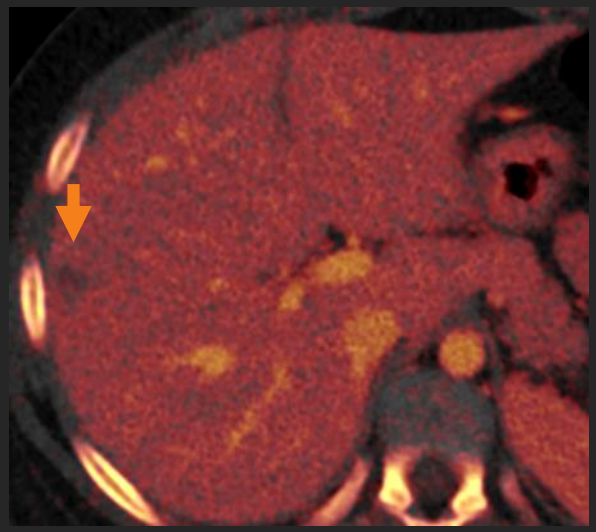

Iodine map increases conspicuity of AAST grade 1 injury right hepatic lobe

DECT – Trauma imaging (Abdomen/Pelvic CT)

8 yo male; MVC trauma with elevated LFTs

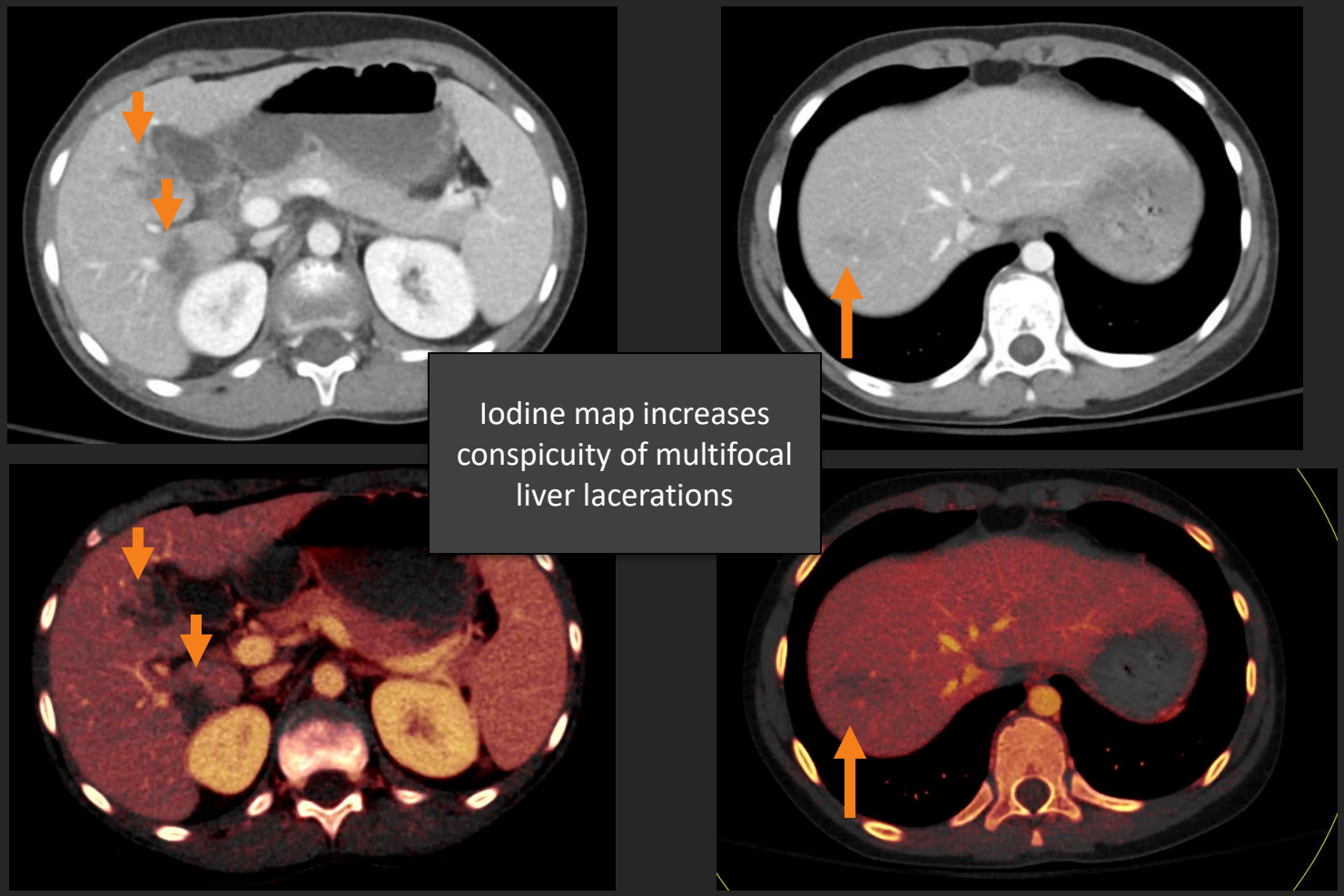

Iodine map increases conspicuity of multifocal liver lacerations

DECT – Trauma imaging (Abdomen/Pelvic CT)

11 yo Female, kicked by horse

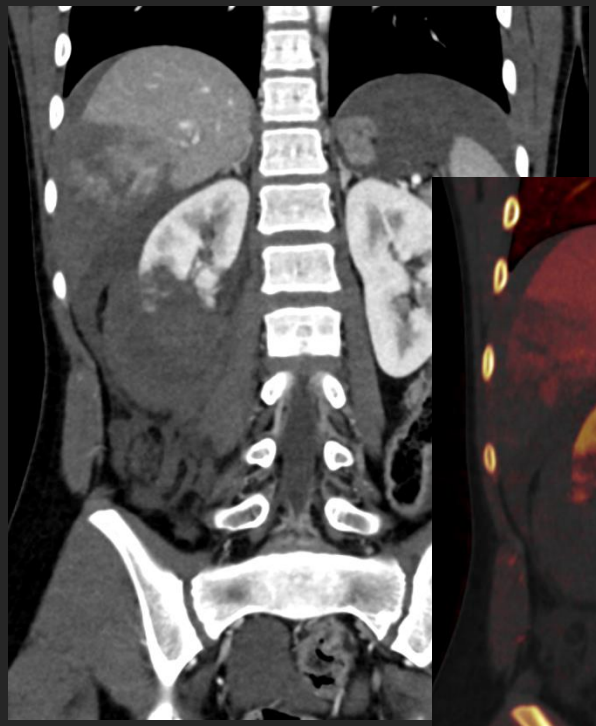

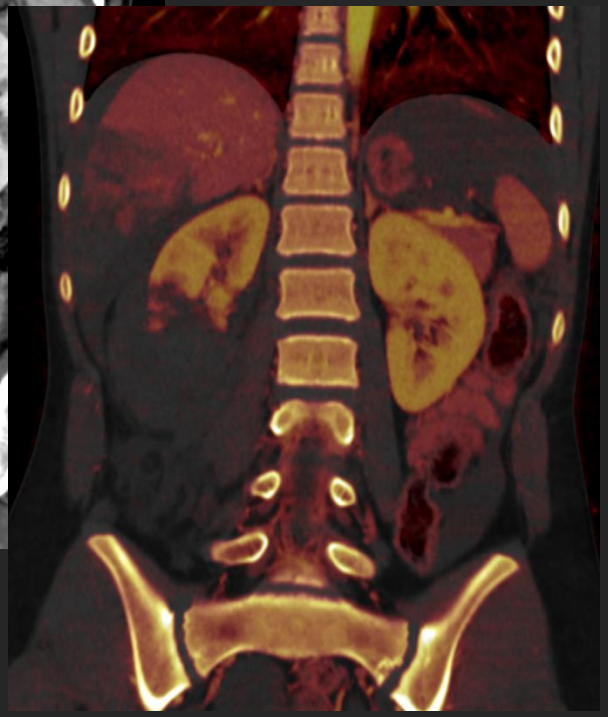

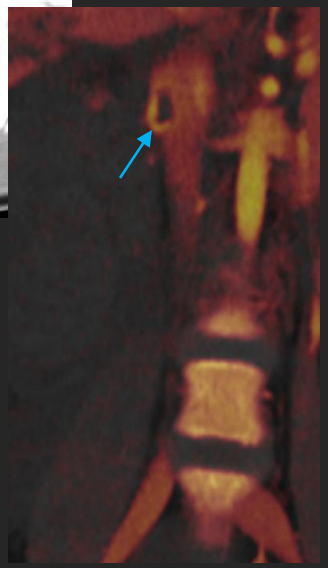

Iodine map also confirms right renal vein thrombus (→).

Grayscale DECT images demonstrate high grade injury of the inferior pole right kidney with large perinephric hematoma. Iodine map confirms lack of perfusion to the affected renal parenchyma (AAST grade 4 injury) and excludes contrast extravasation. Also seen is AAST grade 3 liver injury.

DECT – Trauma imaging (Abdomen/Pelvic CT)

- *DECT* material composition analysis and *virtual monoenergetic images* at *high keV (110-150)* can significantly reduce metal artifacts and improve evaluation of penetrating trauma

15 yo male, GSW to left hip

Virtual monoenergetic images at 150 kV decreases metallic streak artifact from ballistic fragments, improving evaluation of sacral and iliac bone injury

DECT - Vascular imaging

- CT Angiography is routinely used in pediatric patients to evaluate the vascular system

- *DECT* material composition analysis can be used to:
  - Virtually *"subtract"* axial and appendicular skeleton to improve visualization of vessels
  - *Virtual monoenergetic* images improve evaluation of iodine contrast within vessels
  - *Iodine maps* can improve visualization of vessels in situ
  - *Iodine maps* can also be used to evaluate solid organ perfusion

DECT - Vascular imaging

12 yo female, hypertension and elevated renin level

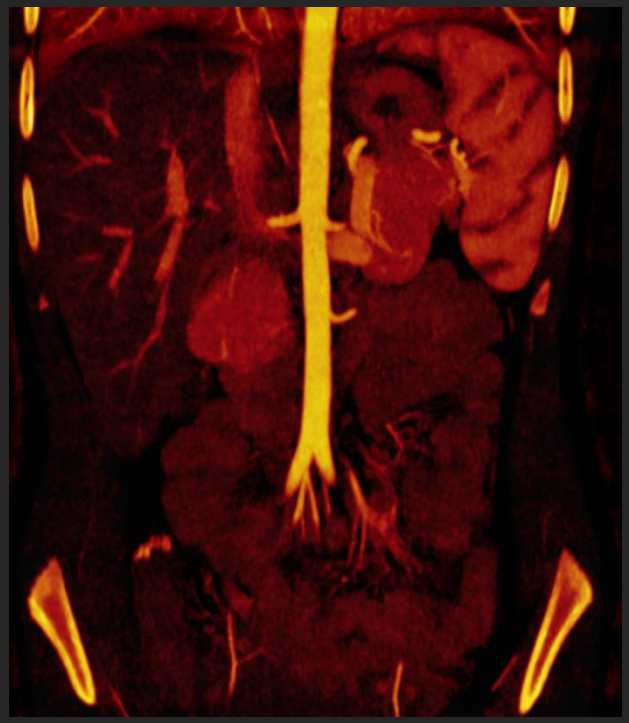

Virtual monoenergetic images at 40 kV and Iodine Map enhances IV contrast conspicuity on abdominal CTA

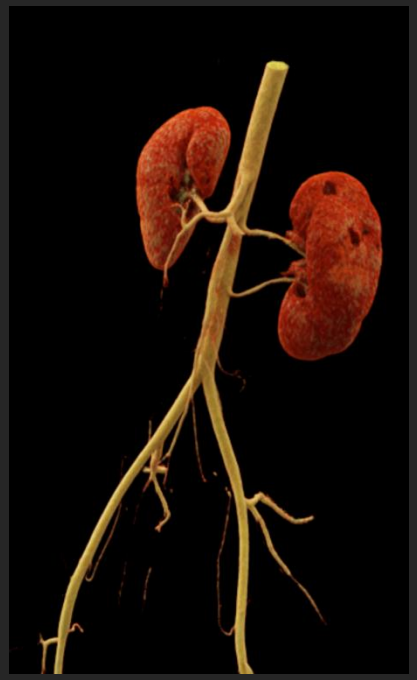

3D rendering with automatic bone removal demonstrates accessory LEFT renal artery, which can be associated with renin-dependent hypertension

Kem DC, Lyons DV, Wenzl J, Halverstadt D, Yu X. *Renin-dependent Hypertension Caused by Non-focal Stenotic Aberrant Renal Arteries – Proof of a New Syndrome*. Hypertension 46; 380-385, 2005.

DECT - Vascular imaging

8 yo F, Gunshot wound (GSW) to the neck

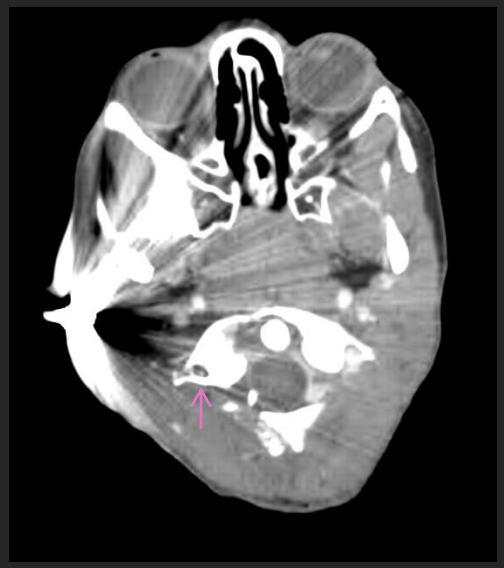

Conventional single energy CT from referring hospital with significant metallic streak artifact from retained ballistic fragment limits evaluation of the right vertebral artery (→)

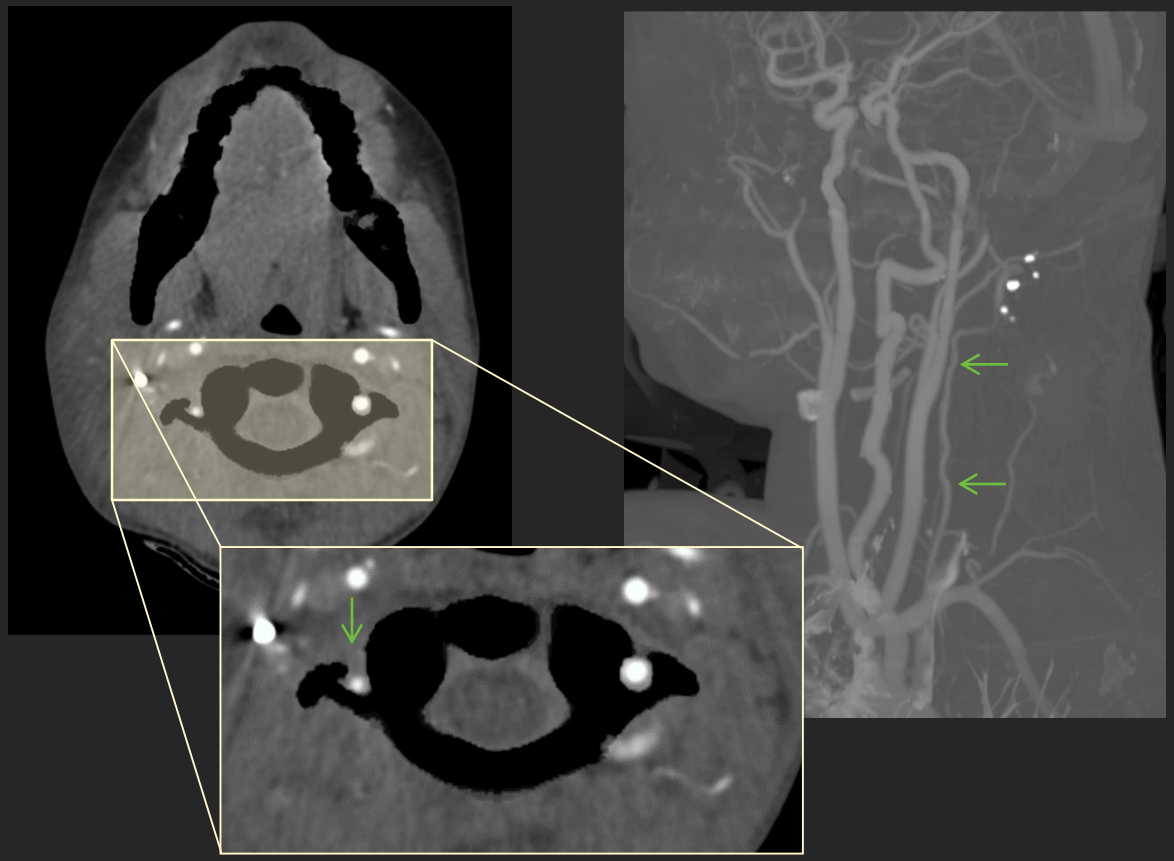

Repeat DECT with bone removal and 3D MIP reformats allows improved visualization of the right vertebral artery (→) and demonstrates Denver grade II vascular injury with >25% luminal narrowing

DECT – Pulmonary Embolus

- Dual-energy CTA is widely used in the evaluation of PE in adult radiology practice
  - Conventional CT angiography provides anatomic information
  - Dual-energy CT allows simultaneous evaluation of *lung vessels* and assessment of *lung perfusion*
    - Perfusion defects seen in 95% of occlusive emboli and in 6%–30% of non-occlusive emboli

- Several studies have shown that perfusion blood volume (PBV) maps can improve detectability of small endoluminal clots in segmental and subsegmental arteries compared with single-energy CT angiography

DECT – Pulmonary Embolus

16 yo female; History of lupus with concern for pulmonary embolism.

- Clot noted on end of dialysis catheter during routine echo.
- Patient reported mid-sternal chest pain and shortness of breath same day.

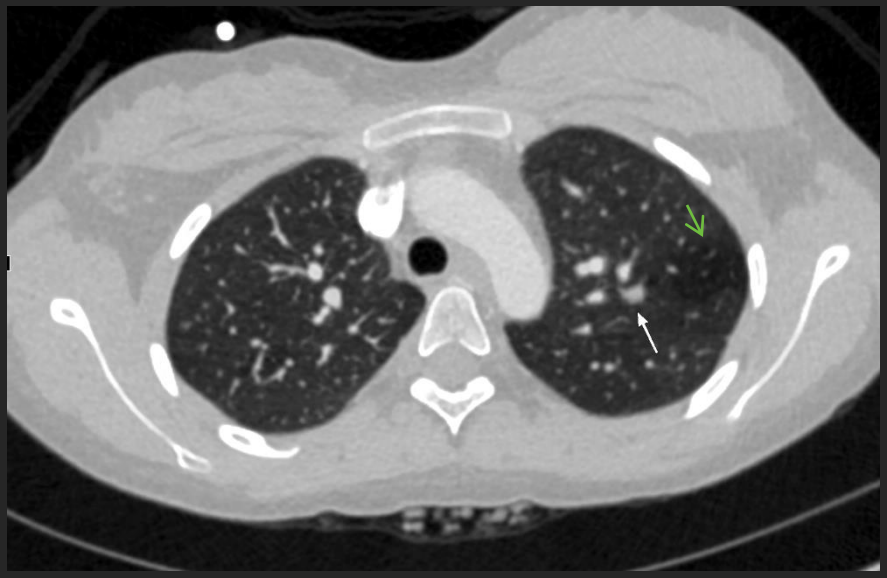

LUL segmental pulmonary artery thrombus (→) and wedge-shaped region of parenchymal oligemia (→)

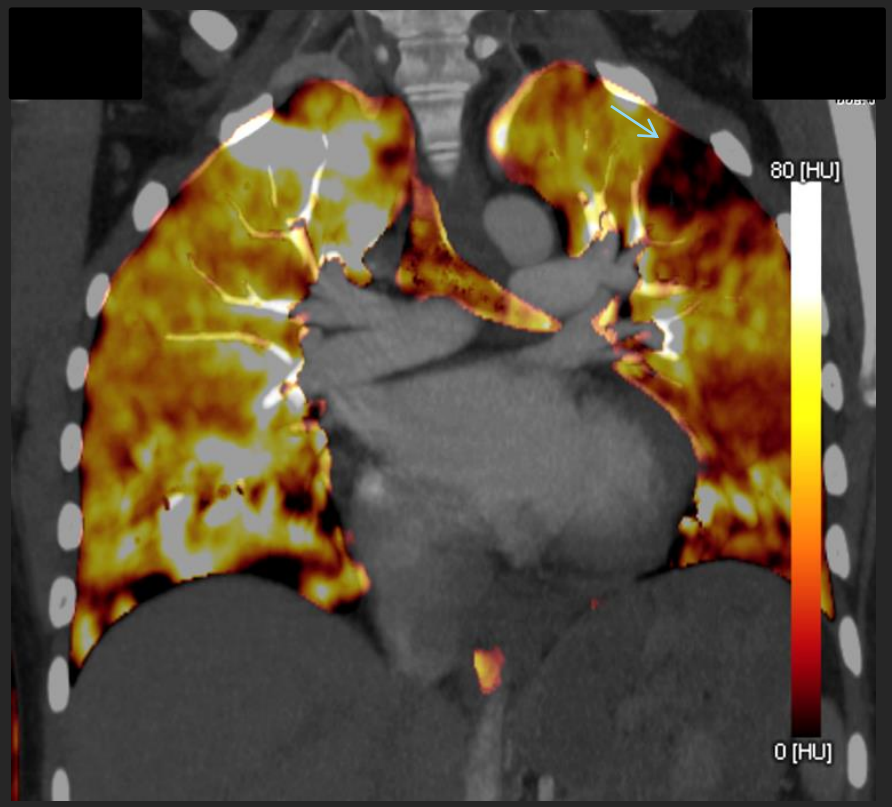

Lung perfusion reformats demonstrate peripheral wedge-shaped defect (→) that corresponds to region of oligemia on grayscale images

DECT – Pulmonary Embolus

- In patients with pulmonary emboli, dual-energy CT perfusion defects have shown good correlation with scintigraphic VQ and SPECT findings

17 yo female; known chronic PE

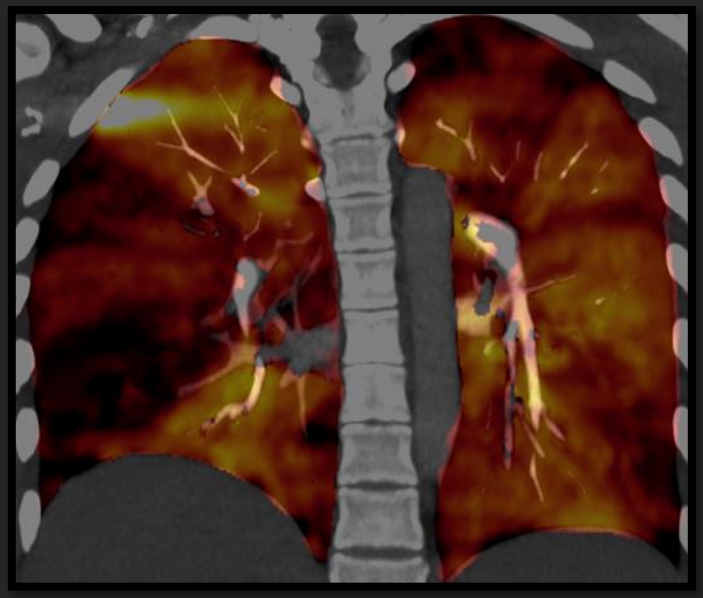

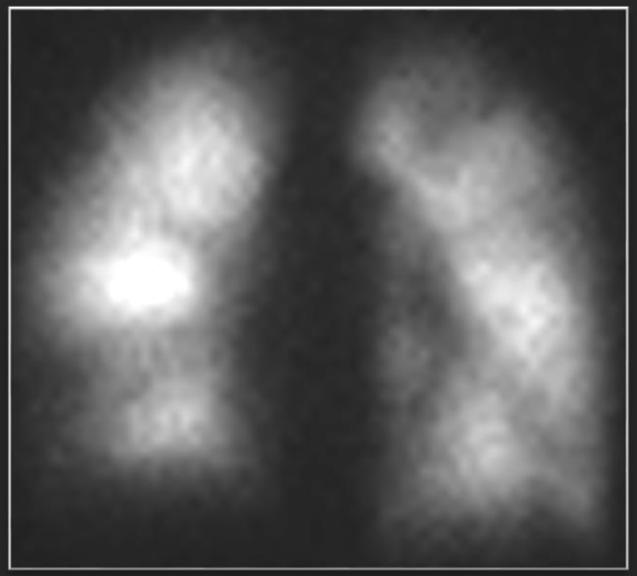

Iodine map and VQ scan performed on the same day show near-identical findings. The pulmonary emboli were no longer visible on CTPA.

DECT – Orthopedic Imaging

- Cross-sectional imaging (CT and MRI) are routinely used for evaluation of pediatric musculoskeletal pathology

- Metallic hardware can cause significant artifact on CT from beam-hardening and photon-starvation effects which degrades image quality, obscures adjacent structures, and decreases diagnostic value of exam

- *DECT virtual monoenergetic images* at *high keV (110-150)* can significantly reduce metal artifacts and improve image quality

DECT – Orthopedic Imaging

- *DECT virtual monoenergetic images* at *high keV (110-150)* can significantly reduce metal artifacts and improve image quality

13 yo female S/p limb salvage for proximal tibial osteosarcoma. New leg pain.

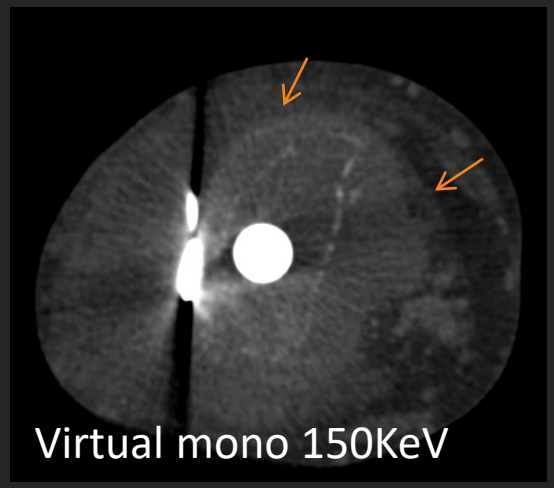

Virtual monoenergetic high kV images allow us to visualize new distal tibial mass (→) with large soft tissue component otherwise obscured by metallic streak artifact.

3D rendering with iodine map demonstrates large metastasis in soft tissues of distal lower extremity (→)

Learning Objectives

1. *Dual Energy CT* (DECT) can *distinguish clinically relevant materials* in the body (calcium, iodine, water, fat) on the basis of k-edge characteristics and differences in attenuation at different kV.

2. With appropriate technical settings *DECT is dose neutral* in pediatric imaging.

3. *Renal stone composition analysis*
   - Differentiate hydroxyapatite from oxalate, cysteine, and uric acid stones to guide treatment

4. *Bone subtraction imaging*
   - Head trauma - Improve conspicuity of intracranial hemorrhage

5. *Iodine material specific images*
   - Trauma imaging - Increase conspicuity of solid organ injury in blunt trauma
   - Oncologic imaging - improve lesion detection and characterization
   - Bowel imaging - evaluation of bowel wall enhancement in inflammatory bowel disease
   - Vascular imaging - Improved vascular definition in CTA
   - Chest imaging - Demonstrate pulmonary perfusion patterns in pulmonary embolus

6. *Virtual monochromatic imaging*
   - Reduce beam hardening artifact from metal stents and orthopedic hardware in pediatric patients

Dual Energy CT (DECT) in Clinical Practice

- Learn more….

REVIEWS AND COMMENTARY • REVIEW

Radiology

Dual-Energy CT in Children: Imaging Algorithms and Clinical Applications

Marilyn J. Siegel, MD • *Juan Carlos Ramirez-Giraldo, PhD*

From the Mallinckrodt Institute of Radiology, Washington University School of Medicine, 510 S Kingshighway Blvd, St Louis, Mo 63110 (M.J.S.); and Siemens Healthineers, Malvern, Pa (J.C.R.G.). Received October 2, 2018; revision requested October 29; final revision received January 21, 2019; accepted January 24. **Address correspondence to** M.J.S. (e-mail: *siegelm@mir.wustl.edu*).

Conflicts of interest are listed at the end of this article.

Radiology 2019; 291:286–297 • https://doi.org/10.1148/radiol.2019182289 • Content codes: CT PD

Thank You!

Corresponding Author:

E. Riedesel, MD

Assistant Professor of Radiology and Pediatrics

Emory University /Children's Healthcare of Atlanta

Erica.riedesel@choa.org

Hepatic subcapsular hematoma in very low birth weight neonates

Haesung Yoon MD, PhD,

Hyun Joo Shin MD, PhD, Myung-Joon Kim MD, PhD, Mi-jung Lee MD, PhD.

Department of Pediatric Radiology, Severance Children's Hospital,
Yonsei University College of Medicine

Disclosures

- All authors have nothing to disclose.

Objectives

- Hepatic hematoma of the liver rarely occurs in neonates and the diagnosis is often missed or delayed.
  We describe the ultrasonographic and MR findings of hepatic subcapsular hematoma of the liver in preterm neonates with very low birth weight.

Patient no.1

- IUP 24+5weeks, 810g, c-sec, male (2014-03-21)
- preterm labor
- APGAR score 1min 2 point, 5min 5 point 10min 6 point.
- Heart rate <100, no respiratory effort

- 2014.03.24
- Brain US: initial Lt. GMH grade 3

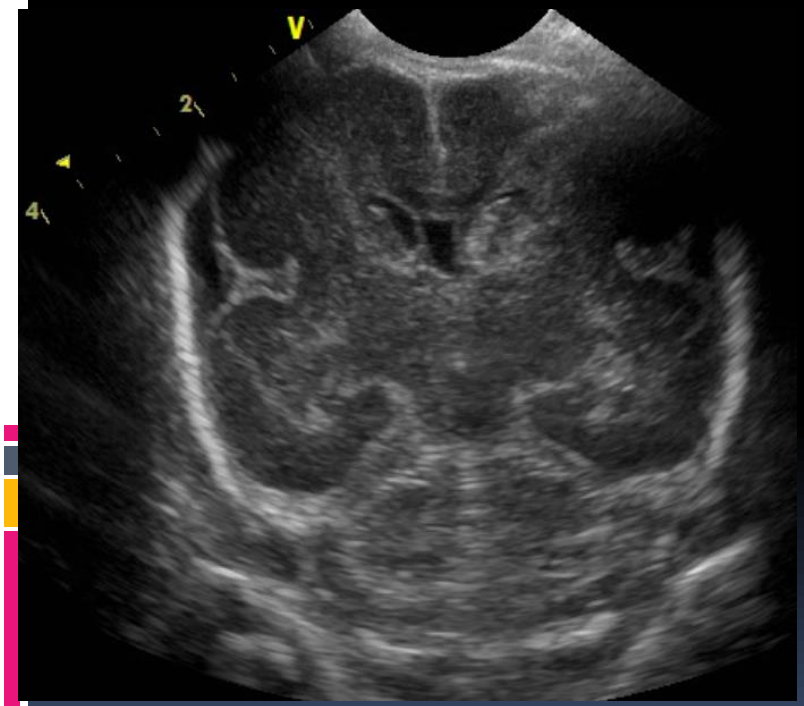

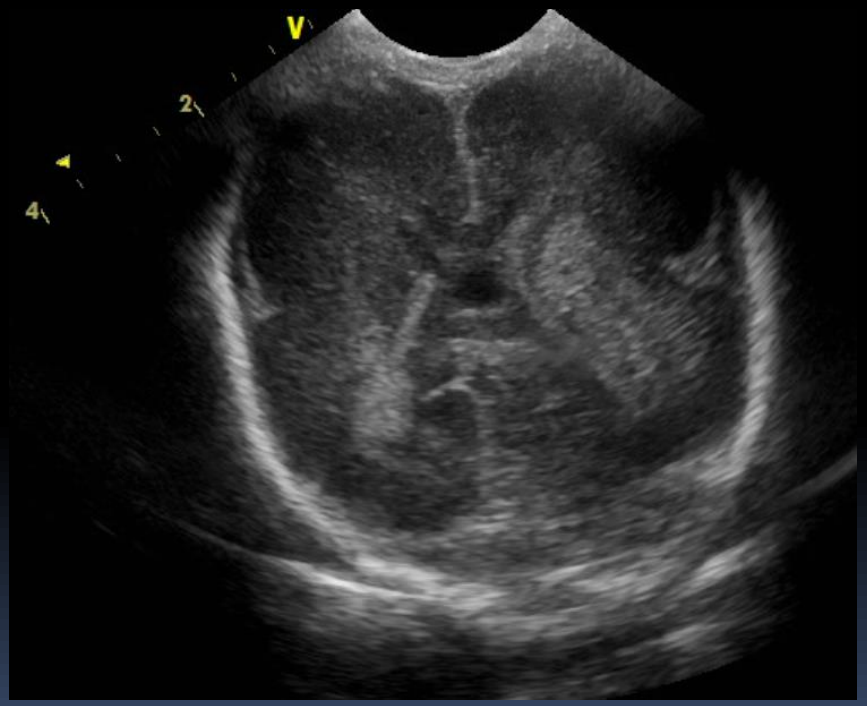

Patient no.1

- s/p bowel perforation due to meconium plug (2014.04.16)

2014.05.19

2014.06.16

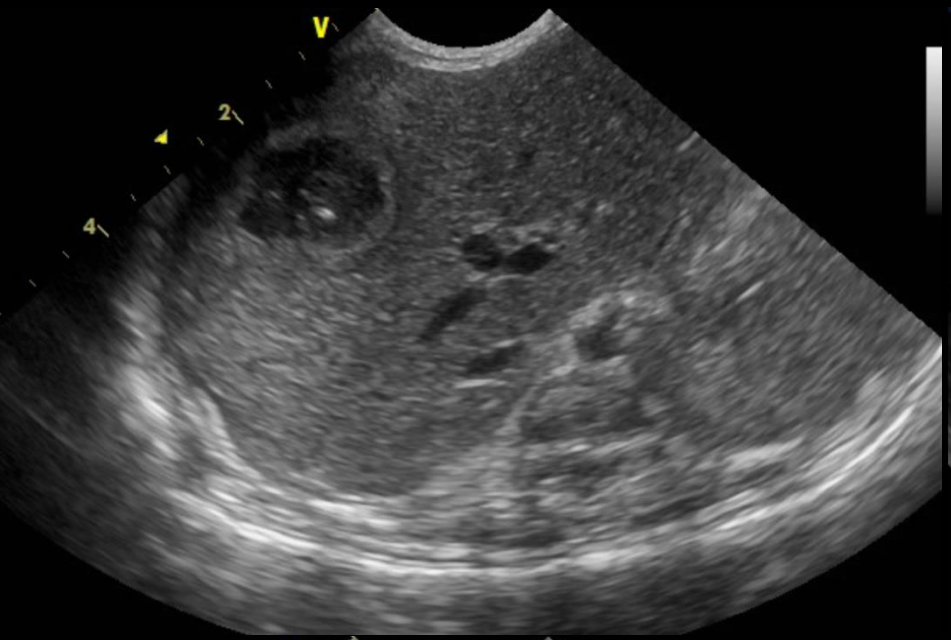

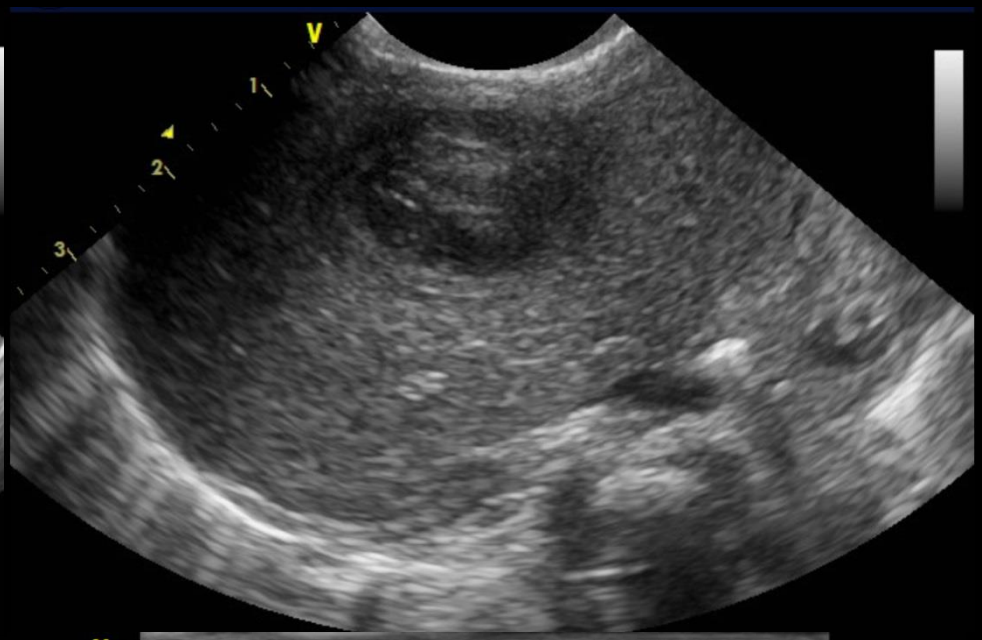

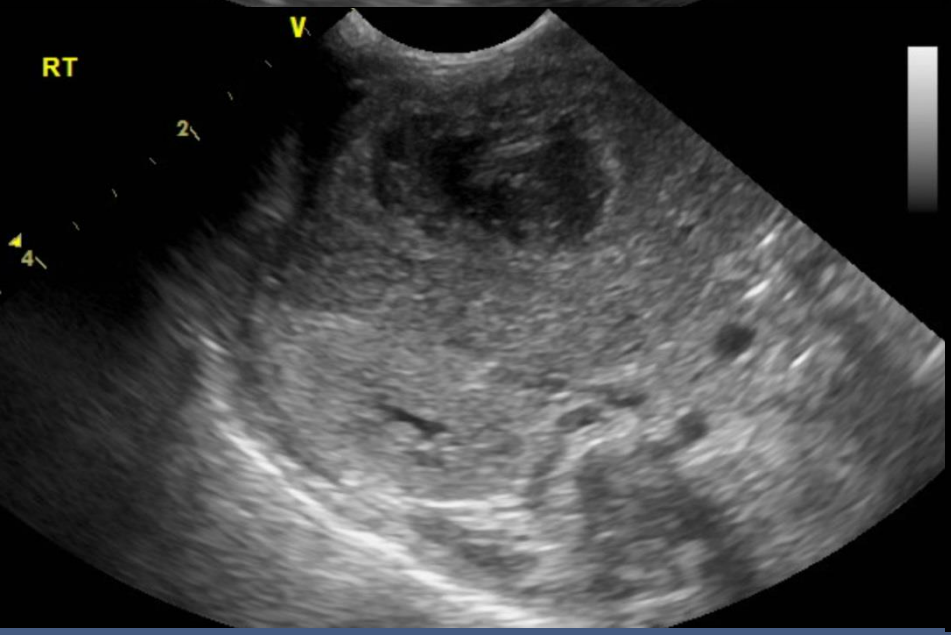

About 2.5cm hypoechoic lesion at Rt lobe subcapsular portion without interval size change for 2 months.

2014.06.20

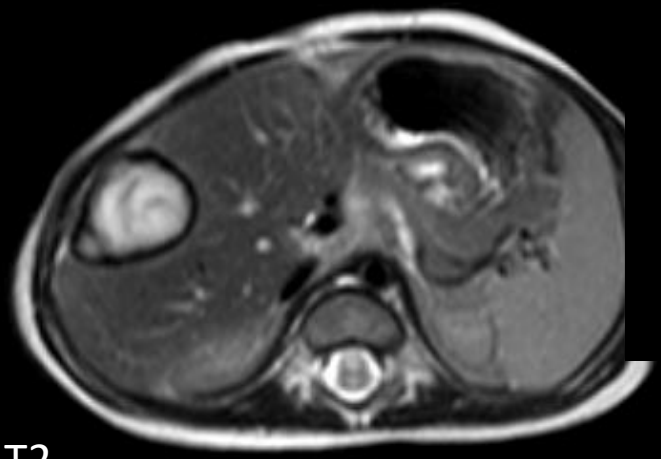

T2

T1

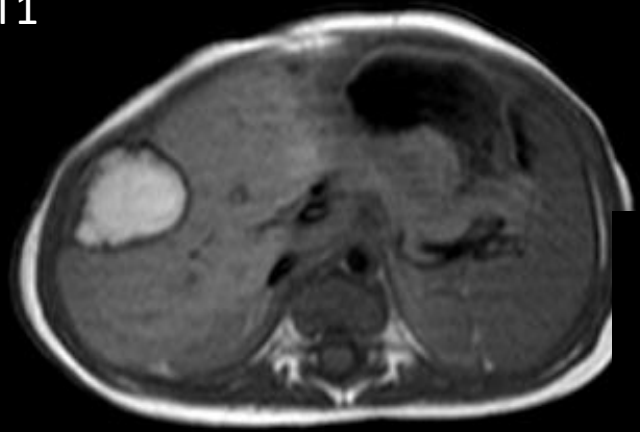

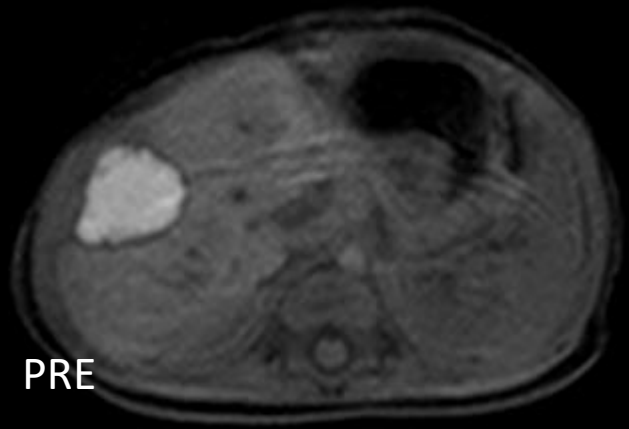

PRE

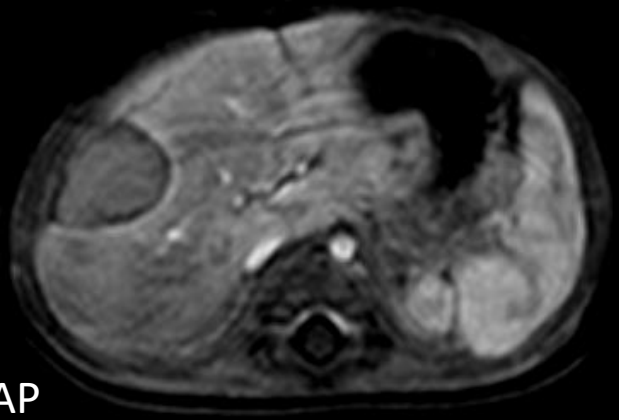

AP

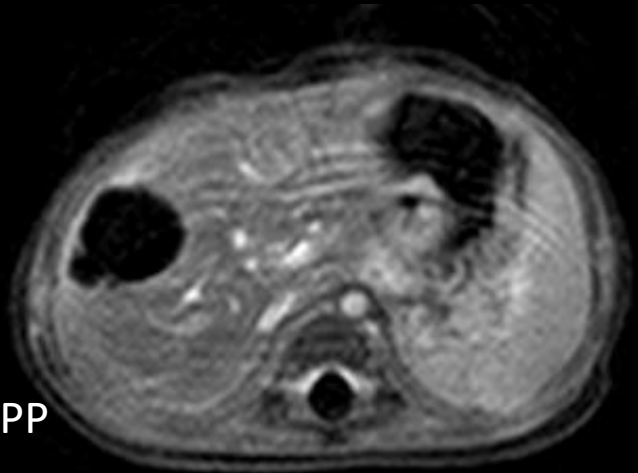

PP

DWI

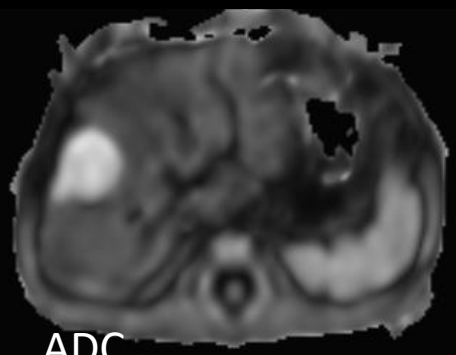

ADC

2014.10.16

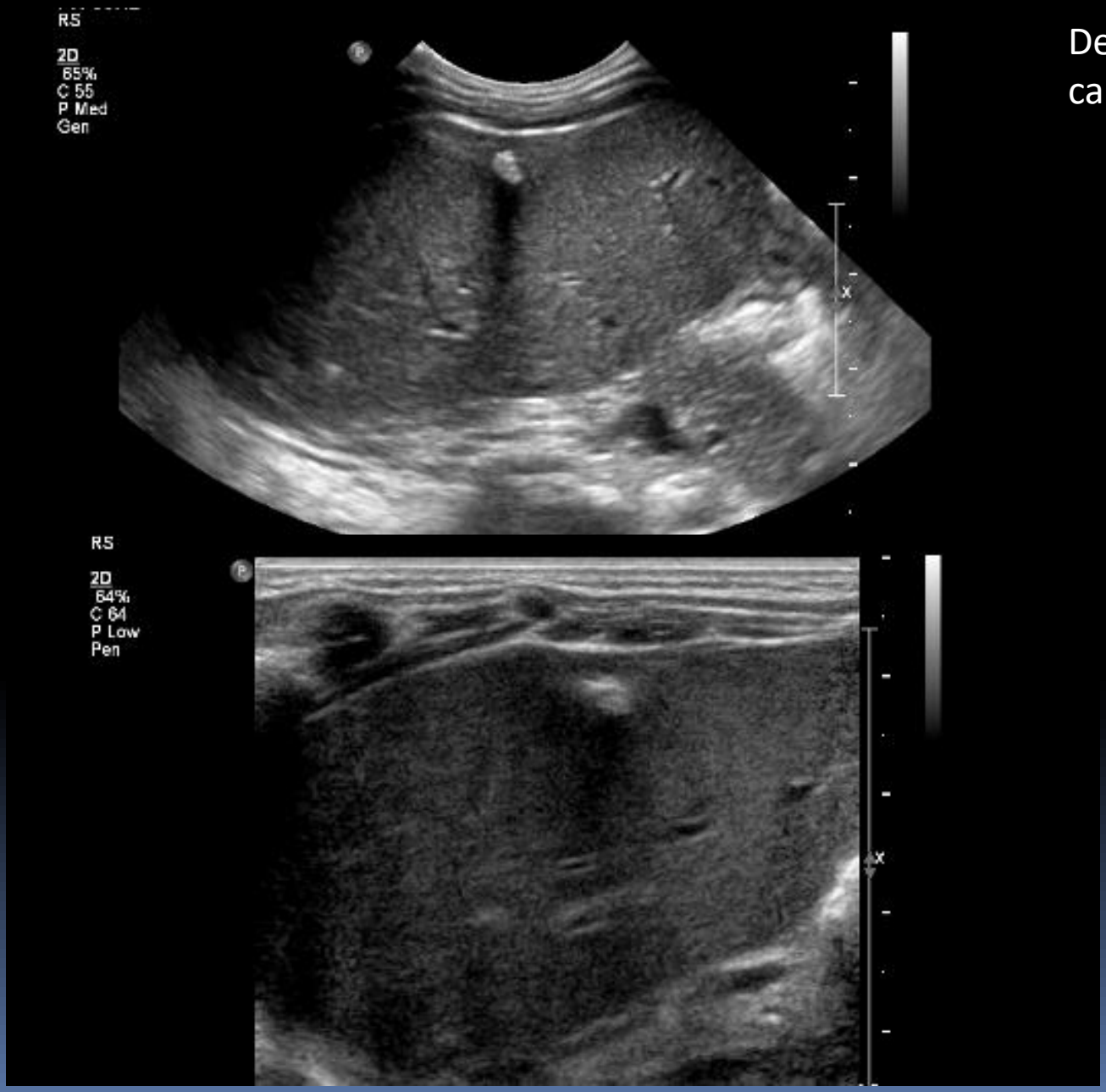

Decreased size with calcification after 5 months

Patient no 2.

- IUP 28+4 weeks, 1.52kg, NSVD. male (2015-03-14)
- Preterm labor,
- APGAR 1min 3 point, 5 min 4 point
- hypotonicity, central cyanosis, no self-respiration at birth
- 2015.03.27 neuro US

Bilateral GMH grade 1

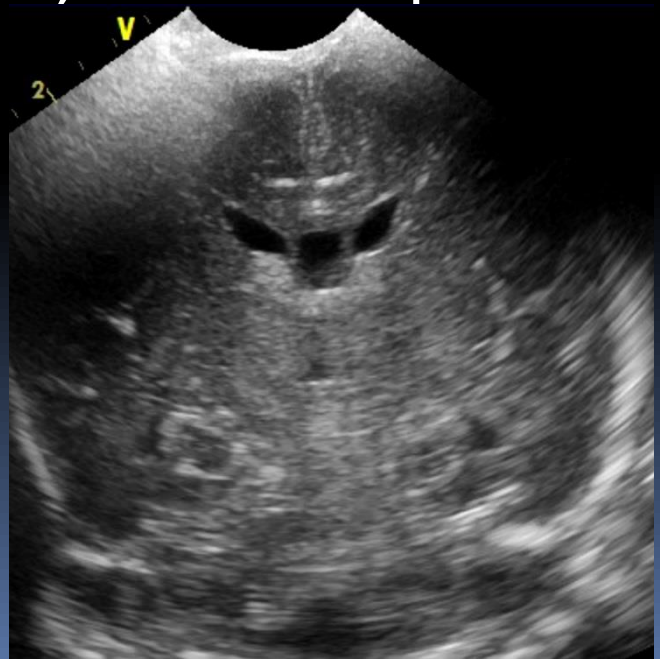

Patient no 2.

- s/p segmental resection of small bowel due to necrotizing enterocolitis and perforation at distal ileum (2015-03-30)

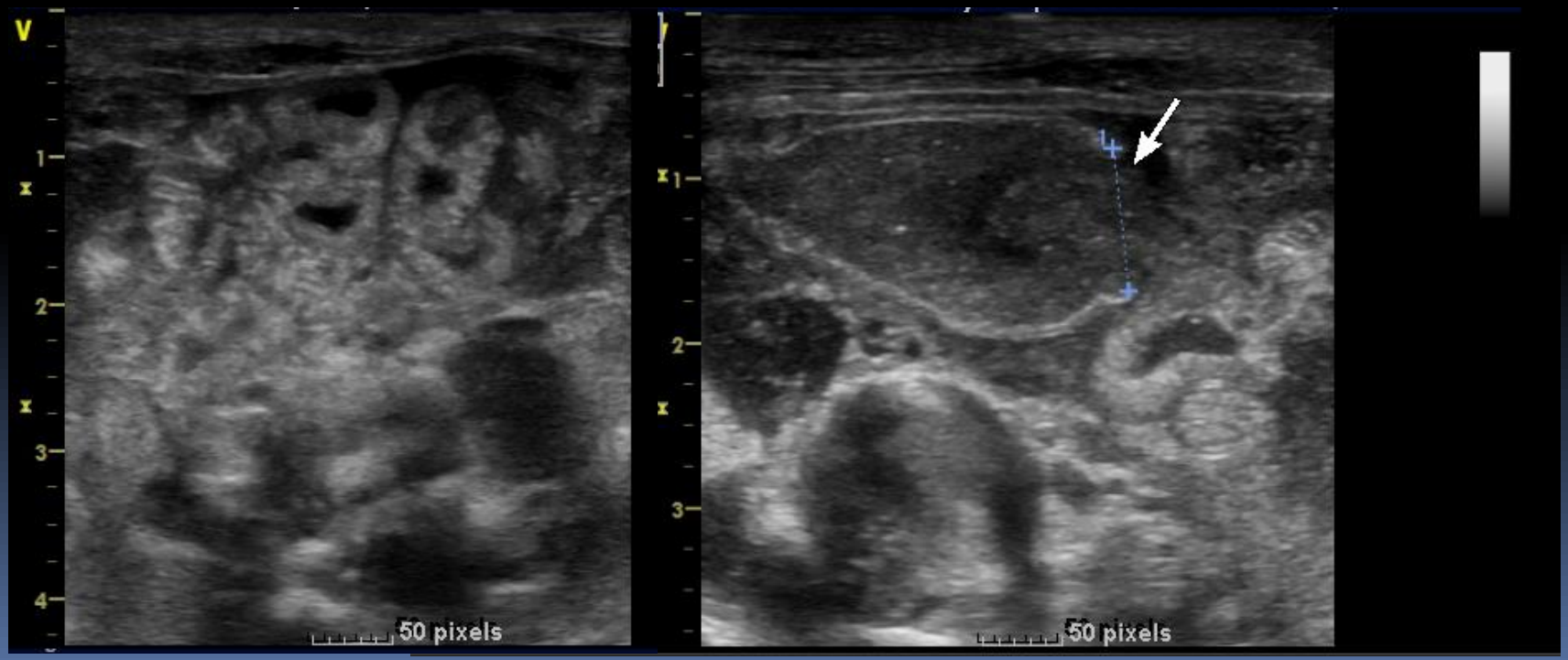

2015.03.31

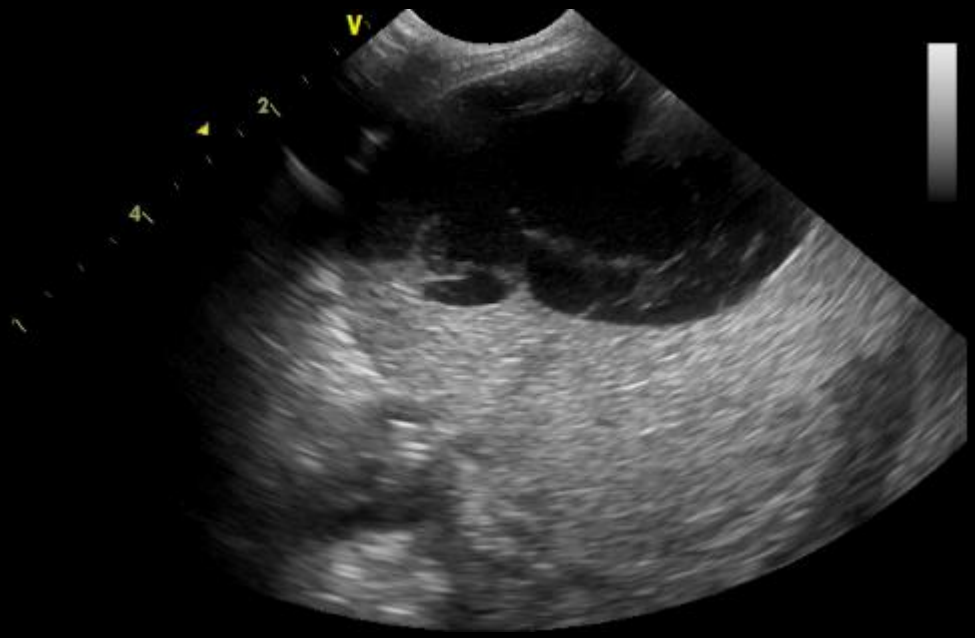

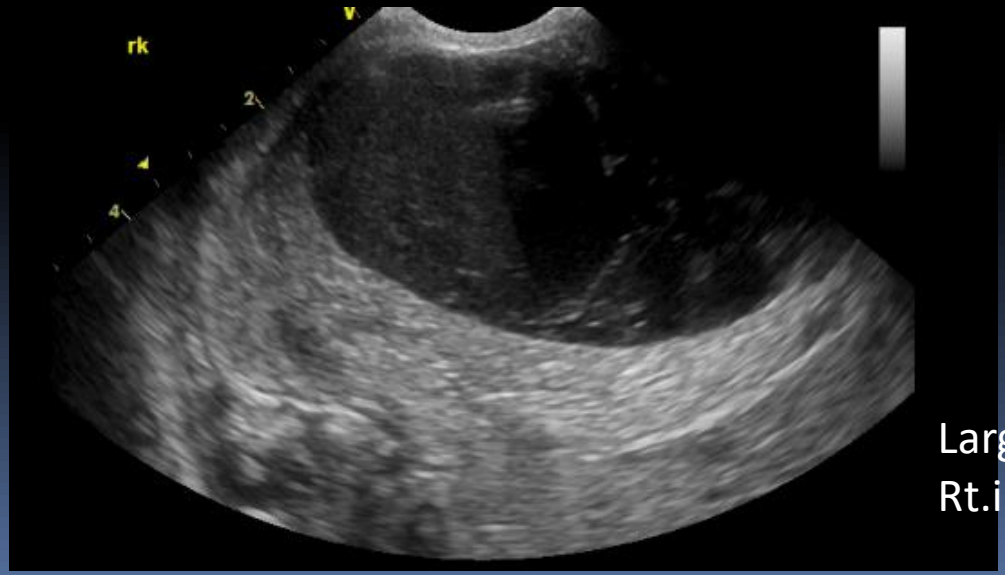

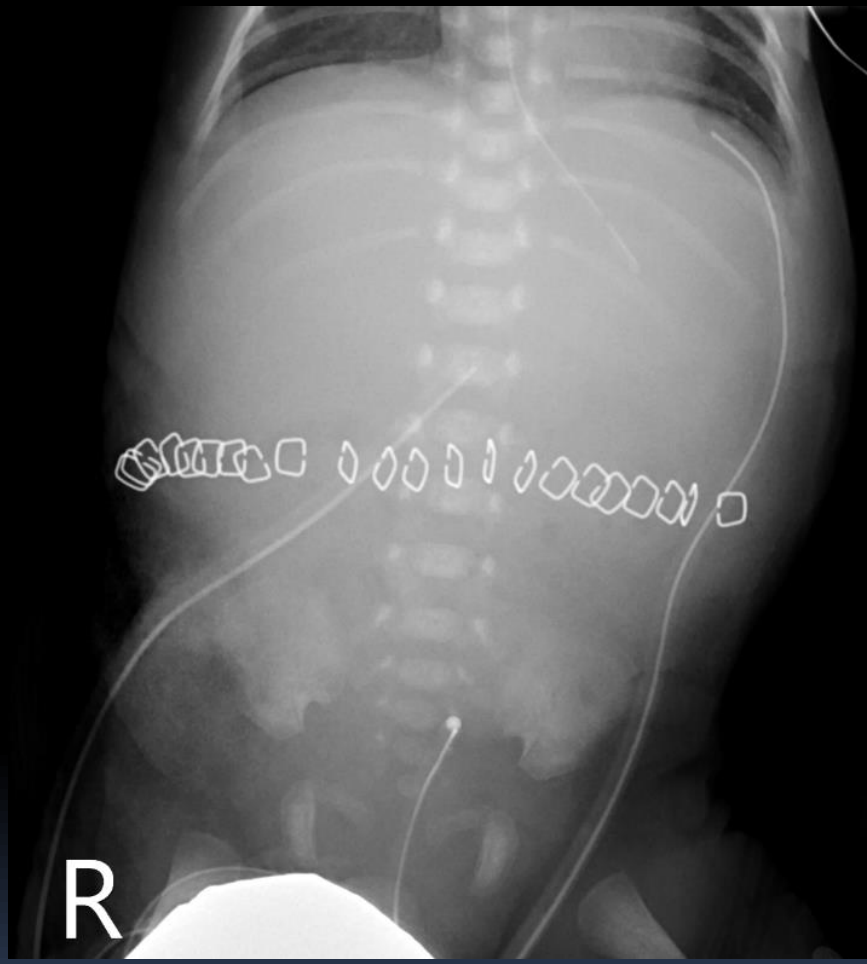

Large hypoechoic lesion with internal debris at Rt.inferior border of liver.(6cm)

2015.04.27

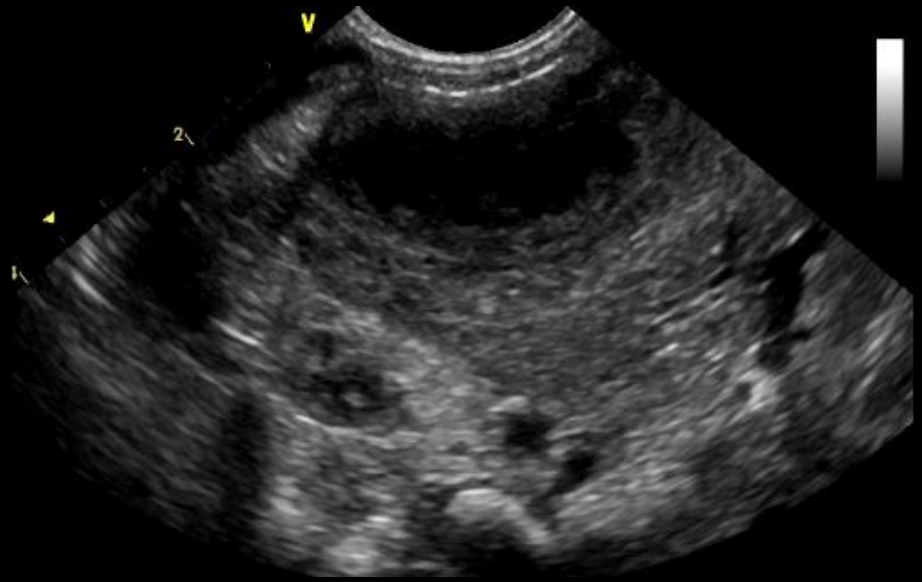

2015.06.03

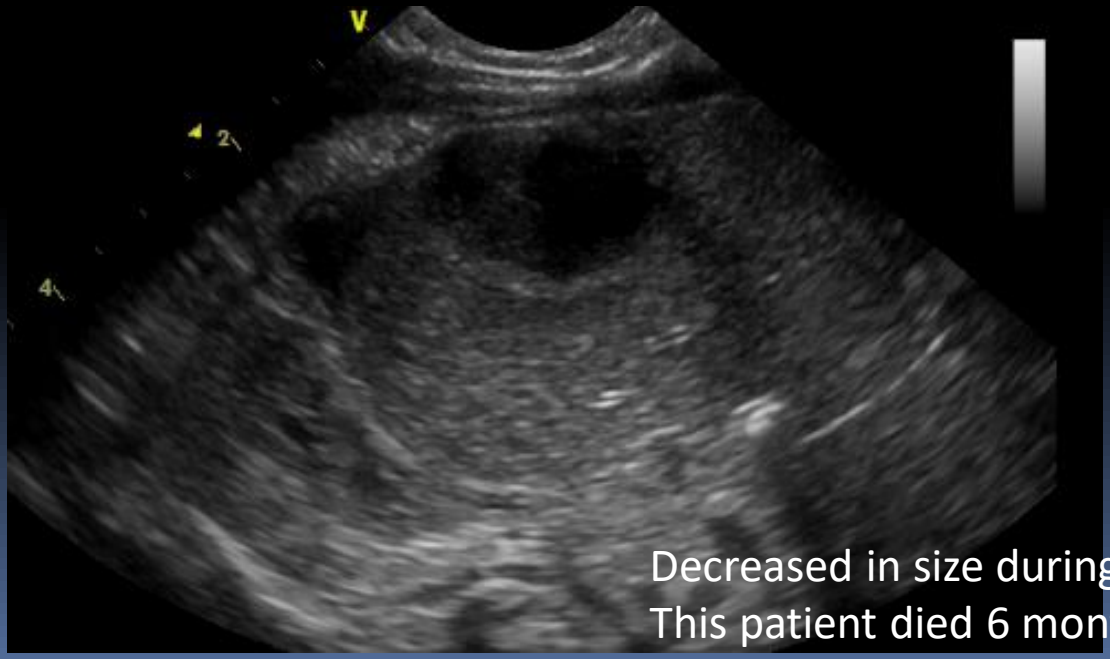

Decreased in size during follow up US
This patient died 6 months later due to sepsis.

Patient no 3.

- IUP 25+3 weeks, 650g, c-sec, male (2018-03-08)
- preterm labor
- APGAR 1min 5 point, 5 min 3 point.
- Hypotonicity, central cyanosis, no self repiration at birth
- BP fluctuation, oliguria (2018.03.12)

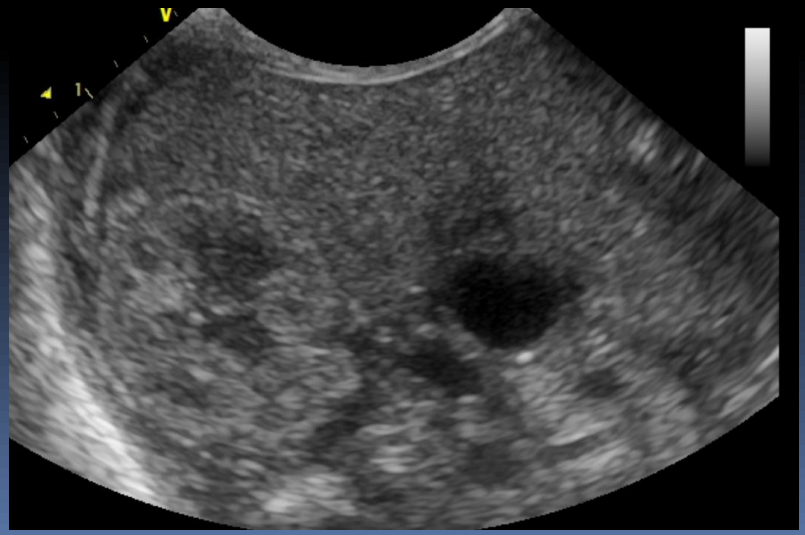

2018.03.12
Initial neuro US: Bilateral GMH grade 1

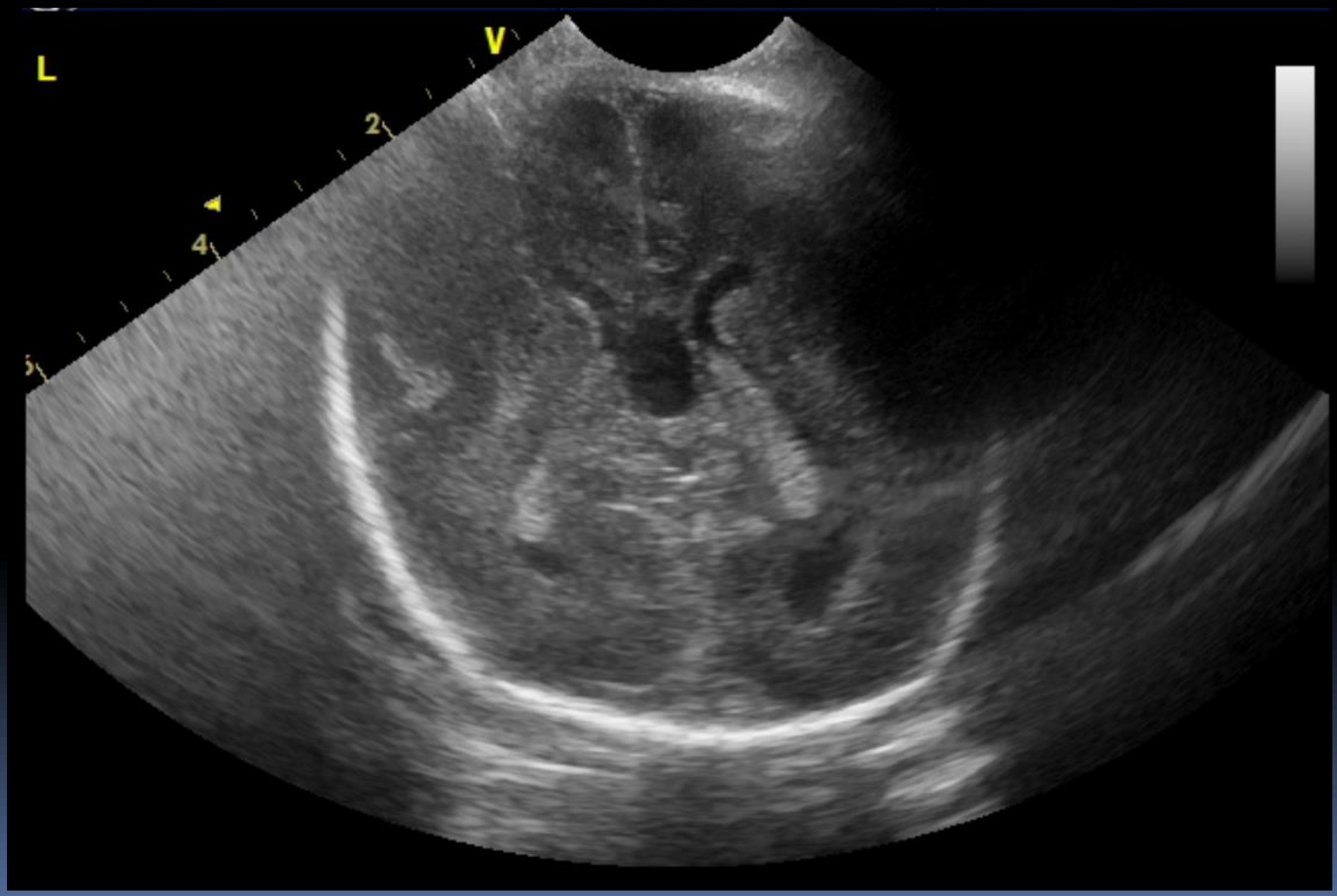

2018.03.13

s/p PD catheter insertion status (2018.03.13)
Chief complaint: bloody PD fluid.

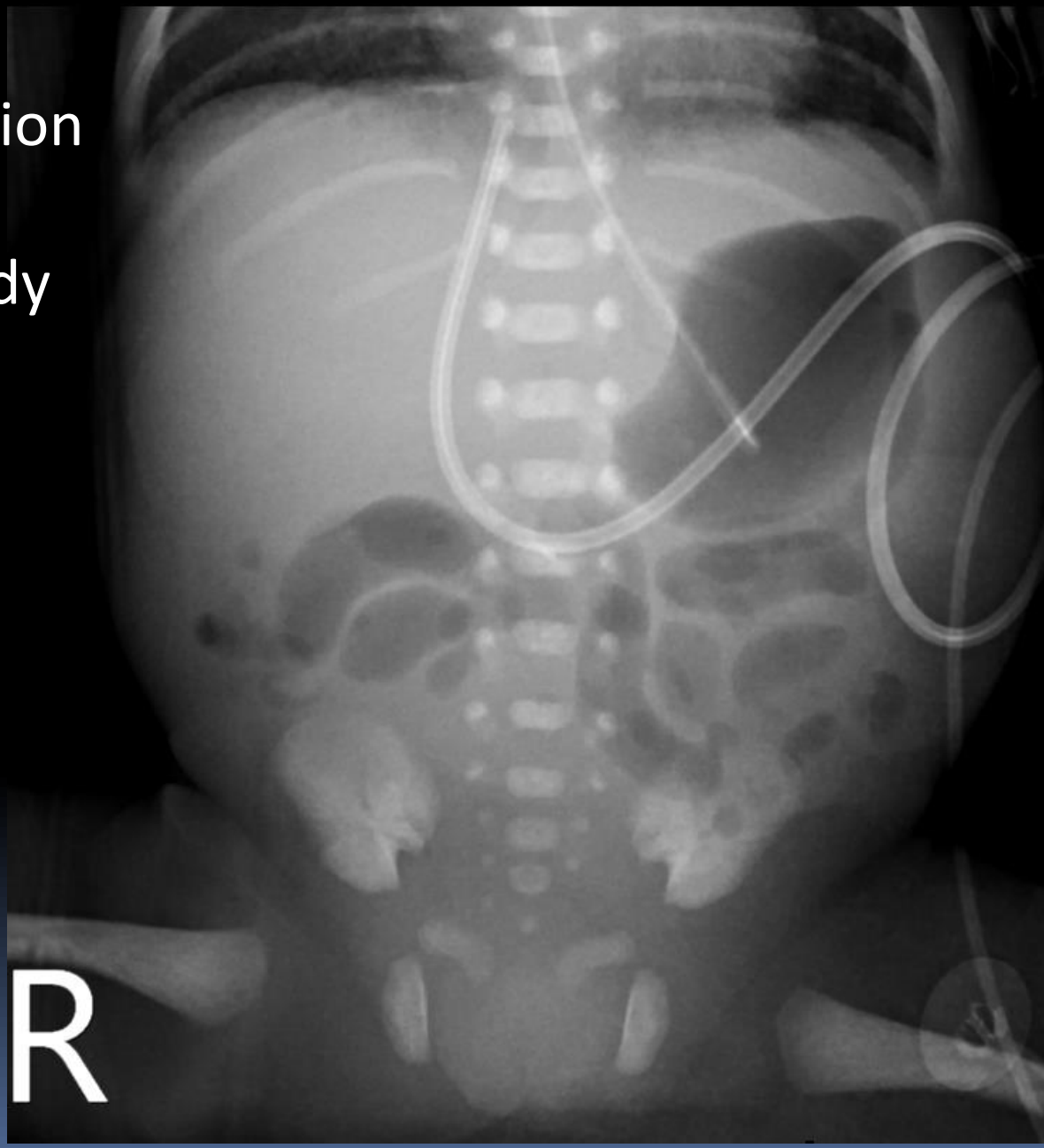

2018.03.13

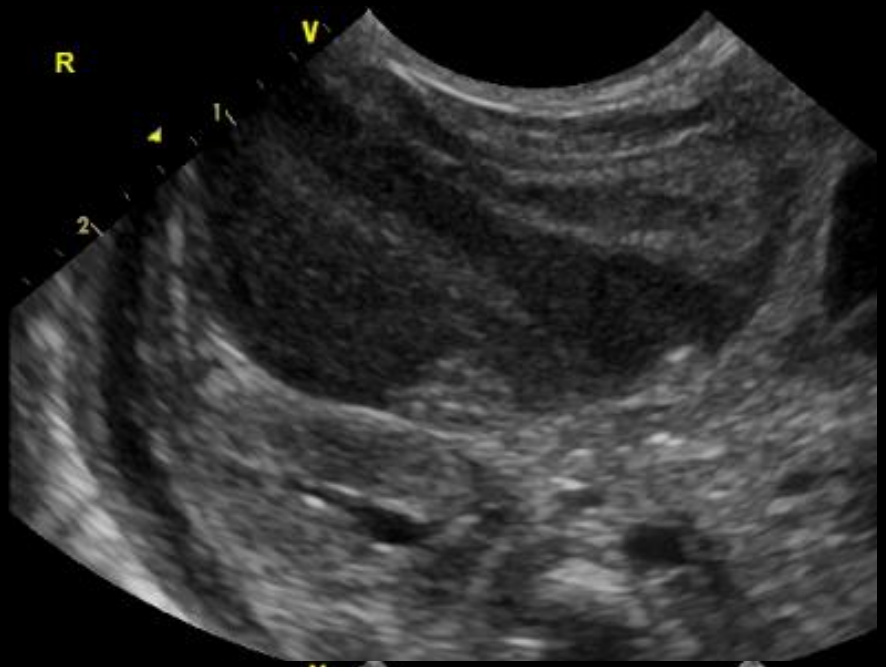

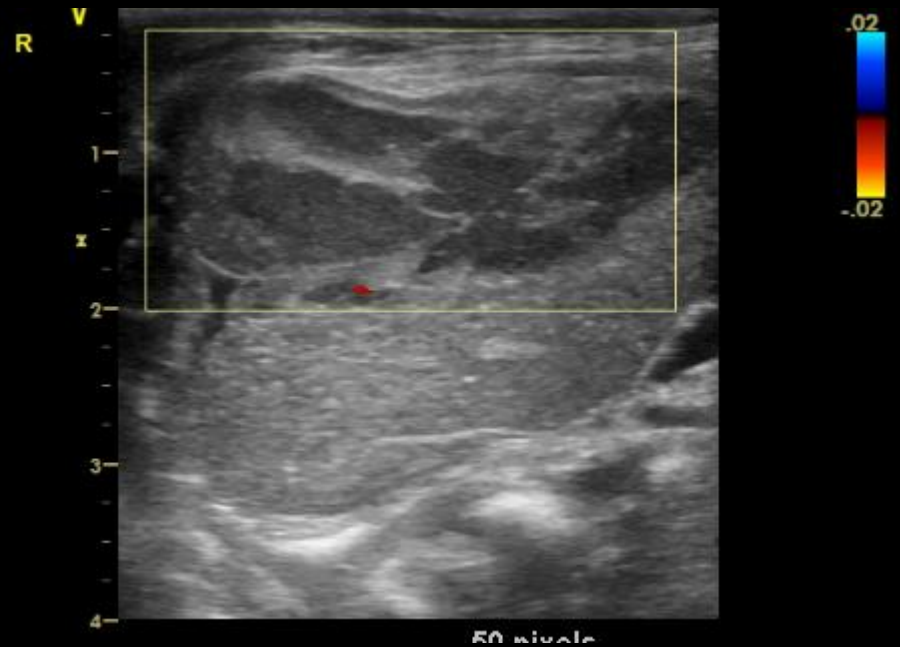

Newly developed heterogenous lesion (3.3x4.6cm) from liver dome to Rt lower abdomen, suggesting hematoma. Another small lesion (0.7cm) at S8 subcapsular area.

2018.03.15

Bilateral GMH grade 3

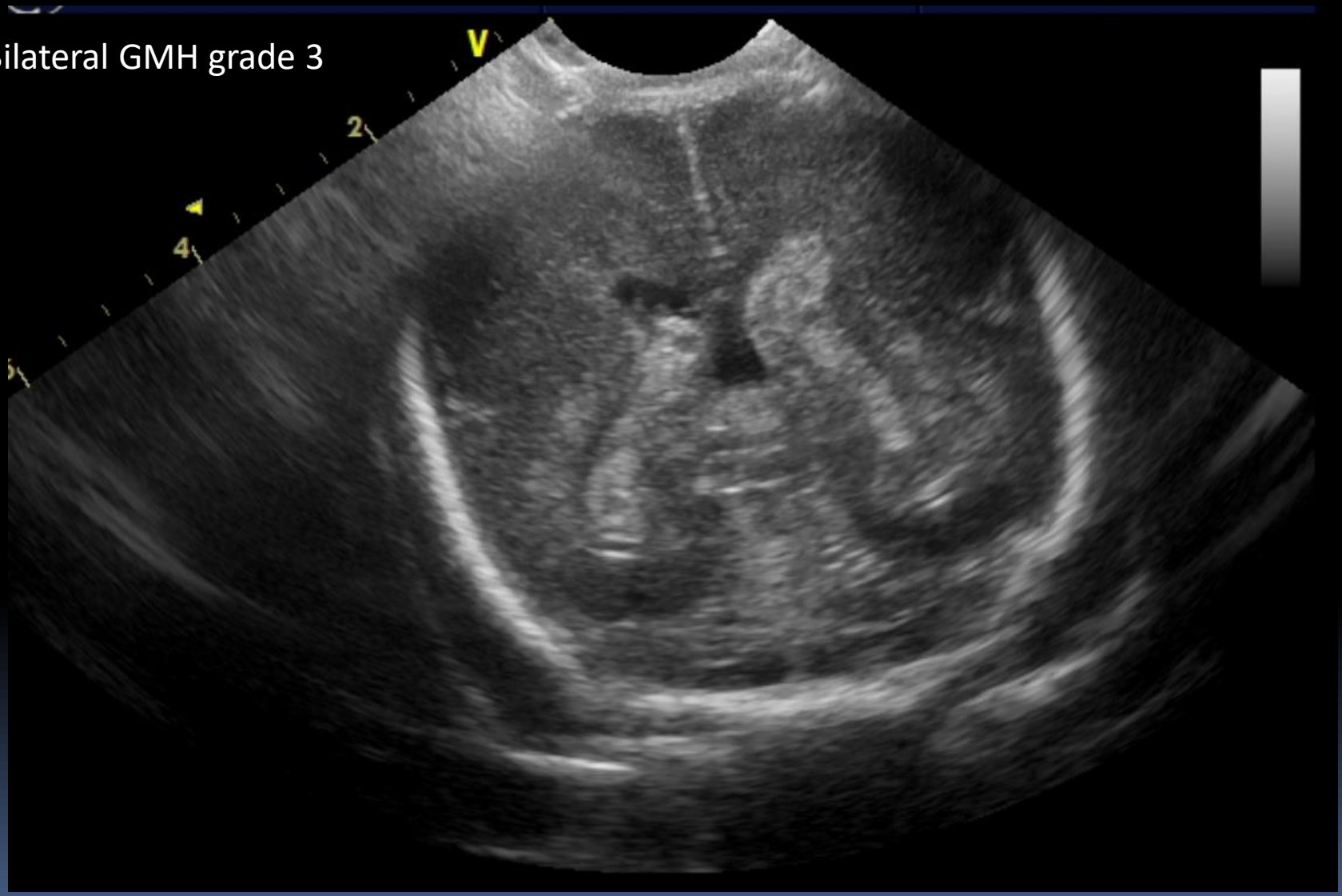

2018.03.27

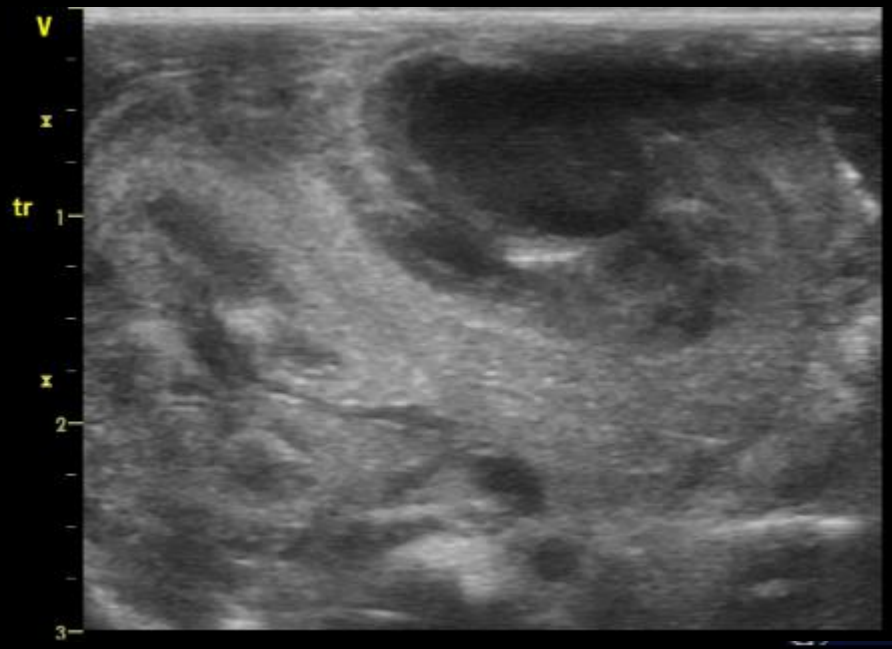

2018.04.02

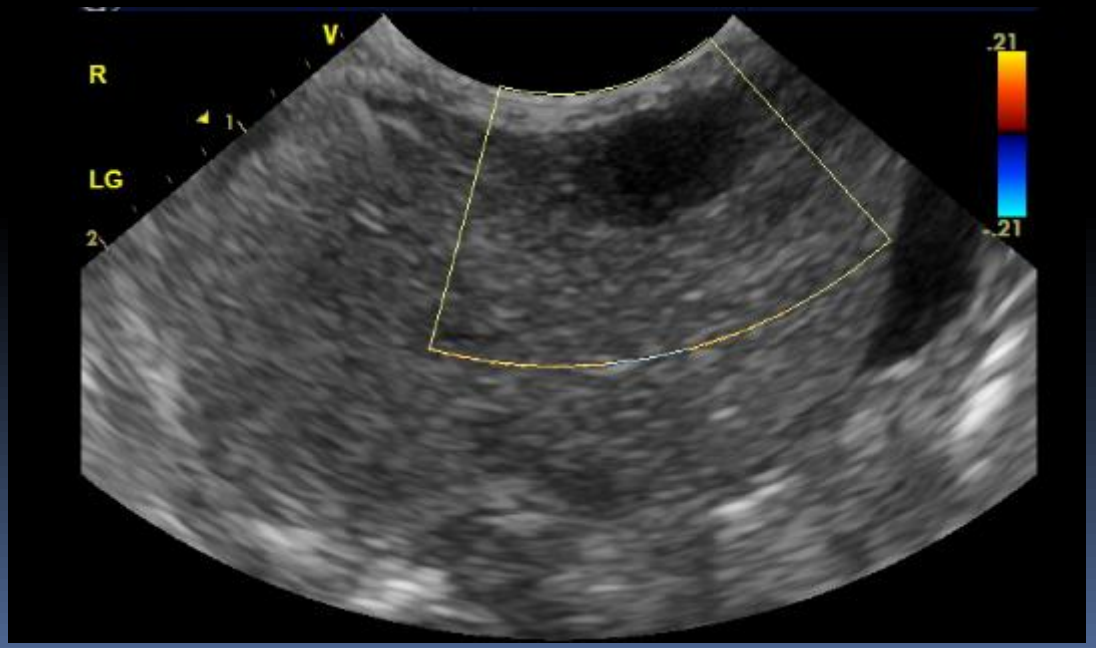

Decreased in size during follow up US

Patient 4

- IUP 27+3week, 700g, C-sec, female (2018-04-18)
- Diabetic mother
- Ventriculomegaly on prenatal ultrasound
- APGAR 1min 3 point, 5 min 6 point
- Initial neuro ultrasound : agenesis of corpus callosum.

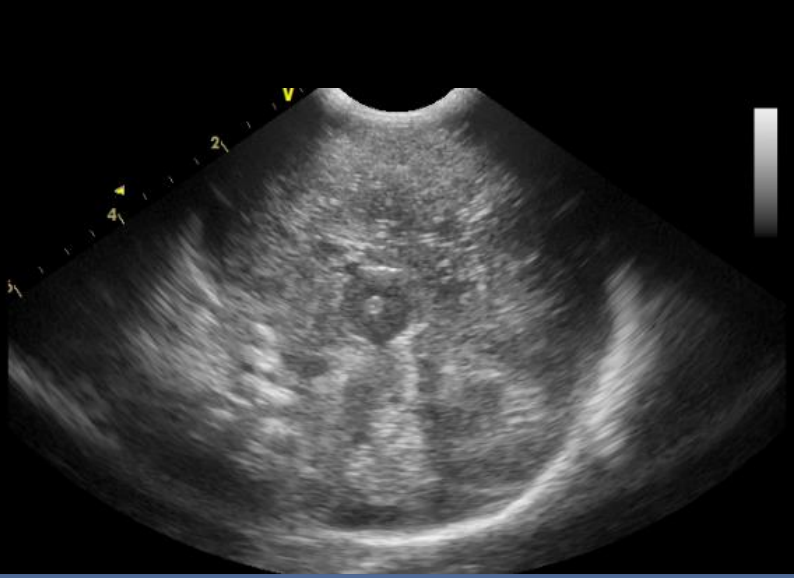

2018.04.22

Clinical history – development of metabolic acidosis

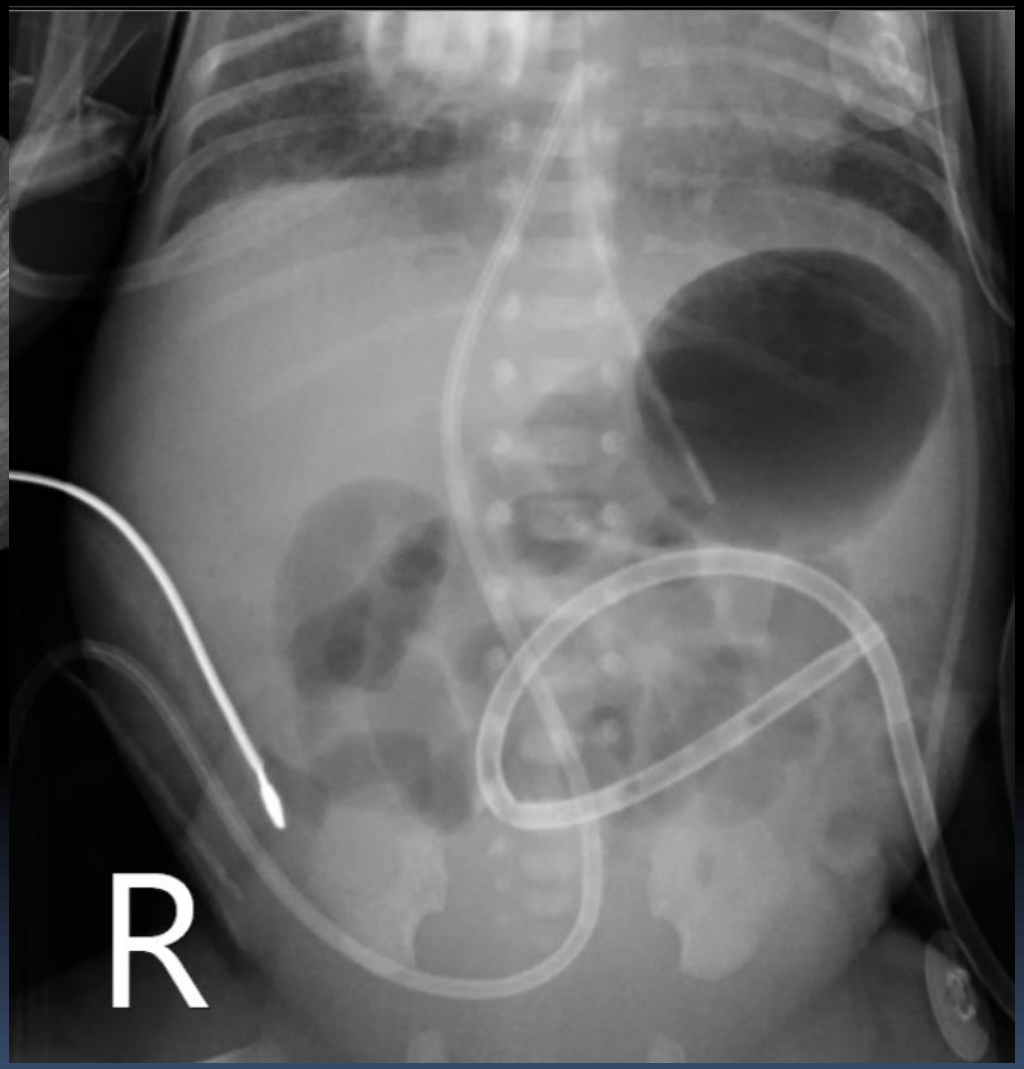

2018.04.26

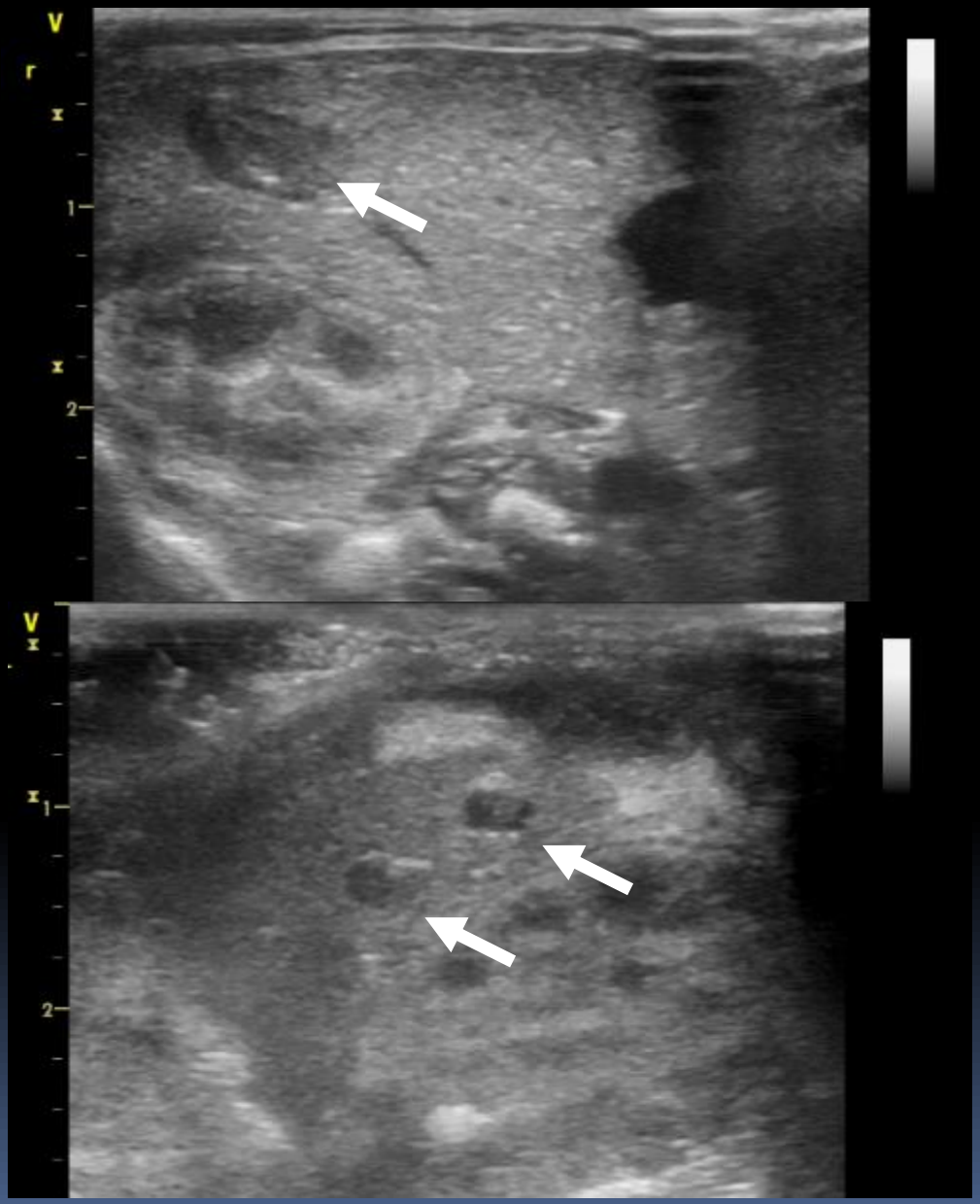

Tiny hypoechoic lesions at Rt lobe subcapsular portion.
All measuring less than 1cm.

Patient 5

- History: IUP 27+0weeks, 1.06kg, NSVD, female
- Born at outside hospital
- APGAR 1min 4 point, 5 min 6 point

- On Day 3, pneumopericardium and cardiac tamponade was developed.
- Cardiac pulmonary resuscitation (CPR) for 20mins and return of spontaneous circulation(ROSC)

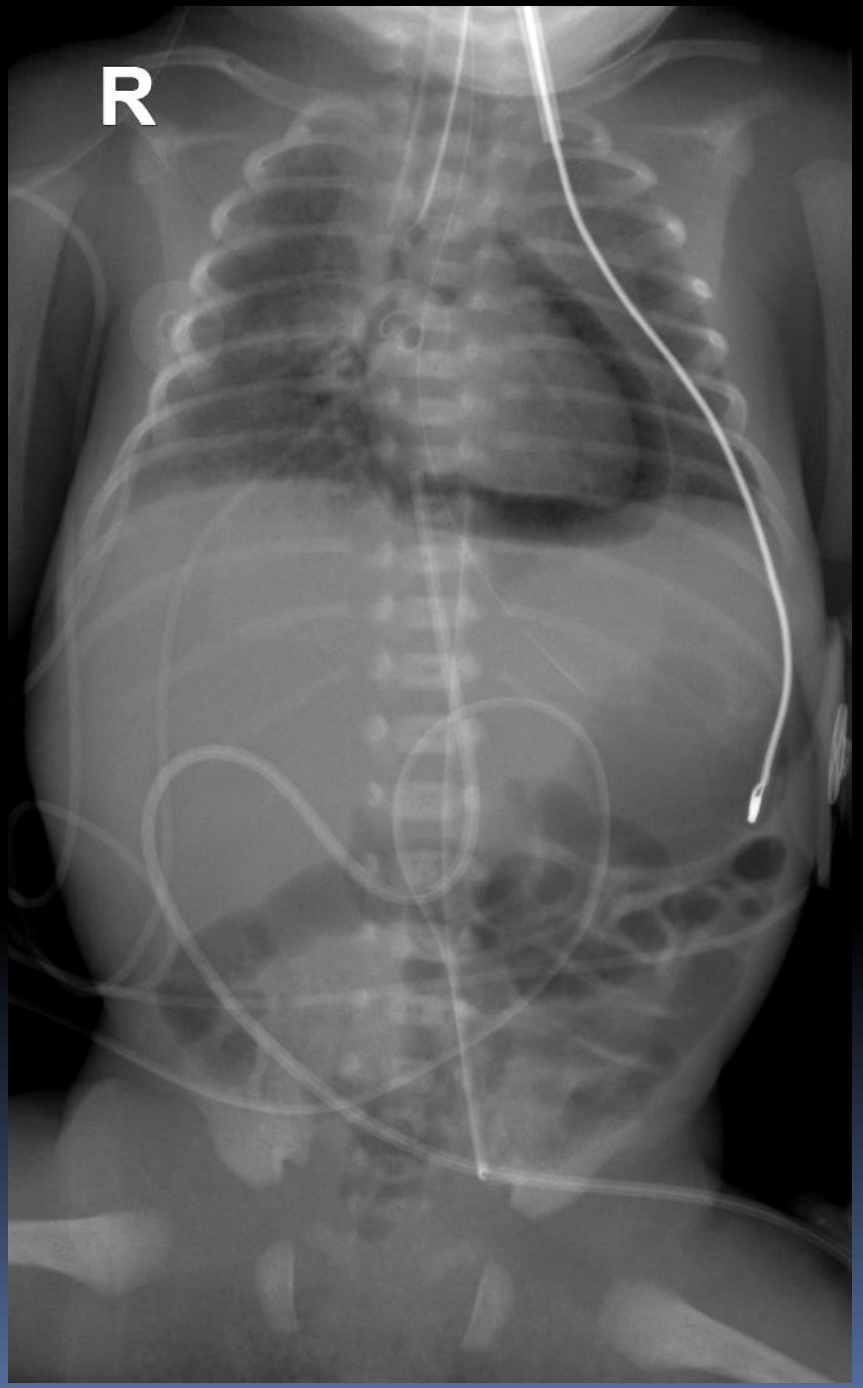

2018.10.10, day 3 outside hospital

Bilateral GMH grade 3.

2018.10.31, outside

Decreased size of heterogenously hypoechoic lesion at subcapsular portion of liver Lt lobe .
No interval change of heterogenously hypoechoic lesion at subcapsular portion of liver Rt lobe.

2018.11.12

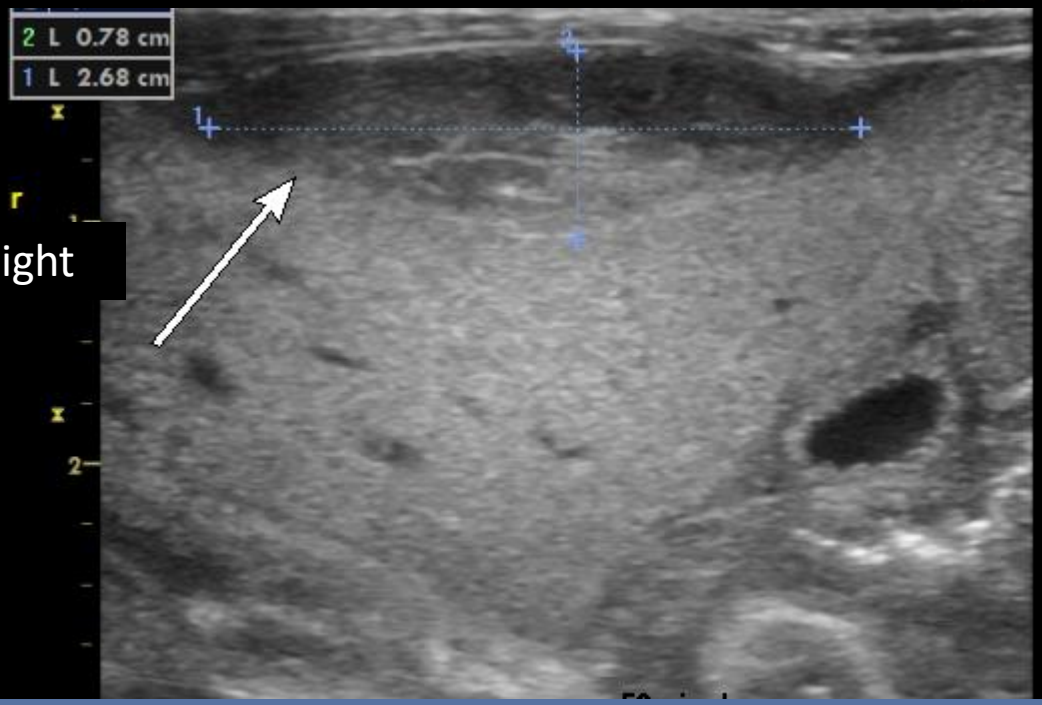

Right

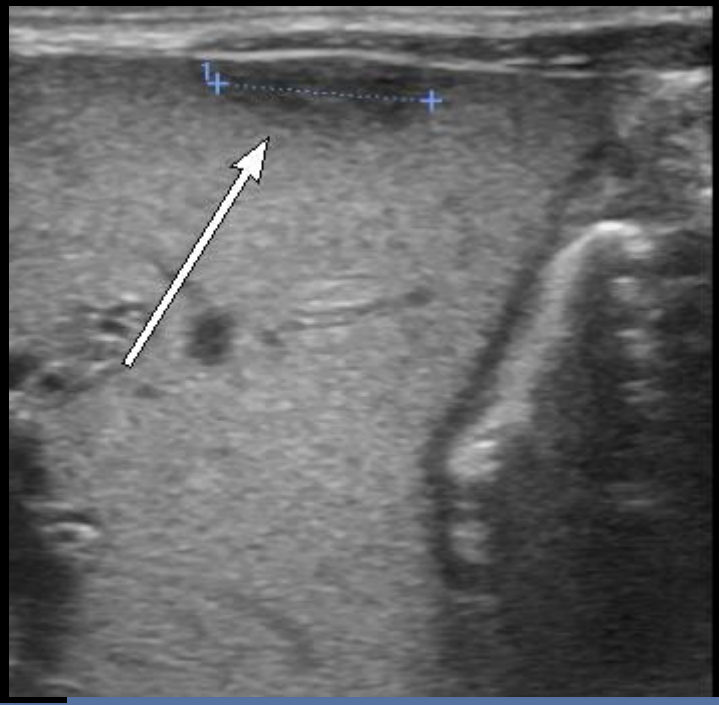

Left

2018.12.07

Decreased size of heterogenously hypoechoic lesion at subcapsular portion of liver Lt lobe and Rt lobe.

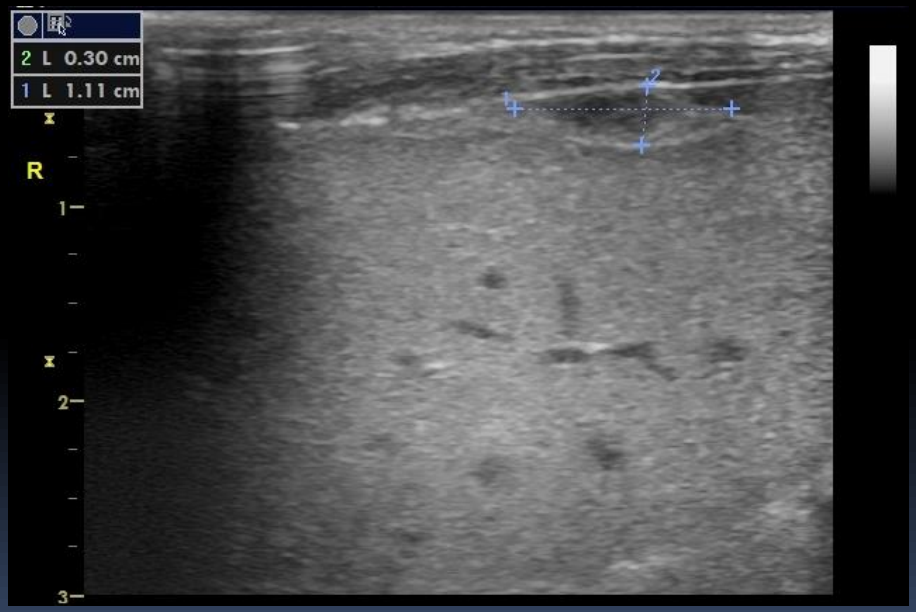

Hepatic subcapsular hematoma

- Subcasular hematoma of the liver is collecting of blood under the Glisson capsule,
  - In adults, it is likely to occur following blunt abdominal trauma.
- This should be distinguished from an intrahepatic hematoma, where bleeding is less extensive and occurs within the liver parenchyma.
- Etiology
  - Traumatic labor, coagulopathies, prematurity, very low birth weight, hypoxia, sepsis, pneumothorax and umblical venous catheterization.
  - Most reported cases are preterm with very low birth weight and condition is extremely rare in term healthy neonates.

Hepatic subcapsular hematoma

- In previous study of 755 perinatal autopsies, hepatic subcapsular hematomas were found in 52 (6.9%) cases, including 31 stillborn fetuses and 21 liveborn infants.
  - Sepsis was associated with 62% of the cases with hepatic subcapsular hematomas and with 25% of the comparison group (P =.0001).
  - Cerebral germinal matrix hemorrhages were present in 35% of the cases with hematomas and in 14% of the comparison group (P =.0001)

Pediatr Dev Pathol. 1999 May-Jun;2(3):215-20.

Hepatic subcapsular hematoma

- Hepatic subcapsular hematoma should be considered in all very low birth weight newborns with unexplained hypovolemia or anemia.
- Acute massive bleeds can present in the immediate neonatal period with hypovolemia and shock.
- Slowly progressing hematoma may manifest with pallor, jaundice, irritability or respiratory distress

Hepatic subcapsular hematoma

- Early detection of a subcapsular hematoma is important in an infant delivered via normal vaginal delivery with no significant clinical symtoms due to the difficulty of recognition of liver laceration.
- If a large amount of peritoneal bleeding progresses the bleeding maybe fatal.

Hepatic subcapsular hematoma

- Abdominal ultrasound shows non-specific findings and intrahepatic hematoma can suggest different diagnosis such as a liver abscess or hepatic mass.
- A follow up US is helpful to confirm the diagnosis of subcapsular hematoma by identifying the lesion with decreased size.

Hepatic subcapsular hematoma

- Treatment
  - Mainly conservative including blood transfusion, correction of coagulopathies and avoiding excessive handling of the baby.
- Conservative treatment is initially performed because of a great extent of subcapsular hematoma is naturally absorbed

Take home points for Hepatic subcapsular hematoma

- Preterm with very low birth weight patient
- With hemodynamically unstable situation
  - surgery, oliguria, metabolic acidosis, post CPR status, sepsis.
  - Germinal matrix hemorrhage are most likely associated.
- US for diagnosis and follow up
- Conservative treatment
- Subcapsular hematoma is naturally absorbed without definite sequelae.

Reference

- Eur J Obstet Gynecol Reprod Biol, 1992. 44(2): p. 161-4.
- Pediatr Radiol, 2004. 34(4): p. 358-61.
- Pediatr Radiol, 2005. 35(11): p. 1139-41.
- Eur J Pediatr, 2008. 167(5): p. 591-3.
- Cases J, 2010. 3(1): p. 32.
- J Perinat Med, 2011. 39(3): p. 353-4.
- Pediatr Int, 2011. 53(5): p. 777-779.
- Pediatr Neonatol, 2012. 53(2): p. 144-6.
- J Gynecol Obstet Biol Reprod (Paris), 2012. 41(4): p. 378-82.
- BMJ Case Rep, 2013. doi:10.1136/bcr-2013-009074


Thank you
YONSEI CANCER CENTER
세브란스병원 SEVERANCE HOSPITAL
Severance

Imaging atlas of soft tissue masses in the backs of neonates and young children

Gayoung Choi, Young Hun Choi, Seul Bi Lee, Yeon Jin Cho, Seunghyun Lee, Jung-Eun Cheon, Woo Sun Kim, In-One Kim

Department of Diagnostic Radiology, Seoul National University Hospital

Disclosures

- Gayoung Choi, Young Hun Choi, Seul Bi Lee, Yeon Jin Cho, Seunghyun Lee, Jung-Eun Cheon, Woo Sun Kim, and In-One Kim have no conflict of interest and nothing to disclosure.

Objectives

- To summarize the list of soft tissue masses that can develop in the backs of neonates and young children
- To present key imaging findings of soft tissue masses in the backs of neonates and young children

Soft Tissue Masses in Children

- Common lesions
  - Benign: Small, well defined, homogeneous, edema (-)
    - Vascular tumors, neurofibroma, fibromatosis, lipoma, ganglion cyst, hematoma, and abscess
  - Malignant: Poorly defined, heterogeneous
    - Liposarcoma, fibrosarcoma, rhabdomyosarcoma

- Imaging study
  - US: Initial examination of choice
    - Cystic or solid
  - MRI: For large lesions to define the extent and its local relationships
  - CT: More limited role

Classifications

- Pseudotumors: Fat necrosis
- Vascular lesions: Hemangiomas, vascular malformations
- Adipocytic tumors: Lipoma, lipoblastoma
- Fibroblastic/myofibroblastic tumors
  - Nodular fasciitis
  - Fibrous hamartoma of infancy
  - Myofibroma/myofibromatosis
  - Lipofibromatosis
  - Infantile fibrosarcoma
- Neurogenic tumor: Neurofibroma
- Unclassified benign tumors
  - Pilomtricoma
  - Epidermal inclusion cyst

PSEUDOTUMORS

Fat Necrosis

- Usually limited to the subcutaneous soft tissues
- Overlying bony prominences
- Subacute or chronic palpable lump or deformity
- Most do not recall a specific traumatic event

- Imaging: Linear or mass-like configuration
- US: Hypoechoic to hyperechoic
- MRI: T1 low SI, T2 high and low SI
- Sequela: Tissue atrophy

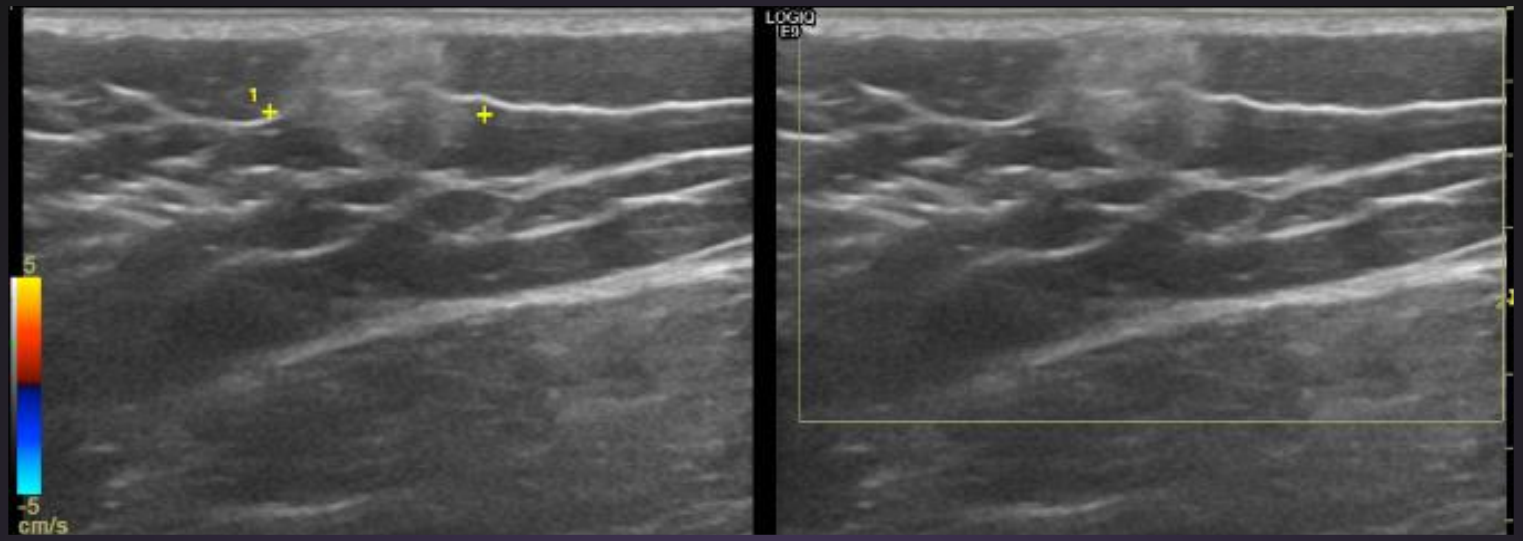

US of a 6-year-old girl with the painful firm mass on the left lower back shows an ill defined hyperechoic lesion in the subcutaneous layer without internal vascularity suggesting fat necrosis.

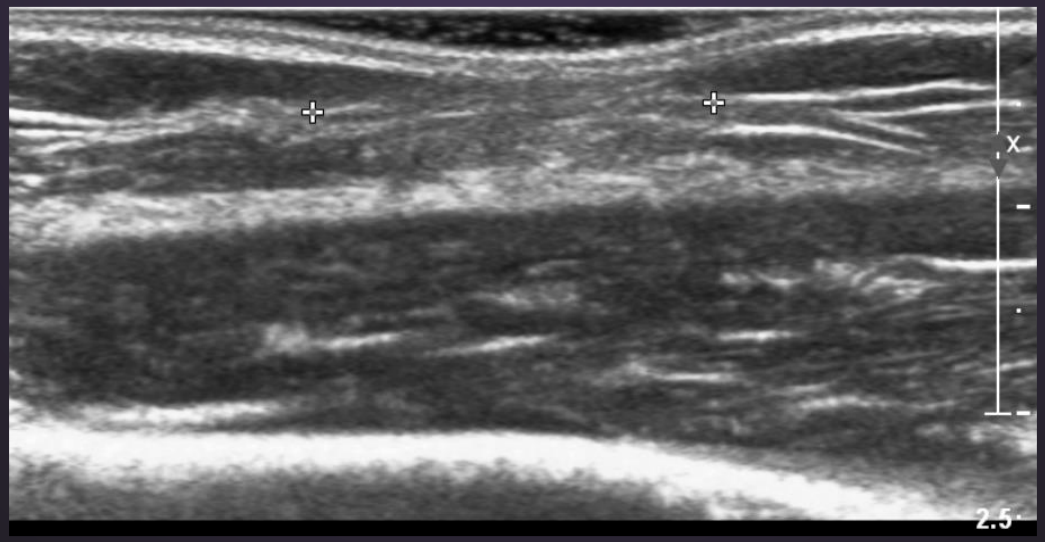

US of a 2-year-old girl with focal dimpling at right lower back shows ill defined hyperechoic lesion in subcutaneous layer with skin contraction which suggests fat necrosis with atrophic change.

VASCULAR LESIONS

Hemangioma

- Benign, slow-growing lesion
- May also contain nonvascular elements: fat, fibrous tissue, smooth muscle
- Usually appear in the first decade of life (often 1st week)
- Rapid growth initially and then usually undergo spontaneous involution

- Imaging
  - Radiography: Soft-tissue mass with possible phleboliths
  - US: Usually hypoechoic, homogeneous or heterogeneous mass
  - Doppler US: Hypervascular
  - CT: Soft-tissue mass with vascular channels, enhancement (+)
  - MRI: T1 low, T2 high SI, marked enhancement (+)
    - Heterogeneity with hemosiderin deposits, fibrosis, fat, calcification, thrombosis, stagnant blood
    - Feeding or draining vessels, muscle atrophy

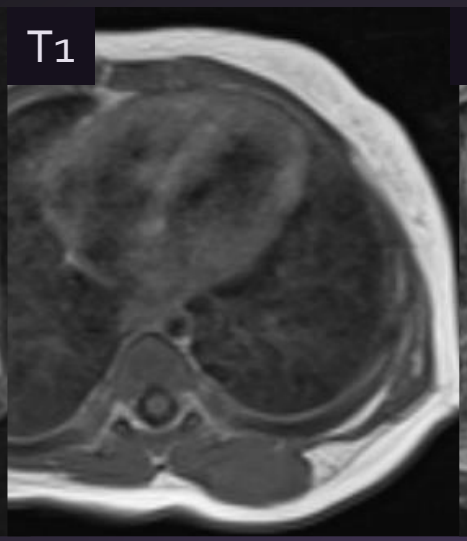

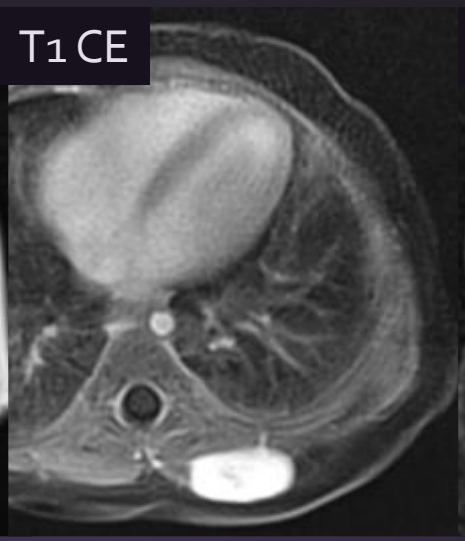

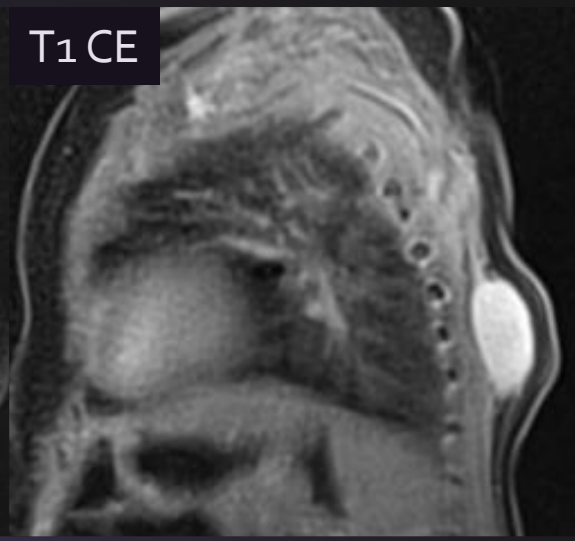

MRI of a 3-year-old boy with palpable back mass shows 2x0.9x2.1cm sized well defined ovoid mass at left upper back with T2 high SI, T1 iso SI, and strong enhancement, confirmed as a hemangioma.

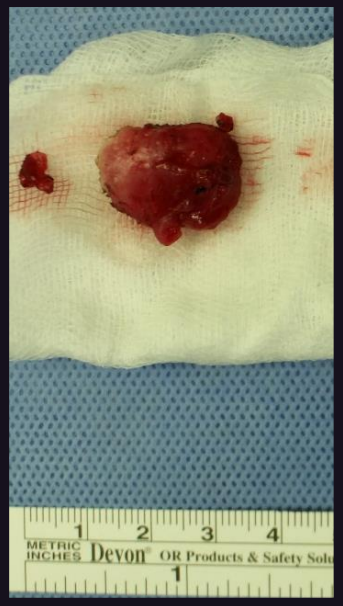

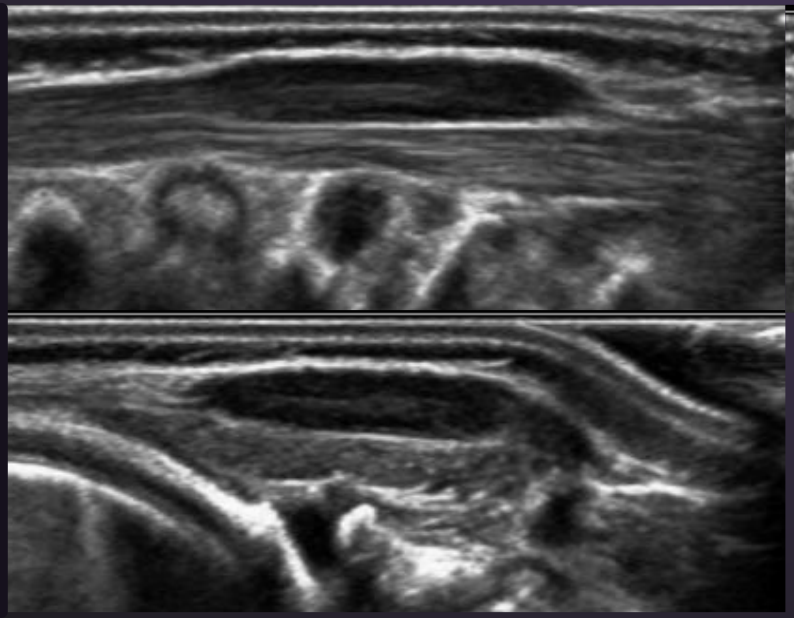

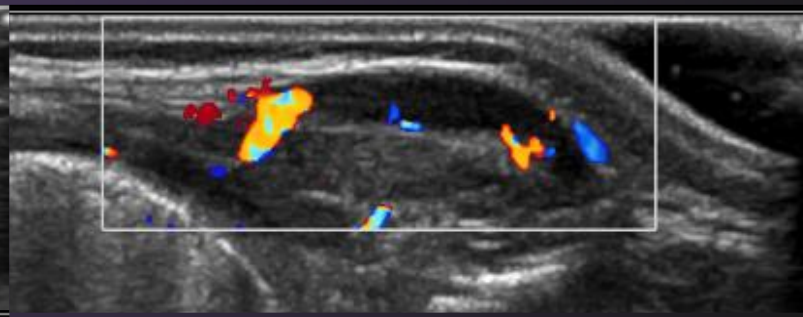

US of the same patient shows well defined hypoechoic mass with vascularity.

Vascular Malformations

- Arteriovenous (AV), venous, capillary, lymphatic malformations
- Usually present at birth and grow with the patient

Vascular Malformations

- AV malformations: high-flow
  - Enlarged feeding arteries and draining veins without an intervening capillary bed
  - US: Complex mass
  - Color Doppler US: High-systolic arterial flow, arterialization of the veins
  - MRI: Dilated feeding and draining vessels, signal voids on Tl- and T2WI, high signal on gradient echo sequences, enhancement (+)

Vascular Malformations

- Venous malformations: slow-flow
  - Abnormal venous spaces and a normal arterial component
  - Soft, compressible masses
  - Normal or bluish color

  - US: Hypoechoic or hyperechoic mass
  - Doppler US: Low monophasic flow or no flow at all
  - MRI: T1 iso- or hypointense, T2 hyperintense mass, absent signal on gradient-echo images, enhancement (+)
    - Rare signal void areas

Vascular Malformations

- Capillary malformations: Port-wine stain
- A collection of small vascular channels in the dermis

- Imaging: Usually normal, increased thickness of the subcutaneous fat and prominent venous channels

Vascular Malformations

- Lymphatic malformations: *Lymphangiomas, cystic hygroma*
- Congenital lesions composed of dilated lymphatic channels
- Usually present <2yrs
- Neck (75%), axilla (20%), mediastinum, retroperitoneum, bone, abdominal organs

- Imaging
  - Thin-walled, multilocular predominantly fluid filled masses
  - Fluid-fluid levels (prior hemorrhage), aneurysmal dilatation of adjacent veins
  - No enhancement of the cystic spaces, minimal/moderate septal enhancement
  - Absence of feeding vessels

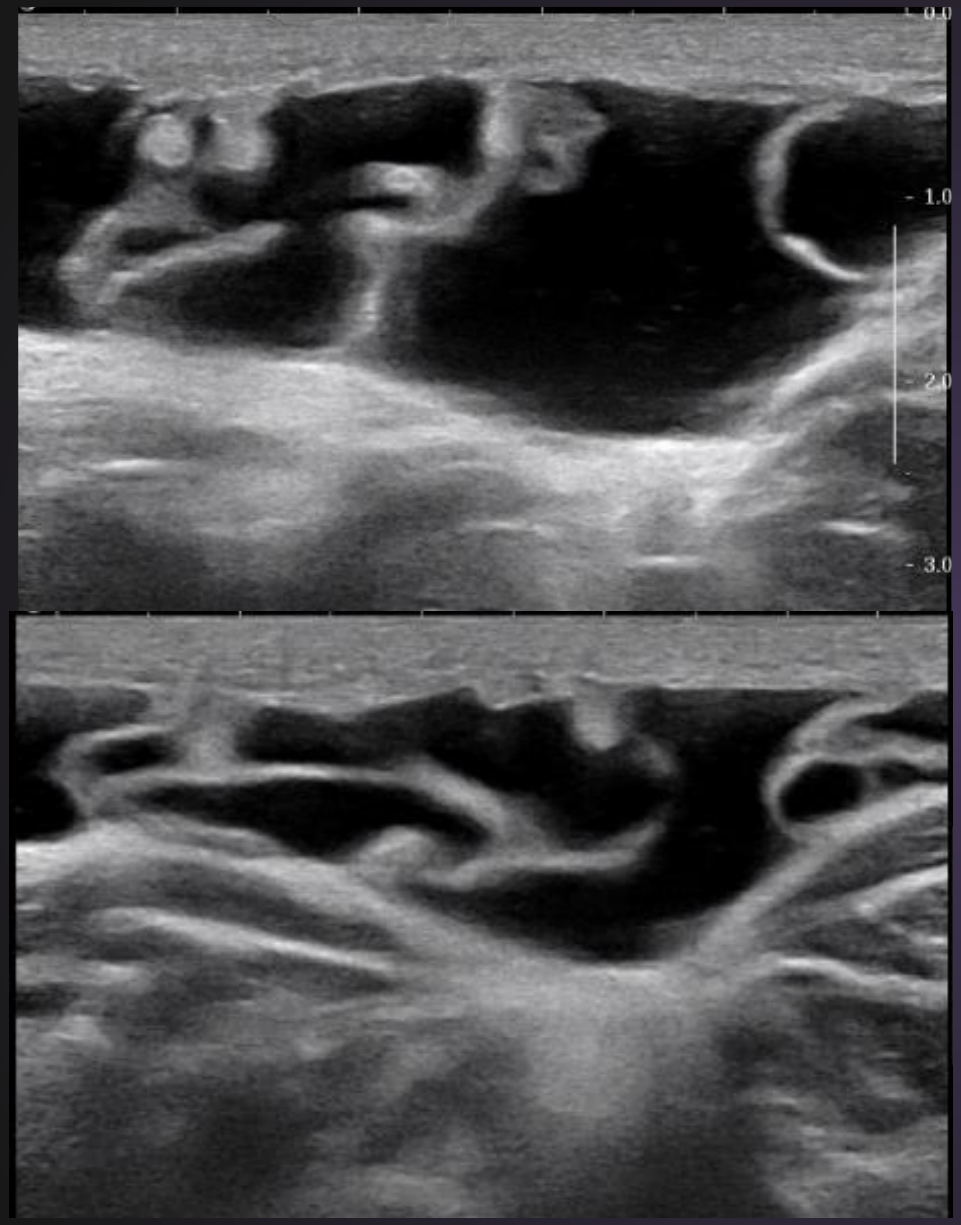

US of a 2-month-old boy shows about 5.3cm sized multiseptated cystic mass at midline upper back, suggesting lymphangioma.

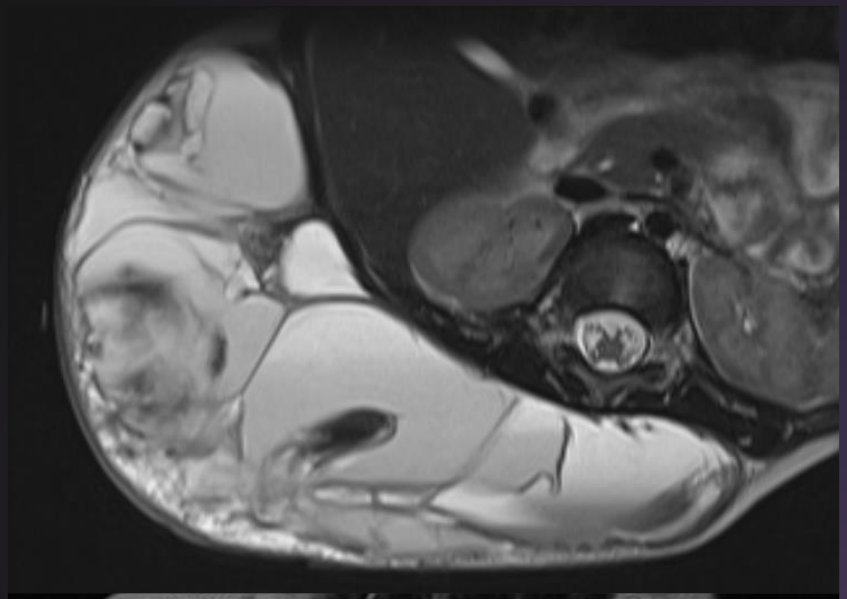

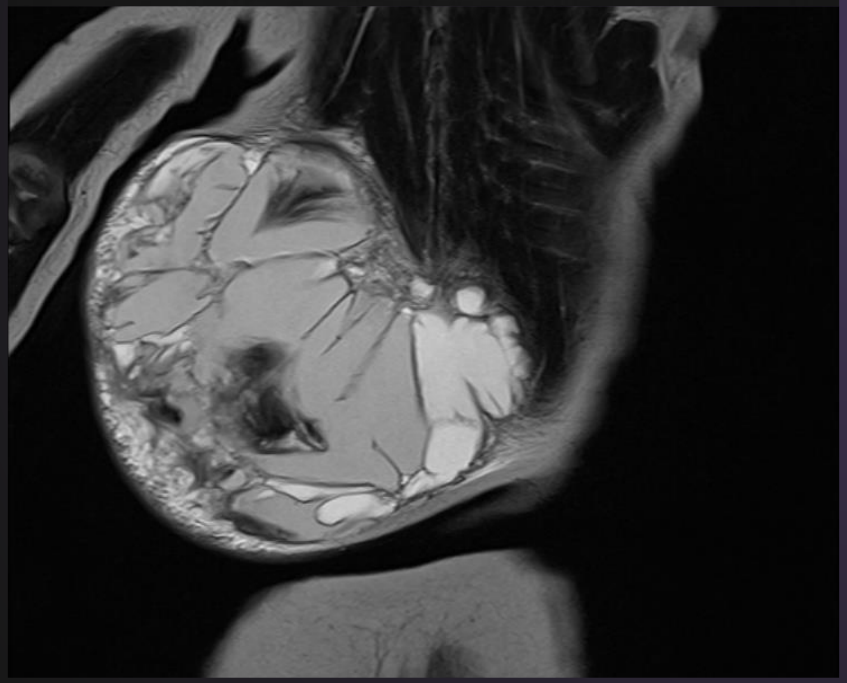

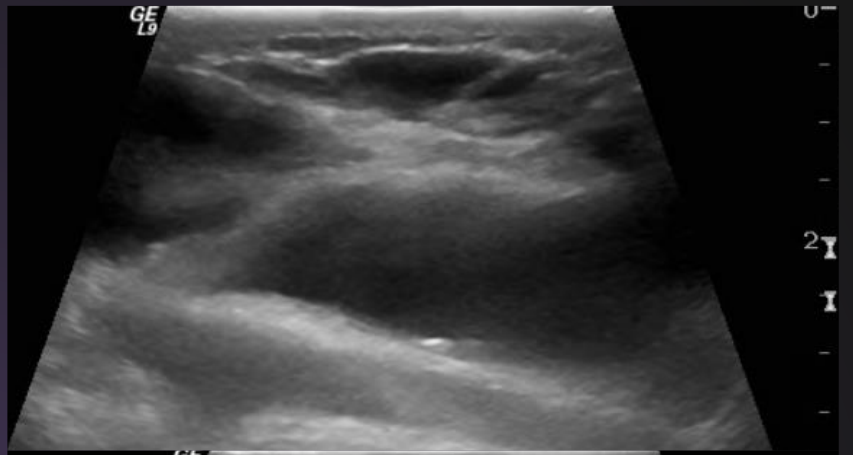

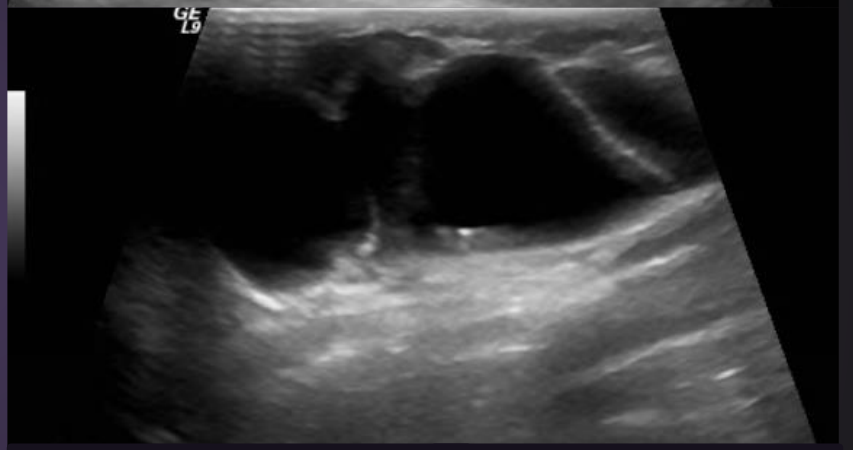

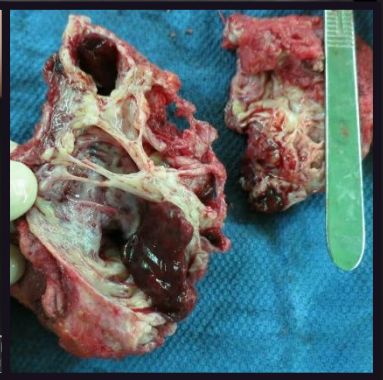

MRI and US of a 10-month-old boy shows about 15x13x10cm sized huge multiseptated cystic mass at right lateral back, confirmed as a lymphangioma.

ADIPOCYTIC TUMORS

Lipoma

- M/C fat containing soft tissue mass in children
- Composed of mature adipose tissue
- Well-defined, homogeneous masses consisting almost entirely of fatty tissue

- US: Homogeneous mass of variable echogenicity
- MRI: Fatty mass, may have a few thin septations, no solid soft tissue component, enhancement (-)

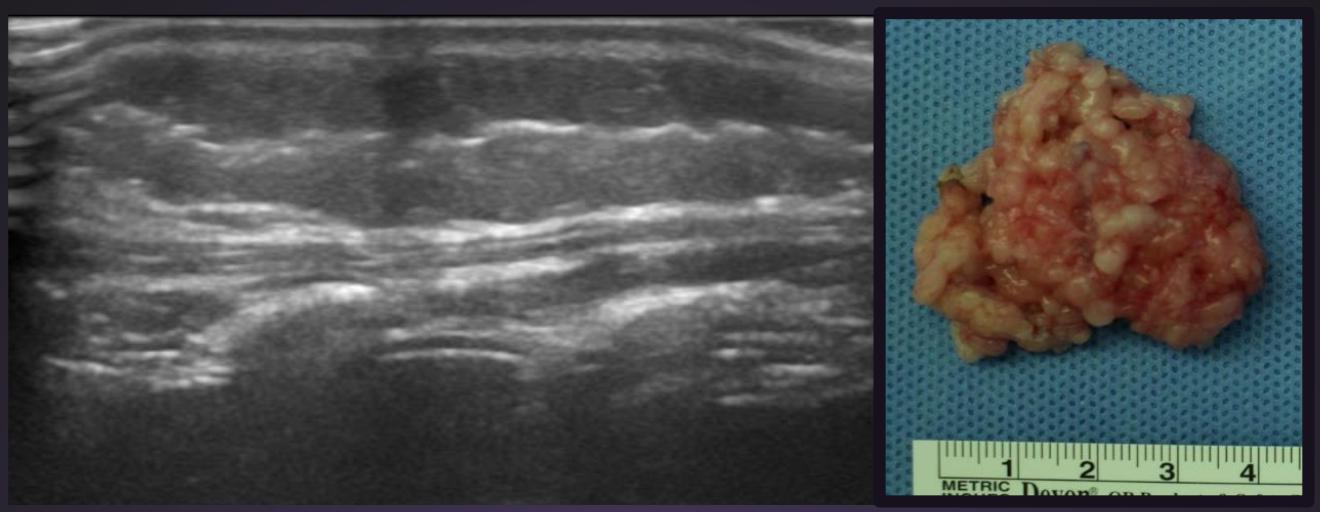

US of a 9-month-old boy shows localized thickening of subcutaneous fat layer at left back, confirmed as a lipoma.

US of a 16-year-old girl shows about 6.7x5.3x1.29cm sized homogeneously hypoechoic mass in the subcutaneous fat layer of left upper back, suggesting lipoma.

Lipoblastoma

- Rare fatty tumor
- Occurs almost exclusively in young children (usually <3yrs)
- Multiple lobules of immature fatty tissue separated by fibrous septa
- Soft tissue or fatty mass
  - Depending on the relative amount of fibrous and lipomatous tissue

- c.f. Liposarcoma: Indistinguishable on imaging, but exceedingly rare in children (<1%)

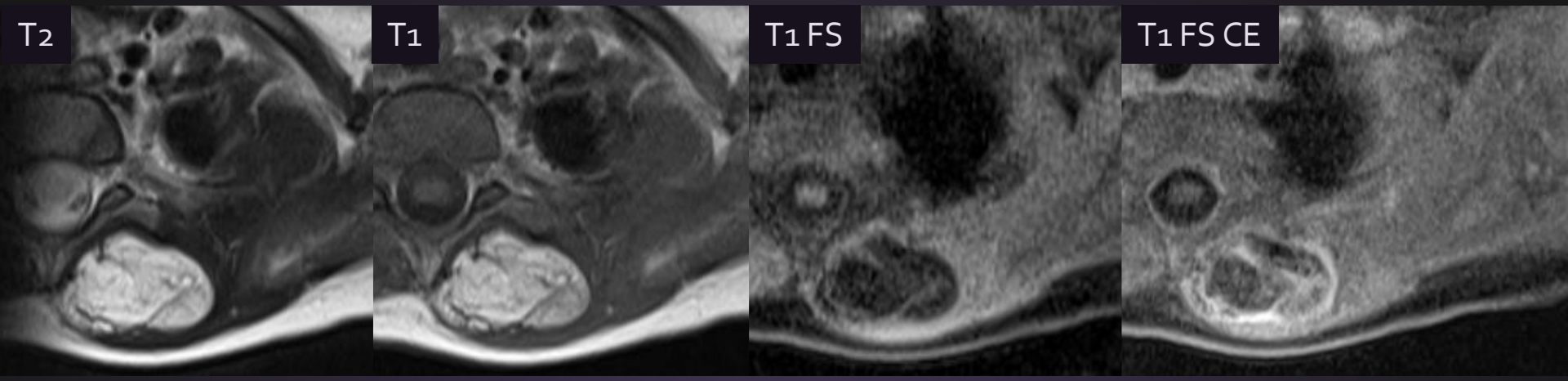

MRI of a 3-year-old boy with palpable mass on left upper back shows lobulated fatty mass with enhancing septations at left paraspinal area, confirmed as a lipoblastoma.

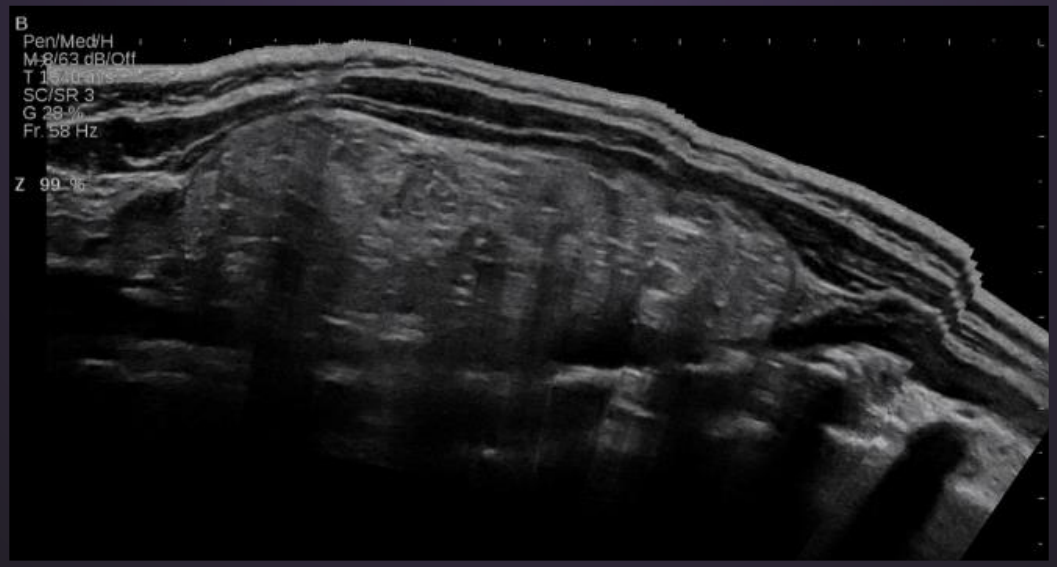

US of the same patient shows heterogeneous hyperechoic fatty mass.

FIBROBLASTIC/MYOFIBROBLASTIC TUMORS

Nodular Fasciitis

- A rapidly growing painless mass
- Benign fibrous proliferation
- Usually subcutaneous, sometimes intra/intermuscular locations
- Cranial form: Almost exclusively <2yrs

- T1WI: Iso to slightly high SI to skeletal muscle
- T2WI: Often high SI (> subcutaneous fat)
- Possible central necrosis
- Fascial tail sign (+): Linear extension along the fascia

Fibrous Hamartoma of Infancy

- Subdermal fibromatous tumor of infancy

- Benign superficial soft tissue mass composed of fibrocollagenous tissue, primitive mesenchymal cells, and mature fat
- Solitary, freely mobile, rapidly growing, usually painless, <5cm
- Anywhere in the body
  - Axilla > upper arm, shoulder > neck, thigh, back, forearm

- 25% congenital, diagnosed in the first 2 yrs of life
- M:F = 2-3:1

Fibrous Hamartoma of Infancy

- Imaging: Rapidly growing, subcutaneous mass in soft tissues adjacent to shoulder in infant
  - Usually <5cm

- Radiographs: Normal to soft tissue fullness, calcification (-)
- CT: Nonspecific soft tissue mass, usually infiltrative
- US: Lobulated/ill defined hyperechoic subcutaneous mass with a hypoechoic peripheral component/serpentine internal strands
- MRI: Variable amount of fat interspersed among heterogeneous soft tissue bands composed of mesenchymal and fibrous tissue
  - Tightly packed strands of T1/T2 iso-low SI and T1 high SI fat component

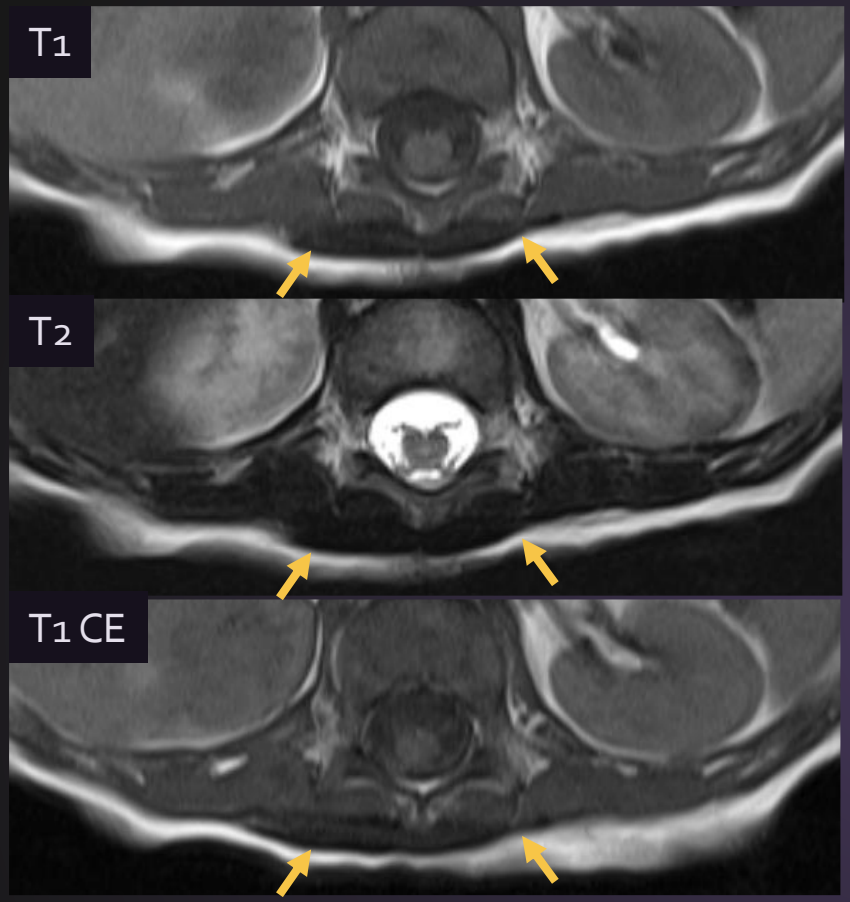

MRI of a 3-month-old boy with palpable mass on mid back shows poorly enhancing T1 and T2 low SI well defined plaque like lesion at superficial fascial layer of median to right paramedian back, confirmed as a fibrous hamartoma of infancy.

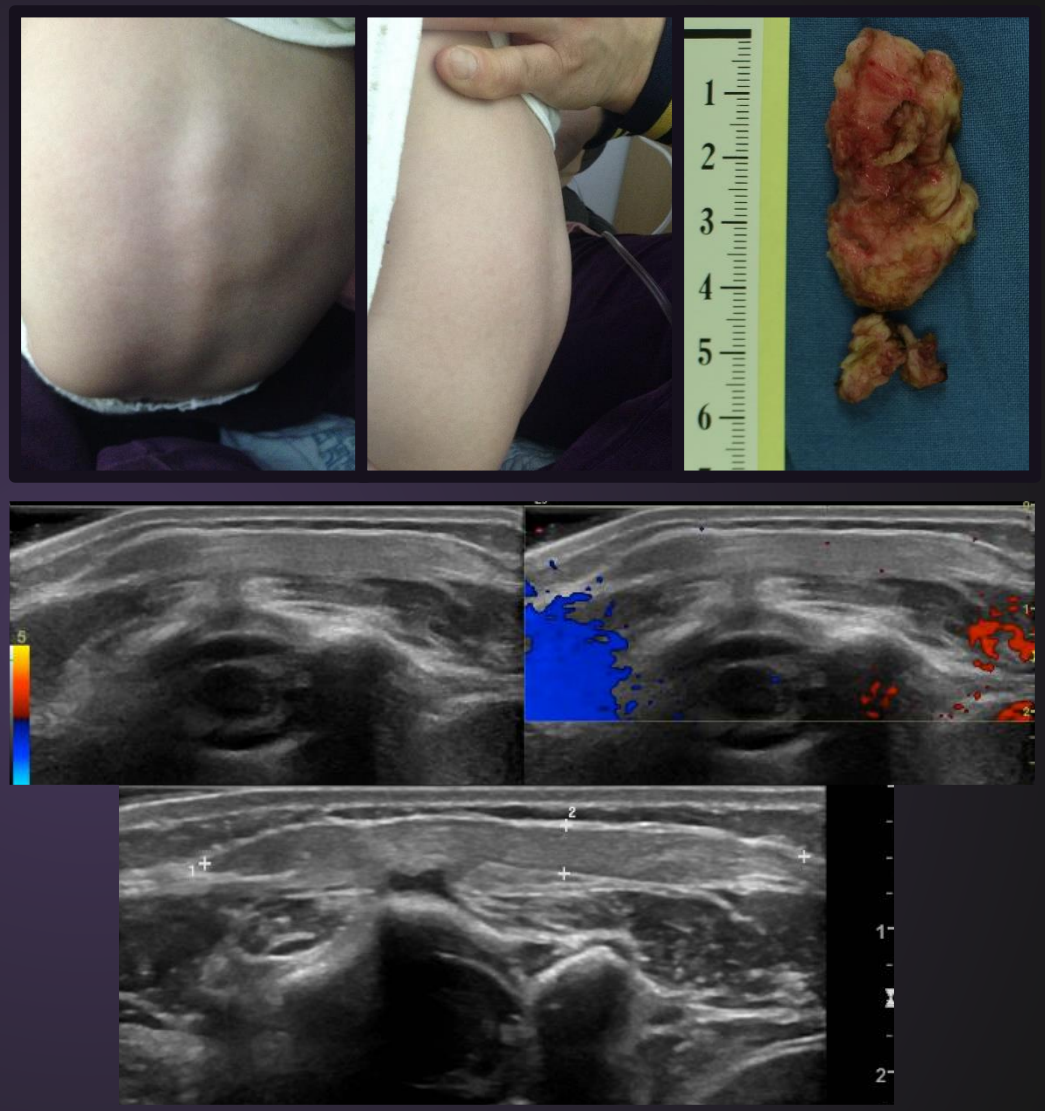

US of the same patient shows well defined plaque like hyperechoic lesion at the superficial layer of back.

FU MRI (2019)

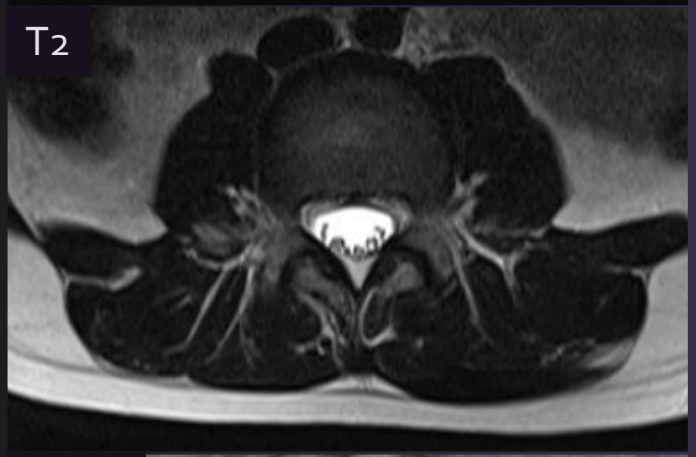

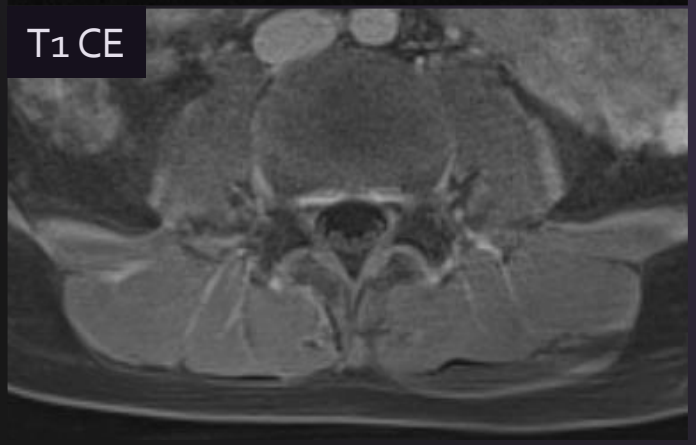

Initial MRI (2015)

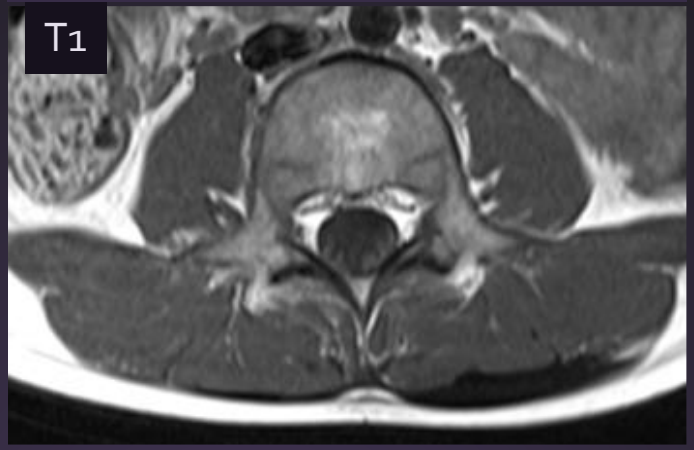

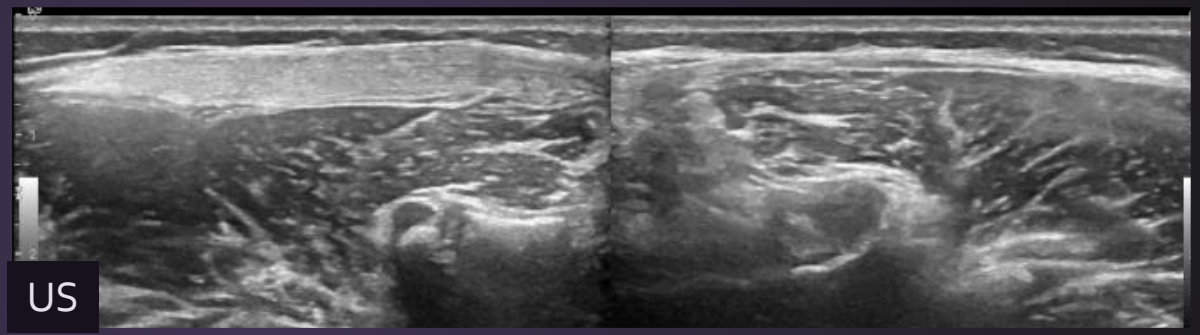

MRI of a 5-year-old boy with back mass shows 6.5x4.5x0.8cm sized T1 dark, T2 dark SI plaque-like lesion at left paramedian superficial fascial layer of paravertebral muscle without significant enhancement, and
US of the same patient shows echogenic plaque-like lesion, suggesting benign fibrous lesion including fibrous hamartoma of infancy and paraspinal elastofibroma*.
This lesion is stable for 4 years of FU.

*Ann Thorac Surg 2015;100:302–4

Myofibroma/Myofibromatosis

- Common benign tumors
- A solitary mass (myofibroma) or multicentric masses (myofibromatosis)
- Nodules formed by 2 components
  - Peripheral: Plump myofibroblasts arranged in short fascicles or whorls
  - Central: Less-differentiated cells usually arranged around hemangiopericytoma-like vessels
- Infantile hemangiopericytoma is part of the spectrum of myofibromas
  - Hemangiopericytomatous component predominates over the myofibroblastic component
- Cutaneous/subcutaneous, muscle, bone (skull)
- Visceral involvement (15-20%): poor prognosis, mortality rates up to 75%
- 88% <2yrs, 60% diagnosed at birth

Myofibroma/Myofibromatosis

- Variable tumor size
- Firm, reddish purple nodules
- Increase in size and number until 1yr → slow spontaneous regression

- US: Variable
  - Target sign: Well demarcated nodules with an anechoic center (necrotic) and a thick hypoechoic wall
  - Solid hypoechoic nodules with or without central calcification
  - Isoechoic nodules
- Color Doppler US: Poorly vascularized
- MRI: T1 low, T2 high SI nodule with a hypointense center (calcification)
  - Diffuse or peripheral enhancement

MRI of a 5-month-old girl with cherry colored nodule on upper back shows T2 high, T1 low SI nodule with enhancement at upper back, confirmed as a myofibroma.

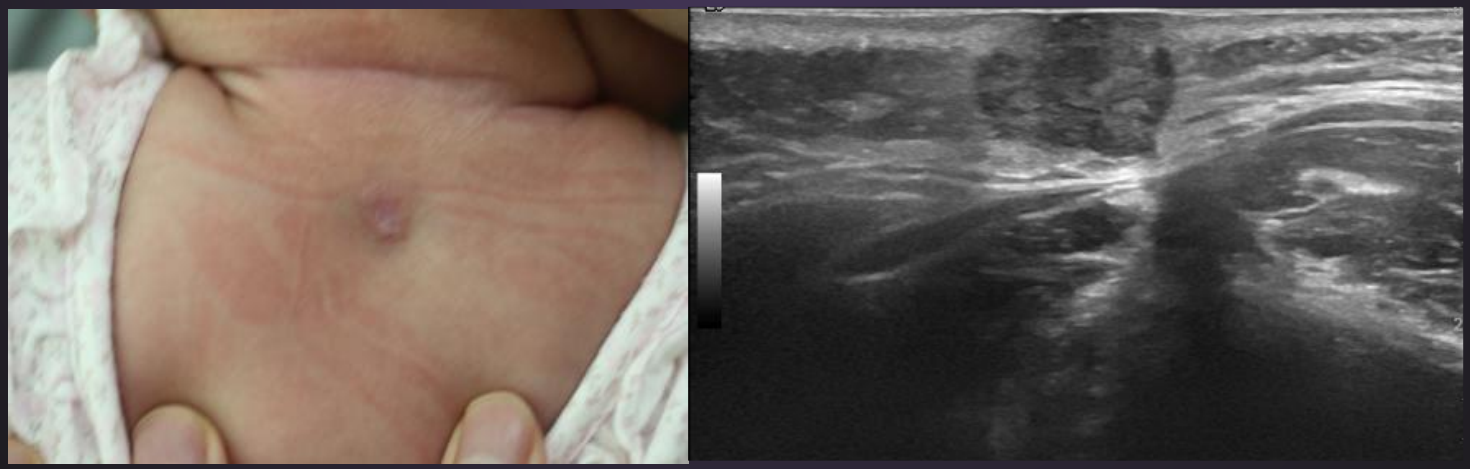

US of the same patient shows well defined hypoechoic lesion at subcutaneous layer of upper back.

Lipofibromatosis

- Rare fibrofatty tumor: abundant adipose tissue traversed by bundles of fibroblast-like cells
- Exclusively in the pediatric age (11 days – 12yrs, median 1yr)
- Ill-defined mass in subcutaneous or deep soft tissues
- Slow growing, nontender, 1-12cm

- US: Heterogeneous, predominantly hyperechoic mass
- Color Doppler: Small internal flow
- MRI: Hypointense strands in intralesional fat
  - Enhancement of the fibrous component

NEUROGENIC TUMOR

Neurofibroma

- Benign peripheral nerve sheath tumor with neoplastic tissue inseparable from normal nerve
- Subtypes: Localized, diffuse, plexiform
  - Localized NF: Painless, slowly growing nodule
  - Diffuse NF: Plaque-like skin elevation
  - Plexiform NF: Limb disfigurement, enlarging mass, weakness, dysesthesia, pain
    - Almost exclusively in neurofibromatosis type 1
    - Extensive plexiform neurofibromas → massive enlargement of body part (elephantiasis neuromatosa)
    - High risk of malignant transformation (8-12%)

Neurofibroma

- Localized neurofibroma (NF): Well-defined, fusiform mass
  - CT: Hypodense relative to muscle
  - MR: T1 Iso to mildly hyper SI, T2 hyper SI
    - Target sign: Central low signal focus
    - Fascicular sign: Multiple, small ring-like structures
    - Split-fat sign: Thin peripheral rim of fat
  - US: Homogeneous hypoechoic mass with mild posterior acoustic enhancement
- Diffuse NF: Ill-defined plaque-like or infiltrative expansion of subcutaneous tissue
  - Nonspecific MR signal characteristics
- Plexiform NF: Long segments of diffusely and irregularly enlarged nerves and nerve branches
  - Multilobulated masses with low attenuation on CT
  - Bag of worms appearance on MR

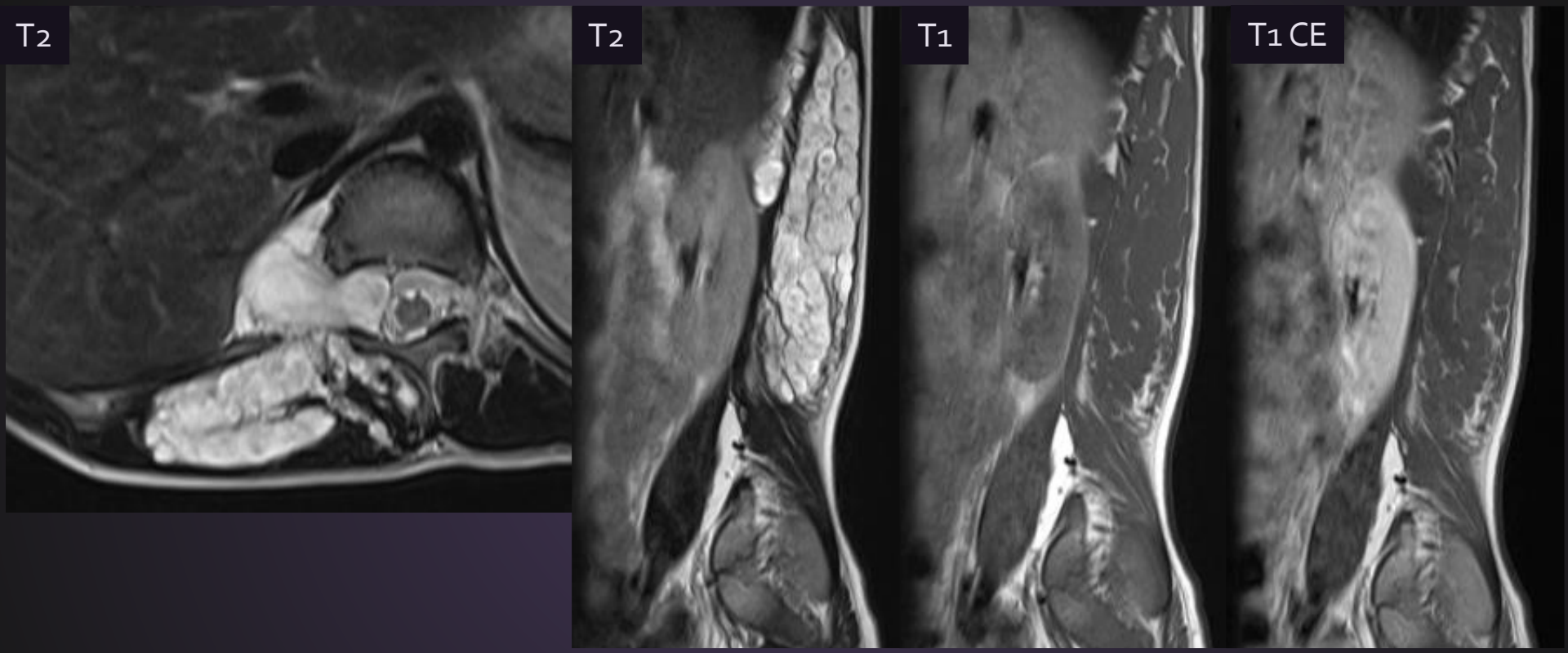

MRI of a 12-year-old boy with NF type 1 shows extensive multilobulated T2 high, T1 iso SI mass at right paraspinal area of lower T-L level, with encasing right L1 nerve root, suggesting plexiform neurofibroma.

UNCLASSIFIED BENIGN TUMORS

Pilomatricoma

- Benign subcutaneous tumor that arises from the hair cortex cells
- Any area of hair-bearing skin
- Slowly grow over months or years, small size (<2cm)
- Nontender, freely movable, hard nodule of irregular surface, bluish discoloration of the overlying skin

- US: Well-defined hyper-/isoechoic nodule with a hypoechoic rim and variable number of internal hyperechoic punctate foci (calcification)
- Color Doppler: Some flow, mainly peripheral (70%)
- MRI: Well-demarcated T1 iso, T2 heterogeneous SI nodule
  - Peripheral, internal patchy/reticular enhancement

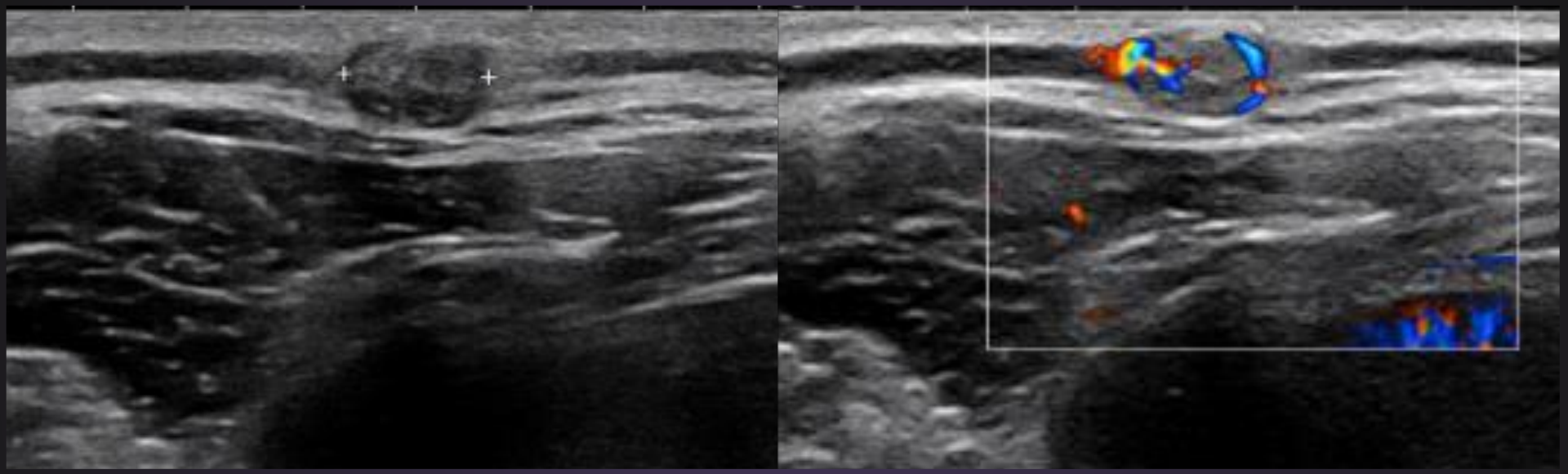

US of a 4-year-old girl with a tiny nodule on back shows about 0.6x0.4x0.9cm sized well defined ovoid mixed echoic nodule with hypoechoic rim, multiple internal hyperechoic foci, and peripheral vascularity suggesting pilomatricoma.

Epidermal Inclusion Cyst

- Common benign lesion of cutis and subcutis that arises from obstruction of hair follicle or deep implantation of epidermis
- Scalp > face > neck > trunk
- Osseous lesions appear lytic with sclerotic margin ± soft tissue swelling

- US: Well-circumscribed, heterogeneously hypo to hyperechoic mass
- CT: Soft tissue density mass in subcutaneous fat
- MR findings
  - Isointense to muscle with mild heterogeneous signal ranging from low to high on T1WI
  - Hyperintense signal plus ↑ or ↓ signal debris (cholesterol crystals or keratin) on T2WI FS
    - Debris may be positionally dependent

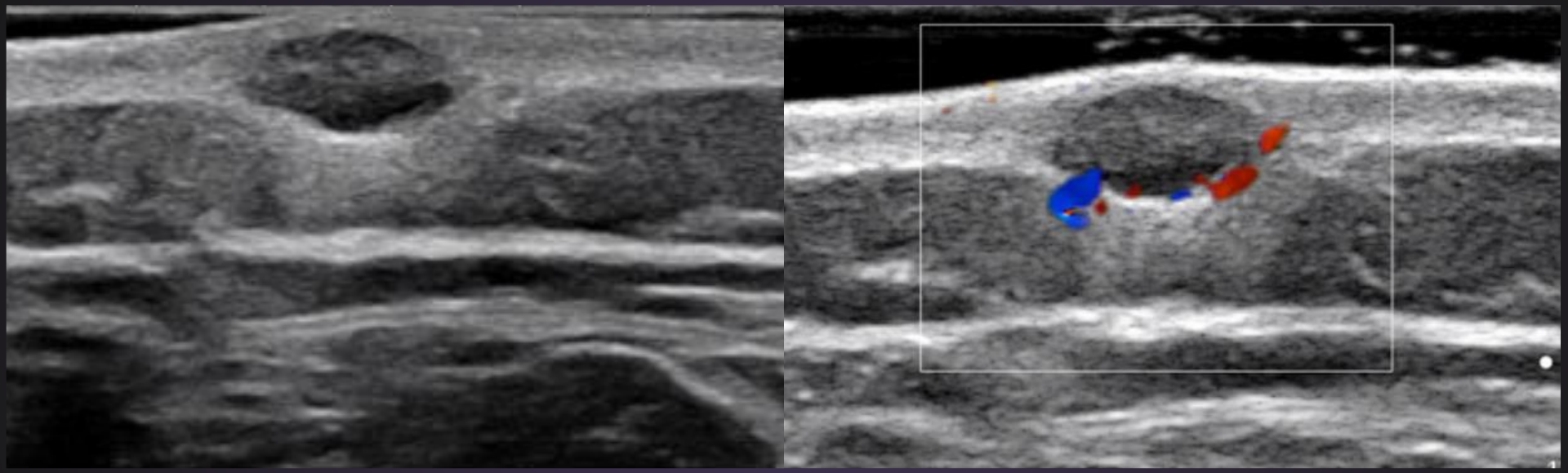

US of a 12-year-old girl with a painless nodule on lower back shows 0.91x0.38x0.51cm sized well circumscribed heterogeneously hypoechoic nodule at skin layer of right paramedian lower back with focal thickening of overlying skin suggesting epidermal inclusion cyst.

References

- O.M. Navarro. Soft tissue masses in children. Radiol Clin N Am 49 (2011) 1235–1259
- O.M. Navarro et al., Pediatric soft-tissue tumors and pseudotumors: MR imaging with pathologic correlation. Part 1. Imaging approach, pseudotumors, vascular lesions, and adipocytic tumors. RadioGraphics2009;29(3): 887–906.
- E.E. Laffan et al., Pediatric soft-tissue tumors and pseudotumors: MR imaging with pathologic correlation. Part 2. Tumors of fibroblastic/myofibroblastic, so-called fibrohistiocytic, muscular, lymphomatous, neurogenic, hair matrix, and uncertain origin. RadioGraphics 2009 29:4, e36.
- A.C. Merrow et al., Elsevier, Diagnostic imaging: Pediatrics, third edition
- B.J. Manaster et al., Elsevier, Diagnostic imaging: Musculoskeletal: Non-traumatic disease, second edition